Spring 5-2013

Phytoplankton Community Distribution and Light Absorption Properties in the Northern Gulf of Mexico

Sumit Chakraborty
University of Southern Mississippi

The University of Southern Mississippi

PHYTOPLANKTON COMMUNITY DISTRIBUTION AND LIGHT ABSORPTION PROPERTIES IN THE NORTHERN GULF OF MEXICO

by

Sumit Chakraborty

Abstract of a Dissertation
Submitted to the Graduate School
of The University of Southern Mississippi
in Partial Fulfillment of the Requirements
for the Degree of Doctor of Philosophy

May 2013

ABSTRACT

PHYTOPLANKTON COMMUNITY DISTRIBUTION AND LIGHT ABSORPTION PROPERTIES IN THE NORTHERN GULF OF MEXICO

by Sumit Chakraborty

May 2013

The theme of this dissertation was to understand the spatio-temporal dynamics of the phytoplankton community, its light absorption properties, and its relationship to underlying physicochemical processes. Understanding these phenomena will benefit efforts to predict pathways of carbon transformation in the ocean, to estimate primary productivity (PP) and to characterize distributions of phytoplankton communities using ocean color remote sensing.

This research entailed four different studies, which address different objectives. The first two studies dealt with phytoplankton community composition and its relationship to environmental variables. A chemotaxonomic approach was used, which was successful in revealing distinct phytoplankton assemblages in distinct water mass regimes. In the second study, a multivariate statistical analysis was used to examine community responses to seasonal variability in relation to different meteorological and environmental forcing. Clear differences in phytoplankton communities existed between stratified and non-stratified periods.

Understanding the variability in the dominant light absorption constituents in the continental margin of northern Gulf of Mexico was the subject of the fourth study. Absorption budgets for the region revealed dominance of colored dissolved organic matter (CDOM). The presence of large contributions from the CDOM and non-algal

particles (NAP) can lead to over- or underestimation of chlorophyll-*a* specific phytoplankton absorption (a^*_φ) and such errors may then propagate to errors in PP estimates using current ocean color algorithms. Additionally, variations in the optical characteristics of phytoplankton also influence PP. Thus, the fourth study focused on describing the main sources of bio-optical variability affecting the spectral signatures of phytoplankton absorptions in the region. Results showed that changes in cell size, pigment composition and photoacclimation strongly affected phytoplankton spectral absorption. Values of a^*_φ were largely influenced by the pigment package effect and cell size followed by pigment composition. The results from this study will benefit efforts to examine the critical role of phytoplankton in biogeochemical cycles of the northern Gulf of Mexico.

The University of Southern Mississippi

PHYTOPLANKTON COMMUNITY DISTRIBUTION AND LIGHT ABSORPTION PROPERTIES IN THE NORTHERN GULF OF MEXICO

by

Sumit Chakraborty

A Dissertation
Submitted to the Graduate School
of The University of Southern Mississippi
in Partial Fulfillment of the Requirements
for the Degree of Doctor of Philosophy

Approved:

Steven E. Lohrenz
Director

Wei-Jun Cai

Donald G. Redalje

Jerry D. Wiggert

Stephan D Howden

Susan A.Silatanen
Dean of the Graduate School

May 2013

ACKNOWLEDGMENTS

I would like specially thank my major advisor, Dr. Steven (Steve) E. Lohrenz, for his encouragements, insights, and academic and financial support during the course of this study. I also want to thank you for your endless patience and the tremendous amount of faith you showed to me. Your **unconventional** guidance techniques helped me to sharpen my thought processes and allowed me to take independently decisions.

I also want to express my gratitude to the members of my dissertation committee, who made time for me on numerous occasions to answer my questions and provided intellectual insights during the course of the study. Special thanks to Drs. Stephan Howden and Jerry Wiggert for their advice on dealing with the physical datasets. Drs Donald Redalje and Wei-Jun Cai also deserve equal thanks for their encouragement and scientific help.

I am particularly grateful to Drs. Simon R. Wright and Harry Higgins for providing the latest version of CHEMTAX (v 1.95), Dr. Donsang Ko for providing the current data from the Intra-Americas Sea Ocean Nowcast/Forecast System (IASNFS), and Joe Metzger for providing the NOGAPS wind reanalysis products.

Financial support for this work came from grants NASA (NNX10AU06G) and NSF (OCE-0752254) awarded to my advisor, Dr. Steven E. Lohrenz.

On personal note I would like to express special thanks to friends and colleagues for their unconditional help: David Rosenfield (for assistance during the processing of the NOGAPS winds and help in developing some complex Matlab scripts), Matt Dornback (for his help during the cruise and analyzing the CDOM samples), Sarah Epps (for sharing her SPM data and help during the cruises). I also want to thank lab technician

Allison Mojzis (for analysis nutrient samples), Merritt Tuel, and Richard Slaughter (for their help during HPLC trouble shooting).

Special thanks to Kevin Martin for acting as chief scientist on three of Gulf Carbon cruises, all other cruise participants, captain and crew of R/V *Cape Hatteras* and R/V *Hugh R. Sharp*.

I would like to take this opportunity thank the Department of Marine Science at The University of Southern Mississippi for providing a very cordial academic environment and all the staff members who provided direct and indirect support to me during the course of my stay at the Department of Marine Science.

Finally I dedicate this dissertation to my parents my parents Samir Kumar Chakraborty and Jyoti Kana Chakraborty, for their endless support and encouragement and love.

TABLE OF CONTENTS

LIST OF TABLES

LIST OF ILLUSTRATIONS

Figure

LIST OF EQUATIONS

Equation

CHAPTER I

INTRODUCTION

Phytoplankton communities contribute to about half of global net primary production (NPP), gross photosynthesis minus the plant respiration (Falkowski et al. 1998, Chassot et al. 2010), and play key roles in marine food-webs. Changes in phytoplankton biomass, production and community composition have implications for global biogeochemical processes. Recent studies have established relationships between phytoplankton diversity and assemblages to climatic processes on long term decadal scales (Chavez et al. 1999, Murtugudde et al. 2002, Chavez et al. 2011). Results from such studies also indicate strong relations between phytoplankton community succession and global carbon cycles (Sabine et al. 2004, Iglesias-Rodriguez et al. 2008). Knowledge about mechanisms driving such succession in different phytoplankton groups will ultimately help in predicting changes in phytoplankton communities and their contributions to global carbon cycling in response to environmental change.

Advances in satellite oceanography over the last three decades have revolutionized our understanding of the distribution of important biogeochemical properties including, for example, concentrations of chlorophyll a (Chl *a*), suspended particulate materials (SPM) and colored dissolved organic matters (CDOM). Over the last three decades, ocean color imagery from orbital platforms has provided long-term, synoptic pictures of biogeochemically important optical properties of the world oceans (McClain 2009). However, challenges remain in developing algorithms to detect different phytoplankton groups in diverse marine environments. Applications of remote sensing approaches in coastal environments have been particularly difficult because of the

complex optical conditions in such regions. Satellite retrieval of water column properties is especially difficult in regions with large riverine inputs of dissolved and sedimentary materials (Chang et al. 2007).

The northern Gulf of Mexico is a coastal ocean margin dominated by large river systems, and shows high variability in the fluxes of organic and inorganic matter, including both dissolved (e.g. CDOM) and particulate (SPM) phases (D'Sa et al. 2007, Green et al. 2008b). Phytoplankton productivity, physiology and community dynamics in the northern Gulf region have been shown to be strongly influenced by the availability of light, as well as other environmental variables (Lohrenz et al. 1999).

Detailed understanding of the variability of light absorbing components (pigments, CDOM, and SPM) and their influence on the quality and quantity of light in coastal margins such as the northern Gulf of Mexico will help in advancing the development of remote sensing algorithms to estimate primary production and to characterize phytoplankton community structure. Additionally, information about these light absorbing components (CDOM and SPM) can contribute to understanding of the transport and cycling of organic matter, both from terrestrial (allocthonous) and *in-situ* (autochthonous) sources. Better understanding of the variability in organic carbon fluxes in the coastal margins is essential for accurate estimation of global carbon fluxes (Coble 2010). Understanding of the carbon cycle in continental margins is critical to determine the role of the oceans in future climatic and anthropogenic changes (Chavez 2007). One important step towards such understanding will be the development of regionally specific carbon budgets. Phytoplankton primary production and community dynamics, among others factors, are important variables in such budgets.

A key aspect in the ability to use satellite-derived biogeochemical proxies in coastal margins will be the development and refinement of regional ocean color algorithms. Such efforts will allow better estimation of primary production and retrieval of phytoplankton size classes and functional types from remote sensing data. The lack of information on the spatial and temporal variability of the important biogeochemical proxies has limited understanding of the contribution of the coastal margins to global carbon budgets. High quality satellite derived biogeochemical products can provide improved spatial and temporal coverage and reduce uncertainties in regional carbon budgets. Such products can also be used in coupled physical and biological models (e.g. Fennel et al. (2011) and Hofmann et al. (2011)) that can also help in reduction of uncertainties in carbon fluxes. Constraining the uncertainties in carbon cycling in continental margins will help efforts to predict changes in carbon in response to climate and human induced impacts and will benefit overall carbon management efforts.

This dissertation provides analysis of phytoplankton distributions and community composition along with contemporaneous observations of optical properties and relationships to environmental variables in the northern Gulf of Mexico. The work systematically examines phytoplankton pigments and community composition, optical variability in relation to light absorbing constituents, phytoplankton light absorption properties, and the application of satellite algorithms to retrieve key optical properties. The dataset covers a wide range of water mass types and seasonal river discharge conditions. The measurement approaches and data analyses involved a combination of contemporary ecological and optical techniques. The results provide a unique baseline of

information that will support efforts to understand the ecology and biogeochemistry of the critically important river-dominated coastal margin of the northern Gulf of Mexico.

Background

This research took advantage of a series of cruises conducted in the northern Gulf of Mexico (NGOM) during which observations were made on the distributions of phytoplankton pigments and light absorption properties. As part of ongoing work in the Gulf of Mexico associated with the Gulf Carbon (www.gulfcarbon.org) study, a series of cruises were conducted in the NGOM (Fig. 1), a large river-dominated coastal margin. The study area may be broadly partitioned into different zones based on their freshwater source. The central zone (89 º 30´W to 91º 70´W) is strongly influenced by the freshwater input from the Mississippi- Atchafalaya (MS-ATF) rivers. To the east of the MS delta (east of 89 ºW), the major source of freshwater is the outflow through Mobile Bay from the Alabama/Tombigbee rivers (second largest in NGOM). West of 92 ºW, the area is outside the direct influence of MS-ATF rivers and the Sabine river is one of the main contributors of freshwater. Apart from these major freshwater sources, a series of inland estuaries and lakes, including Calcasieu Lake, Lake Pontchartrain and inland bays such as Barataria Bay and Terrebonne Bay, flush freshwater into the NGOM. All these different large and small freshwater sources are characterized by different origins, habitats, and flow regimes (volumes of water runoff). This results in different hydrology's and hydrodynamics (e.g., heavily dredged Mississippi River in comparison to the less developed Atchafalaya River, Conmy et al. (2004)). Residence times of these systems also differ (e.g., 2-10 days in the Atchafalaya Bay and in the MS River plume compared to approximately 125 days in Terrebonne Bay and Barataria Bay, Bianchi et.al. (1999)).

Such differences in hydrology and hydrodynamics influence both the quantity and chemistry of organic matter in these systems. Export of organic matter from these different freshwater sources can subsequently influence the biogeochemistry and light fields in the coastal environment, thereby influencing phytoplankton composition, primary production and carbon cycling in the river dominated costal margin of the NGOM.

Patterns in Phytoplankton Biomass, Community Structure and Light Absorption Properties in NGOM

Biological productivity in the NGOM is strongly influenced by the large river systems. The MS River drains ~40% of the continental United States (Dagg et al. 2004) and is the largest source of freshwater, suspended sediments, particulate and dissolved organic matter and nutrients to coastal waters in North America (D'Sa et al. 2006). High nutrient content associated with the MS River plume results in enhanced productivity in the NGOM (e.g., Lohrenz et al., 1999). Apart from the MS River there are about half a dozen other rivers in the NGOM that supply significant amounts of freshwater to the NGOM. A cross-shelf gradient of high chl *a* and dissolved organic matter in association with low salinity water masses exists in the continental shelf due to intrusion of freshwater from the MS River and other rivers (Del Castillo et al., 2001; (Vanderbloemen & Müller-Karger 2001). Distinct patterns in phytoplankton community composition have been observed in river-dominated low salinity waters as compared to high salinity offshore waters(Filardo & Dunstan 1985, Anderson 1986, Jackson et al. 1987). For example, Qian et al. (2003) in the northeastern GOM (east of MS delta to Tampa Bay in Florida) found diatoms, chlorophytes and cryptophytes to be associated with low salinity

waters whereas prymnesiophytes and pelagophytes were associated with high salinity waters. Shifts in the surface picoplankton composition, from *Synechococcus* to *Prochlorococcus* have been observed as MS River plume water extends into the oligotrophic waters of GOM (Wawrik et al. 2003). Other studies in the northwestern GOM (Texas shelf) have reported that nutrient rich inner shelf waters were diatom-dominated (Bontempi 1995) along with cyanobacteria while slope waters had high abundances of pelagophytes, cyanobacteria and prymnesiophytes (Lambert et al. 1998). Chen et al. (2000) similarly found high diatom abundance in water masses influenced by the MS-ATF outflow. However, cyanobacteria and chlorophytes were generally found to dominate phytoplankton biomass elsewhere on the shelf, along with contributions by haptophytes, cryptophytes, chrysophytes, prasinophytes and dinoflagellates.

Despite the known importance of river dominated coastal margins, previous studies documenting phytoplankton composition in the NGOM have been spatially scattered and restricted either to the immediate MS Plume (Bode & Dortch 1996, Dagg et al. 2004, Liu et al. 2004, Wysocki et al. 2006) or focused on the North Western Gulf (Qian et al. 2003), Texas continental shelf (Lambert et al. 1998) and Bontempi (1995) or on the greater Louisiana-Texas shelf (Chen et al. 2000). This study systematically examines the spatial and temporal variations in phytoplankton populations present in the large river dominated coastal margins of the NGOM (from Mobile Bay on the East to Sabine on the West, Chapter II, and Fig.1).

In addition to effects of river inputs, the variable patterns of shelf circulation and large scale circulation features (Loop current) exert strong influences on biological processes in NGOM. Eddies generated from Loop current instabilities may cause

localized upwelling, thereby bringing nutrient rich deep water to the surface (Biggs 1992) and influencing primary production (Biggs & Müller-Karger 1994). This research does not address the details of physical processes within the region, but does examine biological and physical data associated with different water mass types to better understand how physical processes may play a role in influencing biological patterns within the study domain.

Relationship of Phytoplankton Light Absorption to Other Light Absorbing Constituents of Water

Phytoplankton biomass and primary production in the coastal regions of NGOM are strongly influenced by nutrient and light availability (Lohrenz et al. 1999, Lohrenz et al. 2008b). The NGOM is optically complex, characterized largely by Case 2 waters (Sathyendranath 2000) with light fields heavily influenced by absorption of colored dissolved organic matter (CDOM) and non-algal particles (NAP) (D'Sa et al. 2006, D'Sa et al. 2007, Green et al. 2008b). The NGOM receives large inputs of terrestrial organic matter from different freshwater sources; annually the MS river alone delivers ~ 2 x 10^{11} kg of suspended sediments and ~ 3.1 x 10^{9} kg of dissolved organic carbon (DOC) to the Louisiana shelf (Green et al. 2008b). Though riverine inputs are assumed to be the main contributor of CDOM in coastal waters (Siegel et al. 2002, Del Castillo & Miller 2008), biological processes can also contribute a significant amount of CDOM and cannot be neglected (e.g., Nelson et al. (1998), Schofield et al. (2004)). In situ processes such as phytoplankton primary production or photo-degradation and bacterial action on byproducts of phytoplankton can influence the CDOM distribution and its spectral signatures (e.g., Twardowski and Donaghay (2002), Rochelle-Newall and Fisher (2002),

Carder et al. (1989)). Similarly, by-products of the phytoplankton community, such as senescent cells and, extracellular release can also contribute to NAP in addition to a continuous mineral signal background (Loisel et al. 2007). The biology and hydrodynamics of the NGOM (study area, Fig. 2.1) is complex, involving various water mass types including estuarine and inner shelf waters heavily influenced by large river systems (MS-ATF) and mid-shelf and slope waters more characteristic of clear, oligotrophic ocean waters. These strong gradients in optical and biogeochemical properties make the NGOM an appropriate site for studying the relationship between the phytoplankton community and the optical constituents. Knowledge about light absorbing constituents is important in efforts to describe variations in the light field and its influence on phytoplankton photosynthesis and primary production. In addition, the study of optical constituents can provide information on the distribution of key biogeochemical constituents in the coastal ecosystem that can provide information that will aid in understanding of carbon cycling and transport in the coastal margins. Recent studies in the region (D'Sa and Miller 2003, D'Sa et al, 2007, Green et.al 2008b) though temporally restricted have provided critical information on the chemical (e.g. Chen and Gardner, 2004, Conmy et.al., 2004, D'Sa et.al., 2009) and physical (D'Sa and Miller (2003), D'Sa, 2006, 2007, Green. et.al., 2008a, 2008b) nature of the variability among light absorbing constituents in the NGOM. Such studies have pointed out the need to expand the available observations to better constrain the uncertainties associated with OCAs and to allow them to be tuned specifically for the NGOM (D'Sa & DiMarco, 2009).

The Gulf Carbon cruises (See Chapter II, Fig. 1) provided an excellent opportunity to expand the data set of optical measurements for the northern Gulf shelf/slope waters and thereby set the stage for in-depth study of the magnitude and spectral features of the light absorbing components. The aim of this proposed work was to study the seasonal and regional variation in the magnitude, spectral shape of the absorption coefficients of a_{φ}, a_{NAP} and a_{CDOM} in the NGOM and to relate phytoplankton biomass and community structure to these light absorbing properties in the water column.

Objectives

Based on the biological, bio-optical and physical data collected during the five Gulf Carbon cruises on R/V Cape Hatteras (January, April-May, July, 2009 and March 2010) and R/V Hugh R. Sharp (October-November, 2009) in the continental margin of northern Gulf of Mexico (31˚N, 87.5˚E, 95˚W and 27˚S), the study focused on the following objectives.

1. To systematically examine the spatial and temporal distribution of phytoplankton biomass and pigment composition by HPLC pigment analysis and using the chemical taxonomic software CHEMTAX to determine the phytoplankton community structure.
2. To describe the environmental variables and their relationship to the phytoplankton community distribution.
3. To understand the relative contribution of phytoplankton and other biogeochemically important light absorbing constituents to total absorption and its spectral variability over time and space in NGOM.

4. To characterize the spatial and temporal patterns of phytoplankton light absorption and underlying factors contributing to its variability in different water masses along the continental margin of NGOM.

Hypotheses

1. Distinct differences exist between offshore and near shore phytoplankton populations with populations in the region of freshwater influence exhibiting larger temporal and spatial variability and lower diversity than the offshore populations.
2. Large differences in phytoplankton community composition coincide with transitions between stratified and non-stratified periods for all water types in the continental margin of the NGOM.
3. Influence of wind and riverine forcing on spatial and temporal variability in bio-optical properties extends across the continental margin of the NGOM throughout the various environmental domains of estuarine, inner-shelf, mid-shelf, and even offshore waters.
    3.1 Spectral characteristics of CDOM and NAP are influenced by algal processes and consequently will vary in relationship to algal biomass.
4. Spatial variability in phytoplankton light absorption properties can be attributed to variations in phytoplankton cell size and pigment composition in the NGOM.
    4.1 Variability in phytoplankton absorption will be strongest along horizontal (across shelf) as compare to vertical (with depth) gradients and will be related to variations in cell size and pigment composition.

CHAPTER II

PATTERNS OF PHYTOPLANKTON COMMUNITY AND BIOMASS DISTRIBUTION ACROSS THE CONTINENTAL MARGIN OF NORTHERN GULF OF MEXICO: HPLC-CHEMTAX ANALYSIS

Abstract

Information about phytoplankton community composition in relation to environmental variability is critical to understanding food web dynamics and the role of the biological pump in carbon cycling. Phytoplankton community composition was characterized over varying seasonal and river discharge conditions during the course of five research cruises across the continental margin of the NGOM as part of the Gulf Carbon program. The composition of the algal community was examined using HPLC analyses of phytoplankton pigments in conjunction with classification using the CHEMTAX software (v. 1.95). Different patterns in phytoplankton community structure in relationship to seasonal hydrographic structure of the water columns were observed. Estuarine and inner-shelf communities were mainly dominated by diatoms, chlorophytes and cryptophytes with the exception of the stratified periods in summer and fall when cyanobacteria were an important part of the community. Mid-shelf waters representative of the transition zone between the river influenced coastal margin and oligotrophic deep slope waters were associated with maximum diversity in phytoplankton community with increasing importance of haptophytes and prochlorophytes. Typical oligotrophic conditions prevailed at the slope with the surface community dominated by cyanobacteria, haptophytes, prochlorophtes and pelagophytes. A chlorophyll fluorescence maximum (CFM) was a regular feature at the offshore stations that showed

significant seasonal variability. Sharp transitions in the phytoplankton pigment ratios between the surface and the CFM and deeper waters were observed particularly among prochlorphytes, haptophytes, and pelagophytes, which was an indication of different ecotypes and photoacclimation states.

Introduction

The structure of phytoplankton communities is a critical factor influencing the marine ecosystem processes including food web dynamics and efficiency and intensity of the biological pump. Variations in phytoplankton community structure and size distributions have potential impacts on biogeochemical transformations and transport of organic matter as well as linkages to higher trophic levels. Knowledge about characteristics of phytoplankton communities is useful for efforts to apply ecosystem-based management approaches for fisheries and can also aid in efforts to study carbon cycling and the balance between autotrophic and heterotrophic production.

The NGOM is a highly productive region with economically important commercial and recreational fisheries. In addition, large uncertainties exists in coastal carbon budgets in this region (Coble 2010). The net metabolic balance of the NGOM ecosystem is not well constrained (Smith & Hollibaugh 1993, Gattuso et al. 1998, Cai 2011, Guo et al. 2012). Furthermore, as is true for some other large river-influenced margins (e.g., Changjiang River), the continental shelves of NGOM have been subject to intense eutrophication (Cai et al. 2011) to which has been attributed the development of large and recurring seasonal hypoxia events (Rabalais et al. 2002b, Li et al. 2011). The nutrient loads from the two large rivers, the Mississippi and Atchafalaya, increases phytoplankton biomass in the coastal waters (Justić et al. 1993, Green & Gould 2008,

Lohrenz et al. 2008a, Lehrter et al. 2009). The production of organic matter and its subsequent transport and flux to the subpycnocline waters is believed to fuel microbial degradation (oxygen consumption) leading to hypoxic conditions below the pycnocline (Redalje et al. 1994, Bianchi et al. 2010). Therefore, understanding the structure of the phytoplankton community helps in understanding the links between nutrient discharge, organic matter production, consumption and degradation. Studies focusing on the biogeography of phytoplankton groups are relevant and crucial to understand the pelagic ecosystem dynamics, which would help to better address the above mentioned broad scientific questions.

Previous studies on phytoplankton distributions in the large river (Mississippi and Atchafalaya) influenced margins of the NGOM have been limited either seasonally or spatially, having focused on the immediate plume regions of the Mississippi (MS) river and inner shelves of NGOM (Dortch & Whitledge 1992, Redalje et al. 1994, Bode & Dortch 1996, Lohrenz et al. 1999, Wysocki et al. 2006). Other studies have not fully encompassed both the Atchafalaya and Mississippi outflow regions, instead covering the northeastern Gulf of Mexico (Qian et al. 2003) or concentrating more towards the northwestern Gulf of Mexico (Lambert et al. 1998, Chen et al. 2000) . This study region encompasses the river influenced region of the NGOM influenced not only by the Mississippi and Atchafalaya rivers, but additionally by numerous freshwater bays and estuaries to the oligotrophic slope or offshore waters outside the direct influence of the rivers (Fig. 1), thus exhibiting strong gradients in physical and chemical properties. This study is unique in its extent across the northern central Gulf of Mexico and provides an unprecedented temporal and spatial dataset on phytoplankton community distributions.

Variations in phytoplankton community composition in relation to river-ocean gradients have been described in a number of studies (Qian et al. 2003, Wawrik et al. 2003, Wawrik & Paul 2004, Wysocki et al. 2006, Lohrenz et al. 2008b). Variations in phytoplankton community composition can be related to shelf circulation and water column structure. As a general paradigm, nutrient rich coastal (well-mixed) regimes support a classical food chain with large phytoplankton, while oligotrophic open ocean or slope (stratified) waters favor smaller phytoplankton (Hulburt 1963, Chisholm 1992) .

Here the spatial and temporal patterns of phytoplankton pigments and associated taxonomic characterizations are investigated for different water types encountered in the study region. The approach relied on HPLC to analyze pigment composition, followed by the use of CHEMTAX software (Mackey et al. 1996) to estimate the contribution of each phytoplankton group to Chl *a* for each of the different water types studied. Prior studies using CHEMTAX to determine phytoplankton community composition are numerous and extend over a wide variety of geographic regions (Mackey et al. 1998, Higgins et al. 2006, Laza-Martinez et al. 2007, Pinckney et al. 2009, Latasa et al. 2010, Wright et al. 2010, Kozlowski et al. 2011, Mendes et al. 2011, Seoane et al. 2011). However, to date there have been no prior comprehensive studies in the NGOM examining phytoplankton pigment variability in conjunction with the CHEMTAX program to derive phytoplankton community composition. The overall hypothesis of this study was that distinct differences exist between offshore and near shore phytoplankton populations with populations in regions of freshwater influence exhibiting larger temporal and spatial variability and lower diversity than the offshore populations.

Observations were made as part of the Gulf Carbon project, which provided for the comparison of pigment observations to physical data collected simultaneously during the course of five research cruises, four in 2009, January (winter), April (spring 2009), July (summer), October-November (fall) and one in March-2010 (spring 2010). This allowed for investigations of the relationship between the observed patterns of phytoplankton community composition and the regional hydrography and the overall ecology of this important coastal ecosystem.

Materials and Methods

Cruise and Sampling

Five research cruises were conducted in conjunction with the Gulf Carbon project, extensively sampling the continental margin of Northern Gulf of Mexico at approximately 50 locations (Fig. 1). The stations encompassed water types from freshwater -influenced by estuarine and inner shelves to oligotrophic slope waters. Water samples and vertical profiles of temperature (T) and salinity (S) were taken at each station using a rosette sampler equipped with 10-L Niskin bottles and a conductivity–temperature–depth (CTD) instrument profiler (SeaBird SBE911 plus). The instrument package was also equipped with a chlorophyll fluorometer (Chelsea Instruments) and beam transmissometer (Sea Tech, 20 cm, path length).

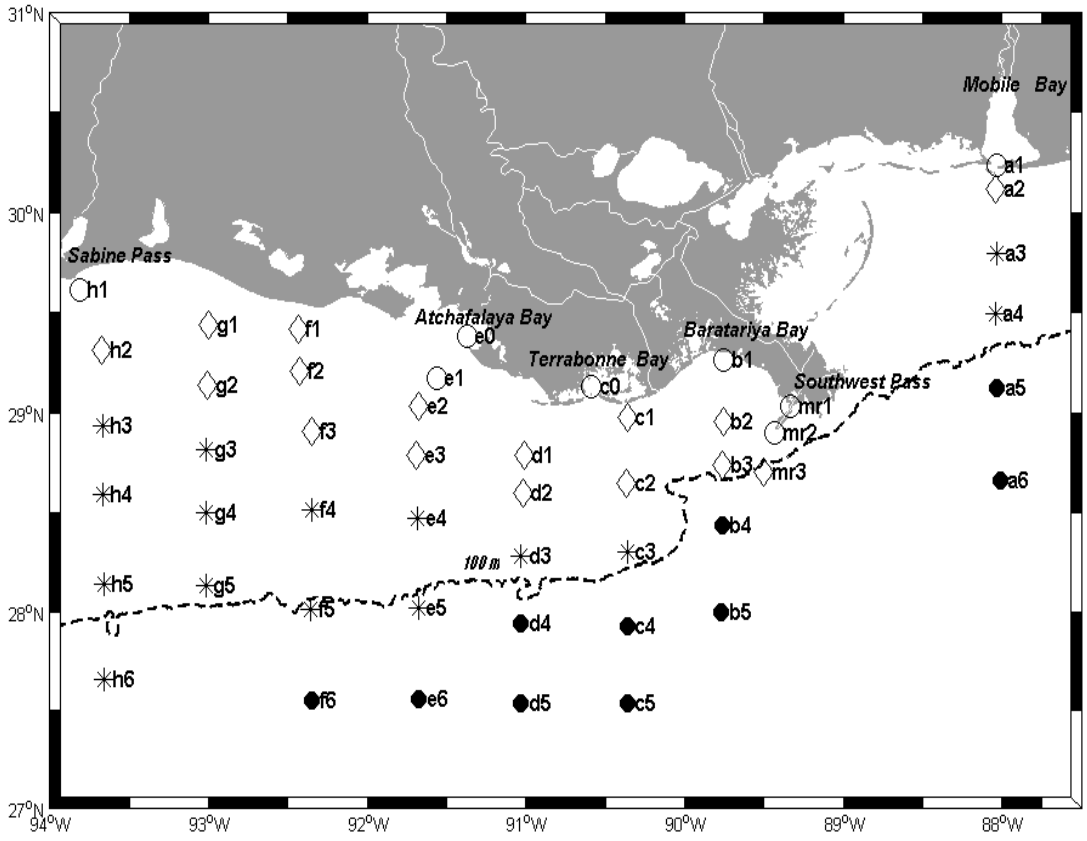

Figure 1. Study area and stations sampled during the Gulf Carbon cruises. The symbols denote the geographical locations of stations demarcating the different water types found in the area, estuaries (○), inner-shelf (◊), mid-shelf (*), and offshore/slope (●) waters.

At very shallow stations (<5m), particularly the estuarine end member stations, a bucket was often used to collect near surface samples. Sampling depths were selected by examining chlorophyll fluorescence profiles and water samples were taken from at least 3-4 depths in the upper 150 m for pigment analysis. Samples were also taken to determine nutrient concentrations at similar depths. At selected stations water samples from the surface, mixed layer and the CFM were taken to examine phytoplankton microscopically. All nutrient concentrations (NO_3-N, NO_2–N, NH_4 and SiO_3 and PHO_4) were measured using flourometric (N species) and spectrophotometric (PO_4 and SiO_3)

methods using an Astoria –Pacific A2+2 nutrient auto-analyzer (Method # A179, A027, A205 and A221; Astoria Pacific International, Oregon USA). In this study we defined dissolved inorganic nitrogen (DIN) as the sum of NO_3+NO_2; NH_4 was usually small for most samples. Samples were kept frozen (− 20 °C) for a few weeks until their analysis.

Statistics

To identify different water types, cluster analysis (using IBM SPSS software version 14) was performed on temperature (T), salinity (S), total chlorophyll *a* (TChl *a*) and bottom depth data. A standard Z scores transformation was performed on the data after which stations were clustered using the Ward's method and City-block distance type (Ward 1963). The results of cluster analysis are summarized in Table 1. To test for significant spatial and seasonal variations, a Kruskal-Wallis test was use with a critical significance value of $p<0.05$. Prior to all tests, normality of the dataset was determined using Shapiro-Wilk and Anderson-Darling tests in SPSS (version 14).

HPLC Pigment Analysis

Seawater samples for pigment analyses were immediately filtered (2-5 L volume) onto *Whatman* 47mm GF/F filters at low vacuum (<0.5 atm). The filters were blotted dry with a laboratory tissue, folded and place in 2 mL cryotubes, and immediately frozen in liquid nitrogen until analysis. Prior to extraction of the pigment samples, the filters were lyophilized (freeze dried) at -47 to -52 °C, 0.100 mbar for 12 h using a (Labconco FreeZone 6 system) to remove water from the filters. The lyophilized filters were immersed in 90% acetone (3 ml), vortexed, and the contents weighed prior to storing overnight at -19°C. The following morning the filters were again vortexed for 1 minute and reweighed to determine any weight loss due to evaporation. We found that there was generally negligible weight loss during the overnight storage. The acetone and filter

contents were transferred to a 5 cc glass syringe and the extracted pigments in acetone were filtered through a 13 mm diameter 0.2 μm PTFE HPLC syringe filter (Alltech, Catalog: 2164). The clarified extracts were collected in disposable microcentrifuge tubes (2 ml) and stored at -19°C until analysis (usually less than 8 hrs). Immediately prior to injection, a 50:50 mixture was prepared using 350 μL of sample extract and 350 μL tetrabutylammonium acetate (TBAA) adjusted to pH 6.5. The mixture A 500 μL injection loop was flushed and filled with the mixture and the contents then injected onto the column. The HPLC analysis was that of Van Heukelem and Thomas (2001) with minor modifications and used an Eclipse XDB C8, 4.6 mm_150 mm column (Agilent Technologies). The HPLC was calibrated using standards from DHI lab products, Denmark. For each sample, the Waters proprietary software package MaxPlot was used to acquire a chromatogram and peak amplitudes were detected as the maximum absorbance of each one second interval across the spectrum from 408 to 480. A threshold of greater than 0.0005 Absorbance Units (AU) was used for peak detection and integration. About 24 pigments were identified with confidence for this study. Co-elution issues of DVChlb and Chlb was not a major problem during the analysis phase, as a distinct shoulder separated the two peaks in the chromatograms and was further validated with library spectral match with pure pigments. The method was included in the recent NASA fifth SeaWiFS HPLC Analysis Round-Robin Experiment (SeaHARRE-5) and was found perform well relative to other methods for identification and quantification of pigments (Hooker et al. 2012, in press).

Quality Assurance (QA) of the Pigment Data

Improper pigment quantification, near the limit of detection (LOD) of pigments and their subsequent reporting in the dataset often leads to false positives and false negatives. This study used QA threshold procedures during processing of the pigment data as described in Hooker et al. (2005). Additionally, the relationship between total chlorophyll *a* (TChl *a*) and accessory pigments (AP) has been used (e.g., Aiken et al. 2004, 2009) as a means of quality control of the HPLC data. Here we have adapted the quality assurance criteria proposed by Aiken et al. (2009) as follows:

(1) The regression between TChl *a* = Σ (MVChla +DVChla) and AP = Σ Peri + 19'-But + Fuco + Viola + 19'Hex + Allo +DDx +DDt + Lut + Zea + Caro + Chlb + TChlc) should have a slope within the range 0.7–1.4 and $r^2 > 0.90$;

(2) For each sample the difference of TChl *a* and AP should be < 30% of the sum of TPig.. Regression analysis of the pigment data set for each Gulf Carbon cruise met the QA criteria, such that the linear relation between TChl *a* and AP had an intercept ranging from 0.011 to 0.02 (SE = 0.011, P<0.001), the slope was in the range of 0.85-0.98, and $r^2 > 0.90$ (Appendix A).

CHEMTAX Analysis

The relative abundance of microalgal groups contributing to total Chl *a* biomass was calculated from the HPLC-derived pigment concentration data using CHEMTAX version 1.95 (Mackey et al. 1996, Wright et al. 2009a). CHEMTAX applies a factor analysis and steepest-descent algorithm to find the best fit of the pigment data to an initial (pigment: Chl *a*) ratio matrix that is used to infer phytoplankton community composition. Initial ratios and relevant taxonomic groups for the analysis were based on previous

studies in the region (Dortch & Whitledge 1992, Redalje et al. 1994, Bode & Dortch 1996, Lohrenz et al. 1999, Chen et al. 2000, Jochem 2003, Qian et al. 2003, Wawrik et al. 2003, Dagg et al. 2004, Wawrik & Paul 2004, Wysocki et al. 2006) as well as a large number of prior studies (Gieskes & Kraay 1986, Jeffrey et al. 1997, Mackey et al. 1998, Schlüter et al. 2000, Schlüter & Møhlenberg 2003, Latasa et al. 2004, Veldhuis & Kraay 2004, Zapata et al. 2004, Rodríguez et al. 2005, Laza-Martinez et al. 2007, Seoane et al. 2009). A total of 11 algal groups were selected for CHEMTAX analysis in this study (Table 1), and were based on the HPLC pigment analyses and limited microscopic observations performed during the field campaigns. Haptophytes were divided into haptophyte-6 (Hapto-6) and haptophyte (Hapto-8) according to (Zapata et al. 2004).Prasinophyte was divided into two types, prasinopyte-I (pras-I) and prasinophytes-II (pras-II), based on Schlüter et al. (2006). Because of wide variations in phytoplankton community composition a hierarchical cluster analysis using SPSS v16 was performed on the ratios of accessory pigments (AP) to TChl *a* in order to organize data into pigment groups with similar characteristics. The pigments used for the analysis are listed in Table 1. The pigment clusters closely followed the water types.

Table 1

List of Major Pigments and Phytoplankton Groups Studied

Abbreviations	Description	Formula	Taxonomic group
Chl *a*	Chlorophyll-a	Chl *a*= Σ (Chla+Chla-epimer+Chla-allomer)	Represents biomass in this study
DVChla	Divinyl Chlorophyll-a		Prochlorophytes
TChl *a*	Total Chlorophyll-a	TChl *a*=Σ(Chla+DVChla+Chllide-a)	Universal
Chlb	Chlorophyll-b		Green algae
DVChlb	Divinyl Chlorophyll-b		Prochlorophytes
$Chlc_2$	Chlorophyll-c_2		multiple
$Chlc_3$	Chlorophyll-c_3		Haptophytes , diatoms
Allo	Alloxanthin		Cryptophytes
19′-But	19'-Butanoyloxyfucoxanthin		Pelagophytes
19′-Hex	19'-Hexanoyloxyfucoxanthin		Haptophytes
DDx	Diadinoxanthin		Diatoms, haptophytes, pelagophytes
Fuc	Fucoxanthin		Diatoms
Lut	Lutein		Green algae
Neo	Neoxanthin		Green algae
Viola	Violaxanthin		Green algae
Per	Peridinin		Dianoflagellates
Pras	Prasinoxanthin		Prasinophytes
Zea	Zeaxanthin		Cyaobacteria & prochlorophytes

Pigment ratios in a given phytoplankton class are subject to changes depending on the availability of the light field (Demers et al. 1991), variations in species composition even within the same class (Gieskes & Kraay 1986), and with depth in the water column (Mackey et al. 1996). To address these issues, a separate cluster analysis (See Appendix C) was applied to the subsurface data which grouped the shelf data into two subgroups

the subsurface (<50m) and bottom waters, the offshore data got partitioned into two depth bins, 50-100m (corresponding to the depth range of maximum chlorophyll) and > 100m. After carefully reviewing the clusters and the pigment ratios, three separate initial input matrices were developed and used for CHEMTAX analysis of different subsets of data that included (1) estuarine-inner shelf and mid-shelf region (2) offshore surface slope waters and (3) deep slope waters.

CHEMTAX Optimization

Optimization of the input ratio matrix was achieved through the construction of a series of 60 different ratio matrices by multiplying each ratio of the initial matrix by a random function as described in Wright et al. (2009a). The average of the best six output results (i.e. 10%, n=6 with smallest residual root mean square) was then run repeatedly in CHEMTAX until a stable ratio matrix was obtained (Latasa 2007). Final pigment ratio matrices were derived for each category using CHEMTAX (Table 3). Each subset (identified through cluster analysis of the pigment data) was processed separately through CHEMTAX.

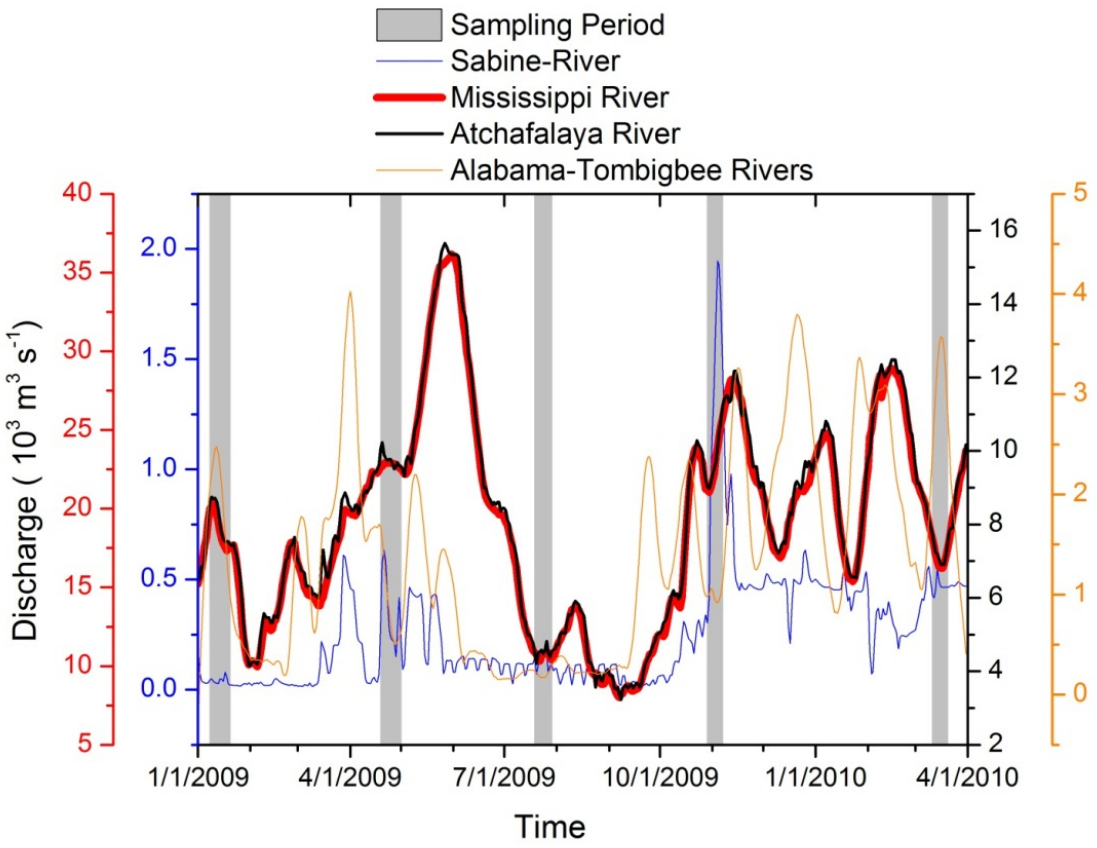

Figure 2. Mean daily discharge of the important rivers in the region from January 2009 to March 2010. The Discharge (10^3 m^3/s) reported on the Y axis, data for Mississippi and Atchafalaya rivers were obtained from US Army Corps of Engineers (http://www.mvn.usace.army.mil/eng/edhd/wcontrol/discharge.asp) and the rest of the data for Sabine, Alabama and Tombigbee were obtained from USGS database (http://waterdata.usgs.gov/nwis/qw). The discharge data for Alabama and Tombigbee was filtered using a Savitsky–Golay second-order polynomial filter with an 18 point of window. Discharge from Alabama and Tombigbee rivers were combined to get the total outflow from Mobile bay. The shaded bars represents the sampling period for each of the five cruises from January 2009 to March 2010.

Table 2

Output Ratios from CHEMTAX for the Three Different Datasets Analyzed.

	Chlc3	Chlc2	Per	19But	Fuco	Neo	Pras	Viola	19Hex	Ddx	Allo	Zea	Lut	chlb
Dinoflagellates														
Estiarine-	-	-		-	-	-	-	-	-	-	-	-	-	-
Innershelf-														
Midshelf			0.8759											
Slope	-	-	0.937	-	-	-	-	-	-	-	-	-	-	-
Deep	-	-	0.674	-	-	-	-	-	-	-	-	-	-	-
Diatoms														
Estiarine-														
Innershelf-	-	0.1522	-	-	0.5356	-	-	-	-	0.102	-	-	-	-
Midshelf														
Slope	-	0.103	-	-	0.413	-	-	-	-	0.0665	-	-	-	-
Deep	-	0.301	-	-	0.801	-	-	-	-	0.1715	-	-	-	-
Chlorophytes														
Estiarine-														
Innershelf-	-	-	-	-	-	0.054	-	0.028	-	-	-	0.0586	0.1859	0.1783
Midshelf														

Table 2 (continued)

	Chlc3	Chlc2	Per	19But	Fuco	Neo	Pras	Viola	19Hex	Ddx	Allo	Zea	Lut	chlb
Cryptophytes														
Estiarine-Innershelf-Midshelf	-	0.0385	-	-	-	-	-	-	-	-	0.2726	-	-	-
Slope	-	0.1105	-	-	-	-	-	-	-	-	0.1915	-	-	-
Deep	-	0.1105	-	-	-	-	-	-	-	-	0.1915	-	-	-
Prasinophyte-I														
Estiarine-Innershelf-Midshelf	-	-	-	-	-	0.055	0.285	0.034	-	-	-	0.0329	0.0059	0.6738
Slope	-	-	-	-	-	0.0417	0.1308	0.083	-	-	-	0.04	-	0.8057
Deep	-	-	-	-	-	0.055	0.1869	0.052	-	-	-	0.02	-	1.014
PrasinophyteII														
Estiarine-Inner-shelf	-	-	-	-	-	0.037	-	0.071	-	-	-	0.0262	0.079	0.7664

Table 2 (continued)

	Chlc3	Chlc2	Per	19But	Fuco	Neo	Pras	Viola	19Hex	Ddx	Allo	Zea	Lut	chlb
Haptophyte-6														
Estiarine-Innershelf-Midshelf	0.1755	0.1876	-	0.007	0.0193	-	-	-	0.78	-	-	-	-	-
Slope	0.1854	0.1826	-	0.0068	0.117		-	-	0.806	-	-	-	-	-
Deep	0.2704	0.244	-	0.007	0.283	-	-	-	1.126	-	-	-	-	-
Haptophyte-8														
Estiarine-Innershelf-Midshelf	0.2702	0.1146		0.204	0.1087	-	-	-	0.261	-	-	-	-	-
Slope	0.1958	0.988		0.189	0.885	-	-	-	0.383	-	-	-	-	-
Deep	0.208	0.114		0.1776	0.098	-	-	-	-	-	-	-	-	-
Pelagophyte														
Midshelf -Slope	0.1963	0.0934	-	0.8651	0.6743	-	-	-	-	0.279	-	-	-	-
Deep	0.66	0.2437	-	0.989	0.1	-	-	-	-	-	-	-	-	-

Table 2 (continued)

	Chlc3	Chlc2	Per	19But	Fuco	Neo	Pras	Viola	19Hex	Ddx	Allo	Zea	DVChlb	Chlb	DVChla
Cyanobacteria															
Estiarine-Innershelf-Midshelf															
	-	-	-	-	-	-	-	-	-	-	-	0.505	-	-	-
Slope	-	-	-	-	-	-	-	-	-	-	-	0.607	-	-	-
Deep	-	-	-	-	-	-	-	-	-	-	-	0.454	-	-	-
Prochlorophyte															
Slope	-	-	-	-	-	-	-	-	-	-	-	0.4793	0.5597	-	1
Deep	-	-	-	-	-	-	-	-	-	-	-	0.242	1.02	-	1

Results

Hydrography

Based on a cluster analysis of T-S, TChl *a* and bathymetry observations, four distinct water types were identified, including (1) estuarine, (2) inner-shelf, (3) mid-shelf, and (4) slope or open ocean. Differences among cruises were observed in the physico-chemical variables of each of the water types (Table 3). The water column was generally found to be homogeneous during January and April of 2009 (Fig. 3) for majority of the inner-shelf stations. Temperatures were highest during July 2009, while lowest values were observed during March 2010 (Table 3). A prominent seasonal cycle was evident in the NGOM (Fig. 3). Water columns were strongly stratified in summer, weakly stratified in fall, and were in transitional phase during the spring 2009 (April-May 2009). Highly stratified conditions were observed at inner-shelf stations during the July 2009, with low salinity layer overlying high salinity subsurface waters (Fig. 3b). In contrast, the water column was completely mixed during winter. Average surface salinity at the shelf slope was > 35, an offshore extension of the MS river plume was observed during the July 2009, a low salinity pool of (mean ± SD 28.9 ± 1.31) occupied several south central slope stations with below average (30.9 ± 3.31) salinity at slope waters during that period (Fig. 3f, inset). Such a feature has been reported in several previous studies (Chen et al. 2000, Walker et al. 2005).

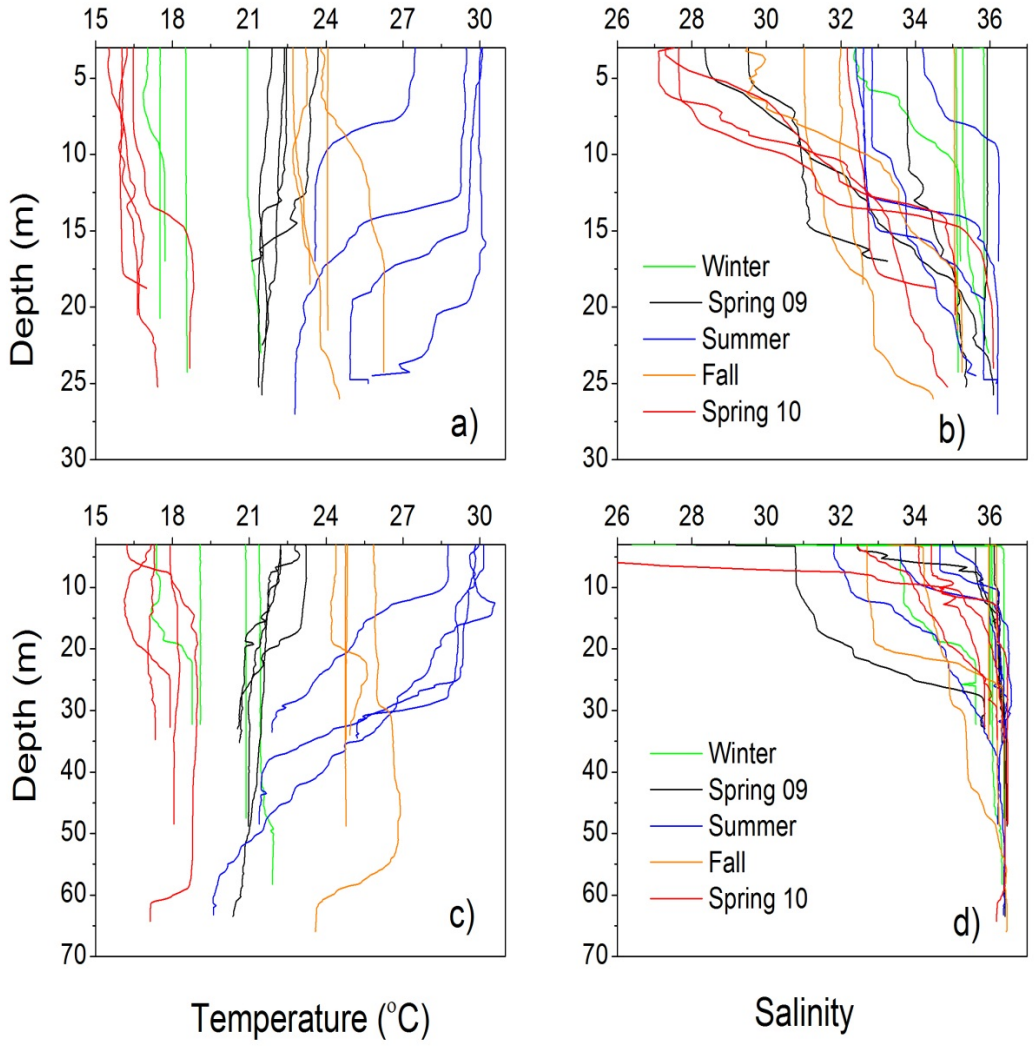

Figure 3. Seasonal variations in Temperature and Salinity profiles at selected stations for inner shelves and estuarine waters (a & b), mid-shelf (c & d) and slope (e & f).

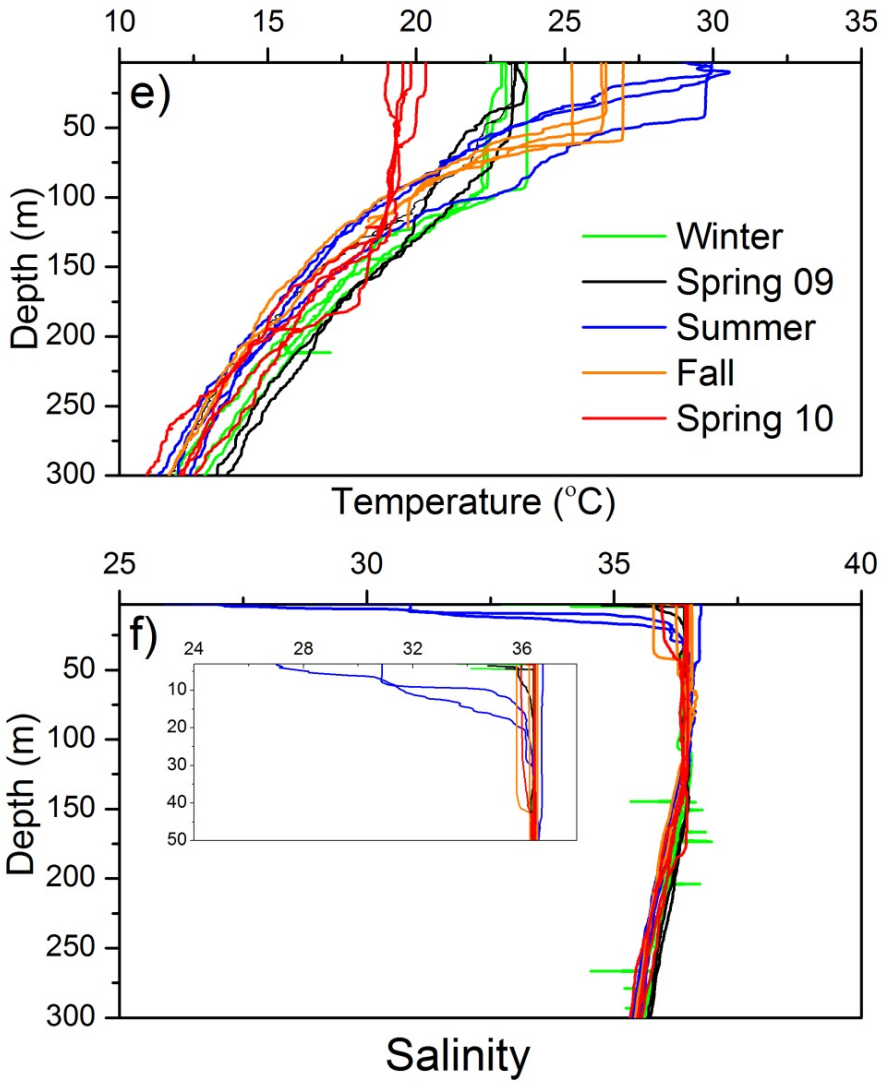

Figure 3. Seasonal variations in Temperature and Salinity profiles at selected stations for inner shelves and estuarine waters (a & b), mid-shelf (c & d) and slope (e & f).

Table. 3

Summary of Regional Physico-Chemical Variables. Means of Each Variable is presented, their Ranges are in Parentheses.

Region	Jan 2009	Apr 2009	Jul 2009	Nov 2009	Mar 2010
		Temperature (˚C)			
Estuarine	13.9 (7.9-19.26)	20.6 (15.2-23.2)	29.2 (28.5-30.3)	16.9 (16.7-17.2)	12.1 (10.5-13.2)
Inner-Shelf	18 (15.2-20.9)	22.5 (22.3-32.6)	29.2 (27.4-30.8)	22.2 (19.8-24.6)	16.5 (15.2-18)
Mid-Shelf	21.3 (19.9-23)	22.6 (20.6-24.7)	29.9 (29.4-30.8)	24.9 (23.3-26.4)	17.8 (15.6-20)
Slope	22.8 (22.3-23.7)	23.1 (22.5-23.5)	29.5 (29.1-30.8)	26 (25.2-27.4)	19.3 (18.4-20.3)
		Salinity			
Estuarine	20.3 (0.2-25.6)	14.9 (0.2-25.9)	13.7 (0.35-28.7)	0.12 (0.08-0.15)	4.2 (0.3-11.6)
Inner-Shelf	33 (26-36)	28.7 (22.3-32.6)	31.9 (27.9-35.7)	25.6 (13.5-33)	25.2 (20-29.2)
Mid-Shelf	36.2 (35.5-36.5)	35.9 (33.8-36.5)	34.7 (30.8-36.8)	35 (31.9-36.6)	33.2 (27.3-36.5)
Slope	36.4 (36.4-36.5)	36.3 (35.7-36.7)	30.9 (27.3-36.7)	35.3 (32.6-36.6)	35.6 (33-2-36.5)
		Chlorophyll *a* (mg m^{-3})			
Estuarine	8.5 (0.4-17.2)	19.5 (4-42.4)	16.5 (1-41)	2.2 (1.4-3)	6.4 (4.4-9)
Inner-Shelf	2.1 (0.4-4.9)	5.5 (0.7-16)	2.2 (0.3-8.8)	5.3 (1.2-13.07)	10.4 (5-22.3)
Mid-Shelf	0.5 (0.1-1)	0.22 (0.04-0.5)	0.4 (0.1-1.3)	0.7 (0.13-2.3)	1.68 (0.3-3.4)
Slope	0.3 (0.1-0.5)	0.15 (0.06-0.27)	0.4 (0.2-1.1)	0.22 (0.13-0.57)	1.58 (0.5-3.8)

Table .3 (continued)

Region	Jan 2009	Apr 2009	Jul 2009	Nov 2009	Mar 2010
		DIN(µM)			
Estuarine	19.6 (0.13-52)	31.6 (0.2-61.4)	49 (0.7-74.3)	36.9 (18.9-54.8)	66.7 (37.3-93)
Inner-Shelf	1.6 (0.12-9)	8.9 (0.25-61.3)	0.73 (0.66-0.8)	4.5 (0.1-22.45)	6.27 (0.2-19)
Mid-Shelf	0.4 (0.1-0.7)	0.25 (0.17-0.3)	0.72 (0.6-0.9)	0.2 (0.04-1.7)	1.8 (0.27-5.9)
Slope	0.2 (0.06-0.35)	0.3 (0.19-0.6)	0.72 (0.67-0.8)	0.08 (0.04-0.15)	1.33 (0.4-2.3)
		Phosphate (µM)			
Estuarine	0.55 (0.09-1.9)	0.95 (0.4-2)	1.9 (0.2-3.66)	2.2 (1.58-2.9)	1.6 (1-1.9)
Inner-Shelf	0.56 (0.95-1.92)	0.61 (0.14-2)	0.1 (0.02-0.27)	0.5 (0.1-1.55)	0.19 (0.1-0.5)
Mid-Shelf	0.28 (0.05-0.4)	1.03 (0.11-1.35)	0.1 (0.02-0.25)	0.08 (0.03-0.2)	0.16 (0.09-0.3)
Slope	0.26 (0.02-0.4)	0.18 (0.03-1.13)	0.1 (0.02-0.25)	0.07 (0.04-0.1)	0.13 (0.01-0.2)
		Silicate (µM)			
Estuarine	36 (1.37-109.9)	47.2 (10.7-101.2)	78.5 (30.5-131.5)	117.2 (113-121)	86.8 (75-109.5)
Inner-Shelf	3.2 (0.13-11.6)	9.65 (0.27-68.6)	6.17 (0.7-14.4)	21 (1.3-63.9)	15.6 (1.8-36)
Mid-Shelf	1.34 (0.8-2)	1.05 (0.38-1.7)	1.5 (0.5-3)	2.6 (1.3-5.2)	2.5 (0.25-11.6)
Slope	1.12 (0.6-1.7)	0.92 (0.6-1.2)	1.3 (0.6-2.2)	1.3 (0.7-1.6)	0.9 (0.17-2.34)

Seasonal and Spatial Patterns in Phytoplankton Biomass

Distinct temporal and spatial patterns in phytoplankton biomass were evident in phytoplankton biomass across the continental margin of the NGOM (Fig. 4a). At the inner shelf stations, large seasonal variations in Chl *a* concentrations were observed, ranging from 0.3-22.3 mg m^{-3} with highest values during spring 2010 and lowest during the winter 2009. Overall, average Chl *a* for all the shallow inner-shelf (≤ 25 m) stations were slightly higher during the March 2010 than April 2009 (Table 3). Bottom waters on the inner-shelf also showed high biomass levels, Chl *a* ranged from (0.12- 14.66 mg m^{-3}) with the greatest during the summer while lowest values (0.9 ± 1.3 mg m^{-3}) were recorded during winter. High biomass levels (>7.5 mg m^{-3}) were generally associated with the stations at the mouths of the inland bays (see locations in Fig.1) including Barataria Bay (41 mg m^{-3} of Chl *a*, summer), Terrebonne Bay (42.3 mg m^{-3} Chl *a*, spring 2009), Mobile Bay (12.5 mg m^{-3} of Chl *a* ,during Fall) and at the outlet of Sabine estuary (13.1 mg m^{-3} of Chl *a*, during winter). In contrast, stations at the mouth of the Mississippi (MR1) and Atchafalaya (E0) in the NGOM (Fig. 1). Average Chl *a* concentrations at those stations were 3.2 ± 2.1 and 5.3 ± 3.1 mg m^{-3}, respectively.

Intermediate levels of Chl *a* were observed at mid-shelf (Fig. 4c) with surface values ranging from ~0.04-3.4 mg m^{-3}. Highest concentrations were observed during March 2010 and lowest values during April 2009. A subsurface maximum was evident at ~ 50% of the stations on the mid-shelf during July 2009, while more than 60% of the stations in April 2009 were characterized by higher biomass level (Chl *a* ≥ 0.84 ≤ 2 mg m^{-3}) in bottom waters relative to surface (0.28 ± 0.17 mg m^{-3}). At other times of the year, the water column was generally mixed with relatively low biomass levels (mean ~ 0.46

mg m^{-3}) in bottom waters during the winter (January 2009), March 2010 and fall (November 2009).

Average surface Chl *a* values in slope waters ranged 30-75 % lower than the shelf stations**.** Prior studies have reported higher Chl *a* levels in offshore Gulf of Mexico water during winter (December-February) than in summer (August-September) (Muller-Karger et al. 1991, Jolliff et al. 2008, Martínez-López & Zavala-Hidalgo 2009). Results from this study (Fig. 4e) were generally consistent with this pattern, with some exceptions. Highest Chl *a* concentrations among the offshore stations were observed during March 2010 (Fig. 4e & 4f), with values ranging from 0.25-1.28 mg m^{-3}. This range extended beyond previously reported climatological means (range 0.2-0.6 mg m^{-3}, (Muller-Karger et al. 1991, Martínez-López & Zavala-Hidalgo 2009)) for the winter period (generally high Chl *a* levels) in the offshore NGOM. On another (summer-July 2009) occasion, high Chl *a* levels were observed at several slope stations including a5, a6, b4, b5, c4 (Fig. 1 & 4f). Chl *a* at those stations ranged from 0.35-1.1 mg m^{-3} during summer, due to an offshore extension of the MS river plume onto the continental shelf. Reversal of wind and current patterns during summer (Walker et al. 2005, Schiller et al. 2011) often leads to extension of low salinity tongues ($S < 30$) of the MS river rich in nutrients and high in Chl *a* in the offshore direction to the south and southeast of the MS river delta.

The presence of a subsurface CFM was a regular feature at the slope stations, particularly during spring and summer. The CFM was observed during fall, but was not as strong as in spring and summer (Fig. 4f, inset). Interestingly no CFM was evident during March 2010 and highest chlorophyll fluorescence values were located in the upper 50 meters of the water column (Fig. 4f, inset). The water column was well mixed (Fig. 3e

& 3f) during March 2010, a period when prevailing winds were northerly (from north) and upwelling favorable (not shown, Huang et al. in prep) conditions were conducive to upward flux of excess nutrients from deep waters. HPLC-derived Chl *a* levels determined from samples collected within the CFM were highest during summer, ranging from 0.08-3.1 mg m^{-3} (mean Chl *a* 0.76 ± 0.95 mg m^{-3}), and were lowest during winter (mean Chl *a* 0.26 ± 0.12 mg m^{-3}). Similar levels were observed during April and November 2009 (mean Chl a ~ 0.36 mg m^{-3}) within the CFM. On average, Chl *a* values in samples collected at the CFM feature were about 3-8 times higher than the surface.

Pigment Composition and CHEMTAX Analysis

Phytoplankton marker pigments and community distributions were closely associated with the earlier defined hydrographic regions. A separate cluster analysis of the marker pigments: Chl *a* ratios similarly differentiated the dataset into different compositional provinces similar to those found for the hydrographic data. These included the following: i) estuarine and inner shelf, ii) the mid-shelf and iii) the shelf-slope boundary communities. Characteristics of pigment and phytoplankton taxonomic composition were examined for each of the compositional provinces distinguished from the cluster analysis in the next few sections.

Estuarine and inner-shelf communities. From the CHEMTAX output showing the proportion of TChl *a* associated with different taxa (Fig. 5a), it was evident that diatoms were consistently the dominant group, accounting for ~ 30 - 40 % of biomass in summer and fall (July, November 2009)

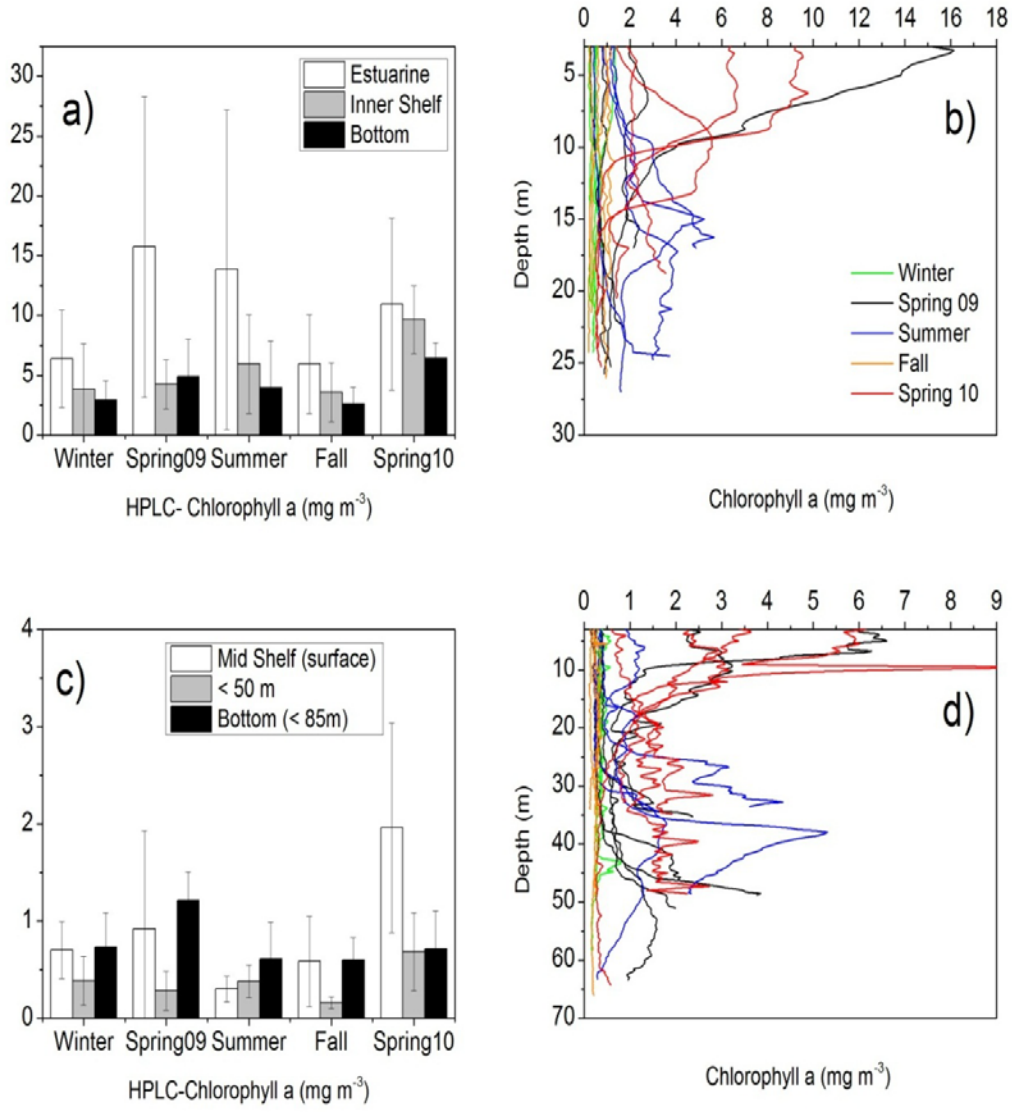

Figure 4. Seasonal distribution of biomass, the bars (mean and standard deviations) of HPLC derived Chlorophyll a (mg m^{-3}) for each water type, estuarine and inner-shelf (a), midshelf (c) and slope (e) and selected vertical profiles of Chlorophyll fluorescence from CTD for each water types estuarine and inner-shelf (b), mid-shelf (d) and slope (f).

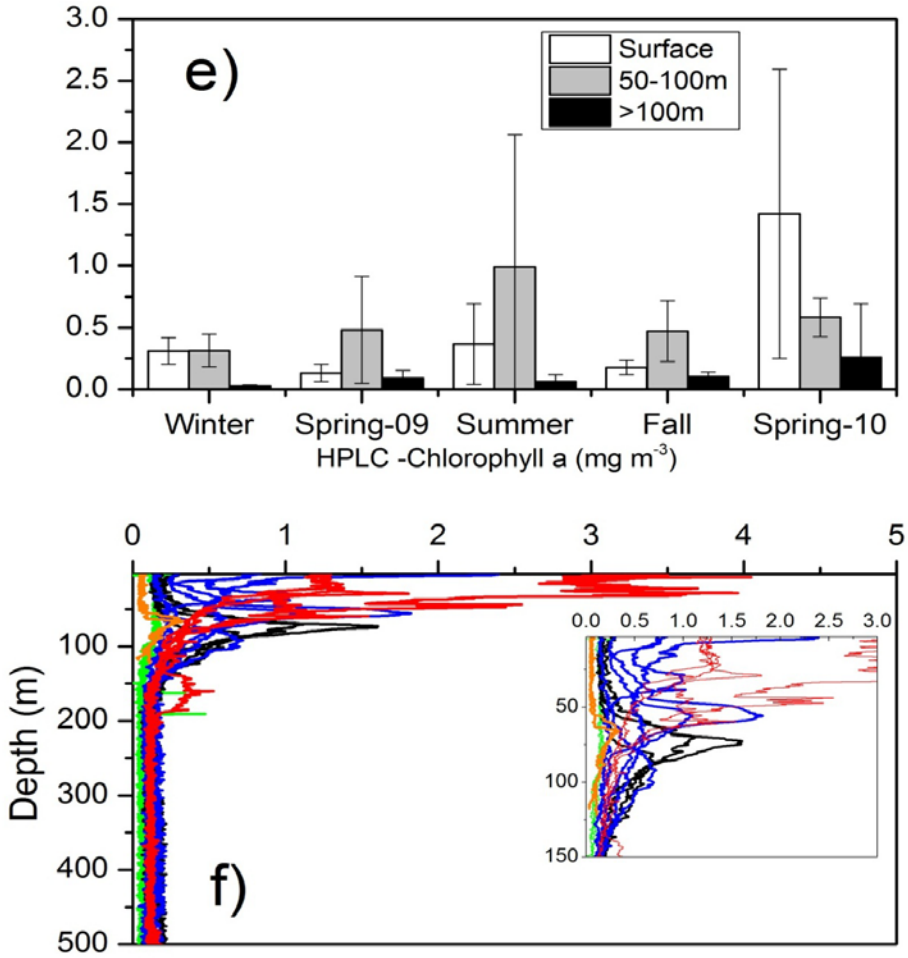

Figure 4. Seasonal distribution of biomass, the bars (mean and standard deviations) of HPLC derived Chlorophyll a (mg m^{-3}) for each water type, estuarine and inner-shelf (a), midshelf (c) and slope (e) and selected vertical profiles of Chlorophyll fluorescence from CTD for each water types estuarine and inner-shelf (b), mid-shelf (d) and slope (f).

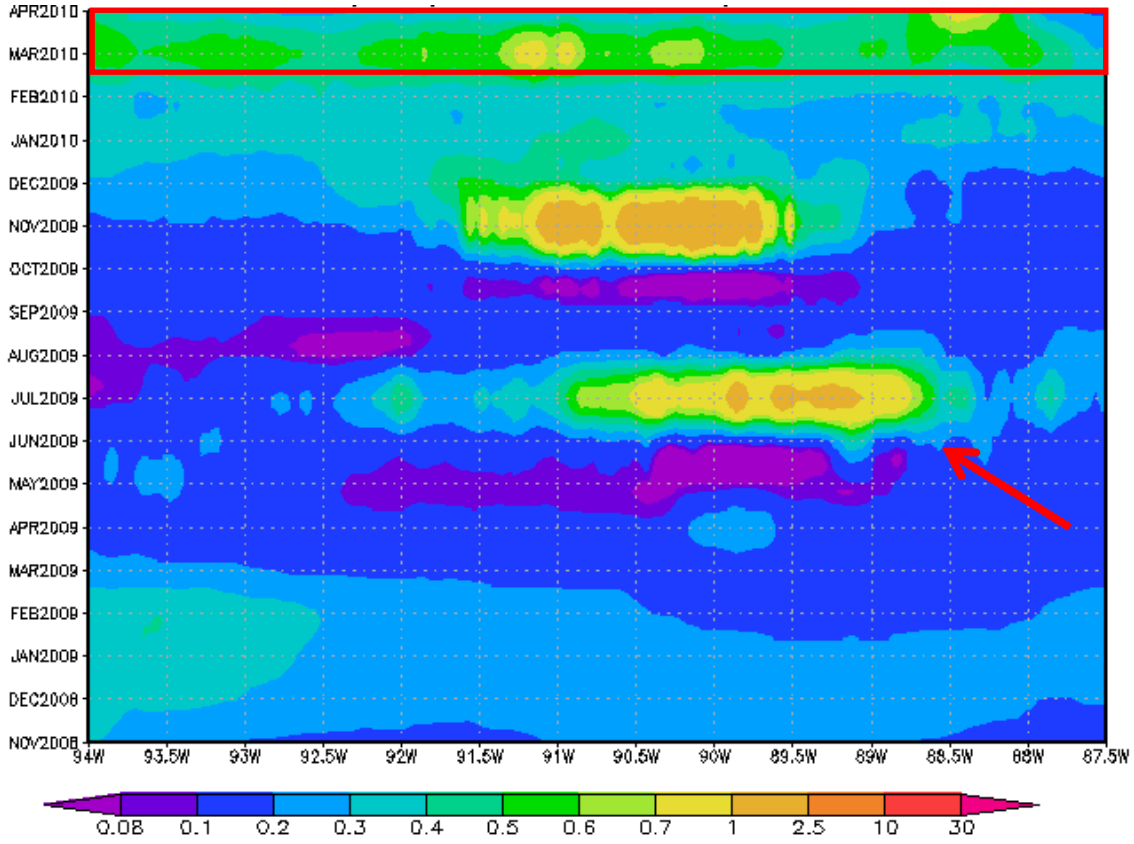

Figure 5. Hovmöller diagram showing the distribution of Chl *a* on the slope water (Lat 28N -27N, Lon- 94 W-87.5W) of the NGOM derived from GIOVANNI MODIS –Aqua at 4Km (November 2008-April-2010). Image produced with the Giovanni online data system, developed and maintained by the NASA GES DISC. The summer (July2009) high is due to the offshore extension of the Mississippi river plume (red arrow). Elevated Chl *a* levels observed during March 2010 (red rectangle) was due to higher river discharge (see Fig 2.2). No cruise was conducted during the observed November-December high.

to ~ 65 -70 % in winter and spring (January, April 2009; March 2010) in the estuary and the inner-shelf provinces respectively. Fucoxanthin (Fuco), a carotenoid characteristic of diatoms, was the dominant accessory pigment ranging from 1.8-5 mg m^{-3} in the region. Cryptophytes (marker alloxanthin) and chlorophytes (Chlb) on average accounted for 20±5% and 7 ± 6% respectively of TChl *a* (Fig. 6a). The chlorophyte fraction of TChl *a* was significantly (ANOVA, $p < 0.05$) higher within the estuaries compared to inner and

mid shelves. Cryptophytes and chlorophytes increased to 25 ± 7% and 10 ± 0.1 % respectively during periods of stratification (summer and fall) when contribution from diatoms dropped (Fig. 6a). Relative contributions of cyanobacteria increased significantly (ANOVA, $p < 0.05$) during the summer (July 2009), occupying ~ 35% of the total biomass, while their contribution was low for other periods, ranged between 3-7 % of the total biomass (Fig. 6a). Dinoflagellates, prasinophytes, and haptophytes (Hapto) were of lesser importance, ranged from 0.1- 5 %. A notable exception was in March 2010, when dinoflagellates contributed nearly 15 % to the total biomass (Fig. 6a). Pelagophytes and prochlorophytes were absent within the estuarine and inner-shelf regions and neither 19´-But nor any divinyl (DV) forms of Chl *a* and Chlb were detected by the pigment analysis.

Mid-Shelf communities. Mid-shelf region was characterized by the most diverse and complex phytoplankton distributions in this study. Diatoms were the dominant algal group during January 2009 and March 2010, contributing 45% and 64% respectively to the total biomass. During March 2010, water column was well mixed (Fig. 3c & 3d) and highest levels of Fuco concentrations were observed (0.29 - 0.91 mg m^{-3}). The cruise sampling followed a period of high river discharge (Fig. 2). The January 2009 cruise also coincided with a smaller discharge peak (Fig. 2) and similar elevated levels of Fuco (0.09-0.27 mg m^{-3}) were observed. Fuco concentrations during winter (January 2009) and March 2010 were about 2-7 times higher than at other times of the year. Cyanobacteria dominated during summer, contributing ~ 50% of total biomass. Zea was the dominant pigment (high Zea : TChl *a*, Fig. 7b) for the mid-shelf region during summer, an observation consistent with that of previous studies (Redalje et al. 1994, Chen et al. 2000) in the region. Seasonal fluctuations were observed in the abundance of the two Hapto

groups, with Hapto-6 (16 % of total biomass) relatively important during the stratified period (July 2009) while Hapto-8 (~ 18% of total biomass) was relatively more abundant during the mixed period (January 2009). Cyanobacteria (22%) and prochlorophytes (17%) were the major groups observed in the partially stratified conditions during fall (Fig. 3c & 3d). DVChla and minor amounts of DVChlb, an indication of the presence of prochlorophytes, were evident during the November 2009 (Fig. 7a & 7b) but were absent in March 2010. Average contributions from cryptophytes, chlorophytes, dinoflagellates, prasinophytes and pelagophytes were small; they ranged between 2-4 % of the total biomass. Diatoms (16-65 %) along with haptophyte-8 (10-30%) dominated the biomass in the subsurface (<50 m) and bottom waters with varying contributions from prasinophyte-I (7-20%) and cyanobacteria (0-23%).

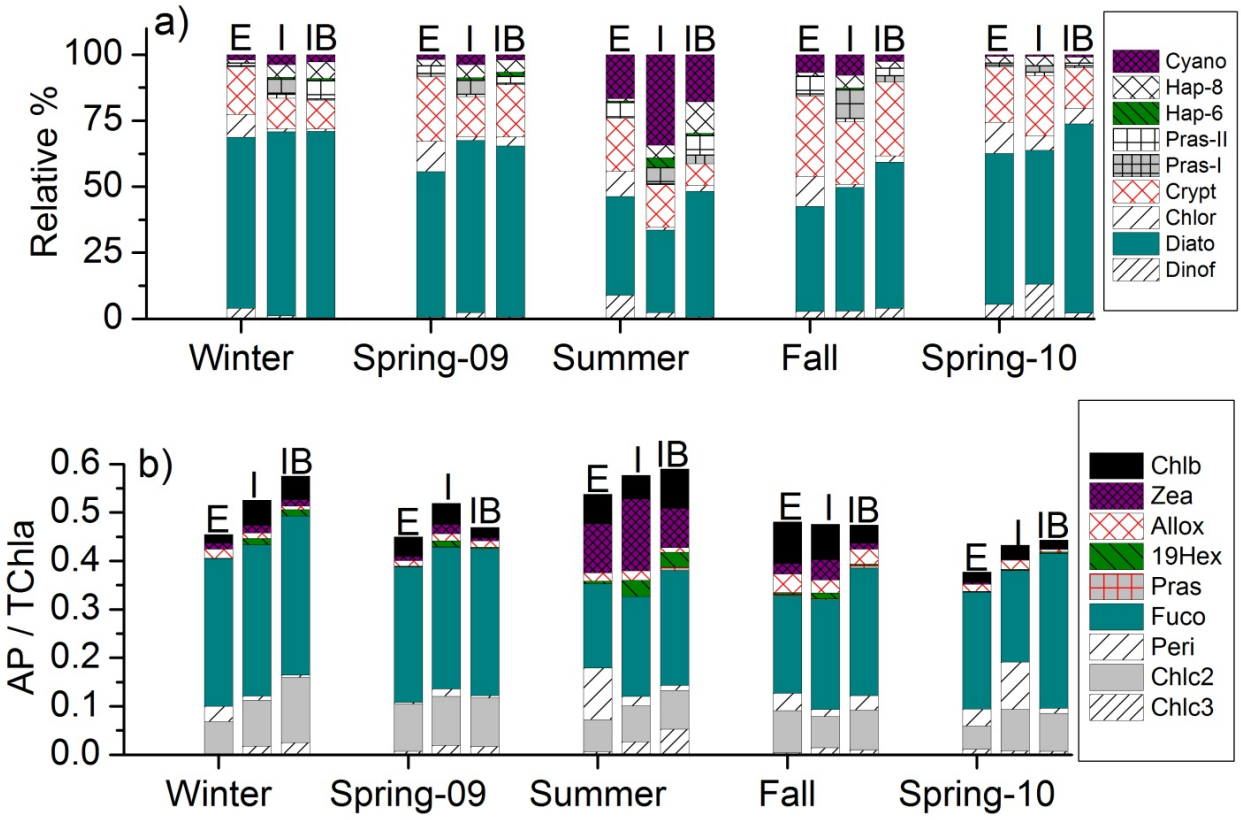

Figure 6. Distribution of major phytoplankton groups at the estuarine and inner shelf as calculated by CHEMTAX (a); accessory pigment:TChl *a* ratios (b); the letters E, I, and IB at the top of each stacked bars in (a) and (b) represents the estuarine surface, inner shelf surface and inner shelf bottom (~25m).

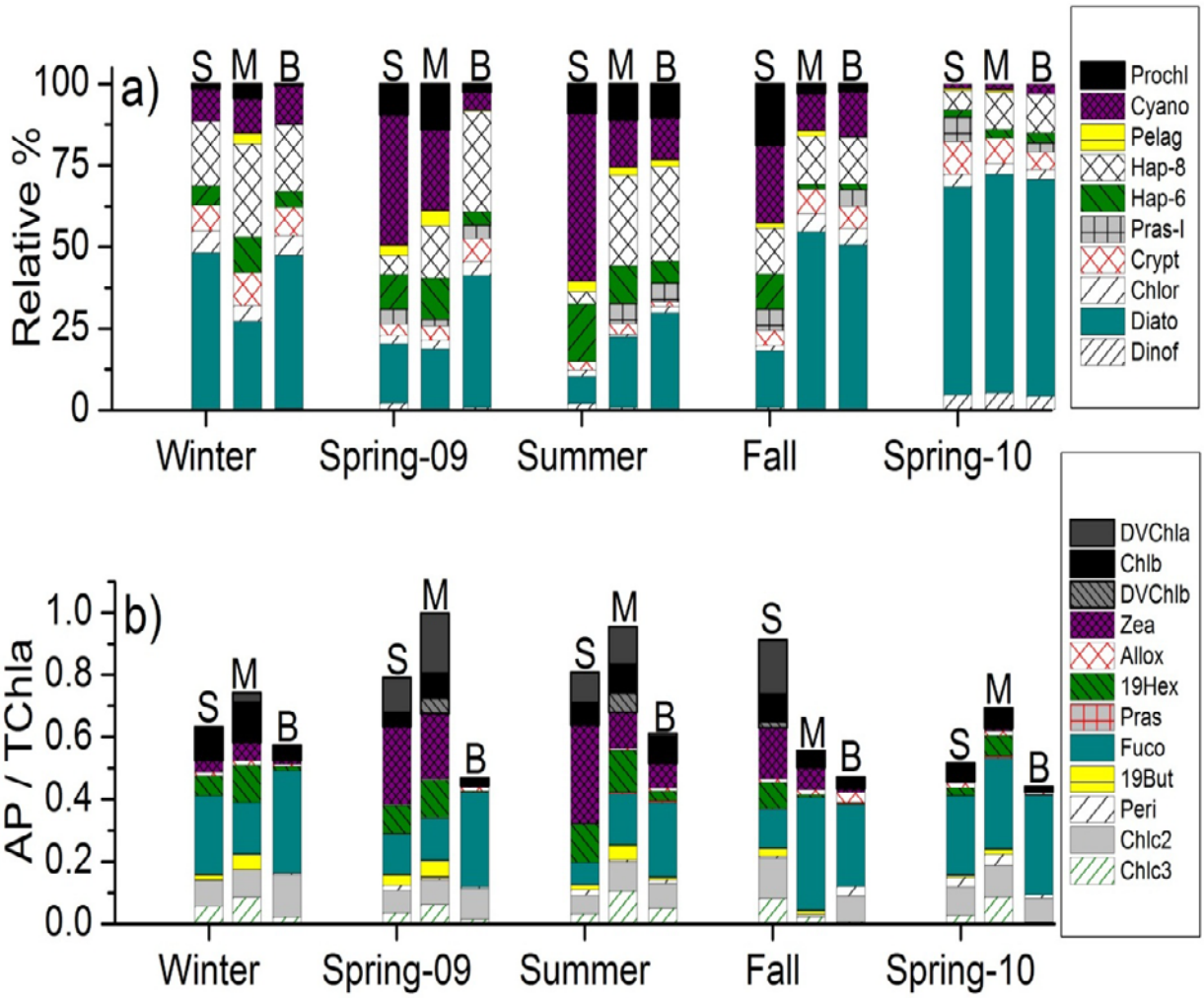

Figure 7. Distribution of major phytoplankton groups at the midshelf as calculated by CHEMTAX (a); change in accessory pigments : TChl *a* ratios (b); the letters S, M, and D at the top of each stacked bars in (a) and (b) represents the surface, mid depths and bottom (<75m)

Slope community. Cyanobacteria dominated (mean contribution, 45.7 ± 4.5 %) the surface slope community for the April, July and November 2009 (Fig. 8a). Pigments Zea along with DVChla were the major pigments in surface slope waters (Fig. 8b), DVChlb was present occasionally indicating an abundance of prochlorophytes and overall dominance of pico sized phytoplankton. A difference in community composition was observed during March 2010 when the predominantly picoplankton (cyanobacteria and prochlorophytes) community was replaced by an assemblage micro- (diatoms) and nanophytoplankton (dinoflagellates, cryptophytes and some haptophytes). Cyanobacterial contribution was minimal (mean 5.1 ± 6.1 % of the TChl *a*) and prochlorophytes were undetectable during March 2010. Prochlorophytes were highest (~32% to the total biomass) during fall (November 2009).

Influence of an offshore extension of MS plume water on phytoplankton distribution was evident during summer 2009. Diatoms dominated (~ 58%) at several offshore stations (a5, a6, b4, b5, c4, Fig. 1) where low salinity (< 31) and high Chl *a* waters (Fig. 5) were observed in comparison to the non-plume impacted stations where the diatoms contribution averaged ~4% (Table 4) Fuco concentrations at plume impacted stations were about 30 times greater than the non-plume impacted slope stations (Table 4), these findings were comparable to those of Wawrik and Paul (2004).

Haptophytes-6 was also an important group in oceanic waters, on average contributing ~ 19 ± 8 % to the total biomass. The total contribution by haptophytes (Hapto-6 and Hapto-8) in the slope region for this study was 25 ± 9 % , which was much less than previous reports of 40-60 % by (Qian et al. 2003) for NEGOM.

Table 4

Differences between Plume Impacted and Non-plume Impacted Stations

Station	Salinity	Chl *a* mg m^{-3}	Fuco mg m^{-3}	Zea mg m^{-3}	Diatom %	Cyanobacteria %
Plume	28.9±1.3	0.23±0.18	0.153±0.12	0.041±0.01	58.9±21.4	23.4 ± 14.4
Non-plume	34.9±1.7	0.125±0.0	0.005±0.00	0.057±0.04	4.2±4.7	56.3 ± 8.9

The presence of a CFM was common feature at slope stations (Fig. 3f, inset). Prochlorophytes, haptophytes and pelagophytes accounted for the majority of biomass at CFM. The largest contributions were from Prochlorophytes (Fig. 8a), contributing between18-59 % at the CFM and 33-63% at greater depths (100-120m). In general, DVChla and DVChlb levels increased with depth and the ratio of DVChlb: DVChla ratios increased from the surface (range 0.1-0.2) to that at or below the CFM (range 1-4.5). These results support the existence of different ecotypes acclimated to high or low light conditions. Depth differentiation among different light-acclimated ecotypes of prochlorophytes have been reported for various parts of the world ocean (Goericke & Repeta 1993, Moore et al. 1995, Moore & Chisholm 1999a, Ting et al. 2002). March 2010 was an exception when the prochlorophyte contribution was minimal in the deep waters > 100m, deep waters were mainly dominated by diatoms (42%) along with relatively small contributions from haptophyte-8 (20%) and cyanobacteria (11%) (Fig. 8a).

The 19′-But: TChl *a* ratio also increased with depth (Fig. 8b) indicating the importance of pelagophytes in deep water, such trends of increasing in 19But:TChl *a* are common in other tropical and subtropical oceans (Gibb et al. 2000, Gibb et al. 2001, Marty et al. 2008, Schlüter et al. 2011). 19′-But: 19′-Hex ratios extended over a wider range in surface (range, 3-7: 1) than at depth (range, 0.3-1.1: 1) (Fig. 8b). The observed pattern of a larger contribution by pelagophytes to total biomass is similar to that reported in other studies and has been attributed to the control of light and nutrients on their vertical distribution (Claustre 1994, Marty et al. 2002).

A significant relationship ($r^2 > 0.8$, $p<0.05$) between Pras and Chlb was found for samples from the CFM. Minor or trace amounts of Viola, Neo and Lut was found during the HPLC analysis, concentrations were mostly below the limit of quantification (LOQ). By following criteria set by Schlüter et al. (2006), only Prasinophyte - I was included in the final CHEMTAX analysis. For this study it was assumed that Chlb from at CFM was mostly associated with prasinophytes containing Pras (i.e., Prasinophyte-I). Consistent with the findings reported in this study, the presence of the prasinophyte-I in deep water has been documented in various parts of world ocean, including the Gulf of Mexico (Paul et al. 2000b, Wawrik et al. 2003, Guillou et al. 2004, Latasa et al. 2004, Worden et al. 2004, Not et al. 2008, Viprey et al. 2008, Hernandez-Becerril et al. 2012). This highlights the importance of this less studied diverse group of picophytoplankton.

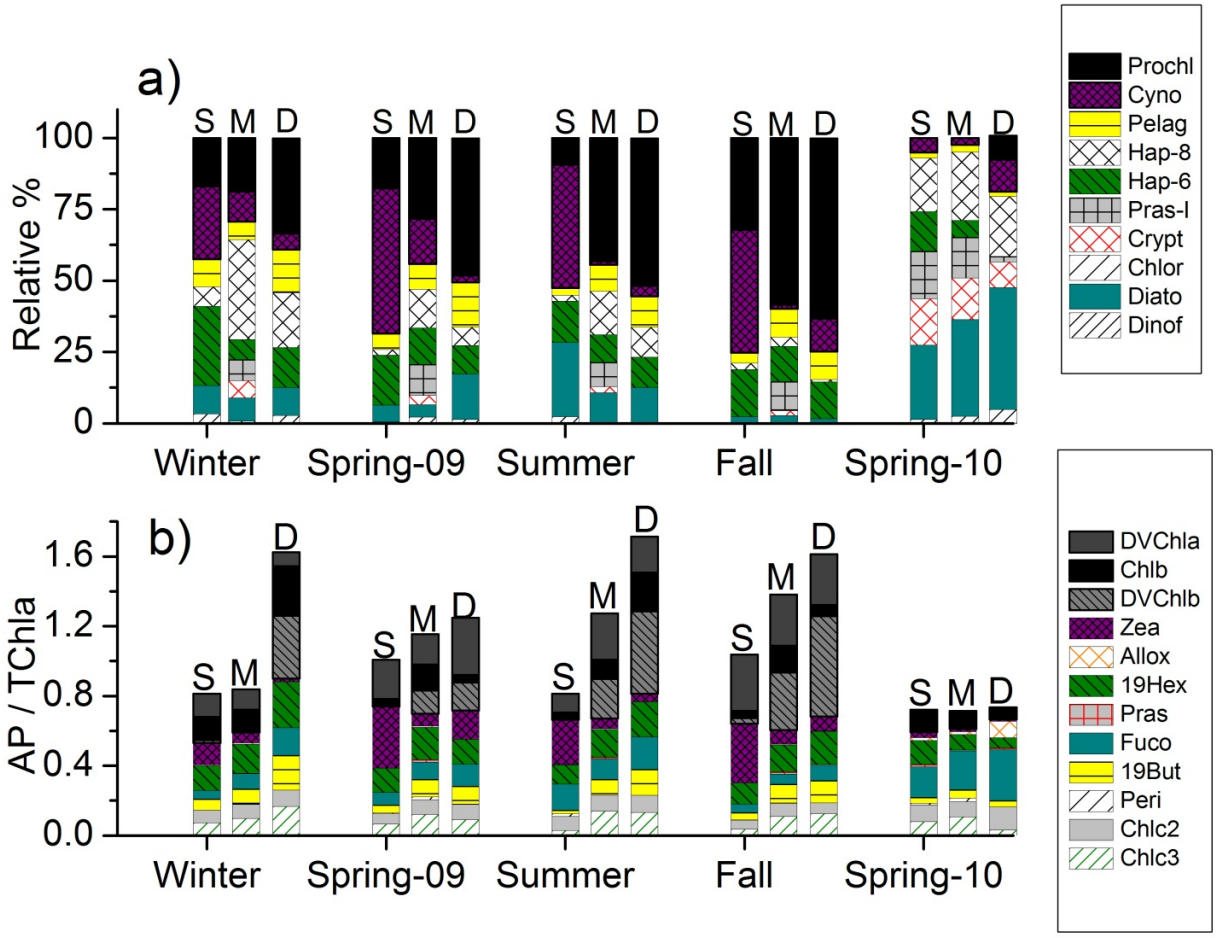

Figure.8. Depth distribution of major phytoplankton groups on the slope as calculated by CHEMTAX (a); change in accessory pigments : TChl *a* ratios with depth (b); the letters S, M, and D at the top of each stacked bars in (a) and (b) represents the surface, mid (50-100m) and deep (>100m).

.

Discussion

Patterns in Phytoplankton Community Composition in Relation to Seasonal Hydrographic Features

Distinct spatio-temporal variations were observed phytoplankton community in the coastal margin of the NGOM. Diatoms along with chlorophytes and cryptophytes, dominated the high biomass estuarine waters, a pattern attributed to the ability of these taxa to exploit relatively high nutrient availability and to tolerate low to moderate salinity conditions. Diatom contributions were reduced under stratified (summer and fall) conditions relative to other periods, while changes in thermal structure of the water column (Fig. 3a) had no noticeable changes in chlorophytes and cryptophytes. Because of their motility the flagellates may have an advantage over diatoms to remain in the euphotic zone in under stratified conditions (Margalef 1978). Cyanobacteria rich in phycocyanin (Murray et al. 1998, Collier 2000) prevailed at the riverine (low salinity) end member stations. The cyanobacteria's were predominant during the summer period. It have been shown that higher water temperatures (Li 1998) and lower discharge conditions (and thus longer residence times, Paerl (1996)) may favor proliferation of cyanobacteria's. Lower discharge conditions probably also contributed to the increased presence of dinoflagellates (Paerl et al. 2003), that were appreciably more important on average accounting for 9-10 % total biomass during summer (Fig. 6a). Dinoglagellate blooms following a cyanobacterial blooms have been reported in the Gulf of Mexico (Walsh et al. 2006, Vargo et al. 2008), and it has been suggested that the releasing NH_4 and inorganic N by the decaying cyanobacterial bloom provides favorable conditions that could initiate a dianoflagellate (particularly *Karenia brevis*) bloom. It is not possible to prove or disprove such a causal mechanism for the observed in increased dinoflagellates

population during in summer in this study, and certainly cannot be generalized for all dinoflagellates

Similar to estuarine waters, diatoms were the dominant taxa in inner shelf waters. Continuous nutrient supplies from the large rivers (MS-ATF) at the inner-shelf have been suggested as the possible reason of diatoms dominance (Dortch & Whitledge 1992, Bode & Dortch 1996, Lohrenz et al. 1999). High nutrient/ high-turbulence inner-shelf systems have been known to favor large celled phytoplankton such as diatoms (Margalef 1978). Cyanobacteria were prominent in inner shelf waters, particularly during summer (stratified conditions) and to a smaller extent during weakly stratified fall (Fig. 6a).Such observations are consistent with reports from previous studies in immediate plume areas (MS river) and the shallow inshore stations of the NGOM (Chen et al. 2000, Paul et al. 2000a, Liu et al. 2004). Dominance of cyanobacteria during summer during summer have been speculated to altered food-web structure (Murrell & Lores 2004) in some estuarine and coastal zones, but no such evidence exists in NGOM. The consequences of the cyanobacteria bloom during summer on the trophic structure needs to be addressed with careful and detailed studies on the abundance, biomass and production of zooplankton and phytoplankton.

Phytoplankton communities as derived from CHEMTAX in mid-shelf regions were primarily composed of small-celled cyanobacteria and procholorophytes, except for the January 2009 and March 2010 periods. Communities during those two periods were dominated by diatoms and nanoflagellates. High river discharge during winter, can spread nutrient-rich river waters to considerable distances across the shelf (Dagg & Breed 2003). At subsurface depths in mid-shelf (i.e., < 50m and bottom), diatoms and Hapto-8

were the dominant phytoplankton groups. The presence of Hapto-8 in subsurface and bottom waters (Fig. 7a) provides a basis for speculation that this group is well adapted to varying light levels and tolerant of widely salinity conditions. Laboratory experiments on *Phaeocystis. globosa* (hapto-8) support of this view. Hoogstraten et al. (2011) have suggested that *P. globosa* can maintain high growth rates at suboptimal light levels. However, high growth rates may not be enough to outcompete diatoms (Meyer et al. 2000). The Hapto-8 ratios used in CHEMTAX for this study were averages from *Imantiana.rotunda* and *P. globosa*. Both species have been known to occur in the GOM (Zapata et al. 2004, Schoemann et al. 2005), and *P. globosa* in particular has been reported frequently in the literature (Zapata et al. 2004, Schoemann et al. 2005).

Phytoplankton communities in surface waters of the slope were subject to the seasonal changes in thermal structure of the upper water column and to mesoscale events such as intermittent pulses of low salinity waters from river systems. During strong thermal stratification (July and November 2009) or in a transitional phase (April 2009), the community in surface waters of the slope regime were chacterized by low surface biomass and dominated by picophytoplankton (cyanobacteria and procholorcoccus dominated 42-75% of total biomass). The peak in prochlorophyte contribution to phytoplankton biomass during fall was associated to several factors, surface DIN: P (~1) were lowest during that period while NH_4 was highest (DIN: NH_4 = 0.3). Prochlorophytes usually dominates low nutrient stratified conditions (Ting et al. 2002, Johnson et al. 2006) and are able to utilize NH_4 very efficiently (Moore et al. 2002). Additionally, several studies have shown prochlorophytes to be particularly sensitive to UV radiation (Sommaruga et al. 2005, Llabrés & Agustí 2006, Agustí & Llabrés 2007).

The erythermal UV dose rate (mW m^{-2}) in the NGOM slope was low during fall, almost half and a third from spring and summer respectively (See Appendix C).

On two occasions during the study, the slope community was dominated by micro and nanophytoplankton (~60% of total biomass). One such instance was during summer in July 2009, when MS plume waters (salinity ≤31) impacted several offshore stations (Fig. 3f, inset), high biomass (Fig. 4e & Fig. 5, Table 4) and micro and nanophytoplankton (≥ 60% to total biomass) dominated those stations while picophytoplankton (~ 71% of total biomass) dominated the non-plume impacted stations. Similar shifts in community were also observed by Qian et al. (2003) and Wawrik and Paul (2004) under scenarios involving offshore transport of MS plume. The second occasion was during March 2010, when diatoms dominated the slope waters. The March 2010 cruise followed a period of high river discharge, was special in a scence that it co-incided with low water temperature, high nutrinet (Table 1) and a mixed (Fig. 3e, deepest observed mixed-layer) upper water column conditions, suitable conditions for diatom proliferation.

During January 2009, biomass at slope stations was high and the water coumn was mixed but dominance by any particular group was not observed. A mixed community comprised of Hapto-6 (~30%), cyanobacteria (~25%) and prochloprophytes (~ 17%) was observed through out the upper water column. High surface TChl *a* observed during winter in NGOM slope is consistent with previous works by Muller-Karger et al. (1991) and Jolliff et al. (2008). Vertical mixing was attributed to the higher biomass, vertical mixing not only supplies the nutrients from depth to the euphotic zone but also allows larger cells (nano and microplankton) to remain in suspension. Therefore

it can hypothesized here that mixing during winter might have eroded the CFM and subsequently brought the deeper community in the well lit surface layers. The low nutrient levels during the period (Table 3) futher suggests efficient removal of the nutrients from deep waters by the phyoplankton community.

CFM was a consistent feature in subsurface slope waters. The depth of the CFM during our study ranged from 45-88 m, was shallowest during summer (55 ± 11m) and deepest during spring 2009 (76 ± 12m). The community composition observed at CFM and deeper (100-120m) depths were very similar to patterns reported for several other regions including the Atlantic Ocean (Gibb et al. 2000, Veldhuis & Kraay 2004), Mediterranean Sea (Marty et al. 2008) and Indian Ocean (Not et al. 2008, Schlüter et al. 2011). Procholorophytes, cyanobacteria along with haptophytes, pelagophytes and prasinophyte-I were the main groups identified in CFM and deeper depths. Diatoms were also present but were a minor part of the community except in spring 2010 (Fig. 8a). Occurrence of diatoms in deeper water has been previously observed by Schlüter et al. (2011) in Indian Ocean. Prochlorophytes were particularly dominant under conditions of strong stratification, and patterns in pigment ratios bears evidence of existence of at least two different light-acclimated ecotypes, a high light adapted surface population with a lower DVChlb : DVChla ratio and a low light adapted deep population with high DVChlb :DVChla ratio. Several studies have found such vertical segregation of genetically and physiologically distinct populations among prochlorophytes (Goericke & Repeta 1993, Partensky et al. 1993, Moore et al. 1995, Moore & Chisholm 1999b, Bouman et al. 2006, Uitz et al. 2006). Recent studies have also found prochlorophytes to be susceptible to UV radiation (Bruyant et al. 2005, Sommaruga et al. 2005), which

might be a reason for their low contribution to the surface water communities. Analyses of phytoplankton absorption revealed UV absorption signatures consistent with the presence of UV photo protective substances (i.e., mycosporine-like amino acids) in surface samples from the slope regime (See Chapter IV).

In addition to procholorophytes and cyanobacteria, phytoplankton group's haptophyte-6, haptophyte-8, pelagophytes were also identified mainly based on the 19′-Hex and 19′-But typical pigments in flagellated phytoplankton but can also occur in some picophytoplankton. Prasinophyte-I identified in CFM and deeper water was based on the presence of the xanthophyll pigment prasinoxanthin. The analytical methods used in this study did not detect the presence of pigments like urolide and micromonal required to distinguish different phylogenetic groups of prasinophytes (Guillou et al. 2004, Latasa et al. 2004). However, a separate study on picophytoplankton in southern GOM (Hernandez-Becerril et al. 2012) reported *Micromonas pusilla* to be the dominant prasinophyte in that region. These results clearly show the need for further studies focused on pico-eukaryotic phytoplankton in NGOM, given their global importance (Not et al. 2008, Liu et al. 2009)

Comment on the Use of CHEMTAX for Determining Phytoplankton Composition.

Applications of the CHEMTAX program have been remarkably successful for the discrimination of phytoplankton groups in a wide variety of marine environments (Mackey et al. 1998, Muylaert et al. 2006, Marty et al. 2008, Latasa et al. 2010, Wright et al. 2010, Kozlowski et al. 2011, Mendes et al. 2011, Schlüter et al. 2011), despite the fact that a number of pigments with varying amounts are shared among different phytoplankton classes. The robustness of this method to discriminate phytoplankton

classes is enhanced if optimization techniques as suggested by Latasa (2007) and Wright et al. (2009b) are followed. This study used a combination of both techniques along with cluster analysis to statistically identify water types with similar pigment characteristics. The previous that used CHEMTAX in NGOM (Wysocki et al. 2006) used the same pigment ratios as used by Qian et al. (2003) for the north-eastern Gulf of Mexico. Qian et al. (2003) used a least square approach to determine the contribution of different phytoplankton groups. Use of such approaches to derive phytoplankton distribution have been cautioned by Mackey et al. (1996), such approached have often been found to provide unrealistic estimations (negative contribution from certain groups).

The final pigment ratio matrices in this study were consistent with those reported in other studies. The final ratios obtained for Per: Chl *a* and Fuco:Chl *a* fell within the ranges reported in the literature (Schlüter et al. 2000, Lewitus et al. 2005, Laza-Martinez et al. 2007). Fuco:Chl *a* ratios in this study increased with waters depths (50-100m and >100m but <150m). Increases in Fuco:Chl *a* ratios with increasing depth have been observed in East China Sea by Furuya et al. (2003) and also in Southern Ocean by Schlüter et al. (2011). In contrast some other studies have found Fuco:Chl *a* to decrease with depth (e.g. Higgins et al. (2006) & Wright and van den Enden (2000)). Understanding the variations in Fuco:Chl *a* ratios is not straight-forward, some culture studies have reported increases in Fuco:Chl *a* ratios in both marine and freshwater diatoms under low light conditions (Goericke & Montoya 1998, Schlüter et al. 2000, Schlüter et al. 2006). Those studies have reported high variability at species level suggesting complex interactions between light and nutrient availability.

The ratios obtained for haptopyte-6 fell were in the range for the several strains studied by Zapata et al. (2004). For haptophyte-8, the ratios found in this study were closer to the ratios observed in *I. rotunda* (Zapata et al. 2004). In this study, the cyanobacteria group represented of both *Trichodesmium* and *Synecochoccus sp*. Zea: Chl *a* ratios can vary largely among strains of cyanobacteria (e.g., *Synechococcus sp*) depending on light conditions (Kana & Glibert 1987). Zea:Chl *a* ratios obtained from this study were comparable to the average ranges found in the literature (Bidigare et al. 1989, Mackey et al. 1998, Schlüter et al. 2000, Veldhuis & Kraay 2004, Marty et al. 2008). Ratio of prochlorophytes were normalized to DVChla and final ratios fell within the range as observed in open oceans (Mackey et al. 1998, Gibb et al. 2001, Veldhuis & Kraay 2004).

Conclusion

The present work will contribute significantly towards the better understanding of phytoplankton dynamics across the continental margin of the Northern Gulf of Mexico. The objective this study was fulfilled by showing distinct phytoplankton community assemblage's for each water types. The findings of this study corroborate some of the widely accepted concepts in phytoplankton ecology, such as ubiquity and stability of communities pertaining to specific water types. Some of the information provided in this such as the observed niche separation among ecotypes would serve as a baseline for future work related to phytoplankton community composition, abundance and diversity.

CHAPTER III

RELATION BETWEEN PHYTOPLANKTON COMMUNITY COMPOSITION AND THE PHYSIOCHEMICAL ENVIRONMENT IN THE CONTINENTAL MARGIN OF NORTHERN GULF OF MEXICO.

Introduction

Seasonal changes in physico-chemical properties of the environment drive changes in phytoplankton populations in the world oceans (Smayda 1980). Community succession of phytoplankton on temporal scales is largely dependent on changes in the physical environment (Margalef 1978, Banse 1994).

The coastal waters of northern Gulf of Mexico are under a range of pressure including anthropogenic (Rabalais et al. 2002a), nutrient enrichment, pollution and climate driven (Bianchi & Allison 2009a) changes. These and other environmental changes are known to alter the temporal and spatial distribution of the phytoplankton community. The present study extends this idea by analyzing the relationship between variability's of the physico-chemical properties in northern Gulf of Mexico to the biological system, especially in determining the responses of phytoplankton community. A series of field campaigns (Gulf Carbon) were conducted across the continental margin of the northern Gulf of Mexico during winter (January 2009), spring (April-May 2009), summer (July-2009), fall (October-November 2009) and spring 2010 (March 2010) where an unprecedented dataset of environmental and biological variables were collected. Most previous studies in northern Gulf of Mexico have been mostly focused on the immediate plume areas of two large rivers (Mississippi and Atchafalaya). The primary hypothesis of this work was large differences in phytoplankton community composition

coincide with transitions between stratified and non-stratified periods for all water types in the continental margin of the northern Gulf of Mexico.

This study uses principal component analysis (PCA) to relate environmental variables to different phytoplankton groups derived from CHEMTAX analysis. PCA is an effective statistical tool to analyze large datasets of field observations and can be used to detect patterns among a suite of variables. PCA has been used widely in oceanographic studies for example Adolf et al. (2006). PCA generates components which can describe significant portion of variability observed in the datasets and can therefore provide insights to the mechanistic relationship between the components and the variables.

Materials and Methods

Cruise and Sampling

Water samples were collected on board R/V Cape Hatteras (January, April-May, July, 2009 and March 2010) and R/V Hugh R. Sharp (October-November, 2009) during 5 cruises that took place in January (winter), April (spring 2009), July (summer), October (fall) 2009 and March 2010 (spring 2010). Eight transects were made across the northern Gulf of Mexico, encompassing large gradients across the continental margin, from highly turbid riverine conditions to oligotrophic slope waters. Water samples were collected at each station using 10 L Niskin bottles mounted on a CTD (SeaBird SBE911 plus) rosette system. For details about phytoplankton pigment analysis and subsequent CHEMTAX (see chapter-II of this dissertation).

Mixed layer depth calculation

Mixed layer depths (MLD) were calculated according to Lorbacher et al. (2006) and Kara et al. (2000). Temperature at 2 m depth was chosen to be the initial reference temperature for determining MLD. Besides the mixed layer was also established each at

each station with a criterion of a change in density of 0.05 kg m^{-3} (Greg Mitchell & Holm-Hansen 1991).

Nutrient Analysis

Nutrient samples were filtered through glass fiber filters (GF/F) and subsequently collected into 250-mL acid –washed brown polyethylene bottles which were kept frozen (− 20 °C) for a few weeks until their analysis. All nutrients (NO_3-N, NO_2–N, NH_4 and SiO_3 and PO_4) were measured using fluorometric (N species) and spectrophotometric (PO_4 and SiO_3) methods on the Astoria –Pacific A2+2 nutrient auto-analyzer (Method # A179, A027, A205 and A221; Astoria Pacific International, Oregon USA).

Winds and Current data

Sea surface currents were obtained from Intra-Americas Sea Ocean Nowcast/Forecast System (IASNFS; Ko (2003); Chassignet et al. (2005)) which provides experimental near-real-time predictions of Gulf of Mexico and Caribbean waters. The IASNFS consists of a 1/24 degree (~6 km), 41-level sigma-z data-assimilating ocean model based on the Navy Coastal Ocean Model (NCOM) ((Martin 2000). Three hourly wind stresses used in this study were obtained from the Navy Operational Global Atmospheric Prediction System (NOGAPS, http://hycom.org/dataserver/nogaps).

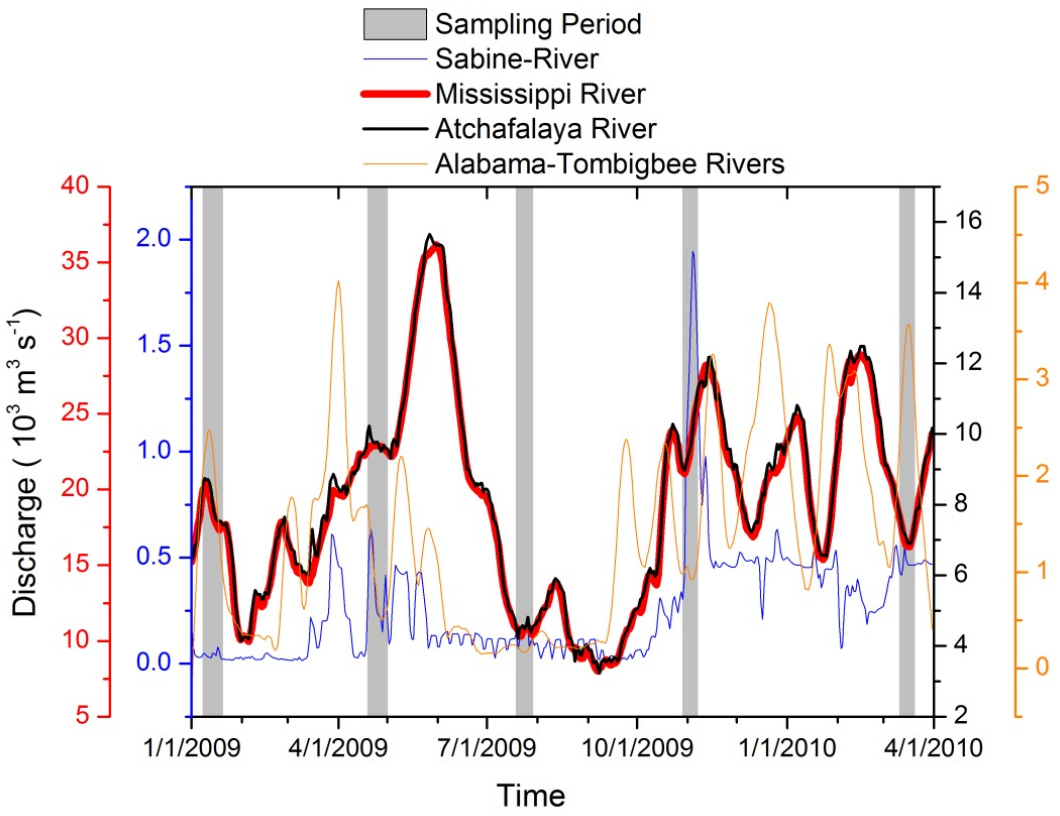

Figure 9. Mean daily discharges of major rivers in the region. The discharge data for the Mississippi and the Atchafalaya was obtained from the United States Army Corps of the Engineers (USACE) for Tarbert Landing and Sommesport in Louisiana. Discharge from Alabama and Tombigbee Rivers were combined to represent the total outflow through the Mobile Bay. The discharge out of Sabine Bay was obtained from the Sabine River. The discharge data were obtained from the United States Geological Survey (USGS). None of the cruise caught the peaks of Mississippi and Atchafalaya River discharge, only the October, 2009 cruise caught the a peak in Sabine River and the March 2010 caught the peak in Alabama/Tombigbee Rivers.

Data Analysis

Principal component analysis (PCA). Principal component analysis (PCA) was used as a data reduction technique to examine patterns within the datasets. PCA reduces a large data matrix of several variables with some level of correlation into uncorrelated (orthogonal) variables which are known as principal component (PCs). The first PC accounts for most of the variability in the dataset followed by the other PCs each of which explains progressively less variability (Meglen 1992). The PC loading are

eigenvectors of the correlation matrix which provides information about the relative contribution of each PC and while the derived scores describes the relationship between the PCs and the individual observations. PCA have been successfully used in many oceanographic studies (Adolf et al. 2006, Álvarez-Góngora & Herrera-Silveira 2006, Massolo et al. 2009) to examine the relative importance of environmental factors in control of phytoplankton community. The physical variables used in this study composed of temperature (T), Salinity (S), mixed layer depth (ZM), dissolved inorganic nitrogen (DIN = sum of nitrate (NO_3) + nitrite (NO_2)), phosphate (PO_4), ammonia (NH4), silicate (SIO3), sea surface currents (u vector (SSCu), v-vector (SSCv)), wind stress vectors u (SSWu), wind stress vector v (SSWv). Biological variables that were included in the analysis were TChl *a* (TCHLA), diatoms (DIA), cryptophytes (CRYP), haptophytes (HAP) and prochlorophytes (PRO). The phytoplankton groups selected for this study was derived using CHEMTAX version v 1.95 (Mackey et al. 1996, Wright et al. 2009b) details of which have been discussed in chapter II of this dissertation. The above four phytoplankton groups were chosen because they showed largest variability and were the major groups of phytoplankton representing major size classes in the region. The dataset was separated into different regional (estuarine, inner shelf, mid-shelf and slope) and vertical subsets (surface and bottom for estuarine, inner shelf, mid-shelf, and surface, 0-50 m and $\geq$ 100m for slope waters). Estuarine and inner shelf was combined and was treated as a single dataset in this study.

Results and Discussion

Hydrography

Regional hydrography and water column structure have been described previously in chapter-II. Differences among cruises were observed in the environmental variables in each the water types and are summarized in Table 5, 6 and 7. The environmental conditions from two specific periods (summer 2009 and spring 2010) are discussed in greater details here, regional variations in winds and currents significantly affected physico-chemical properties in the continental margin of northern Gulf of Mexico during those periods. On average surface salinity at the shelf slope was > 35, except during July 2009 (Fig. 10a) when an offshore extension of the Mississippi river plume was observed and impacted some slope station (the dotted ellipse, Fig. 10a) where surface salinity < 31 was observed. Offshore movement of the plume during summer 2009 impacted slope stations were identified by the presence of a low salinity pool (mean ± SD 28.9 ± 1.31) in the southwestern and south central direction of the Mississippi delta. Offshore flow evidenced during summer (July 2009) was facilitated by the prevailing winds mostly from the southwest direction (Fig. 10a & Fig 10c). Previous studies in the region have also evidence of such offshore extension of the Mississippi river plume (Chen et al. 2000, Walker et al. 2005)

The March 2010 cruise followed a large peak in Mississippi and Atchafalaya (in February 2010, Fig. 9) when the average discharge of both Mississippi and Atchafalaya was 38.7 x 10^3 m^3 s^{-1} (combined discharge Mississippi and Atchafalaya). Surface salinity during the march 2010 period was significantly low (ANOVA, $p< 0.05$) for the entire margin (Table 5). Low salinity waters (Fig. 10b) extended a wide area in the shelf. High river discharge prior to the March 2010 cruise presence of winds from north-east

directions facilitated the extension of river plume in southern direction. TChl *a* levels were significantly higher ($p < 0.05$) than the rest of the study period (See Chapter II for details, Fig. 4c). Though for most of the study period the currents were towards the west along the shelf but offshore flow was observed in March 2010 following the winds from the north (Fig 10d).

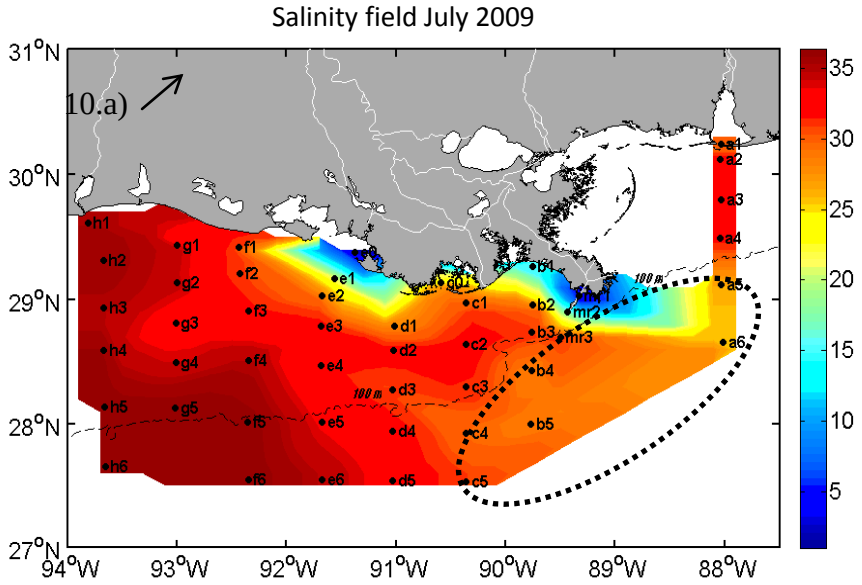

Figure 10. Surface plots of salinity during summer 2009 (a) and spring 2010 (b), sea surface currents during summer (c) and spring 2010 (d) the broad white arrows on the plots depicts the general direction of the current flow. The averaged wind speed during summer for the region was 3.45 ± 1.67 m s^{-1} and ranged between 0.59-6.27. The average during spring 2010 was 6.77 ± 2.33 m s^{-1} and ranged between 0.50- 11.84 m s^{-1}

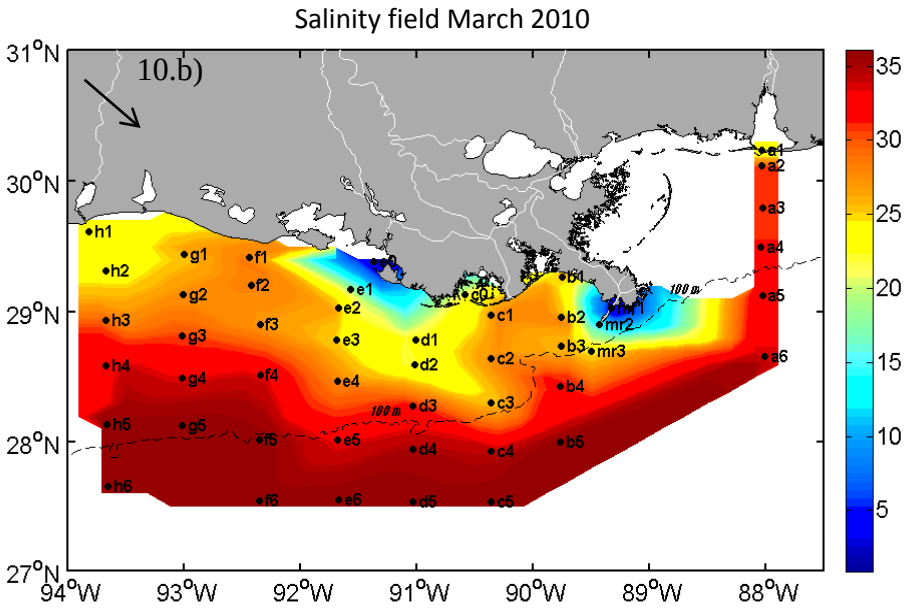

Figure 10. Surface plots of salinity during summer 2009 (a) and spring 2010 (b), sea surface currents during summer (c) and spring 2010 (d) the broad white arrows on the plots depicts the general direction of the current flow. The averaged wind speed during summer for the region was 3.45 ± 1.67 m s^{-1} and ranged between 0.59-6.27. The average during spring 2010 was 6.77 ± 2.33 m s^{-1} and ranged between 0.50- 11.84 m s^{-1}.

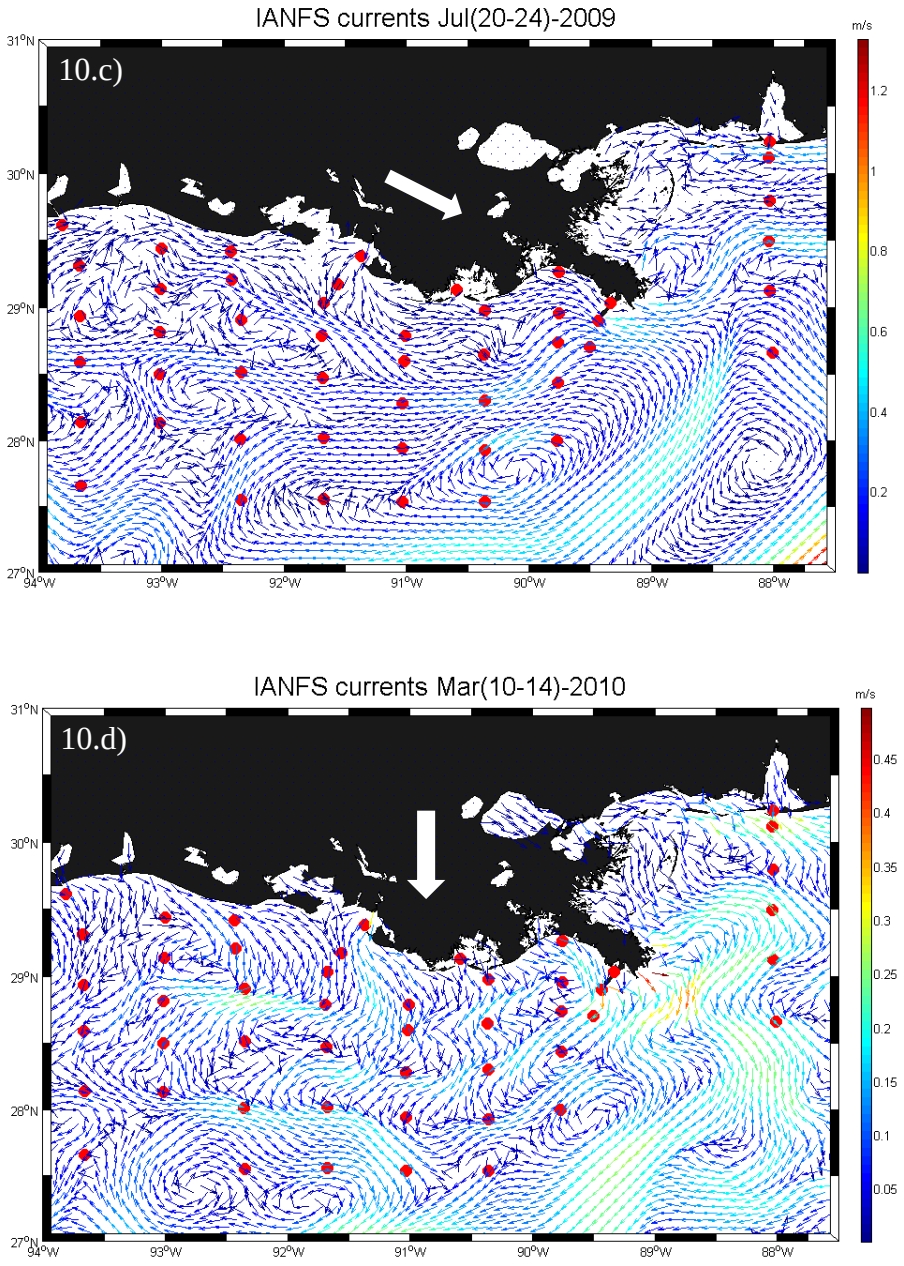

Figure 10. Surface plots of salinity during summer 2009 (a) and spring 2010 (b), sea surface currents during summer (c) and spring 2010 (d) the broad white arrows on the plots depicts the general direction of the current flow. The averaged wind speed during summer for the region was 3.45 ± 1.67 m s^{-1} and ranged between 0.59-6.27. The average during spring 2010 was 6.77 ± 2.33 m s^{-1} and ranged between 0.50- 11.84 m s^{-1}

Table 5

Descriptive Statistics of the Environmental Variables in Estuarine and Inner Shelf

Variables		N	Mean	Std. Dev	Minimum	Median	Maximum
Salinity	January	17	29.19626	5.63119	15.357	29.9911	35.1973
	April 2009	19	28.06489	2.86705	23.1199	28.4614	32.6314
	July	15	29.43719	6.12274	15.0816	30.8852	35.6762
	October	23	26.48532	5.4212	13.4837	27.4244	33.2679
	March 2010	21	24.6903	3.94214	11.6179	25.417	29.1725
Temperature	January	17	16.3882	1.97375	13.3462	17.0616	19.385
	April 2009	19	22.75492	0.85406	21.23	22.9225	24.6887
	July	15	29.46539	1.02318	27.4586	29.5143	30.8175
	October	23	22.17118	1.58876	17.3619	22.6463	24.5983
	March 2010	21	16.28987	1.00551	13.2145	16.347	17.9956

Table 5(continued)

Variables	Months	N	Mean	Std.Dev	Minimum	Median	Maximum
	January	17	6.32574	12.89284	0.122	1.075	52.084
	April 2009	19	8.15639	15.14483	0.22324	1.322	61.32416
DIN	July	15	4.83448	12.67104	0.69489	0.75219	49.05
	October	23	4.56804	5.3997	0.085	3.183	22.451
	March 2010	21	9.79319	15.06107	0.125	7.458	69.84
	January	17	10.79965	15.97897	0.137	4.057	64.4
	April 2009	19	10.66296	15.85348	0.27835	5.967	68.645
SIO_3	July	15	15.6336	22.35955	0.638	5.075	75.496
	October	23	19.13287	16.85071	1.309	14.942	63.913
	March 2010	21	18.3619	15.52581	1.842	16.815	74.963

Table 5(continued)

Variables		N	Mean	Std.Dev	Minimum	Median	Maximum
	January	17	0.31088	0.43019	0.095	0.187	.921
	April 2009	19	0.65611	0.39386	0.302	0.541	2.059
PO_4	July	15	0.27767	0.4675	0.018	0.176	1.855
	October	23	0.44848	0.3689	0.093	0.285	1.551
	March 2010	21	0.27705	0.3602	0.111	0.151	1.771
	January	17	0.33541	0.442	0.063	0.107	1.503
	April 2009	19	0.46916	1.14315	0	0.024	4.315
NH_4	July	15	0.64072	0.39819	0.25783	0.5312	1.53946
	October	23	0.72526	0.36429	0.282	0.694	1.815
	March 2010	21	0.52714	0.71074	0.157	0.298	3.468
	January	17	10.90294	6.022133	4	9.4	43.2
	April 2009	19	6.592105	3.790715	2.5	8	25.75
ZM	July	15	7.016667	5.592139	2.5	7.25	25
	October	23	11.13333	5.281059	2.5	9.75	100
	March 2010	21	6.855263	2.388217	2.5	7.75	40

Table 6

Descriptive Statistics of the Environmental Variables in Mid- Shelf

Variables		N	Mean	Std. Dev	Minimum	Median	Maximum
	January	11	35.53198	0.94936	33.5855	35.8421	36.4035
	April 2009	8	33.95756	1.91894	30.7968	33.85595	36.3566
Salinity	July	11	33.78174	1.23684	31.8471	34.0333	35.7799
	October	11	35.10998	1.29483	32.7016	35.8221	36.5505
	March 2010	9	29.5889	2.88341	24.6044	30.7956	33.0744
	January	11	19.46487	1.46961	17.419	19.098	21.6951
	April 2009	8	22.52481	0.42514	22.1204	22.384	23.2455
Temperature	July	11	29.8333	0.60754	28.7393	29.9843	30.8175
	October	11	24.91378	0.58897	24.0638	24.8182	25.833
	March 2010	9	16.71068	0.87179	15.5709	16.607	18.0712

Table 6(continued)

Variables		N	Mean	Standard Deviation	Minimum	Median	Maximum
	January	11	0.34646	0.19425	0.111	0.301	0.74352
	April 2009	8	0.30184	0.12051	0.17608	0.271	0.526
DIN	July	11	0.74061	0.06122	0.6635	0.73139	0.87628
	October	11	0.12791	0.07653	0.078	0.09	0.319
	March 2010	9	4.19644	5.85029	0.534	1.76	18.964
	January	11	1.22009	0.5754	0.551	1.125	2.446
	April 2009	8	0.83247	0.36109	0.27835	0.89691	1.20619
SiO_3	July	11	1.22373	0.50203	0.548	1.256	2.121
	October	11	2.70927	0.96331	1.329	2.865	3.967
	March 2010	9	6.971	5.95191	2.453	4.065	20.172
	January	11	0.26436	0.09201	0.047	0.294	0.357
	April 2009	8	0.90925	0.42328	0.144	1.0875	1.355
PHO_4	July	11	0.06164	0.0613	0.02	0.041	0.209
	October	11	0.08445	0.05016	0.037	0.07	0.213
	March 2010	9	0.17467	0.03521	0.127	0.188	0.226
	January	11	34.79636	13.95651	12.55	32.46	62
	April 2009	8	14	3.76544	9.75	13.875	21
ZM	July	11	13.77273	7.43678	5.75	10.5	25.5
	October	11	31.56818	11.73461	10	34.5	43.25
	March 2010	9	21.77778	11.45742	11.5	22.25	47

Table 7

Descriptive Statistics for Environmental Variables in Slope Waters

Variables		N	Mean	Standard Deviation	Minimum	Median	Maximum
Slope							
	January	12	36.37257	0.0863	36.1333	36.3898	36.4641
	April 2009	13	36.26278	0.33444	35.775	36.4148	36.7
Salinity	July	15	32.75824	3.58139	27.3743	33.2382	36.7778
	October	11	35.82925	1.32206	32.603	36.5235	36.6298
	March 2010	15	35.64043	1.17691	33.2883	36.3865	36.4875
	January	12	22.29345	0.87781	20.3116	22.45355	23.7056
	April 2009	13	23.14228	0.30043	22.4612	23.2298	23.4954
Temperature	July	15	29.63214	0.38639	29.0887	29.7112	30.5424
	October	11	26.11288	0.61243	25.2322	26.2516	26.9543
	March 2010	15	19.13483	0.67951	18.1277	19.0622	20.3111
	January	12	0.29457	0.18948	0.058	0.2513	0.69171
	April 2009	13	0.27544	0.10737	0.19266	0.25382	0.579
DIN	July	15	0.71406	0.03242	0.66058	0.71496	0.76715
	October	11	0.09418	0.02571	0.064	0.09	0.149
	March 2010	15	1.20033	0.85177	0.082	0.843	2.757

Table 7(continued)

Variables		N	Mean	Standard Deviation	Minimum	Median	Maximum
Slope							
	January	12	1.30975	0.33117	0.821	1.2365	1.843
	April 2009	13	1.11895	0.28185	0.79381	1.10309	1.72165
SIO_3	July	15	1.34607	0.43601	0.586	1.5	2.228
	October	11	1.373	0.29887	0.724	1.335	1.863
	March 2010	15	0.9454	0.80939	0.167	0.598	3.037
	January	12	0.30458	0.07501	0.15	0.3205	0.416
	April 2009	13	0.53231	0.5363	0.029	0.12	1.133
	July	15	0.1152	0.07558	0.018	0.137	0.255
	October	11	0.05673	0.02656	0.028	0.045	0.115
	March 2010	15	0.13527	0.04935	0.094	0.115	0.267
	January	12	0.05675	0.04293	0	0.0785	0.103
	April 2009	13	0.02485	0.04213	0	0	0.142
NH_4	July	15	0.4797	0.32312	0.22815	0.35087	1.33424
	October	11	0.30073	0.08893	0.162	0.294	0.481
	March 2010	15	0.224	0.15183	0.07	0.21	0.698
	January	12	76.74083	16.63917	45	84	90
	April 2009	13	28.05769	11.91601	7.25	32.5	47.25
ZM	July	15	19.86667	14.07279	4.25	12.75	43.75
	October	11	48.83091	14.4672	13.25	53.25	60.9
	March 2010	15	41.7	10.89323	23	44.5	63

Principal Component Analysis

The relationship between the variables for the different regions and seasons were examined using principal component analysis. The first two principal components accounted for 48-60% of the total variance for surface across the continental margin of northern Gulf of Mexico. The total variance explained by the first two PCs was comparable to that found in other studies (Farnham et al. 2003, Massolo et al. 2009). The sign of the loading reflected the relationships between variable and respective PCs (Table 8) while the magnitude of the loading indicates the influence of the variable on each PC.

Estuarine and Inner Shelf. The first two PCs determined by the PCA analysis explained ~ 57 % of the variability in the estuarine and inner shelf (Fig 11a & 11b), for the surface samples (Fig 11a) the first two PCs explained 57% of the total variance. The positive PC1 for the estuarine and inner shelf dataset was mainly characterized by high nutrients, cryptophytes followed by TChl *a*, while the negative PC1 included salinity, cyanophytes, haptophytes. PC1 also separated the end member estuarine stations; most of the data were clustered together on the same plate (Fig. 11a) of PC1 axis. The end member stations were characterized by low salinity (range for all season 0.02 -25.6,) and high nutrient levels (for all season DIN range was 0.13- 73). Most of the summer data was clustered together (Fig. 11a) and were very different rest of the dataset both in physical and biological properties. The summer samples located on the positive PC2 axis were characterized by high temperature, high cyanobacteria and eastward sea surface current and northward wind vector. While the negative PC2 were mainly characterized by high diatoms followed by cryptophytes. Haptophytes were of lesser importance

(contribution on average ranged between 4-5 %) in the estuarine and inner shelf waters, it showed little variations, very closely placed to the origin.

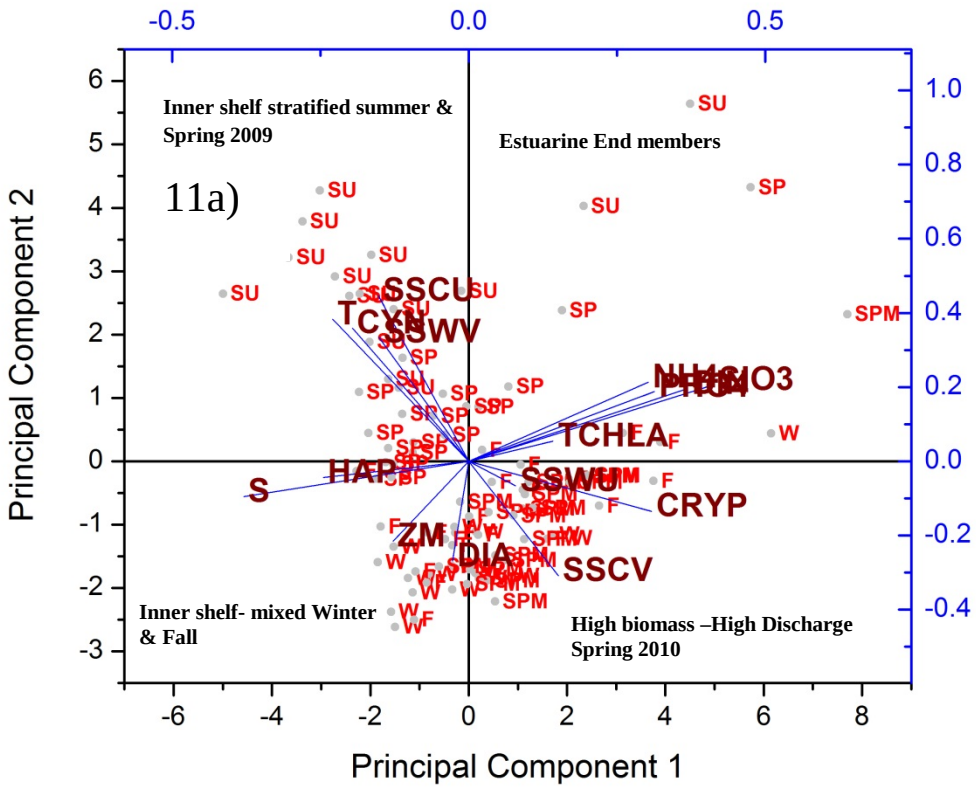

Figure 11. PCA bi-plot for estuarine and inner shelf surface (a) and bottom (b) waters. The objects are coded according to the sampling periods (W= winter, SP= spring 2009, SU = summer, F= fall, SPM = spring 2010(March 2010)). The symbols used for physical and chemical variables are as follows T= temperature, S= Salinity, ZM = mixed layer depths, DIN= sum of nitrate and nitrite NO3+ NO2, NH4= ammonia, SIO3 = silicate, PHO4 = Phosphate, SSWU= wind speed u, SSWV= wind speed v, SSCU= current u, SSCV = current v. The symbols used for biological samples are TCHLA = total Chlorophyll a, DIA = diatom, HAP = haptophytes, CYN = cyanobacteria, PRO = prochlorphytes.

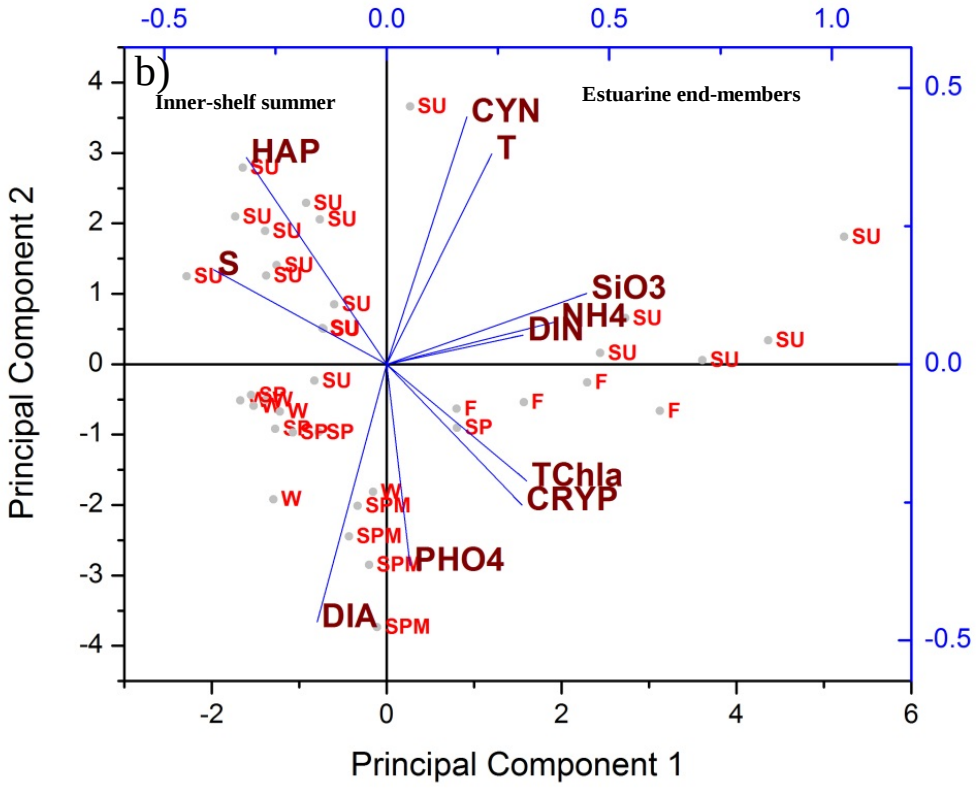

Figure 11. PCA bi-plot for estuarine and inner shelf surface (a) and bottom (b) waters. The objects are coded according to the sampling periods (W= winter, SP= spring 2009, SU = summer, F= fall, SPM = spring 2010(March 2010)). The symbols used for physical and chemical variables are as follows T= temperature, S= Salinity, ZM = mixed layer depths, DIN= sum of nitrate and nitrite NO3+ NO2, NH4= ammonia, SIO3 = silicate, PHO4 = Phosphate, SSWU= wind speed u, SSWV= wind speed v, SSCU= current u, SSCV = current v. The symbols used for biological samples are TCHLA = total Chlorophyll a, DIA = diatom, HAP = haptophytes, CYN = cyanobacteria, PRO = prochlorphytes

Mixed layer depths were important (Table 8) in the PC2 axis but had a lesser impact than temperature, suggesting temperature and salinity (or freshwater discharge) was the main factors controlling the community distribution in estuarine and inner shelf waters. Variations in physical and biological factors were also assessed for the bottom waters for the inner shelf and estuaries (Fig 11b). The first principal component (PC1) separated the end member estuarine stations from inner shelf characterized by some of

the highest levels of nutrients and low salinities (average ranged between 23.9 – 28.9) corresponding to the end-member stations collected during the fall (October-November 2009) and summer (July 2009) cruises. Effects of river discharge and subsequent nutrient availability on the phytoplankton community was also explained by the PC1 axis. During low discharge periods (summer, Fig 10) inner-shelf waters had higher haptophyte (11 ± 9 %) than cryptophytes (8.3 ± 4 %) (negatively related to salinity, Fig. 11a, Table 8). PC2 axis was mainly controlled by the temperature differentiating the summer from the rest when cyanophytes dominated the community in contrast to diatoms which was otherwise the dominant phytoplankton group at both depths in estuarine and inner shelf waters.

Thus it appears that seasonal fluctuations in phytoplankton community were mainly controlled by temperature and salinity (river discharge) in the estuarine and inner-shelf waters. Temperature had a larger influence on cyanophytes and diatoms while haptophytes and cryptophytes were mainly driven by salinity (river discharge) and subsequent high nutrient delivery. The results suggest that both river discharge and nutrients (mainly DIN and SiO_3, Table 8) was strong predictor of TChl *a*. Previous studies in the region have shown strong correlation between river discharge and nutrients loads (Lohrenz et al. 2008b, Lehrter et al. 2009). Long-term studies in the region have also demonstrated correlation between river discharge, nutrient loads and phytoplankton productivity (Justić et al. 1993) along with Chlorophyll-*a* (Chl *a*) and primary production (Lehrter et al. 2009). In contrast with some studies e.g., Green and Gould (2008) this study show a secondary role of mixing in regulating phytoplankton community composition. Seasonal reversal of winds and currents during summer was found to be strongly related to cyanobacteria dominated phytoplankton community (Fig. 11a).

Table 8

PCA results for Surface Station for different Water Types. Extracted eigenvectors from the PCA for the first two PCs. Bold number denotes the dominant variables in each PCs indicated by high loading values

	Estuarine & Inner-shelf		Mid-shelf		Slope	
	PC1	PC2	PC1	PC2	PC1	PC2
TChla	0.41215	0.05451	**0.39428**	0.10229	-.33154	-0.19886
Diatom	-0.02704	**-0.26905**	0.28519	-.15503	**-.41286**	0.01549
Cryptophytes	**0.38086**	-0.13544	0.31345	0.03658	Not used	Not used
Haptophyta	-0.24517	-0.04358	-0.25317	-.00825	0.2364	-0.2239
Cyanophyta	-0.19603	**0.35923**	**-.29376**	**0.26922**	0.28135	**0.34137**
Prochlorophyta	Not used	Not used	-.16945	-.05832	**0.36431**	0.03499
Salinity	**-0.37936**	-0.099481	**-.31337**	-.30972	**0.29266**	-0.31026
Temperature	-0.22957	**0.38319**	-0.30684	**0.25396**	0.09901	**0.45018**
DIN	**0.36887**	0.19609	**0.27868**	0.23044	**-0.31372**	-0.05973

Table 8 (continued).

	Estuarine & Inner-shelf		Mid-shelf		Slope	
	PC1	PC2	PC1	PC2	PC1	PC2
SiO3	**0.41418**	0.20681	**0.33796**	0.16175	0.03941	0.14573
PO_4	0.31341	0.18787	-0.09582	-0.09029	0.11238	0.06587
NH_4	0.30258	0.21383	0.04649	0.31661	-0.24907	**0.28027**
Zm	-0.12712	**-0.21524**	0.04813	**-0.38586**	0.25645	**-0.32907**
SSCu	-0.15209	**0.44649**	-0.19385	0.38211	0.04738	0.20714
SSCv	0.15097	-0.3086	0.0412	-0.16996	0.00451	-0.14808
SSWu	0.07916	-0.06611	**0.21681**	0.17953	**-0.30683**	-0.27446
SSWv	-0.15146	0.33467	-0.08864	**0.4291**	-.11776	**0.30048**

Mid-shelf. The first principal component explained 51.2 % of the total variance.in the mid-shelf (Fig. 12a) and was governed by the seasonal variations in river discharge. The positive PC1 (Fig. 12a) was characterized by high nutrient, high TChl *a*, high cryptophytes and high diatoms and the negative PC1 axis was defined by salinity,

temperature and cyanobacteria. PC1 mainly separated the spring 2010 (March 2010) samples and some stations in spring 2009 when high biomass (0.3- 3.4 mg m^{-3}) and high nutrient levels (0.27 – 5.9 µM) were observed in the mid-shelf. PC2 axis separated the stratified from non-stratified periods at mid-shelf (Table 8), mixed layer depth (ZM) being the major controlling factor in the negative PC2 space while the positive PC2 was mainly characterized by temperature and cyanobacteria. Clustering of the summer (July 2009) data in the same quadrant suggest strong relationship between temperature and cyanobacteria.

Mixed layer depths were deepest during winter (35.07 ± 14.6 m, median 36.73 m suggesting a well-mixed water column, diatoms were the dominant phytoplankton group during that period. Water column was strongly stratified during summer, mixed layer depths were shallow (13.77 ± 7.43 m, median 10.5 m) and cyanobacteria dominated the phytoplankton community. Diatoms were also dominant during spring 2010, physical advection of freshwater to the shelf following a high river discharge (Fig. 9) and subsequent high nutrient delivery led to enhanced biomass and facilitated diatoms and cryptophytes. Winds coming from the northeast blowing in the southeast direction during that period (Fig 10b) also facilitated offshore transport of low salinity waters (29.58 ± 2.88), into the mi-shelf waters. Mixed layer depths during spring 2009 and fall fell between the two extremes (shallowest during summer and deepest during winter, Table 8) and prochlorophytes and haptophytes were more important between the intermediate mixing period in fall and spring 2009 (Fig 12a).

From the above results it can be concluded that river discharge, stratification and water column mixing plays an important role in shaping the phytoplankton community structure at the mid-shelf stations in the northern Gulf of Mexico.

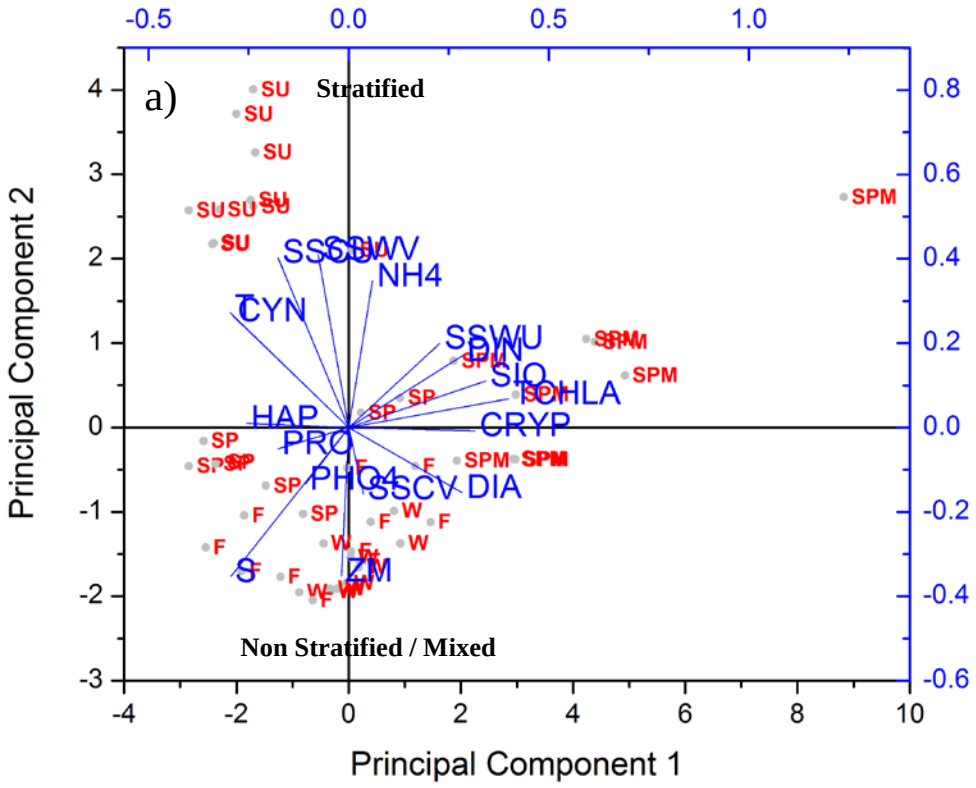

Figure 12. PCA bi-plot of the surface mid-shelf surface (a) and bottom (b) waters. The objects are coded according to the sampling periods (W= winter, SP= spring 2009, SU = summer, F= Fall, SPM = spring 2010(March 2010)). The symbols used for physical and chemical variables are as follows T= temperature, S= Salinity, ZM = mixed layer depths, DIN= sum of nitrate and nitrite NO3+ NO2, NH4= ammonia, SIO3 = silicate, PHO4 = Phosphate, SSWU= wind speed u, SSWV= wind speed v, SSCU= current u, SSCV = current v. The symbols used for biological samples are TCHLA = total Chlorophyll a, DIA = diatom, HAP = haptophytes, CYN = cyanobacteria, PRO = prochlorphytes.

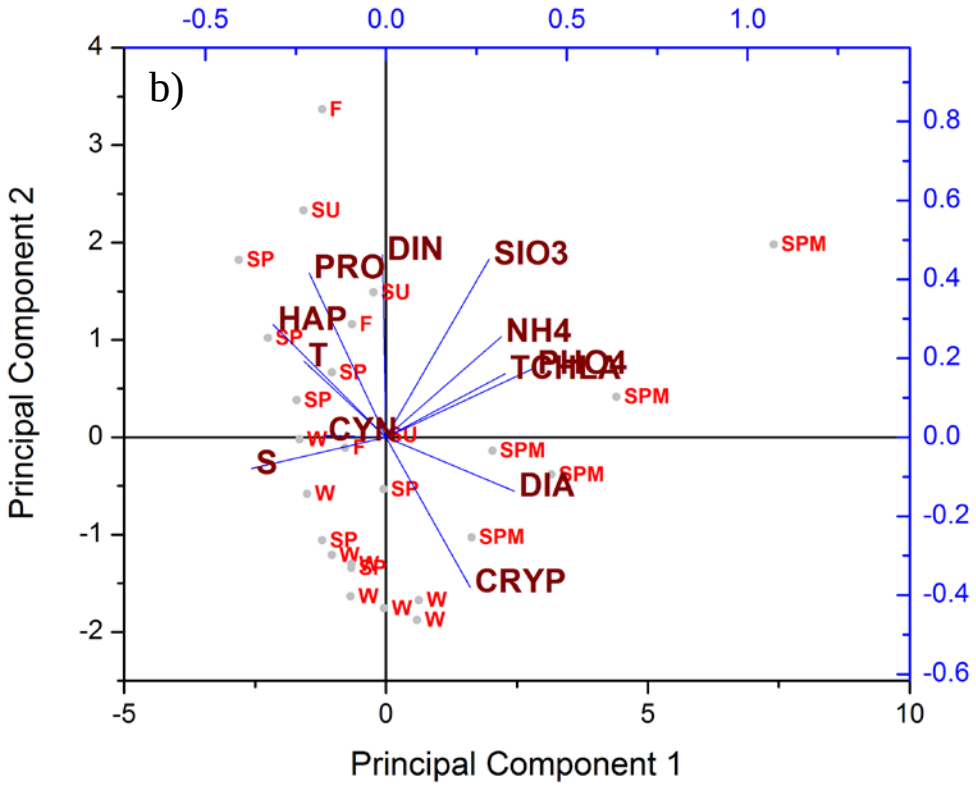

Figure 12. PCA bi-plot of the surface mid-shelf surface (a) and bottom (b) waters. The objects are coded according to the sampling periods (W= winter, SP= spring 2009, SU = summer, F= Fall, SPM = spring 2010(March 2010)). The symbols used for physical and chemical variables are as follows T= temperature, S= Salinity, ZM = mixed layer depths, DIN= sum of nitrate and nitrite NO3+ NO2, NH4= ammonia, SIO3 = silicate, PHO4 = Phosphate, SSWU= wind speed u, SSWV= wind speed v, SSCU= current u, SSCV = current v. The symbols used for biological samples are TCHLA = total Chlorophyll a, DIA = diatom, HAP = haptophytes, CYN = cyanobacteria, PRO = prochlorphytes

As for the surface PC1 for the bottom samples at the mid-shelf were described on the positive axis by nutrients, TChl *a*, diatoms and cryptophytes and the negative axis by salinity and temperature. PC1 differentiated the spring 2010 from other periods when water temperature (18.09 ± 0.74 ˚C) and salinity (34.30 ±2.61) were lower in comparison to the average temperature (20.25 ± 2.38˚C) and salinity (35.70 ± 1.34) at those depths. Positive correlations were observed between the prochlorophytes, haptophytes and

temperature at the positive PC2 axis while cryptophytes and diatoms were negatively correlated with temperature. Thus phytoplankton community at the bottom depths showed strong dependence on the temperature of the water column.

Slope. For the slope surface waters the PC1 explained ~ 40 % of the total variance by positive loadings. Clear seasonal patterns were evident where the positive PC1 co-ordinate represented periods of lower biomass (0.23 ± 0.22 mg m^{-3}) and low DIN (0.44 ± 0.26 μM) levels corresponding to spring, summer, fall and winter of 2009 (Fig. 13a). The phytoplankton community was dominated by cyanobacteria (45 ± 4.4 %) and prochlorophytes (20 ± 11%) during spring (April-May 2009), summer (July) and Fall (October-November). While the negative PC1 included spring 2010 (March 2010) and some summer (July 2009) samples having high levels of surface TChl *a* (~ 4 times higher than average TChl *a* in the slope), DIN (~ 1.75 times higher than the average) and high contributions from diatoms (41.21 ± 23.6 %). The proportions of cyanobacteria for those samples were low (12.12 ± 13.5 %) and prochlorophytes were nearly absent during that period (See Fig. 7, Chapter II).

The principal component two was mainly influenced by temperature and mixed layer depth. It separated warmer summer and spring 2009 (range 22.23 – 30.54 ˚C) with shallow mixed layer depths (median depths for summer 12.75 m and median depths for spring 2009 32.5m) from colder seasons winter and spring 2010 (range 18.12 – 23.31 ˚C) with deeper mixed layer depths (median depths for winter 84 m and for spring 2010, 44.5 m). In other words PC2 differentiated periods of stratified ocean from non-stratified or mixed conditions. The occurrence of mixed layer depths (ZM, Fig. 13a) and haptophytes (HAP) in the same co-ordinate plate shows that phytoplankton assemblages during those

periods (winter, W in Fig. 13a) were dominated by haptophytes. Mixed layer depths were deepest (76.7 ± 16.6 m) during winter (January 2009) and it was hypothesized in the previous chapter (Chapter II) that winter mixing eroded the chlorophyll fluorescence maximum (CFM) and subsequently brought the deeper community in the well lit surface layers along with nutrients facilating nano and microphytoplankton growth and abundance.

The phytoplankton community in the northern Gulf of Mexico was strongly controlled by mixed layer depths. The increase of relative abundance of haptophytes winter (See Fig 7, Chapter II) and spring 2010 with increased mixing were in agrrement with findings from other studies (Lindell & Post 1995, Steinberg et al. 2001) which suggests better adaptive ability of small-eukaryotes in higly dynamic environment in contrast with picoprokaryotes (cyanobacteria and prochlorophytes).

Previous studies in the Gulf of Mexico (Muller-Karger et al. 1991, Jolliff et al. 2008) have shown the occurance of high Chl *a* in slope and offshore waters of the Gulf of Mexico associated with deeper mixed layers and cooler temperature conditions. It can be concluded the thermal mechanism as described in those studies was also driving the phytoplankton community distribution during this study in slope waters. Deeper mixed layer and high TChl *a* suggest phytoplankton growth were fueled by upward flux of nutrients.

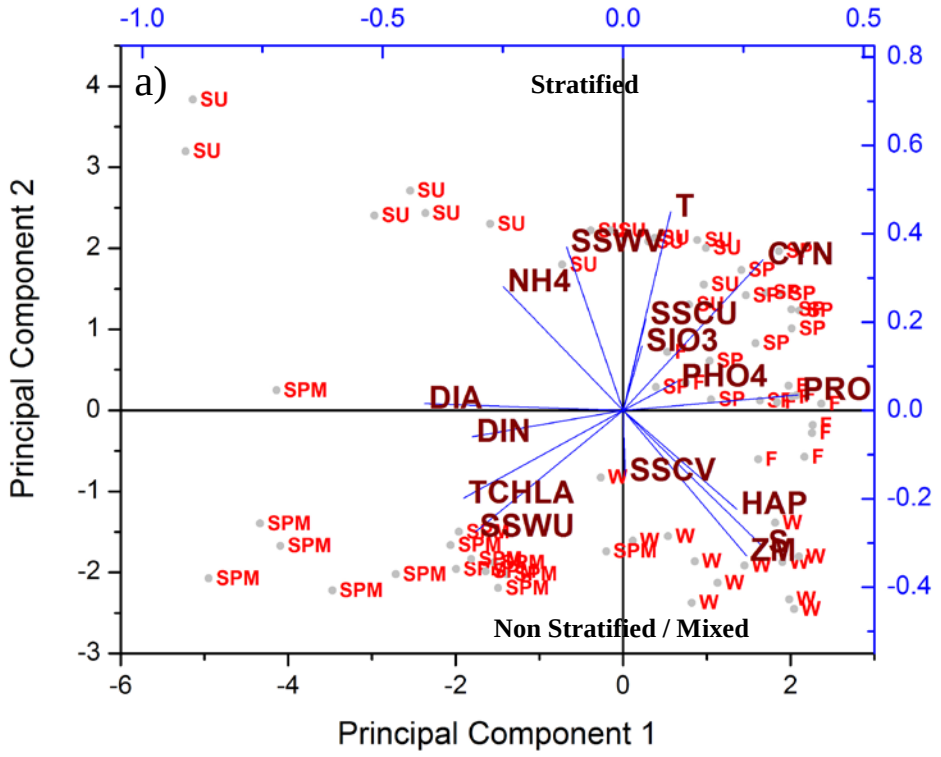

Figure 13. PCA bi-plot of the slope waters, surface (a), mid-depths (b) and deep (c). The objects are coded according to the sampling periods (W= winter, SP= spring 2009, SU = summer, F= Fall, SPM = spring 2010(March 2010)). The symbols used for physical and chemical variables are as follows T= temperature, S= Salinity, ZM = mixed layer depths, DIN= sum of nitrate and nitrite NO3+ NO2, NH4= ammonia, SIO3 = silicate, PHO4 = Phosphate, SSWU= wind speed u, SSWV= wind speed v, SSCU= current u, SSCV = current v. The symbols used for biological samples are TCHLA = total Chlorophyll a, DIA = diatom, HAP = haptophytes, CYN = cyanobacteria, PRO = prochlorphytes.

The effects of winds were also observed at the slope waters. Both diatoms and southwesterly (negative SSWU and SSWV) were negatively co-related with prochlorophytes and cyanobacteria, suggesting abundance of diatoms during east winds (Fig 10c). That was the case during summer when offshore transport of the Mississippi river occurred and resulted in high diatom abundance at several slope stations (See Fig. +8, Chapter II). The effects of winds and currents were also evident on the negative PC2

axis where most of the spring 2010 data clustered. The negative PC2 (Fig. 13a) axis showed that northwesterly (negative SSWU and positive SSWV) and TChl *a* (TCHLA) were negatively related to cyanobacteria (Table 8). High river discharge prior to the spring (March 2010) 2010 (Fig. 9) cruise and the northeasterly winds (Fig. 10a) facilitated the offshore extension of the river plume (i.e.in southern direction) leading to high TChl *a* and abundance of diatoms in the slope waters.

The slope waters at both depths (CFM and deeper waters) revealed interesting community variations. Fig. 13b for the mid-depths (50-100 m) mostly represents CFM samples except for winter (W, January 2009) and March 2010 (SPM) when no CFM was observed and water column was mixed (See Chapter II, Fig. 3e & 3f). The positive PC1 axis corresponded to CFM samples with biomass (range: 0.16 – 3.59 mg m^{-3} TChla) mostly dominated by prochlophytes (43.78 ± 22.5 %) during the stratified periods of summer, fall and some samples from spring 2009 (April-May 2009). Negative PC1 represented mixed periods, when samples collected from mid-depth (50-100 m) had low proportions of prochlorphytes (8.21 ± 12.61 %). Therefore the variability in the PC1 axis was mainly driven by the differences in phytoplankton community as function of water column stratification that was positively related to temperature (Table 8 and Fig. 13b). Positive PC2 axis for mid-depth clearly differentitaed high biomass and high nutrients from low biomass and low nutrient conditions

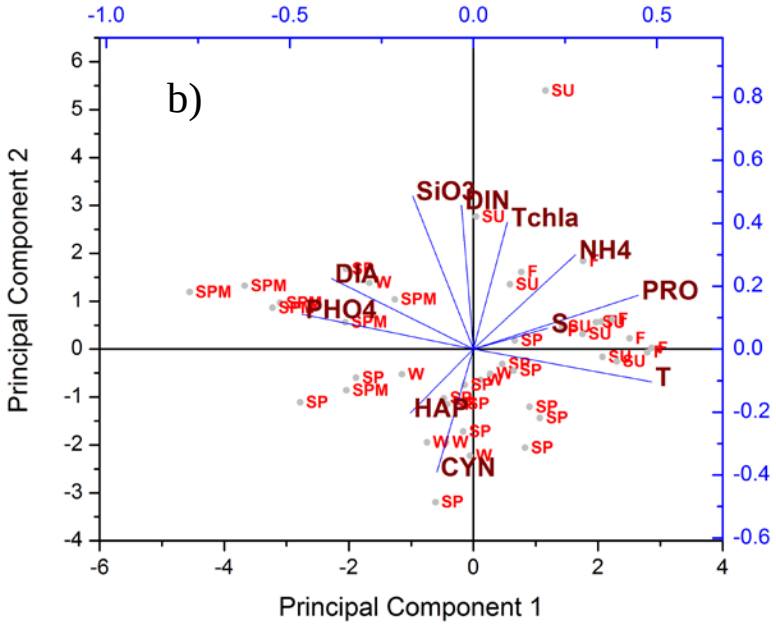

Figure 13. PCA bi-plot of the slope waters, surface (a), mid-depths (b) and deep (c). The objects are coded according to the sampling periods (W= winter, SP= spring 2009, SU = summer, F= Fall, SPM = spring 2010(March 2010)). The symbols used for physical and chemical variables are as follows T= temperature, S= Salinity, ZM = mixed layer depths, DIN= sum of nitrate and nitrite NO3+ NO2, NH4= ammonia, SIO3 = silicate, PHO4 = Phosphate, SSWU= wind speed u, SSWV= wind speed v, SSCU= current u, SSCV = current v. The symbols used for biological samples are TCHLA = total Chlorophyll a, DIA = diatom, HAP = haptophytes, CYN = cyanobacteria, PRO = prochlorphytes

The slope mid-depth waters at slope had high biomass (1.25 ± 1.75 mg m^{-3} TChla) during summer (July 2009), fall (Oct-Nov, 2009) and March 2010, while winter (January2009) and spring 2009 (April-May) had much lower (0.422 ± 0.14 0.43 mg m^{-3} TChla) biomass levels. During winter (W) and spring 2009 (SP) nutrients levels were lower (DIN= 0.77 ± 0.41 µM and SiO3 = 1.38 ± 0.48 µM) and community was mainly dominated haptophytes and cyanobacteria in contrast to diatoms during March 2010 (SPM).

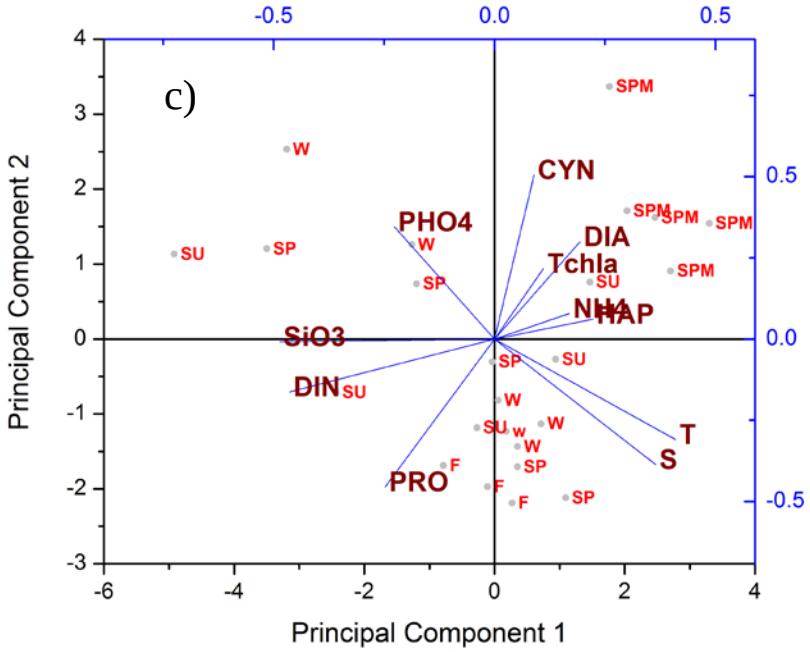

Figure 13. PCA bi-plot of the slope waters, surface (a), mid-depths (b) and deep (c). The objects are coded according to the sampling periods (W= winter, SP= spring 2009, SU = summer, F= Fall, SPM = spring 2010(March 2010)). The symbols used for physical and chemical variables are as follows T= temperature, S= Salinity, ZM = mixed layer depths, DIN= sum of nitrate and nitrite NO3+ NO2, NH4= ammonia, SIO3 = silicate, PHO4 = Phosphate, SSWU= wind speed u, SSWV= wind speed v, SSCU= current u, SSCV = current v. The symbols used for biological samples are TCHLA = total Chlorophyll a, DIA = diatom, HAP = haptophytes, CYN = cyanobacteria, PRO = prochlorphytes.

For deep (≥ 100 m) waters (Fig. 13c) the PC1 axis was mainly influenced by the physical and chemical properties of the water rather than the biology (Table 9). PC2 axis showed community differences. The close clustering of the March 2010 samples (SPM in Fig. 13c) shows that prochlorophytes were virtually absent during that period and cyanobacteria and diatoms dominated the community even at greater depth (≥ 100 m).

Table 9.

Factor Loading Matrix from Principal Component Analysis (first two PCs only) for Subsurface and Deep Samples only forEach Water Type. Extracted Eigenvectors from the PCA for the First two PCs. Bold number Denotes the Dominant Variables in each PCs Indicated by High Loading Values

	Estuarine Inner-shelf		Mid-shelf bottom		Slope CFM		Slope deep	
	PC1	PC2	PC1	PC2	PC1	PC2	PC1	PC2
TChla	**0.31484**	-0.21104	0.32871	0.17656	0.09243	**0.40373**	0.11046	0.21698
Diatom	-0.1565	-0.46655	**0.35733**	-0.13964	**-0.38701**	0.22438	0.19356	**0.29933**
	0.3038	-0.25472	0.23525	-0.36395				
Haptophyta	-0.31502	0.37438			-0.17175	**-0.2029**	0.22289	0.06147
Cyanophyta	0.18022	0.44788	**-0.31638**	0.37856	-0.09944	**-0.39069**	0.08948	**0.50506**
Prochlorophyta			-0.17081	-0.12723	**0.44864**	0.17125	-0.24707	**-0.45529**
Salinity	**-0.38933**	0.17093	-0.21313	0.36865	0.20247	0.06629	**0.3645**	-0.38661
Temperature	0.23638	0.38106	**-0.37304**	-0.05143	**0.48562**	-0.10374	**0.40959**	-0.30912
DIN	**0.30663**	0.05266	-0.22518	-0.01936	-0.03259	**0.45786**	**-0.46347**	-0.16236
SiO_3	**0.4495**	0.12835	-0.05565	0.5124	-0.16562	**0.48636**	**-0.48602**	-0.00826
PO_4	0.05214	-0.36397	0.27932	0.38275	-0.4673	0.11112	-0.22666	0.34569
NH_4	0.38226	0.07754	0.40525	0.14436	0.2781	0.29972	0.16904	0.07889

Conclusions and Implications

The main objective of this study was to use principal component analysis (PCA) to relate environmental variables to different phytoplankton groups derived from CHEMTAX analysis. The results from this study provide strong evidence of associations of different phytoplankton groups with specific environmental conditions. In the northern Gulf of Mexico diatoms and cryptophytes dominated phytoplankton assemblages in the estuarine and inner shelf water while cyanophytes and prochlorophytes dominated the slope waters. Haptophytes were found to be ubiquitous in all water types and co-existed with other major groups at different periods during the study. Based on the variables examined in this study, it can be concluded that shifts in phytoplankton community in the estuarine and inner shelf waters for most of the study period were controlled by river discharge (salinity) and nutrient dynamics. Thermally driven water column mixing regime was found to be the dominant physical forcing controlling the phytoplankton community in mid-shelf and offshore slope waters. Seasonal variations in wind and current directions in the region also played a strong role in phytoplankton community distribution.

Sea surface temperature, water column stability is projected to change under future global warming scenarios. The relationships showed in this studies will be helpful in understanding the critical role of phytoplankton in the food-web structure and biogeochemical cycles (i.e., easily grazed diatoms and consequent transfer of energy to higher trophic levels versus smaller prochlorophytes and cyanobacteria) under current and potential future changes occurring in the northern Gulf of Mexico. The environmental factors that were primarily linked to the phytoplankton community structure, such as temperature, mixed layer depths, winds, and salinity are measurable by

satellites. The relationships from this study would also be useful in modeling studies trying to predict future climate change scenarios using satellite data products.

CHAPTER IV

VARIATION IN LIGHT ABSORPTION COEFFICIENTS OF PHYTOPLANKTON, NON-ALGAL PARTICLES AND COLORED DISSOLVED ORGANIC MATTER IN THE RIVER INFLUENCED CONTINENTAL MARGIN OF NORTHERN GULF OF MEXICO.

Introduction

Continental margins despite their relatively small size (~ 7% of world ocean surface area) may contribute significant to global biogeochemical cycles. This is particularly apparent in the case of large river systems, which are characterized by large exports of freshwater and terrestrial organic and inorganic materials. The northern Gulf of Mexico (NGOM) is a large river dominated continental margin (D'Sa et.al. 2006, 2007; Green et al. 2008) strongly influenced by the Mississippi-Atchafalaya river system. The NGOM receives a large amount of terrestrial organic matter from different freshwater sources; annually the Mississippi (MS) River alone delivers ~ 2 x 10^{11} kg $yr^{-1}$of suspended sediments and ~ 3.1 x 10^{9} kg $yr^{-1}$of DOC (Green et al. 2008) into the NGOM shelf. The lack of knowledge or understanding of the different biogeochemical processes occurring in the continental margins have left them largely ignored in estimates of global carbon budgets (Robbins 2009). Scientific community has directed much of its attention towards a regular monitoring of the coastal waters of NGOM for some time now to understand the key biogeochemical processes in the region (Cai 2003, Green et al. 2006, Dagg et al. 2008, Lohrenz et al. 2008a, Bianchi et al. 2010, Bianchi 2011, Fennel et al. 2011).

Use of remote sensing has been shown to be a n effective tool in monitoring various coastal regions (Ref). Various algorithms have been developed that derive inherent optical properties (IOPs) such as absorption, attenuation, scattering and backscattering from remotely sensed water leaving radiances or remote sensing reflectance (Morel & Maritorena 2001, IOCCG 2006). In addition, various algorithms have also been developed for estimation of important biogeochemical variables including Chl *a*, phytoplankton taxonomic groups and cell size (Ciotti et al. 2002, Brewin et al. 2011), particle composition and size distribution (Boss et al. 2004, Kostadinov et al. 2012), particulate organic carbon (POC) by Stramski et al. (2008), Son et al. (2009) and (Allison et al. 2010), dissolved organic carbon (DOC), (Siegel et al. 2005). The application of remote sensing for characterizing the variability of these biogeochemical parameters has been critically important in advancing our understanding of carbon cycling processes and transport of organic matter in coastal and open ocean waters. However application of such remote sensing algorithms in coastal waters are particularly challenging because of their optically complex environment. The NGOM, influenced by Mississippi (MS) and Atchafalaya (ATF) rivers provide a clear example of a system largely dominated by Case 2 waters (i.e., optical variability is influenced by non-phytoplankton materials such as colored dissolved organic matter (CDOM) and non-algal particles (NAP) that may or may not co-vary with phytoplankton) CDOM(Sathyendranath, 2000). Prior work in this region have demonstrated that retrieval of IOPs in NGOM may be hampered by relatively high abundance of CDOM and NAP (D'Sa et al. 2007, Green et al. 2008b). Recent studies in the region (D'Sa & Miller 2003, D'Sa et al. 2007, Green et.al 2008b) though temporally restricted have provided critical

information on the chemical (e.g. Chen and Gardner, 2004, Conmy et.al., 2004, D'Sa et.al., 2009) and physical (D'Sa & Miller 2003, D'Sa et al. 2006, D'Sa et al. 2007, Green et al. 2008b), nature of the variability among light absorbing constituents of NGOM. Such studies have pointed out the need to expand the available observations to better constrain the uncertainties associated with ocean color algorithms (OCAs) and to allow them to be tuned specifically for the NGOM (D'Sa and DiMarco, 2009).

There are few IOP measurements that extend beyond the 100m isobaths in the NGOM. This study describes an unprecedented set of bio-optical data acquired during five cruises from January 2009 to March 2010 covering the major portion of the river influenced continental margin of NGOM (Fig. 14). The combination of large inputs of freshwater and associated terrestrial materials coupled with strong gradients in salinity and associated biogeochemical processes in the NGOM result in complex (both spatially and temporally) optical conditions. To better address such complexity , the NGOM was partitioned into different domains, including 1) nutrient rich, high biomass estuarine and large and small inland bay (<20m) waters, 2) inner shelf (<50m) waters heavily influenced by large river systems (MS & ATF) and 3) transitional mid shelf waters (~50-200m), and 4) oligotrophic slope or offshore (> 200m) waters outside the direct influence of rivers having optical characteristics of open ocean ; oligotrophic conditions. The primary hypothesis of this chapter was that winds and river forcing strongly influences the spatio-temporal variability of bio-optical properties in NGOM. Effects of winds and river extend beyond the source of freshwater discharge across the continental margin to the midshelf and slope waters.. A secondary hypothesis was also examined, that the

spectral characteristics of CDOM and NAP are influenced by algal processes and consequently will vary in relationship to algal biomass.

One of the goals of this study was to explore and analyze the spatial and temporal variations of the major light absorbing components (phytoplankton, NAPs, CDOM) in each of the environmental domains and the relationships to riverine inputs and other controlling factors. A secondary objective was to create an absorption budget for the continental margin of NGOM in an effort to assess the relative importance of each light absorbing component to total non-water light absorption. Finally, the performance was assessed of an ocean color algorithm, the Quasi-Analytical Algorithm (Lee et al. 2002), was tested in these waters for retrieval of the dominant light absorbing constituents using ocean color water leaving radiance or remote sensing reflectance.

Materials and Methods

Data Collection

Water samples were collected on board R/V Cape Hatteras (January, April-May, July, 2009 and March 2010) and R/V Hugh R. Sharp (October-November, 2009)during 5 cruises that took place in January, April, July, October 2009 and March 2010. Eight transects were made across the NGOM, encompassing large gradients across the continental margin, from highly turbid estuarine conditions to clear blue open ocean (slope) waters. Water samples were collected at each station using 10 L Niskin bottles mounted on a CTD (SeaBird SBE911 plus) rosette system. Samples were subsequently filtered for particulates, CDOM absorption and phytoplankton pigment analysis.

CDOM Absorption Measurements

Seawater samples were filtered under low vacuum through 0.22 µm polycarbonate filters pre-rinsed with 50ml Milli-Q water. The filtrate was immediately stored at 4˚C in acid cleaned and Milli-Q rinsed 250 ml amber glass (Teflon-capped) bottles . Prior to analysis, the samples were allowed to come to room temperature to reduce the chance of any bias occurring due to temperature difference between the sample and the Milli-Q reference. CDOM absorbance of the filtered water was measured at 1nm intervals from 250-800 nm in a 10 cm quartz cuvette using a bench top spectrophotometer (Cary 300). A baseline correction was made by subtracting the mean absorbance between 650-680 nm from the spectrum to remove instrument baseline drift and refractive effects. The measured absorbance (A [λ]) values were converted into absorption coefficients, a_{CDOM} (λ) (m^{-1}) according to

$$a_{CDOM}(\lambda) = \frac{2.203 \cdot A(\lambda)}{l} \quad (1)$$

where *l* was the path length of the cuvette. The spectral slope (S_{CDOM}) for each spectrum was calculated by applying a nonlinear, least-square fit to the measured a_{CDOM} (λ) values between 350-500nm (Babin et al. 2003b). The fit was performed using the raw (i.e. non log-transformed) data (Twardowski et al. 2004):

$$a_{CDOM}(\lambda) = a_{CDOM}(\lambda_r) e^{(-S_{CDOM}(\lambda - \lambda_r))} \quad (2)$$

In addition, the spectral slope for the 275-295 nm wavelength range, $S_{275\text{-}295}$ (nm^{-1}), was also calculated by assuming an exponential form and using a linear fit of log-linearized a_{CDOM} (λ) (Helms et al. 2008).

Phytoplankton and NAP Absorption Measurements

For particulate absorption measurements, seawater volumes of 0.2-2.5 l, depending on the amount of material present in the sample, were filtered onto 25mm Whatman GF/F glass-fiber filters at low vacuum. Immediately following filtration the filters were stored in liquid N_2 until laboratory analysis. The absorption spectrum of the particles ($a_p(\lambda)$) retained on the filter was measured with a bench top spectrophotometer (Cary 300) using the quantitative filter pad technique (Lohrenz et al. 2003b). Filters were placed on a glass slide and moistened with a few drops of 0.2 µm filtered seawater. A clean GF/F filter soaked in 0.2 µm filtered seawater was used as a reference blank. The spectrophotometer (Cary 300) equipped with a 70 nm (diameter) integrating sphere (Labsphere, Model DRA-CA-30I), absorbance was measured between 300-800 nm. All spectra were baseline-corrected by subtracting the mean absorption for the range 750-800 nm from the entire spectrum. Total particulate absorption, a_{fp}, was calculated from absorbance according to Lohrenz (2000) as follows;

$$a_{fp} = \frac{a_s^*}{\beta\, d_g\,(1-a_s^*)} \qquad (3)$$

where a_s* is the global sample absorption as defined by Tassan and Ferrari (1998), β is the path-length amplification factor, and d_g is the geometric path-length, equivalent to the product of volume filtered and the clearance area of the filter. The above-mentioned equation was applied to total and methanol-extracted absorption spectra to obtain total and detrital (NAP) absorption. For determination of absorption coefficients of NAP, $a_{NAP}(\lambda)$, pigments were extracted from the filters by soaking in hot methanol for 30 min. The extracted filters were rinsed with small volumes (10-20 mL) of Milli-Q water to

ensure removal of the biliproteins and the excess methanol and finally rinsed with filtered (0.2 µm) seawater. $a_{NAP}(\lambda)$ was estimated from absorbance using an approach analogous to that for $a_p(\lambda)$. Phytoplankton absorption coefficients ($a_\varphi(\lambda)$) were determined by subtraction of non-algal particulate absorption from total particulate absorption as:

$$a_\phi(\lambda) = a_p(\lambda) - a_{NAP}(\lambda) \quad (4)$$

A non-linear exponential function was fitted to all NAP spectra to determine the spectral slope coefficient of NAP (S_{NAP})

$$a_{NAP}(\lambda) = a_{NAP}(\lambda_r)e^{(-S_{NAP}(\lambda - \lambda_r))} \quad (5)$$

where λ_r is the absorption at the reference wavelength (443 nm). The fit was performed according to Babin et al. (2003b) on the raw (i.e., not log-transformed) data. Each fitted curve was individually checked for any kind of spectral artifacts and subsequently twenty two spectra out of 475 were discarded.

SPM

Concentrations of SPM in seawater were determined by filtering 0.05-3.5 l of seawater under low vacuum onto pre-weighed 0.4 µm Nucleopore filters. The volume filtered was a function of the amount of material in the water and filtration continued until flow slowed due to accumulation on the filter. After filtration, the filters were rinsed with deionized water to remove residual salts. The filters were preserved in a -20˚C freezer for the duration of the cruise and subsequently in a -80˚C freezer until analysis. Within two months of the sampling date, the dry mass of the particulate material on the filter was determined by drying the membrane filters for 12h at 80˚C and weighing with a

OHAUS Discovery microbalance (resolution 0.00001 mg) The drying and weighing were repeated until weights were stable.

Statistics

Station groupings corresponding to the cluster analysis in Chapter II were used in this study. Pair-wise comparisons were made of mean values of optical parameters and significant differences were identified according to the criteria given by Sokal and Rolf (1973). Kolmogorov-Smirnov and Shapiro-Wilk tests were employed to test the normality of the distribution for each of the variables including total chlorophyll a (TChl *a*), a_{φ} (440), a_{CDOM}(440) and a_{NAP}(440). All data were log-transformed prior to statistical analyses according to Campbell (1995). Additionally, post-hoc Tukey HSD (honestly significant difference) and Fisher LSD (Least Significant difference) multiple comparisons were made to verify statistical significance of difference between data pairs. In the case of non-normal distributions, the non-parametric Kruskal Wallis test was used, which is analogous to an ANOVA.

Satellite Data Processing

Level 2 daily satellite derived chlorophyll data from Aqua-MODIS were acquired from the National Aeronautics and Space Administration (NASA) Ocean Biology Processing Group (OBPG), website (http://oceancolor.gsfc.nasa.gov/) for the cruise periods except the summer cruise when no good image was available from Aqua-MODIS. The Aqua-MODIS Level-2 Chl *a* daily data was derived using the OC3 empirical algorithm (O'Reilly et al. 2000).The derived Chl *a* product was fit to a Mercator projection using SeaDAS 6.2 (http://seadas.gsfc.nasa.gov/) with a nominal spatial resolution 1km. A time window of ± 24 hours between in-situ sampling and satellite overpass was chosen for the data match-ups and comparison.

The Quasi Analytical Algorithm (QAA) (Lee et al. 2002) was applied to the MODIS remote sensing reflectance (R_{rs},(sr^{-1}) products to produce satellite-derived estimates of $a_{\varphi}(\lambda)$ and $a_{dg}(\lambda)$. These products were compared to *in-situ* observations of a_{φ} (λ) and $a_{CDOM}(\lambda) + a_{NAP}(\lambda) = a_{dg}(\lambda)$. QAA cannot separately retrieve $a_{CDOM}(\lambda)$ and a_{NAP} (λ) as would be directly analogous to the in situ measurements. This necessitated a comparison to the combined product of $a_{dg}(\lambda) = a_{CDOM}(\lambda) + a_{NAP}(\lambda)$. In addition to the QAA algorithm, there are other semi analytical algorithms (IOCCG 2006). However, the analyses here was restricted to the QAA because of its simplicity in application and additionally it generated greater positive absorption values and fewer pixel failures in comparison to others algorithms (e.g., GSM) for the conditions in this study. Satellite matchups were estimated as the mean of a 3 x 3 pixel (1km/pixel) window centered on the location of a given in situ observation within a time interval of ± 24 hours between in-situ sampling and satellite overpass.

The performance of ocean color algorithms for estimation of absorption constituents and total chlorophyll was evaluated by comparison to in-situ data collected during the field campaigns. Algorithm performance was evaluated using the mean absolute percentage difference ($|\psi|$) estimated as

$$|\psi| = \left(\frac{1}{N}\sum_{i=1}^{N}\frac{|y_i - x_i|}{xi}\right).100\% \quad (6)$$

Root mean square errors (RMSE) were determined for both linear and log scales as

$$RSME = \sqrt{\frac{1}{N}\sum_{i=1}^{N}(y_i - x_i)^2} \quad (7)$$

$$RSME\_log = \sqrt{\frac{1}{N}\sum_{i=1}^{N}(logy_i - logx_i)^2} \quad (8)$$

Finally, bias (δ) in derived products was determined as

$$\delta = \frac{1}{N}\sum_{i=1}^{N}(logy_i - logx_i) \quad (9)$$

Chl *a* and IOPs data from ship-based observations were log transformed prior to computation of RMSE and bias metrics as described in Campbell (1995).

Results

Seasonal Variations in River discharge and Wind fields.

The physico-chemical properties of the different water types encountered during the study have been discussed previously in Chapters II and III. In summary, four major water types were identified (See Chapter II, Fig, 1); (1) Estuarine waters (2) Inner-shelf, (3) Mid-shelf, and (4) Slope. The region is largely influenced by the discharge from Mississippi and Atchafalaya rivers. Discharge from the rivers varied in phase with one another as flow through the Atchafalaya from the Old River Control Structure is maintained such that about 25% of the Mississippi water is diverted (Goolsby et al. 1999). This flow is subsequently joined by the Red and Ouachita Rivers to form the Atchafalaya River, with a combined flow of about 30% of the total Mississippi-Atchafalaya discharge. High discharge occurred in 2009 occurred during late spring and discharge was lowest during summer(Table 10 and Fig. 14). Discharge from all major rivers remained relatively high in late 2009 and into early 2010. Winds in the region were predominantly from northern directions for the major portion of the study period (January 2009 to March 2010). Winds were generally southwesterly in summer (July 2009), southwesterly winds during summer facilitated offshore transport of the Mississippi river plume; this was previously discussed in Chapter III of this dissertation. Changes in wind direction have been shown to have a major effect on the direction of the Mississippi river

plume and the associated transport of terrigenous materials on to the continental shelf of NGOM (Salisbury et al. 2004).

Table 10

River Discharge table: Mean ± Standard Deviation (SD) of Flow Rates of the Mississippi, Atchafalaya, Alabama and Sabine Rivers in 10^3 $m^3 \cdot s^{-1}$ During the Respective Cruise Periods.

	Winter (Jan 2009)	Spring 09 (Apr-May)	Summer(July 2009)	Fall(Oct-Nov 2009)	Spring 10 (Mar-2010)
Mississippi	18.74 ± .1.18	22.77 ± 0.15	10.68 ± 0.22	22.85 ± 1.78	17.05 ± 0.8
Atchafalaya	7.44 ± 0.54	9.77 ± 0.2	4.53 ± 0.15	9. 76 ± 0.77	7.26 ± 0.34
Alabama	1.96 ± 0.71	0.92 ± 0.54	0.18 ± 0.03	1.08 ± 0.2	3.2 ± 0.91
Sabine	0.04 ± 0.014	0.33 ± 0.017	0.13 ± 0.03	1.21 ± 0.06	0.04 ± 0.03

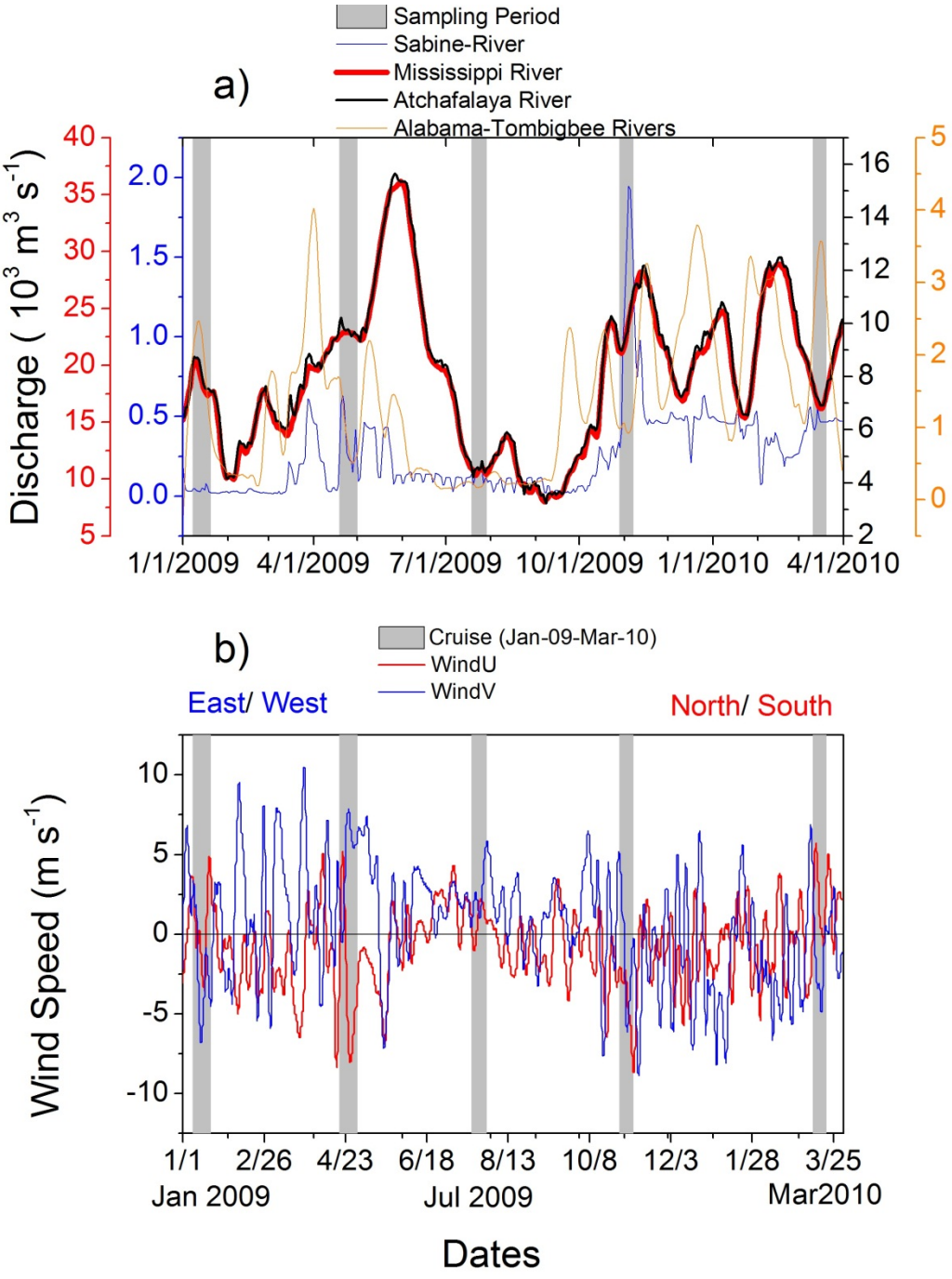

Figure 14. Daily discharge (10^3 m^3 s^{-1}) of the important rivers in the study region. (a) and b) Area averaged (biweekly) wind speed for the period of the study. River discharge was collected from (http://www.mvn.usace.army.mil/eng/edhd/wcontrol/discharge.asp) and the rest of the data for Sabine, Alabama and Tombigbee were obtained from USGS database (http://waterdata.usgs.gov/nwis/qw). Wind data were from MERRA available at http://disc.sci.gsfc.nasa.gov/giovanni/overview/index.html. Data have a resolution of 1.25 x 1.25.

Spatial and Temporal Variation in Absorption Components: CDOM

In general of CDOM absorption was characterized by relatively high coefficients of absorption ($a_{CDOM}(\lambda)$ (m^{-1})) in estuarine and inner shelf waters and lower values in mid-shelf and offshore waters (Fig. 15). The spectral shape of $a_{CDOM}(\lambda)$ (m^{-1}) could be represented by an exponential curve with increasing a_{CDOM} (λ) (m^{-1}) at decreasing wavelengths. Overall highest values of a_{CDOM} (412) were associated with estuarine and inland bays for all seasons with mean values ranging from 0.08-5.73 m^{-1}, and annual mean ± SD= 1.33 ± 1 m^{-1}. Values were particularly high at the end member stations of the Mississippi and Atchafalaya rivers (Fig. 16) and in some of the shallow stations near the mouth of the bays including Barataria (station B1), Terrebonne (C1), and Mobile Bay (A1) (See Chapter II, Fig.1). On average a_{CDOM} (412) in the estuarine region was highest (2 ± 1.64 m^{-1}, mean ± SD) during fall (Oct-Nov 2009) and lowest (0.88 ± 0.53 m^{-1}) during summer (July 2009) which corresponded with the periods of low and high river discharge (Fig 14a and Table 10), consistent with the hypothesis of riverine influence on the bio-optical properties. Besides fall coincides with the peak period of plant litter shedding in the swamps (Shen et al. 2012) of southern Louisiana, and previous works (Benner et al. 1990, Opsahl & Benner 1995, Hernes et al. 2007) have shown that plant litter can readily leach CDOM and lignin into the system. Seasonal differences were also significant in inner shelf waters between winter and summer (0.35 ± 0.27 $m^{-1}$and 0.22 ± 0.86 m^{-1}, respective mean ± SD) and spring 2010 (0.58 ± 0.18 m^{-1}. For the rest of the shelf , a_{CDOM}(412)) was significantly (ANOVA, $p<0.05$) higher in spring 2010 (March 2010 than in other periods (Fig 15 a & 15b). Exceptions occurred in slope during summer (July 2009) when several stations were impacted by the offshore transport of

Mississippi river plume waters. For these stations, $a_{CDOM}(412)$ levels (range 0.35 ± 0.14 m^{-1}) were on average ~ 7 times higher than at the non-plume impacted station (Fig 15d). The range of $a_{CDOM}(412)$ (0.02 - 5.7 m^{-1}) and a_{CDOM} (440) (0.0092- 3.6 m^{-1}) values observed during this study were comparable to previous studies in the NGOM continental margin (D'Sa 2008, Green et al. 2008b, Jolliff et al. 2008, D'Sa & DiMarco 2009, Schaeffer et al. 2011a, Shank & Evans 2011) and in other coastal waters at temperate latitudes (Vodacek et al. 1997, Babin et al. 2003b, Odriozola et al. 2007) and open ocean water (Siegel et al. 2002, Bricaud et al. 2010). Seasonal differences were also observed between surface and bottom a_{CDOM} (m^{-1}) (not shown, See Appendix G for differences in S_{CDOM}).

River discharge strongly influenced CDOM distributions in the continental margin of NGOM. A significant inverse relationship was observed between the a_{CDOM} (412) and salinity (Fig. 16), a regression relationship given by a_{CDOM} (412) = -0.069 + 2.5 (r^2 = 0.81, $p < 0.001$). This near conservative relationship was consistent for the entire continental margin during the study, a trend observed in other studies in the region (D'Sa et al. 2006, Del Castillo & Miller 2008, D'Sa & DiMarco 2009). Though similar in trend, the regression slope obtained from this study was higher than regression slopes previously reported by Del Castillo and Miller (2008) (-0.036) and -0.040 by D'Sa and DiMarco (2009). This study reports measurements from all five cruises (from Jan-Nov 2009 and March 2010) for the full salinity range 0-36 at the continental margin of NGOM, while the other two studies compared in Fig. 16a, were either limited in their salinity range (18-36) for D'Sa and DiMarco (2009) or in their spatial extent in being restricted within the Mississippi plume outflow region (Del Castillo & Miller 2008). The

regression slopes were comparable when narrower salinity (S) ranges were used, for example, -0.05 for inner shelf (S = 14-36) and -0.039 for mid-shelf and slope (S = 25-36) waters (regressions not shown). Despite a significant relationship between salinity and a_{CDOM} (412), large scatter in the data existed at salinities below 20 and at $a_{CDOM}(412) > 1.5\ m^{-1}$. Large differences in the $a_{CDOM}(412)$ values were observed between the Mississippi and Atchafalaya end member (S = 0) stations (Fig 16a), a consequence of the different degree of river-watershed interactions between those two systems (Chen et al. 2004, Conmy et al. 2004).

Spectral slopes of the a_{CDOM} are useful in characterizing CDOM as they vary in relationship to the composition, source and diagenetic processes (Zepp & Schlotzhauer 1981, Carder et al. 1989, Twardowski et al. 2004, Helms et al. 2008). Spectral slope values calculated in this study (Fig. 17a) spanned over the range 0.0085-0.0302 nm^{-1} with an average value of $0.0168 \pm 0.00257\ nm^{-1}$ and 15.4 % coefficient of variation (CV). Average $S_{CDOM(350-500)}$ values were similar to those reported by other studies for the region (e.g., D'Sa and DiMarco (2009) and in other coastal areas at similar latitudes (Babin et al. 2003b). However, the variability in $S_{CDOM(350-500)}$ observed in this study was larger than that observed by Babin et al. (2003b) for European coastal waters, but were similar to ranges reported by Ferreira et al. (2009) and Bricaud et al. (2010), these latter studies also encompassed different environmental regimes as encountered during the current study.

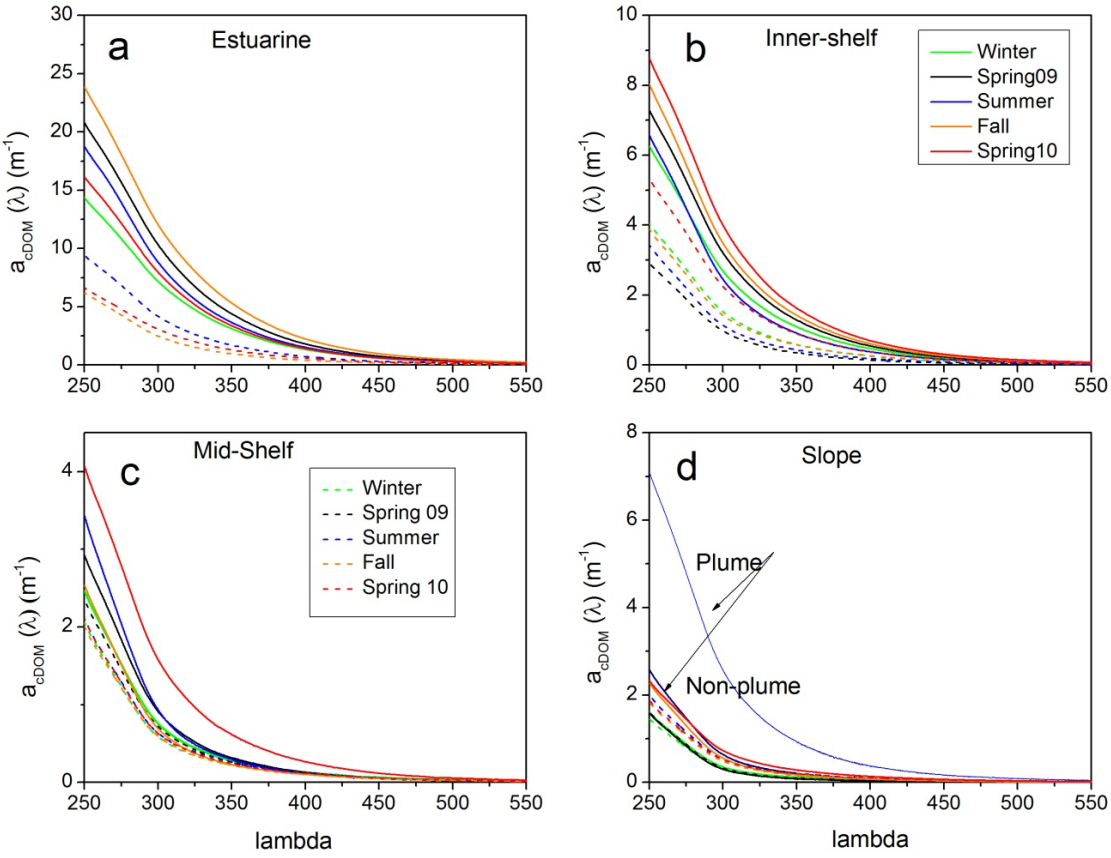

Figure 15. Mean spectra of CDOM absorption (a_{CDOM} (λ)) for all samples collected during each cruise at respective environmental domains (a-d). The differences in the average a_{CDOM} (λ) during summer at the slope stations are highlighted (d). The bold (‾) lines represents surface samples while the dashed (--) lines represents bottom and subsurface for estuarine (a), inner shelf (b) and midshelf (c) and deep samples for slope waters(d).

In addition to $S_{CDOM(350-500)}$, $S_{CDOM\ (275-295)}$ was calculated in this study as it has been reported to be good proxy of CDOM molecular weight (MW) and photo bleaching in aquatic environments (Helms et al. 2008). $S_{CDOM(275-295)}$ increased exponentially with salinity (Fig. 17b), and ranged between 0.014-0.034 in inner shelf and estuarine waters, with highest values occurring during the summer. $S_{CDOM(275-295)}$ ranges were higher in slope waters, ranging between 0.022-0.048. Lowest values of $S_{CDOM(275-295)}$ in slope

waters were observed in spring 2010 and summer 2009. Figure 18a & 18bshows the relationship between the two calculated slopes with CDOM absorption. A clear inverse trend was observed for $S_{CDOM(275-295)}$ (nm^{-1}) with increasing a_{CDOM} (440), and could be fit using a power law relationship given by $S_{CDOM(275-295)}$ (nm^{-1}) = 0.015 [a_{CDOM} (440)] $^{-0.2356}$ (r^2=0.91; N = 247). Such a relationships was not evident for $S_{CDOM(350-500)}$ (nm^{-1}) (Fig. 18a), rather a complex and variable pattern was observed. Such lack of consistent relationships between in $S_{350-500}$ (nm^{-1}) and CDOM absorption have been previously observed in several other studies (Vodacek et al. 1997, Babin et al. 2003b, Del Vecchio & Blough 2004, Helms et al. 2008).

Inverse relationships similar to that for $a_{CDOM(440)}$ were also observed between $S_{275-295}$ and total chlorophyll a (TChl *a*) (data not shown). A non-linear power law fit (See Appendix F) yielded the relationship $S_{CDOM(275-295)}$ (nm^{-1}) = 0.027 [TChl *a*] $^{-0.181}$(r^2 = 0.75, N= 235). Low values of $S_{CDOM(275-295)}$ (nm^{-1}) corresponded to high TChl *a* in the rivers and at slope water stations during spring 2010 and summer (plume stations). In contrast, no discernible pattern existed between TChl *a* and $S_{CDOM(350-500)}$.

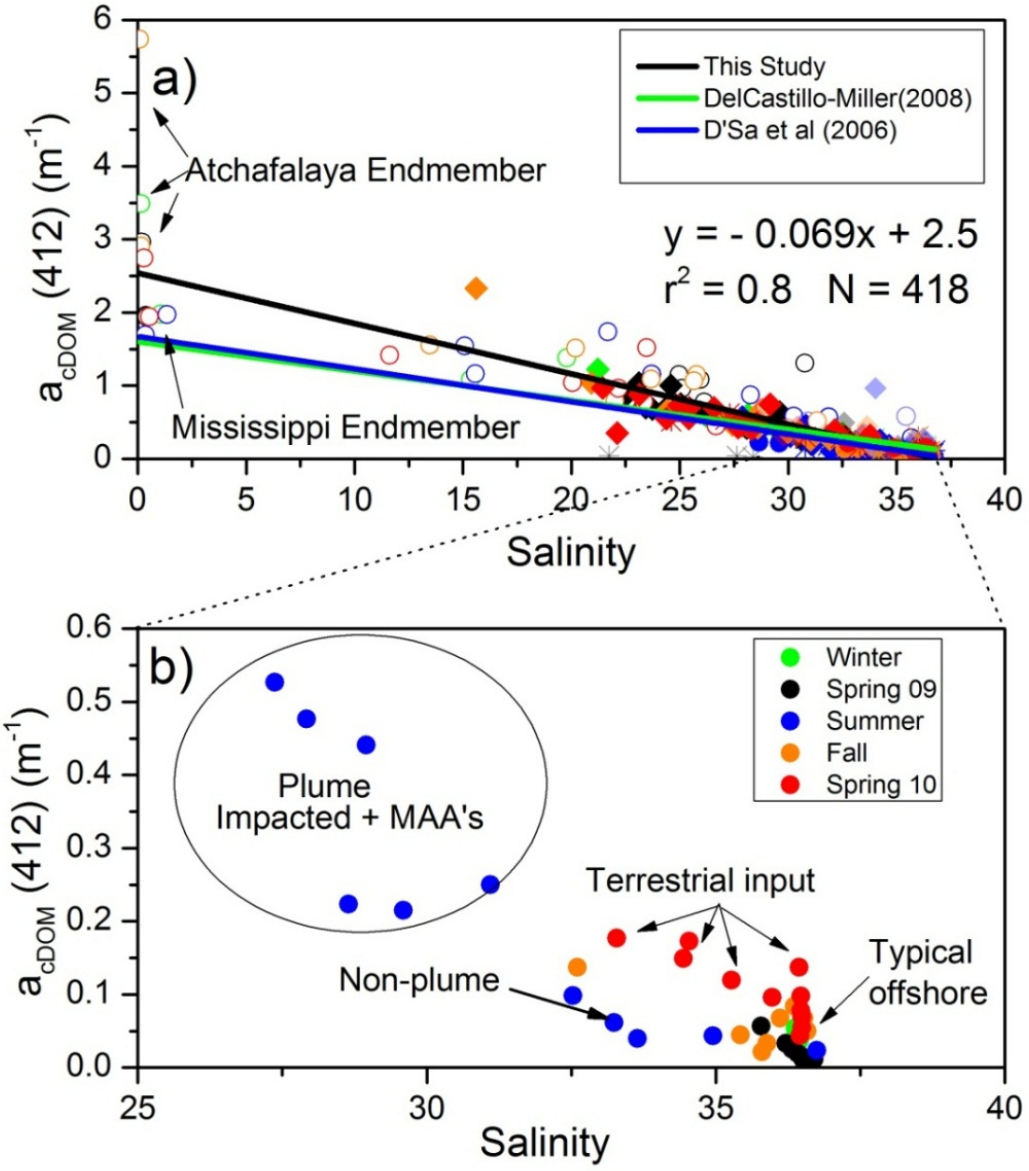

Figure 16. CDOM absorption at 412 nm as a function of salinity for the entire margin (a) and for the slope waters (b) to highlight the seasonal differences in surface CDOM absorption. The regression lines for this study (red) are compared with other studies (blue and green) in the region, reasons of differences among the regression lines are discussed in the results and discussion section.

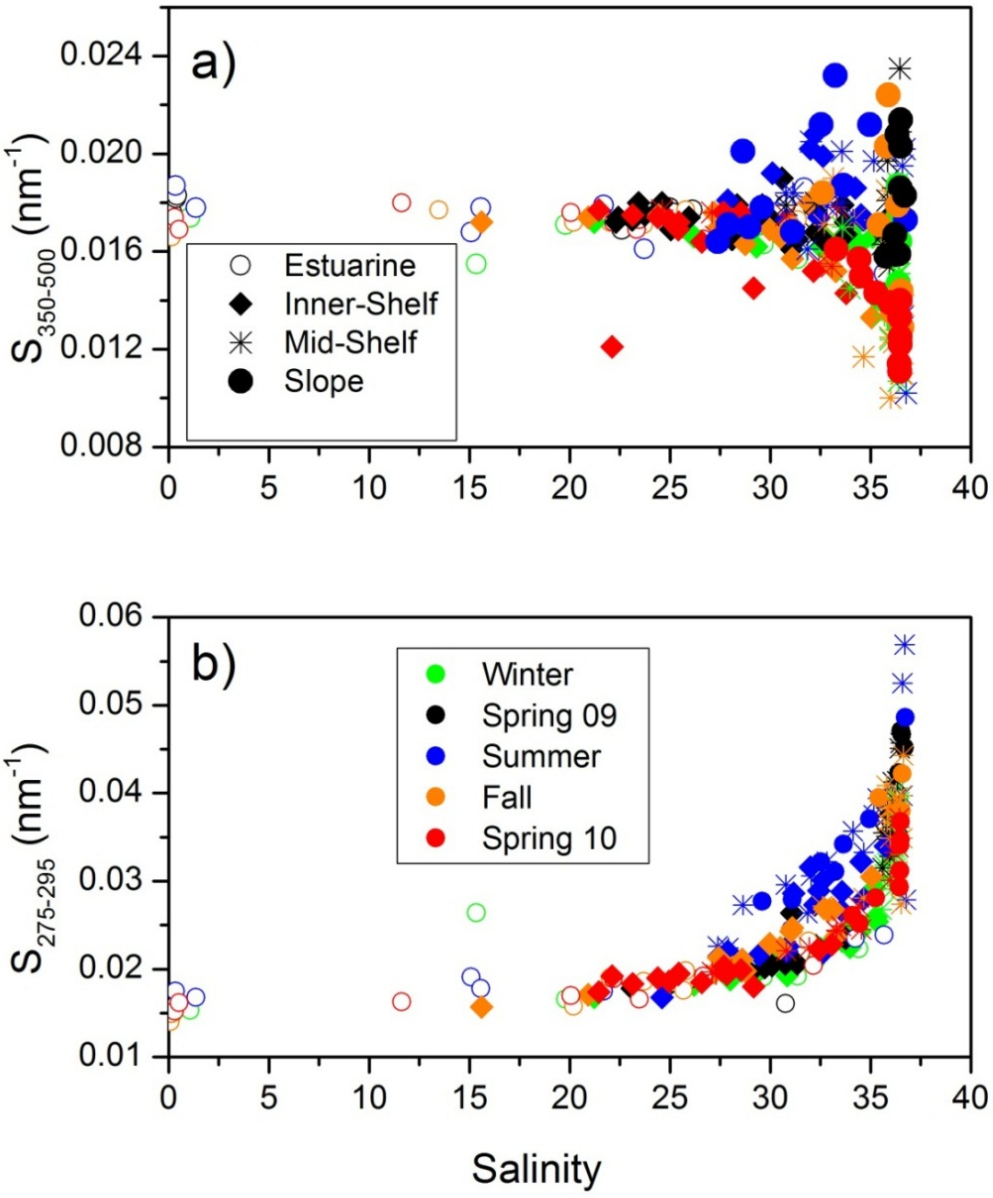

Figure 17. Relationship between salinity and CDOM spectral slope coefficients for wavelength ranges 350-500 (a) and 275-295 (b) for all cruise periods and water types. Note that water mass types were designated by symbol type and seasons by symbol color.

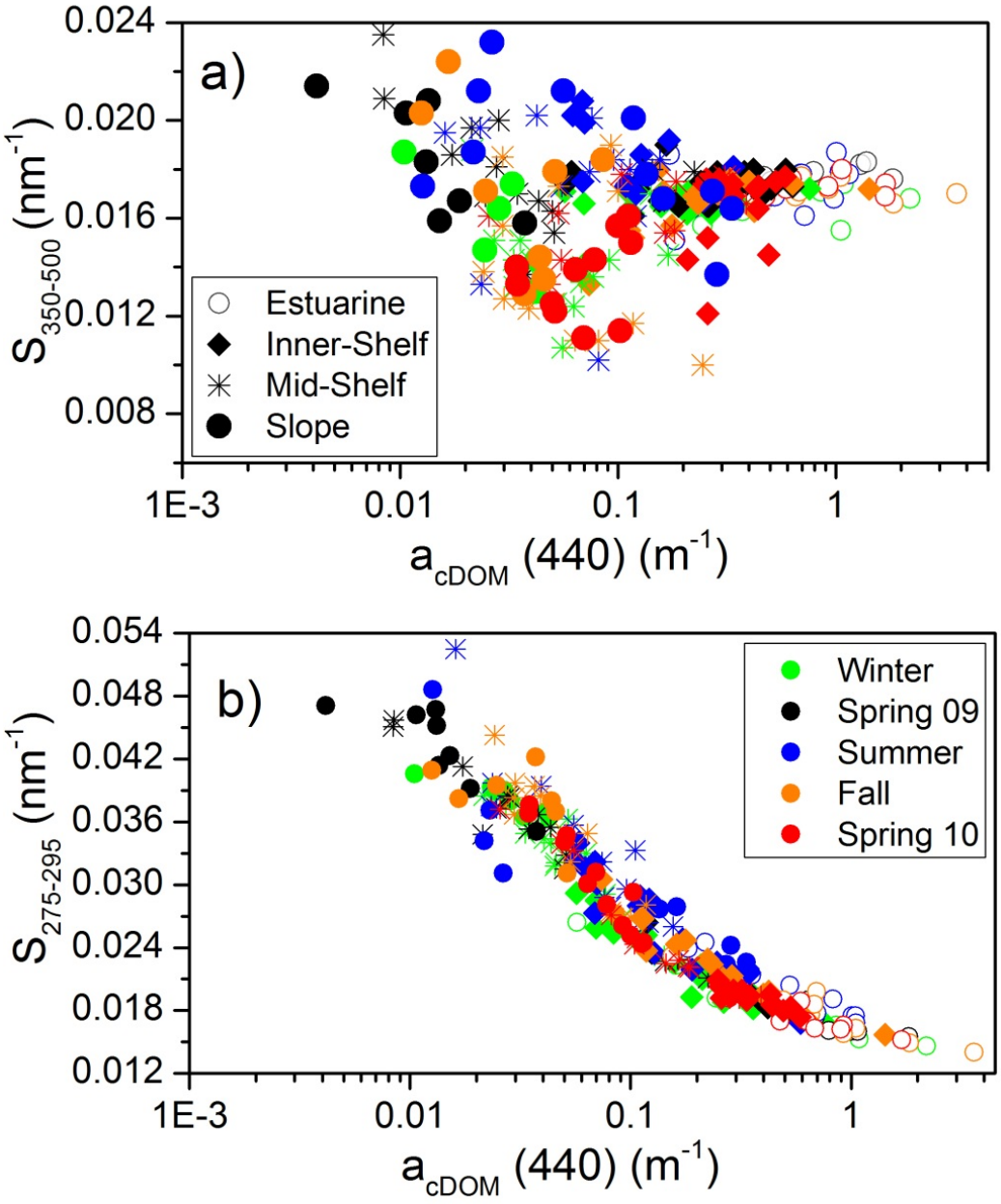

Figure 18. Relationship between $a_{CDOM}(440)$ and CDOM spectral slope coefficients for wavelength ranges 350-500 (a) and 275-295 (b) for all cruise periods and water mass types. Symbols as in Fig. 17.

Spatial and Temporal Variation in Absorption Components: Non-algal Particulate matter (NAP)

Large spatial and some seasonal variability in $a_{NAP}(440)$ were observed for the different water types (Figs. 19 and 20a). High values were mainly associated with the estuarine (range 0.14- 14.28 m^{-1}, mean ± SD = 2.18 ± 3.09 m^{-1}) and the inner shelf (0.06-4.29 m^{-1}, 0.17 ± 0.49 m^{-1}) water types. Seasonal variations in river discharge were reflected in the $a_{NAP}(440)$ values. $a_{NAP}(440)$ in estuarine waters was low during summer (low discharge) compared to other periods (ANOVA, $p < 0.05$), approximately 25 % of the mean $a_{NAP}(440)$ values (2.6 ± 3.44 m^{-1}). For inner shelf waters, $a_{NAP}(440)$ was higher during high discharge (Fig 14a and Table 10) in spring 2009 (0.427 ± 1.08 m^{-1}) and fall (0.162 ± 0.17 m^{-1}) , in comparison to other cruise periods (range, 0.5-0.11 m^{-1}) (ANOVA, $p <0.05$). Seasonal highs in $a_{NAP}(440)$ were associated with the end member stations for the Atchafalaya (E0) and Mississippi (MR1) rivers, and ranged from 2.25 to 10.92 m^{-1} and 1.45 to 14.28 m^{-1} respectively. a_{NAP} (440) values exhibited a significant relationship with salinity (ANOVA, $p< 0.05$), decreasing with increasing salinity (Fig. 20a) away from the direct influence of rivers.

The overall mean ± SD of a_{NAP} (440) in mid-shelf waters was 0.018 ± 0.02 m^{-1}(salinity range = 27-36.4) and 0.007 ± 0.0071 m^{-1} in slope waters (salinity range = 27.3 - 36.7) (Fig. 19, Fig 20a). a_{NAP} (440) at mid-shelf and slope waters also differed significantly between high and low discharge periods (Fig. 19c & 19d) $a_{NAP}(440)$ was also closely related to suspended particulate matter (SPM) (g m^{-3}) concentrations (Fig 20b), as evidenced by a strong relationship between them ($r^2 = 0.91$, $p < 0.001$, N= 229). The regression slope of the $a_{NAP}(440)$-SPM relationship observed in this study was

similar to the average regression slope reported for the area previously (D'Sa et al. 2007) and for other regions of world ocean (Babin et al. 2003b). Differences were also observed in a_{NAP} (440) between surface and bottom waters. These differences were particularly evident in inner shelf waters during summer and fall when NAP absorption was significantly higher in the bottom waters (not shown, See Appendix H).

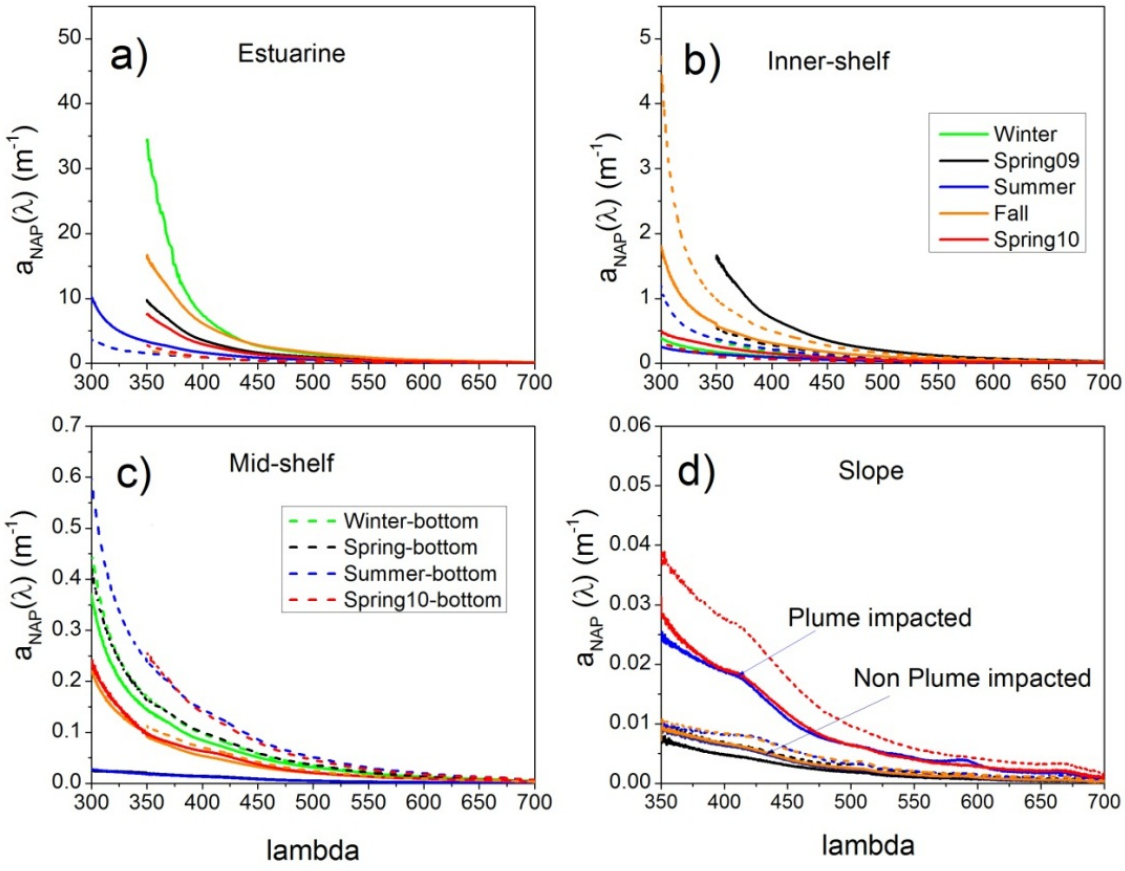

Figure 19. Mean spectra of NAP absorption (a_{NAP} (λ)) for all samples collected during each cruise at respective water mass domains (a-d). The differences in the average $a_{NAP}(\lambda)$ for plume- and non-impacted stations during summer at the slope stations are indicated (d). The solid (-) lines represents surface samples while the dashed (--) lines represents bottom and subsurface for estuarine (a), inner shelf (b) and mid-shelf (c) and deep samples for slope waters(d).

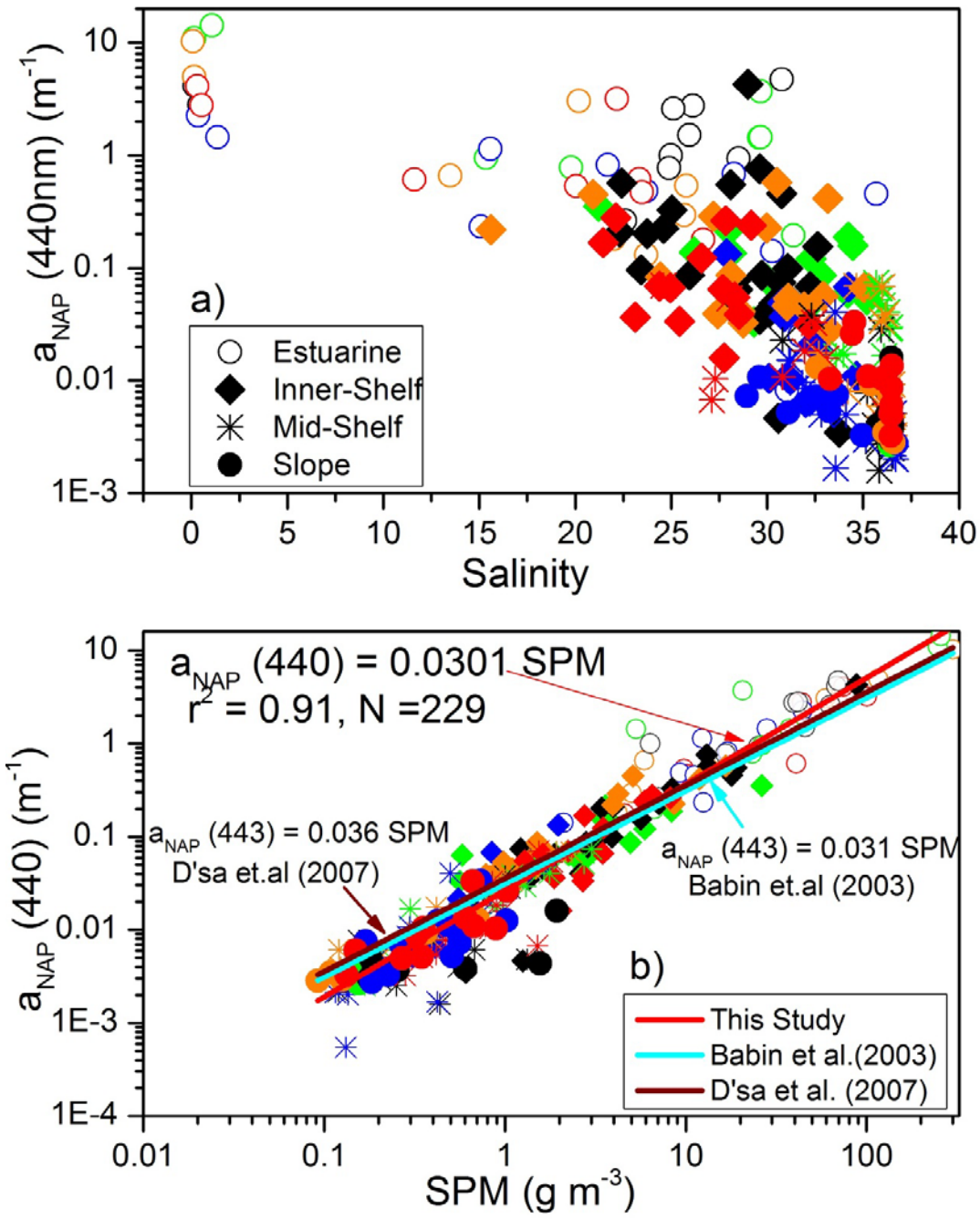

Figure 20. Scatter plots showing relationship between $a_{NAP}(440\ m^{-1})$ and salinity(a) and $a_{NAP}(440\ m^{-1})$ and SPM (g m^{-3}) at the continental margin of NGOM during the study(surface samples). The regression lines from Babin et.al (2003) and D'Sa et.al (2007) are plotted for comparison. Different cruise periods were indicate by symbol color as winter (January in green), spring (April in black), summer (July in blue), fall (Oct-Nov in Orange) 2009 and spring 2010 (March 2010, in red).

The spectral slope of the a_{NAP} (nm^{-1})-wavelength relationship, S_{NAP} (m^{-1} nm^{-1}), was determined for the wavelength range between 300-700 nm after (Babin et al. 2003b) Values of S_{NAP} spanned over a large range, from 0.008 to 0.02 m^{-1} nm^{-1} as observed previously in other studies in coastal waters (Roesler et al. 1989, Nelson & Guarda 1995). Variability in S_{NAP} (nm^{-1}) can be attributed to differences in particle size and composition (Babin et al. 2003a, Ferrari et al. 2003b, Bowers & Binding 2006). Babin et al. (2003b) in their study in European coastal waters observed a much narrower range of S_{NAP} (nm^{-1}) values (0.0116-0.0130 nm^{-1}). The wider range of S_{NAP} (nm^{-1}) values in the NGOM could be explained by the existence of various kinds of mineral and organic particles that are likely to affect the spectral properties of the non-algal component S_{NAP} (m^{-1} nm^{-1}) values observed in this study fell well within the range of S_{NAP} (m^{-1} nm^{-1}) previously published (Ferrari et al. 2003a, Binding et al. 2005, Bricaud et al. 2010) for similar water types.

High S_{NAP} values were observed in most estuarine and inner shelf stations and lower values associated with the mid-shelf and slope waters (Fig. 21a).Highest slopes (S_{NAP}) were mainly observed at the end member stations of the Mississippi and Atchafalaya rivers (Fig. 21a, open circles). Some exceptions to this trend existed particularly at several inner shelf stations (near the mouth of Terrebonne and Barataria Bay) where S_{NAP} values were consistently low throughout the course of the study despite of high TChl *a* (Fig. 21a).

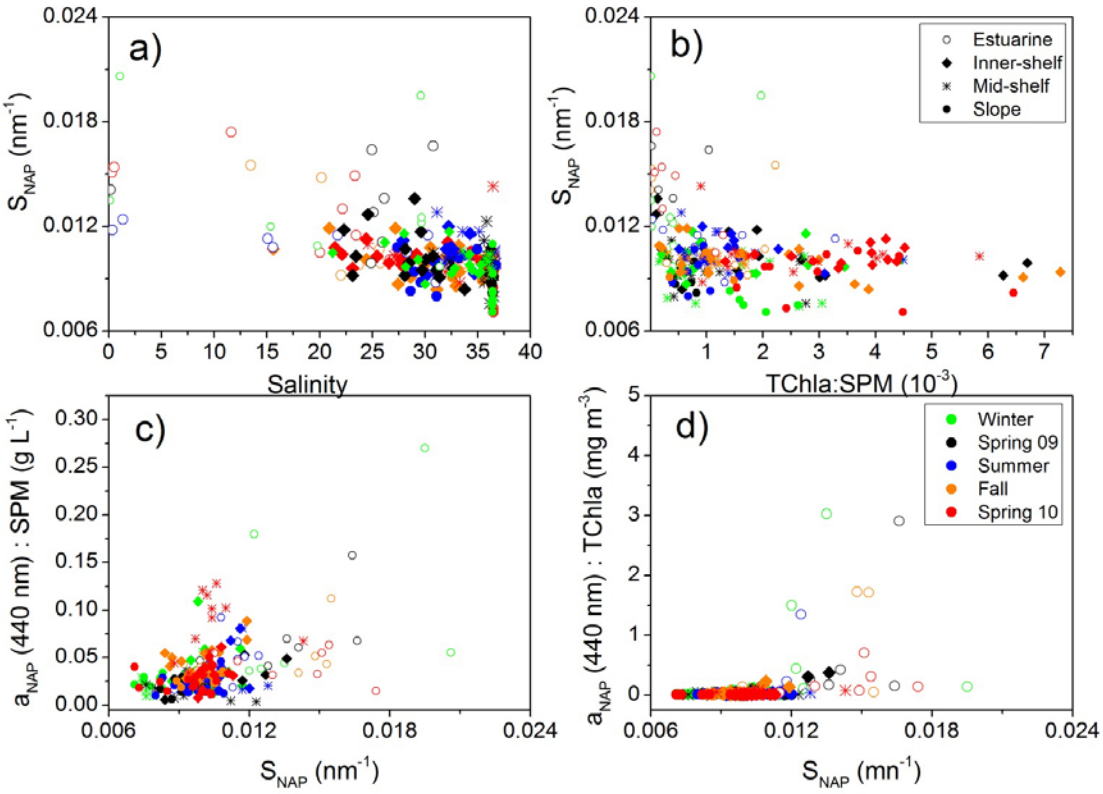

Figure 21. Relationship of spectral slope S_{NAP} with salinity (a), the ratio of TChl *a*: SPM (b), a_{NAP} (440) normalized to SPM (c), and TChl *a* (d) across the different water types in NGOM.

Spatial and Temporal Variation in Absorption Components: Phytoplankton Absorption

Variability in phytoplankton light absorption a_φ (λ) was observed both spatially and temporally (Fig 22a, b, c, d). Values of a_φ(440) were significantly (ANOVA < 0.05) higher in estuarine (0.37 ± 0.24 m^{-1}, mean ± SD) and inner-shelf (0.15 ± 0.12 m^{-1}) water types than in mid-shelf (0.03 ±0.03 m^{-1}) and slope (0.03 ± 0.023 m^{-1}) waters. Significant differences among stations (ANOVA, $p < 0.05$) were also observed within water types. Mean values of a_φ(440) at the estuarine stations of Terrebonne bay (C0) and the Atchafalaya (E1) and Mississippi (MR2) rivers were consistently higher (approximately

three times greater) than other estuarine stations (overall mean for all cruises of 0.28 ± 0.19 m^{-1}). Those estuarine stations with high $a_\varphi(440)$ values were also associated with some of the highest values of TChl *a* during the study. Previous studies in the region (e.g., Lohrenz et al. (1999)) have shown high biomass and productivity in the mid-salinity region of the Mississippi river plume (MR2 in this case).

Seasonal differences were also observed within each region. For the inner shelf waters, values of $a_\varphi(440)$ were significantly higher during both the 2009 and 2010 spring cruises (average 0.21 ±0.14 m^{-1}) compared to that of winter (0.1 ± 0.1 m^{-1}), fall (0.12 ± 0.017 m^{-1}) and summer (0.08 ± 0.06 m^{-1}). Values of a_φ (440) during spring 2010 were twice the mean a_φ (440) values observed for other seasons (0.03 ± 0.02 m^{-1}, median 0.026 m^{-1}). Similarly, for slope waters a_φ (440) was significantly higher during spring 2010, ranging 0.026-1.1 m^{-1}, compared to other periods (mean $\pm$ SD, 0.02 ± 0.011 m^{-1}). Additionally, during summer 2009 Mississippi river water extended onto the continental slope of the NGOM and impacted several stations. Values of $a_\varphi(440)$ for those stations (0.032 ± 0.013 m^{-1}) were double that of the non-plume impacted stations (0.015± 0.005 m^{-1}) (Fig. 24c)

Phytoplankton absorption in the UV. In order to understand the variability of phytoplankton absorption spectra in the UV range measurements were extended into the ultraviolet region for a subsets of samples of UV absorption properties among water types and cruise periods (Fig. 22). Absorption peaks were observed around 320 nm for summer (in slope waters) and spring 2010 indicating presence of microsporine-like amino acids (MAAs). Production of MAAs by algal cells has been previously described (Morrison & Nelson 2004), and observations in this current study of absorption

signatures characteristic of MAAs particularly during the summer months is consistent with a photo protection function as previously described. The presence of absorption peaks typical of MAAs were primarily restricted to surface waters, and were also mainly present at the non-plume impacted stations. The ratio of $a_{\varphi}(320)/ a_{\varphi}(365)$, often used as an index of MAA (Bricaud et al. 2010), ranged from 2.1- 4.4 at all the non-plume stations during summer in slope waters, while values for plume impacted stations were less than 2. Differences in UV absorption features were also observed among different spectra, which was probably due to the presence of different types of MAAs (Laurion et al. 2003, Laurion et al. 2004).

The relationship of $a_{\varphi}(440)$ to TChl *a* (mg m^{-3}) for all cruises was highly significant ($r^2 = 0.76$, N=264, $p<0.001$) (Fig. 23a, Table 11). The relationship found in this study was similar to that reported by other previous studies with larger spatial domains (Bricaud et al. 1998, Bricaud et al. 2004). A strong relationship was also observed between $a_{\varphi}(676)$ and TChl *a* (Table 11 and Fig.23b). This was expected as Chl *a* is the primary absorbing pigment at 676 nm, while at blue wavelengths around 440nm, other pigments besides Chl *a* also contribute to absorption. In addition to pigment composition, phytoplankton light absorption can also be significantly affected by the differences in size structure and pigment packaging (Kirk 1994, Bricaud et al. 1995, Bricaud et al. 2004)

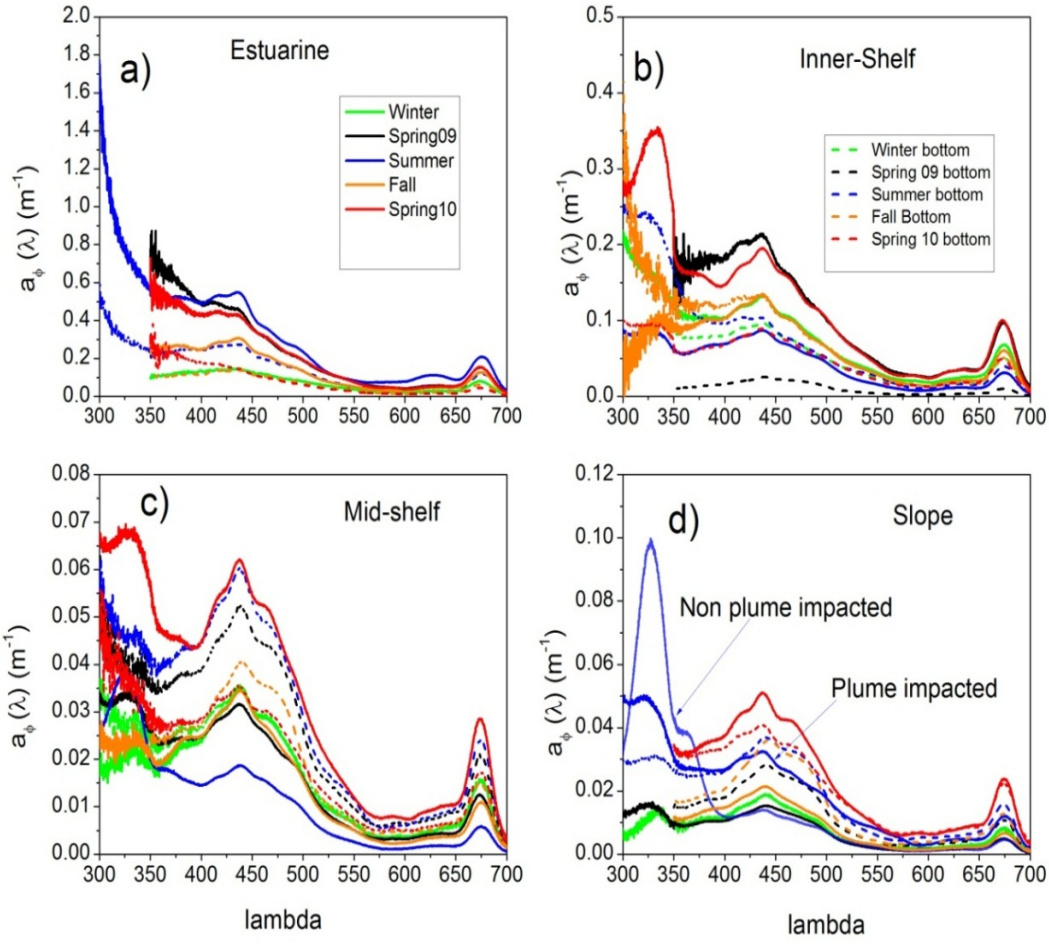

Figure 22. Mean spectra of phytoplankton absorption ($a_\varphi(\lambda)$) for all samples collected during each cruise at respective water mass domains (a-d). Mean values of $a_\varphi(\lambda)$ for plume and non-plume impacted stations during summer for slope waters are highlighted (d). The solid (-) lines represent surface samples while dashed (--) lines represent bottom and subsurface for estuarine (a), inner shelf (b) and midshelf (c) and deep samples for slope waters(d).

.

Table 11

Regression Parameters and Coefficients of the Power Law Fit Expressed as $a_\varphi(\lambda) = A_\varphi(\lambda)[TChla]^{E\varphi(\lambda)}$ at 440 and 676 nm for this Study. Results from Bricaud (1995) and Bricaud (2004) Representing the Global Ocean are also shown for comparison.

	a_φ (440)			a_φ (676)		
	A	E	r^2	A	E	r^2
Winter	0.038	0.79	0.89	0.013	0.93	0.94
Spring 09	0.046	0.77	0.87	0.01	0.78	0.9
Summer	0.015	1.34	0.91	0.014	0.9	0.9
Fall	0.076	0.69	0.8	0.019	0.76	0.76
Spring 10	0.015	1.22	0.84	0.016	0.76	0.87
Total	0.062	0.677	0.76	0.015	0.85	0.9
Bricaud 1995	0.038	0.65	0.9	-	-	-
Bricaud 2004	0.065	0.73	0.9	-	-	-

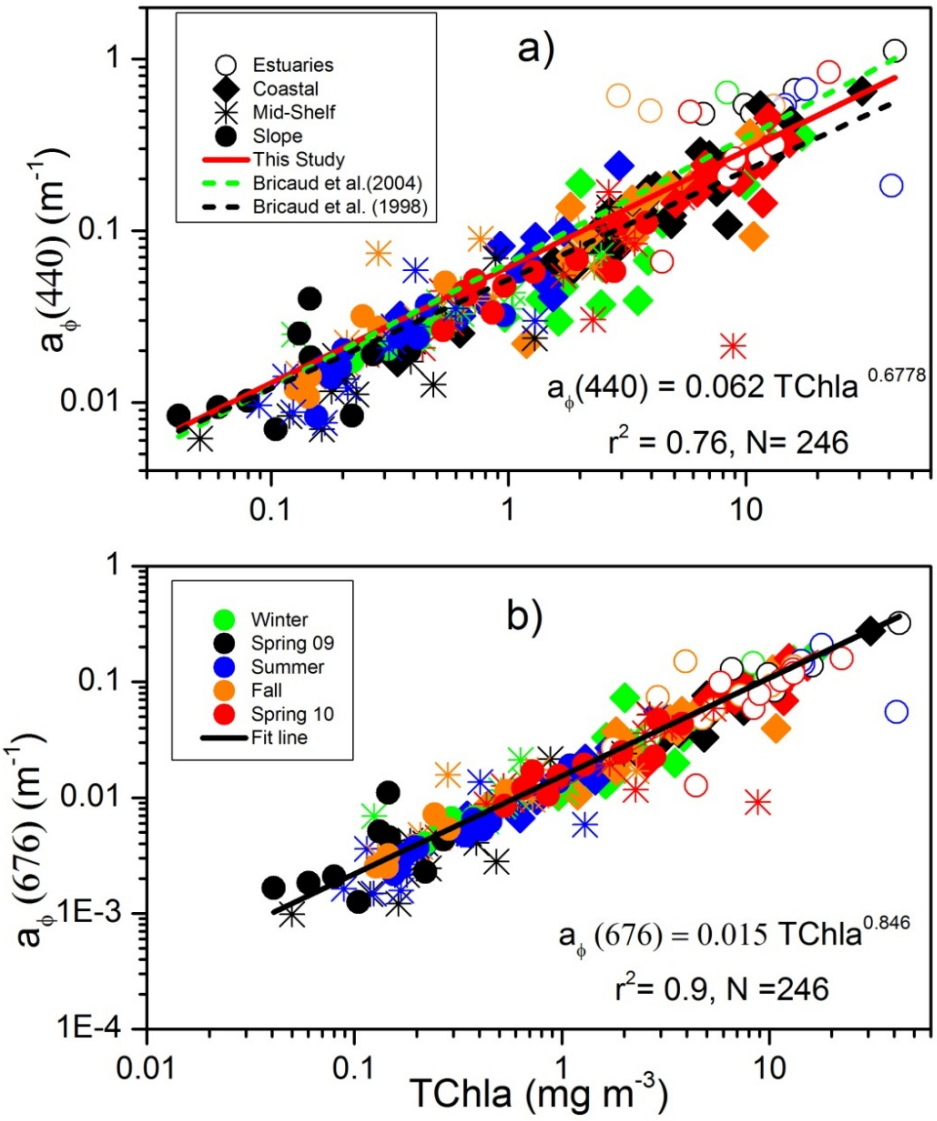

Figure 23. Scatter plot showing the phytoplankton absorption coefficients at 440(a) and 676 (b) nm as a function of TChl *a* (mg m^{-3}). Regression lines of a power law fit are shown in red (a) and in black (b). Regression relationships from Bricaud et al. (2004) and Bricaud et al. (1995) are plotted for comparison (a).

Absorption Budget for NGOM

The light absorption budget for the continental margin of NGOM was examined at eight wavelengths that are relevant to ocean color remote sensing. Relative contributions of $a_{\varphi}(\lambda)$, $a_{NAP}(\lambda)$ and $a_{CDOM}(\lambda)$ to total non-water absorption ($a_{t\text{-}w}(\lambda)$) were compared using the triangular classification scheme for natural waters following Prieur and Sathyendranath (1981) (Fig. 24).

Irrespective of the wavelength a general pattern existed, CDOM and NAP were the major contributors to $a_{t\text{-}w}(\lambda)$ for estuarine and inner shelf waters, while CDOM and phytoplankton dominated $a_{t\text{-}w}(\lambda)$ with minimal contributions from NAP in mid-shelf and slope waters. CDOM contributions in estuarine and inner shelf waters ranged 40 % -57% for all wavelengths except 620 nm and 665 nm (Fig. 24). In mid-shelf and slope waters, values of a_{CDOM} ranged 52% -79% of $a_{t\text{-}w}(\lambda)$. The ranges of contributions of $a_{CDOM}(\lambda)$ to $a_{t\text{-}w}(\lambda)$ observed in this study were consistent with the findings of Babin et al. (2003b) for coastal ocean waters (≥41 %) and Siegel et al. (2002) for open ocean waters (> 50%). Contributions of $a_{CDOM}(\lambda)$ decreased with increasing wavelength. Values of $a_{CDOM}(\lambda)$ in the estuarine and inner shelf waters ranged between 64-55% at UV (370 nm) and violet (412 nm) wavelengths. The relative contribution of $a_{CDOM}(\lambda)$ decreased to approximately 3% at longer (665 nm) wavelengths.

Values of $a_{NAP}(\lambda)$ in estuarine and inner shelf waters varied within a much narrow range (27-40 %) for all wavelengths (Fig. 24) than $a_{CDOM}(\lambda)$. Maximum values of $a_{NAP}(\lambda)$ were observed at estuarine end member stations and $a_{NAP}(\lambda)$ was the major contributor to $a_{t\text{-}w}(\lambda)$ at some estuarine stations. The relative contributions of $a_{NAP}(\lambda)$ to total non-water absorption at 370 nm and 412 nm (28-34%), and at 665 nm (31%)) were

lower in comparison to 510 and 555nm (~38%) (Fig. 24). Values of a_{NAP} (λ) decreased significantly (ANOVA, $p < 0.05$) going from estuarine and inner shelf to mid-shelf and slope waters. The relative contributions of mean values of a_{NAP} (λ) for all cruises and across all wavelengths ranged between 9 - 28 %.

Values of phytoplankton pigment absorption, a_{φ} (λ), were lower in estuarine and inner shelf waters as compared to mid-shelf and slope waters (Fig. 24). In addition, the relative contribution of $a_{\varphi}(\lambda)$ to $a_{t\text{-}w}(\lambda)$ varied with wavelength. The percentage contribution was lowest at 370 nm and 412 nm (0.08- 15%) and increased to 69% at 665. Similarly, in mid-shelf and slope waters, the contribution of a_{φ} (λ) to $a_{t\text{-}w}(\lambda)$ ranged between 11-22 % in the UV (370nm) and violet (412 nm), 22- 35 % in blue (440, 490 nm), 24-30 % in blue-green (510 and 555nm) and between 33-75% in orange (620 nm) and red (665 nm).

The magnitude and relative contribution of different light absorption coefficients also varied among cruises for given water type. The tables (Table 12, 13 and 14) provided shows seasonal variability in absorption properties at 440 nm for surface water. The 440 nm wavelength was chosen as it is representative of a major peak in phytoplankton absorption (Soret band) and also has measurable contributions from absorption by CDOM and NAP.

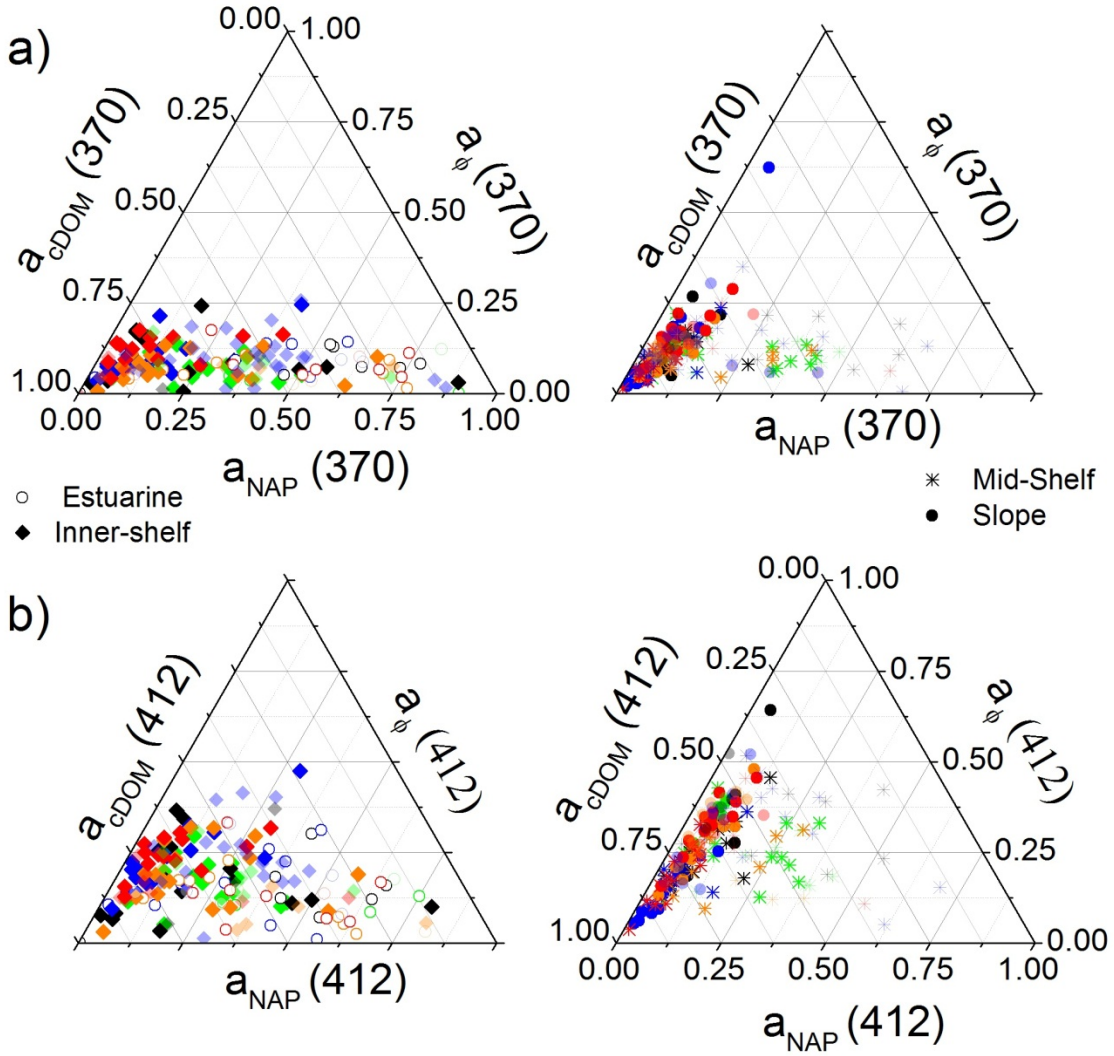

Figure 24. Ternary plots showing the relative proportions (scaled 0-1) of the absorption coefficients of phytoplankton $a_{\varphi}(\lambda)$, CDOM ($a_{CDOM}(\lambda)$) and non-algal particulates ($a_{NAP}(\lambda)$) for all data. The symbol type and color follow the same convention as for Fig. 17. The higher the proportion of absorption coefficients for a given sample the closer it is to its corresponding axes. The scales on each axis are same for all the figures.

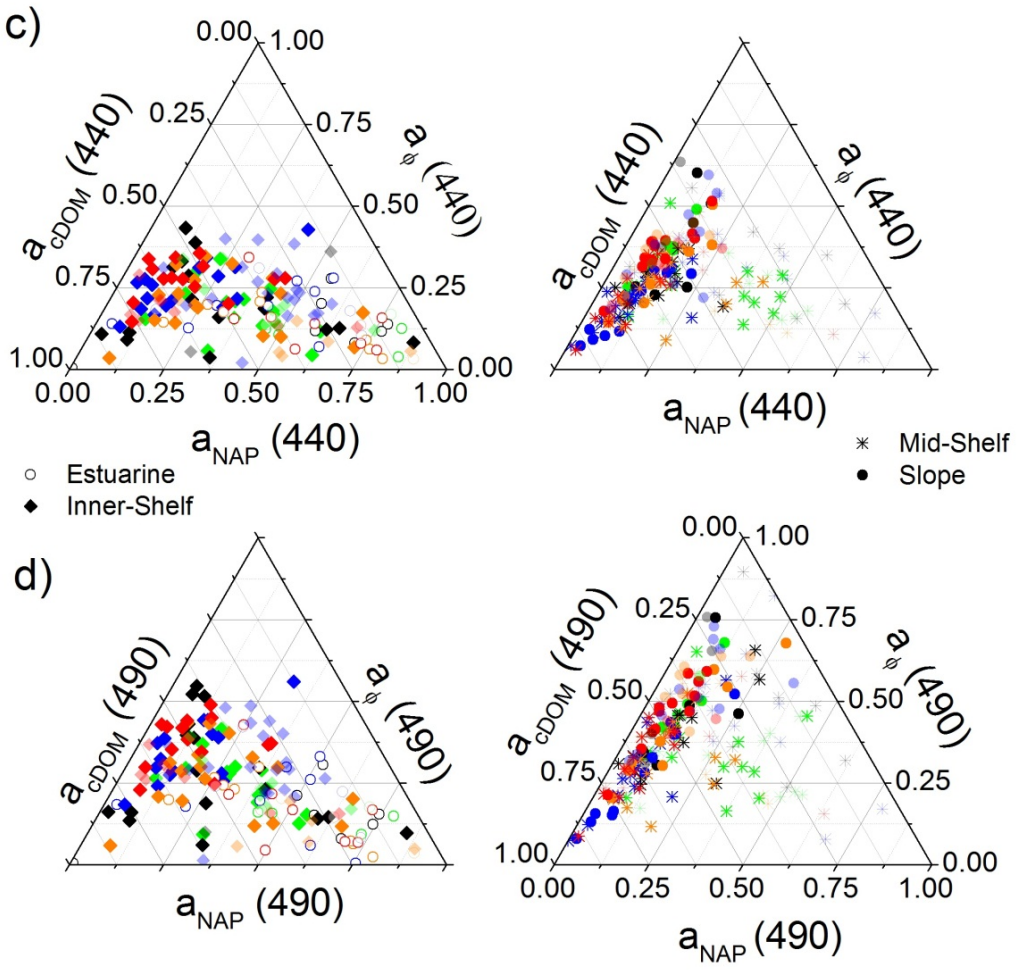
c)
0.00
0.25
0.50
0.75
1.00
a cDOM (440)
a ϕ (440)
a NAP (440)
Estuarine
Inner-Shelf
Mid-Shelf
Slope
d)
a cDOM (490)
a ϕ (490)
a NAP (490)

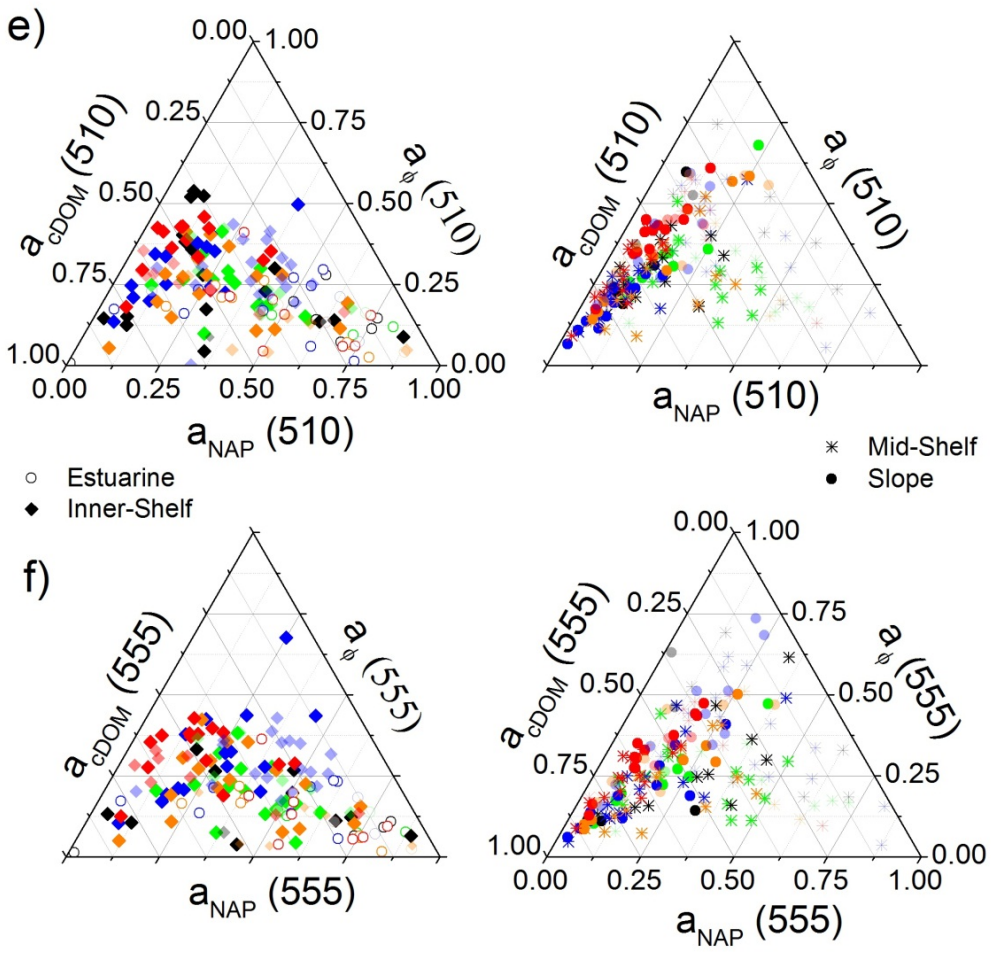
e)
0.00
1.00
0.25
0.75
0.50
0.50
0.75
0.25
1.00
0.00
0.00 0.25 0.50 0.75 1.00
a cDOM (510)
a ϕ (510)
a NAP (510)
Estuarine
Inner-Shelf
Mid-Shelf
Slope
f)
a cDOM (555)
a ϕ (555)
a NAP (555)

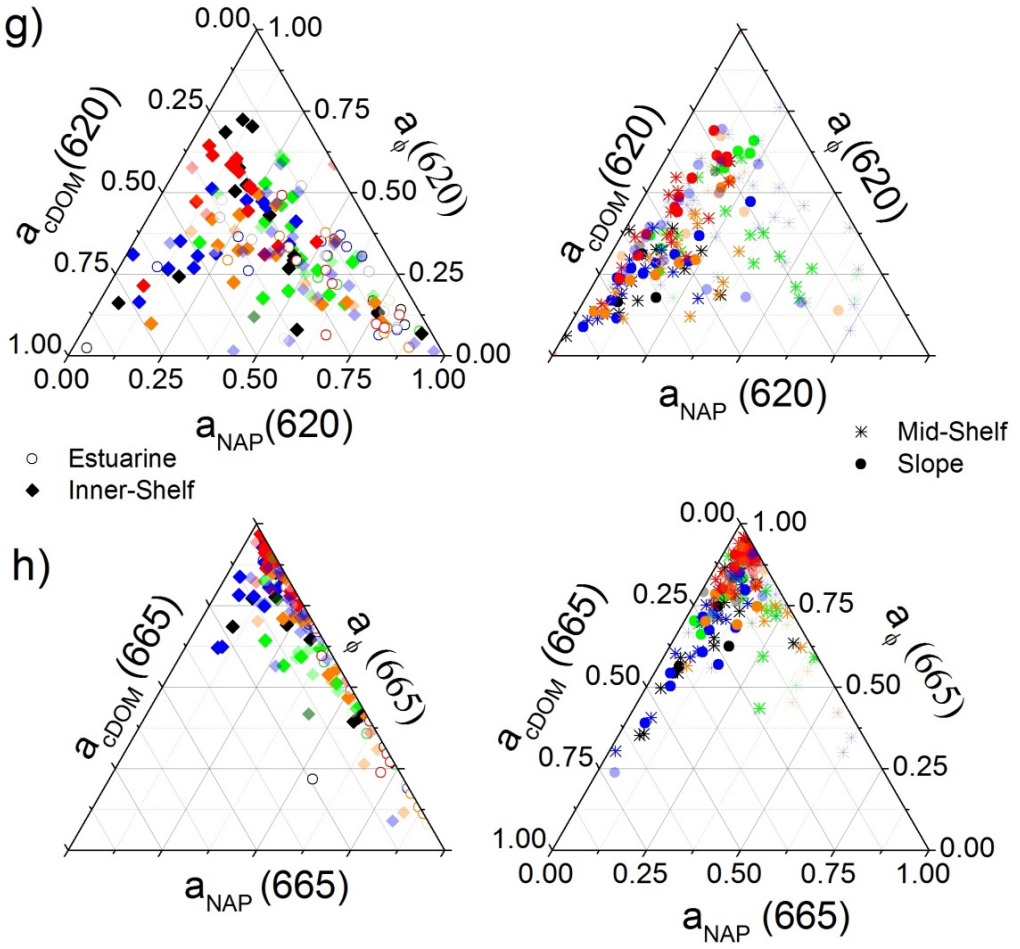

Figure 24. Ternary plots showing the relative proportions (scaled 0-1) of the absorption coefficients of phytoplankton $a_{\varphi}(\lambda)$, CDOM ($a_{CDOM}(\lambda)$) and non-algal particulates ($a_{NAP}(\lambda)$) for all data. The symbol type and color follow the same convention as for Fig. 17. The higher the proportion of absorption coefficients for a given sample the closer it is to its corresponding axes. The scales on each axis are same for all the figures).

Table 12

Descriptive Statistics for a_{NAP} (440)/ $a_{t\text{-}w}$(440) for Surface Samples. The asterisk (*) Denotes Significant Differences Based on ANOVA and Subsequent Post-Hoc Tukey HSD and FisherPro LSD Tests at p< 0.05. Normality of Distributions was Confirmed using Komolgorov-Smirnov and Shapiro-Wilk Tests.

Season	Region	N	Mean	SD
Estuarine **s**	Winter	3	0.52616	0.22535
	Spring 2009	7	0.49954	0.24365
	Summer*	8	0.32821	0.1684
	Fall	8	0.41199	0.2484
	Spring 2010	8	0.48157	0.18509
Inner-shelf **s**	Winter	16	0.29494	0.12622
	Spring 2009	17	0.23874	0.2276
	Summer*	16	0.13446	0.08674
	Fall	17	0.24655	0.17867
	Spring 2010*	14	0.13477	0.09976
Mid-shelf **s**	Winter *	15	0.20734	0.14425
	Spring 2009	14	0.10394	0.06051
	Summer*	15	0.0717	0.0513
	Fall	14	0.13767	0.08921
	Spring 2010*	14	0.06419	0.03338
Slope **ns**	Winter	8	0.0766	0.01478
	Spring 2009	6	0.10475	0.04245
	Summer	11	0.07868	0.04202
	Fall	8	0.0936	0.04245
	Spring 2010	12	0.07388	0.03224

Table 13

Descriptive Statistics for a_{CDOM} (440)/ $a_{t\text{-}w}$(440) for Surface Samples. The asterisk (*) Denotes Significant Differences Based on ANOVA and Subsequent Post-Hoc Tukey HSD and FisherPro LSD Tests at p< 0.05. Normality of Distributions was Confirmed using Komolgorov-Smirnov and Shapiro-Wilk Tests.

Season	Region	N	Mean	SD
Estuarine **ns**	Winter	3	0.33599	0.22281
	Spring 2009	7	0.34322	0.29823
	Summer	8	0.45519	0.21706
	Fall	8	0.42167	0.1721
	Spring 2010	8	0.35468	0.14032
Inner-shelf **ns**	Winter	16	0.48362	0.10765
	Spring 2009	17	0.51994	0.20359
	Summer	16	0.57573	0.15326
	Fall	17	0.51393	0.17499
	Spring 2010	14	0.54533	0.12191
Mid-shelf **s**	Winter*	15	0.47499	0.13567
	Spring 2009	14	0.58896	0.10394
	Summer*	15	0.69705	0.10711
	Fall	14	0.55859	0.12775
	Spring 2010*	14	0.67269	0.1184
Slope **s**	Winter	8	0.51065	0.0982
	Spring 2009	6	0.44467	0.15868
	Summer*	11	0.69911	0.14919
	Fall	8	0.56279	0.16641
	Spring 2010	12	0.51778	0.10835

Table 14

Descriptive Statistics for a_{φ} (440)/ $a_{t\text{-}w}(\lambda)$, for Surface Samples. The asterisk (*) Denotes Significant Differences Based on ANOVA and Subsequent Post-Hoc Tukey HSD and FisherPro LSD Tests at p< 0.05. Normality of Distributions was Confirmed using Komolgorov-Smirnov and Shapiro-Wilk Tests.

Season	Region	N	Mean	SD
Estuarine **ns**	Winter	3	0.13785	0.00715
	Spring 2009	7	0.15724	0.10657
	Summer	8	0.2166	0.08871
	Fall	8	0.16634	0.09689
	Spring 2010	8	0.16374	0.11265
Inner-shelf **ns**	Winter	16	0.22144	0.08118
	Spring 2009	17	0.24132	0.13857
	Summer	16	0.2898	0.09215
	Fall	17	0.23952	0.10524
	Spring 2010	14	0.3199	0.06449
Mid-shelf **ns**	Winter	15	0.31768	0.10516
	Spring 2009	14	0.30719	0.07867
	Summer	15	0.23125	0.07702
	Fall	14	0.30374	0.09902
	Spring 2010	14	0.26311	0.10295
Slope **s**	Winter	8	0.41275	0.08578
	Spring 2009	6	0.45058	0.17251
	Summer*	11	0.22221	0.11222
	Fall	8	0.34361	0.13442
	Spring 2010	12	0.40835	0.08651

Evaluation of Ocean Color Bio-Optical Algorithms

The comparison between Chl *a* values obtained from the OC3 algorithm and from HPLC analysis from in-situ sampling extended over a large range of values from estuarine to slope water conditions (Fig. 25). The OC3 algorithm largely overestimated Chl *a* values for most of the continental shelf of NGOM, except in estuarine waters where satellite-derived estimates underestimated ship-based observations (Table 15). The absolute percentage differences (|ψ|) were particularly high > 100% for inner shelf and slope waters.

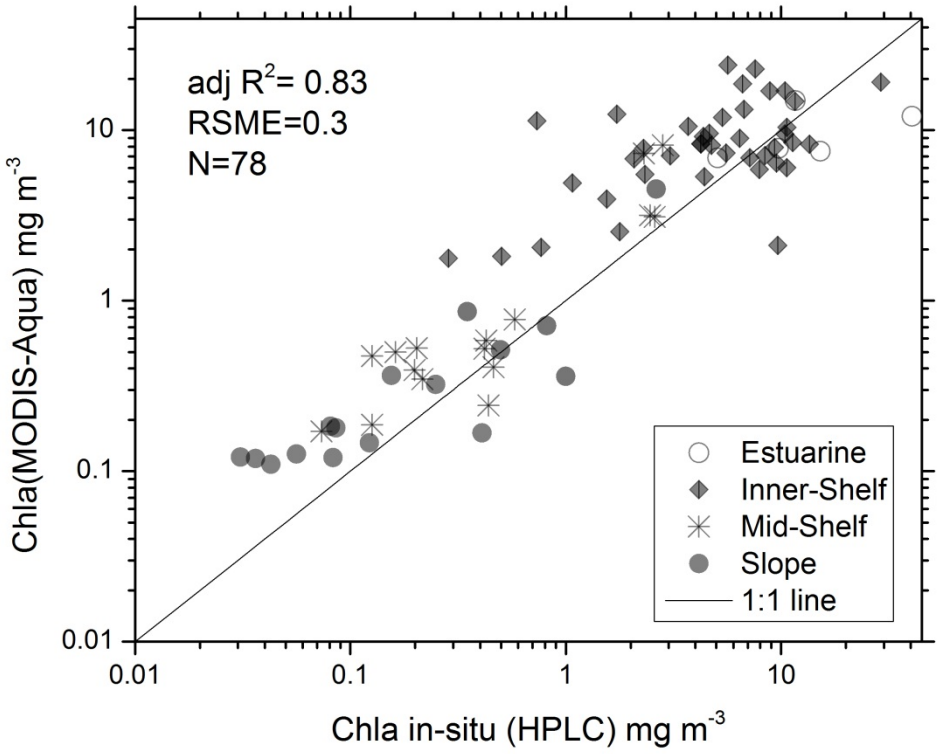

Figure 25. Scatter plot showing Chl *a* derived from the OC3 algorithm (MODIS-Aqua) versus *in-situ* HPLC measured data.

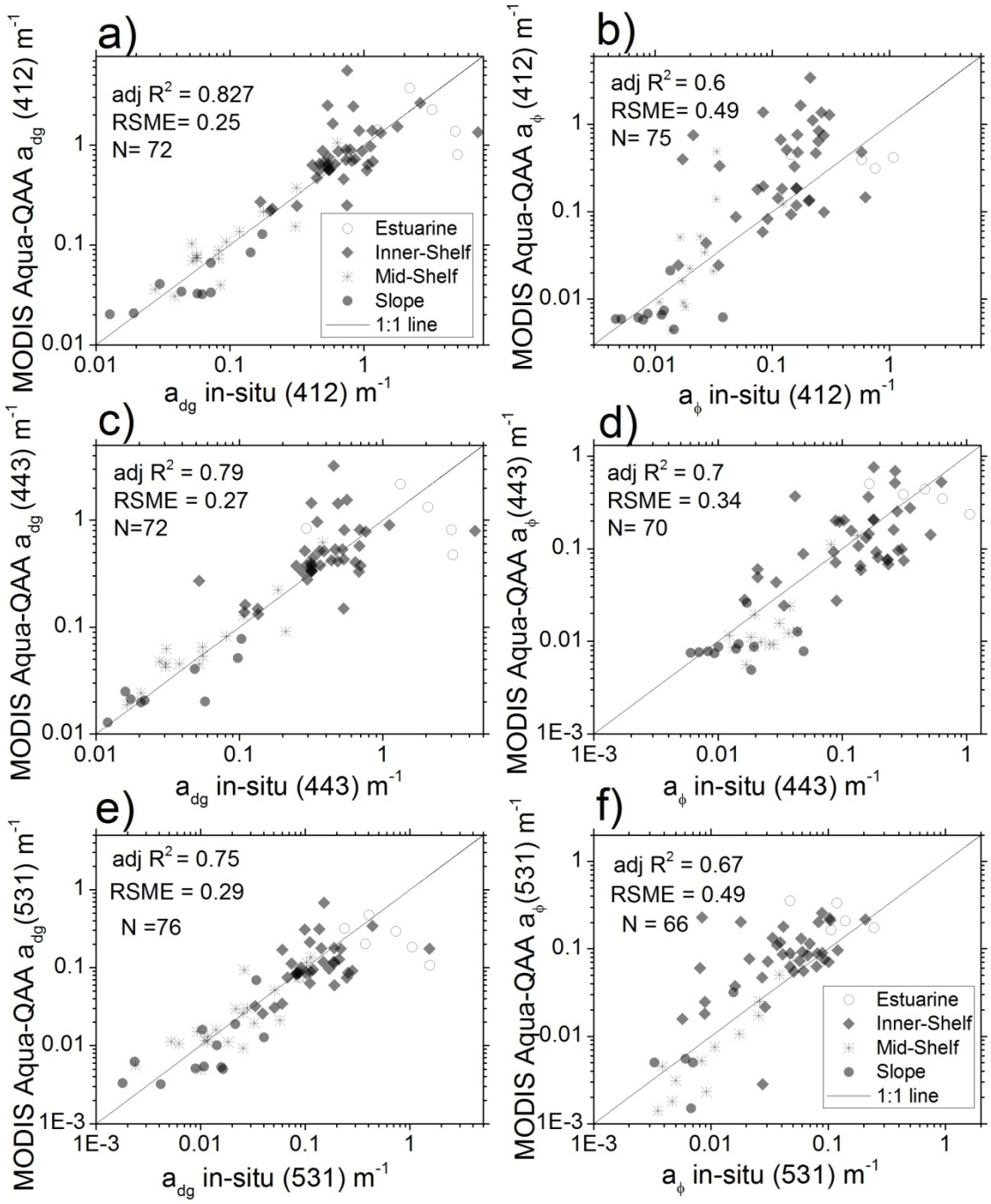

Figure 26. Scatter plot showing comparison between log-transformed in-situ a_{dg} and QAA derived a_{dg} (MODIS Aqua) at 412 (a), 443 (c), 531 (e) and similarly b, d, and f shows the relationship between log-transformed QAA derived a_{φ} versus in-situ a_{φ} at 412 (b), 443 (d), and 531 (f).

In general QAA over-estimated $a_{dg}(\lambda)$ at the inner-shelf regions and underestimated at the estuarine and offshore waters (Fig. 26). Comparisons between log-transformed in-situ $a_{dg}(\lambda)$ data and log-transformed QAA derived $a_{dg}(\lambda)$ showed reasonable agreement with r^2 values between 0.82-0.99 and the slopes ranging from 0.91-1.00 (model I, Table 16).Stations for which the QAA retrieved negative values were excluded from the match-up analysis. The results obtained for QAA_a_{dg} were promising and shows better results in uncertainty measurements (smaller values, Table 15). The biases were quite low (range ± 0.04 -0.08) even in complex inner-shelf waters (Table 15).

QAA retrievals for $a_{\varphi}(\lambda)$ were characterized by r^2 values of 0.6-0.7, slopes of 0.95-1.25 (model I, Table 16), and RSME of 0.34-0.49. The QAA retrieved a large number of negative values for $a_{\varphi}(\lambda)$ at higher wavelengths (e.g., 667 and 678) mainly because of the greater contribution of pure water at those wavelengths. This hinders accurate determination of $a_{\varphi}(\lambda)$ from $R_{rs}(\lambda)$ at these wavelengths as previously discussed by Lee and Carder (2004).

Table 15

Statistics for Comparison QAA Derived Products for N Match-Ups in Different Water Types in the NGOM.

Region		N	R^2	|ψ| (%)	RSME	RSME_Log	δ
Estuarine	OC3	5	0.25	40.8	13.3	0.28	-0.13
	QAA_a_ϕ412	4	0.12	90.1	0.43	0.38	-0.11
	QAA_a_ϕ443	5	0.7	70	0.42	0.38	-0.07
	QAA_a_ϕ531	5	0.45	193	0.17	0.45	+0.3
	QAA_a_{dg}412	5	0.26	53.23	2.25	0.44	-0.24
	QAA_a_{dg}443	5	0.2	94.8	1.76	0.55	-0.28
	QAA_a_{dg}531	7	0.22	49.7	0.66	0.56	-0.35
Inner-shelf	OC3	41	0.34	157	6.29	0.41	+0.24
	QAA_a_ϕ412	37	0.17	389	0.72	0.61	+0.35
	QAA_a_ϕ443	38	0.26	87.3	0.17	0.37	-0.03
	QAA_a_ϕ531	37	0.21	206	0.07	0.47	+0.26
	QAA_a_{dg}412	40	0.33	57.4	1.28	0.26	+0.04
	QAA_a_{dg}443	40	0.27	70	0.79	0.33	+0.07
	QAA_a_{dg}531	34	0.24	54.9	0.26	0.34	-0.08
Mid-Shelf	OC3	17	0.79	94	1.78	0.31	+0.22
	QAA_a_ϕ412	14	0.59	163	0.12	0.43	+0.07
	QAA_a_ϕ443	15	0.73	41.2	0.015	0.31	-0.23
	QAA_a_ϕ531	15	0.84	45.9	0.011	0.43	-0.24
	QAA_a_{dg}412	17	0.85	19.8	0.11	0.16	+0.04
	QAA_a_{dg}443	17	0.8	64.2	0.06	0.25	+0.11
	QAA_a_{dg}531	23	0.73	32.5	0.017	0.23	+0.02
Slope	OC3	15	0.73	106	0.54	0.35	+0.19
	QAA_a_ϕ412	10	0.2	39.4	0.01	0.33	-0.17
	QAA_a_ϕ443	10	0.2	40.4	0.02	0.35	-0.21
	QAA_a_ϕ531	9	0.22	70.7	0.01	0.42	-0.38
	QAA_a_{dg}412	10	0.76	34.6	0.03	0.2	-0.1
	QAA_a_{dg}443	10	0.76	28	0.02	0.19	-0.05
	QAA_a_{dg}531	12	0.5	63.71	0.013	0.32	-0.09

Table 16

Regression Model I and II Regression Slopes and Coefficients

	λ	Regression slopes- model-I	Intercept Model I	Regression slopes Model II	Intercept Model II
Chl *a*		0.8428	0.2329	0.9208	0.2186
$a\varphi(\lambda)$	412	1.1083	0.2799	1.3591	0.1386
	443	0.9494	-0.1748	1.1334	0.1796
	531	1.2461	0.4621	1.5223	0.108
$a_{DG}(\lambda)$	412	0.9165	-0.0365	1.008	0.2027
	443	0.8369	-0.07274	0.9421	0.2147
	531	1.0039	-0.0066	1.0089	0.2025

Discussion

This study focused on the contrasting bio-optical properties of estuarine, inner shelf, mid shelf and the continental slope waters of northern Gulf of Mexico, where, large differences both in spatial and temporal scales was observed.. In the remainder of this section the observed variability in each of the bio-optical properties is discussed primarily based on the hypotheses formed at the beginning of this chapter.

Influence of River Discharge and Wind Patterns on the Bio-optical properties in NGOM.

The light absorption properties obtained in this study compared well with previous studies in the region and was mainly influenced by the Mississippi and Atchafalaya river systems. Besides the major impact of the large rivers in the system, seasonal changes in wind fields can also largely affect the bio-optical properties in the region.

The absorption budgets presented in Fig 24 and in tables 12 & 13 shows that $a_{CDOM}(\lambda)$ and $a_{NAP}(\lambda)$ jointly contribute the major portion of the total non-water absorption in the estuarine and the inner shelf waters. Freshwater discharge provides a major source of CDOM and suspended sediments into the continental margin of the NGOM. Bianchi et al. (2004) and Meade (1996) reported that annually the Mississippi river alone delivers ~ 3.1 x 10^9 kg $yr^{-1}$of DOC and ~ 2 x 10^{11} kg $yr^{-1}$of suspended sediments in the Louisiana shelf. The dependence of $a_{CDOM}(\lambda)$ on the freshwater was shown by the near conservative relationship $a_{CDOM}(412)$ and salinity (Fig. 16a) and largely aggress with other studies in the region (D'Sa & Miller 2003, Del Castillo & Miller 2008). However, indication of different sources, due to presence of two very distinct physical environments in the Mississippi and Atchafalaya were evident at the end-member stations. High $a_{CDOM}(412)$ was associated with the Atchafalaya end members. The Atchafalaya river basin which in comparison to the Mississippi has been less disturbed (by anthropogenic activity and less dredged), maintains a relatively pristine environment and therefore has a higher potential to leach organics into the system Besides the differences in land use and geomorphology, the difference in the vegetation between the two river basins (Mississippi and Atchafalaya) also explains some of the observed variability. The Atchafalaya basin is dominated by deciduous gymnosperms and hardwood forest which are known to produce high amounts of lignin (a chromophore and a part of DOM) in comparison to a basin (the Mississippi River basin) primarily covered by agricultural crops (Shen et al. 2012). The scatter observed in the Fig. 16a at the mid-salinity range (20-25) could be due to addition of CDOM from in-situ biological processes (primary production or its bacterial decomposition) or due to mixing of two or

more water types with different CDOM signatures (Chen et al. 2004, Chen & Gardner 2004, Conmy et al. 2004).

a_{CDOM} (412)-salinity relationship also varied in the continental slope waters (Fig. 16b). High values of a_{CDOM} (412) were associated with stations impacted by the offshore transport of Mississippi plume (salinity < 31) during summer. Seasonal reversal of wind fields (Salisbury et al. 2004, Walker et al. 2005, Schiller et al. 2011) from north-east to north-west (i.e., winds coming from south-west, Fig 14b) usually facilitates offshore transport of the Mississippi river plume. High river discharge prior to the spring 2010 cruise may have favored the transport of terrigenous dissolved organic materials onto the NGOM slope leading to high a_{CDOM} (412) during that period. River discharge for the entire month of February 2010 ($27 \pm 1.8 \times 10^3$ m^3 s^{-1} and 12 ± 0.8 10^3 m^3 s^{-1} for Mississippi and Atchafalaya respectively) was almost double that of spring 2010 (March 2010, Fig. 14, Table 10). High river discharge coupled with northwesterly winds (Fig. 14b) likely resulted in high a_{CDOM} (412) values offshore.

The variability in a_{NAP}(440) in each water type was related to regional hydrodynamics. High a_{NAP} (440) values were associated with low salinity with high SPM, end members stations, such as stations located close to the outflow regions of rivers or near the mouths of the Terrebonne and Barataria bays. Presence at of mineral rich particles having higher particle densities and refractive indices (Johnson & Kelley 1984) may likely be the reason of the observed high $S_{NAP.}$ Besides, high a_{NAP} (440) at those shallow stations is also consistent with adsorption of CDOM, preferential sorption of high molecular weight DOM (as indicated by low $S_{275\text{-}295}$ in estuarine and inner shelf water types) on to fine particulate (e.g., silty clay) material (Zhou et al. 1994,

Aufdenkampe et al. 2001) may have occurred. Zhou et al. (1994) and Shank et al. (2005) has shown strong associations can exist between mineral surfaces and organic molecules**.** Lowest values of $a_{NAP}(440)$ in inner shelf waters coincided with periods of low river discharge in summer (Fig. 14a), while large increases in river discharge before the spring 2010 cruise (Fig. 14a) resulted in to high $a_{NAP}(440)$ in slope waters. Differences in a_{NAP} (440) values were observed between stratified (summer and spring 2009) and non-stratified periods and partially stratified (winter 2009 and spring 2010, Fig. 19b and Fig. 3, Chapter II, vertical profiles of temperature and salinity) in mid-shelf. Seasonal shifts in winds from predominantly northeasterly to southerly and south-westerly winds (Fig. 14b) mediated the transport of the Mississippi plume to the slope waters (Walker et al. (2005) and Schiller et al. (2011). Offshore transport of plume waters led to high a_{NAP} (440) at several slope stations. Values of $a_{NAP}(440)$ and SPM at plume-impacted stations were approximately three times higher than the non-plume impacted stations.

Significant differences among cruise periods were observed in $a_{NAP}(440)/ (a_{t-w}(440))$ (Table 12) for estuarine, inner shelf and mid-shelf water types. The differences can be attributed to seasonal changes in wind stress and river discharge. Green et al. (2008b) found wind speed followed by river discharge to be the strongest predictors of a_{NAP} in the region. In the current study, low river discharge (Fig 14a) and associated low wind speeds out of southwest directions (Fig 14b) were likely the reason for low $a_{NAP}(440)/ (a_{t-w}(440))$ in the estuarine and inner-shelf during summer. Decrease in a_{NAP}((440) led to high light availability and increase biomass production (Lehrter et al. 2009), high of a_{φ} (440)/ $a_{t-w}(\lambda)$ during summer (Table 14) observed during the study supports this idea. Enhanced light availability during summer due to light attenuation (K_d) has

been found to co-vary with river discharge in the region (Lehrter et al. 2009, Schaeffer et al. 2011b). Prior studies have reported lower K_d and increased euphotic zone depths (Z_{eu}) during summer, in some cases exceeding bottom depths (Chen et al. 2000, Lehrter et al. 2009). High wind leading to bottom re-suspension values (Allison et al. 2000) during the unstratified winter period could explain the high $a_{NAP}(440)/ (a_{t\text{-}w}(440))$ in mid-shelf waters (Table 12). Consistent these results, strong correlations between high wind speed and suspended detrital material in the water column have been previously reported by Salisbury et al. (2004) and Green et al. (2008b) in the shelf waters of northern Gulf of Mexico.

Influence of algal Processes on the Spectral Characteristics of CDOM and NAP.

Based on the significant relationship between $S_{CDOM(275\text{-}295)}$ and TChl *a*, it could be inferred that phytoplankton-derived organic matter may have been an influencing factor on $S_{CDOM(275\text{-}295)}$ characteristics, which supports the second hypotheses. However, Fichot (2012) demonstrated that microbial degradation can quickly neutralize the effects of plankton DOM on $S_{CDOM(275\text{-}395)}$.In the same study, he further revealed that photo bleaching was the primary factor regulating $S_{CDOM(275\text{-}295)}$ in the NGOM. Therefore the second hypothesis cannot be fully satisfied further work on important phytoplankton groups under controlled and natural environment is required. However, results from this study are consistent with the findings of Fichot (2012) and other previous studies (Chen et al. 2004, Helms et al. 2008, Shank & Evans 2011, Fichot 2012) and support the view that the presence of chromophores of different origin and composition along with photo bleaching likely has a greater effect than in-situ processes on spectral properties and composition of CDOM in NGOM.

Generally, smaller particles in aquatic regimes have a relatively higher mineral fraction and low POC:SPM ratios as compared to larger particles (Woźniak et al. 2010). Highest slopes (S_{NAP}) were mainly observed at the end member stations of the Mississippi and Atchafalaya rivers (Fig.21a, open circles) The ratio of TChl *a*:SPM was used in this study (Fig. 21b) as an indicator of the relative contribution of phytoplankton-derived organic matter to total particulate material. The TChl *a:*SPM ratios were low at the river end member stations. Light limitations due to high suspended load from the rivers would have constrained phytoplankton growth and can explain the low TChl *a*:SPM ratios. Babin et al. (2003b) hypothesized, that high values of S_{NAP} usually correspond to particles with higher organic matter fractions. The results shown in Figs. 22b and seems to contradict the Babin et al. (2003b) hypothesis, since high S_{NAP} values were observed at estuarine and inner-shelf stations where the importance of the phytoplankton contribution to non-pigmented particulate organic matter are expected to be relatively small. Here particle size can be a factor controlling the S_{NAP} values. Presence of larger particles has been observed in near shore and estuarine regions of NGOM (Estapa et al. 2012), large particles due to their large surface area has higher probability of organic matter accumulation (Mayer 1994) in comparison to smaller sized particles. The spectral slope of backscattering (γ) has been shown to be related to the particle size distribution (Babin & Stramski 2004). D'Sa et al. (2007) attributed low γ in estuarine and inner shelf waters of NGOM to the presence of larger size particles. Additionally, they also found a general inverse relationship between γ and Chl *a* (given by $\gamma = 2.82 - 0.19\text{Chla}$, $r^2 = 0.62$) suggesting high biomass associated with larger particles in estuarine and coastal waters. Adsorption of dissolved organic matter (DOM) on to

particle surfaces are known to occur in inner shelf and estuarine waters (Zhou et al. 1994, Uher et al. 2001). Soils particularly rich in clay minerals have been found to adsorb DOC efficiently (Suess 1970, Binding et al. 2008). This study also found some of the highest CDOM values to be associated with inner shelf and estuarine stations. Such processes if occurring can lead to substantial removal of DOM in estuarine and inland bays and can have significant consequences for the DOM reservoir in the continental margin of NGOM.

The poor relation of S_{NAP} with TChl *a*: SPM observed in this study suggests a limited role of the phytoplankton organic fraction in contributing to non-algal particulate absorption. Estapa et al. (2012) suggested that mineral fractions, mostly oxides and hydroxides of iron derived terrestrially or through resuspension (Allison et al. 2000, Green et al. 2008b) processes may have significant role in the light absorption by the NAP in the coastal regions of NGOM.

Variations in QAA Derived Bio-optical Properties in Northern Gulf of Mexico.

Factors that might affect the a_φ (λ) estimates include variations related to phytoplankton pigmentation and package effects (Bricaud et al. 1998, Bricaud et al. 2004). Large variability in pigment composition in the region as described in Chapter II might account for some of the variability observed between satellite-derived and in situ data. The large absolute percentage difference values at 412 nm for a_φ may be due to the high ratios (>1.1) obtained for derived a_φ (412) and a_φ(443) an exclusion threshold; IOCCG 2006, 30 out of 75 of the match-up samples ratios between derived a_φ (412) and a_φ(443) was > 1.1. Similar problems as observed here with QAA_a_φ (412) data from MODIS-AQUA were also observed for SeaWIFS data in a study in European coast

(Mélin et al. 2007). Retrieval of R_{rs} at shorter wavelengths is particularly challenging in coastal waters given the high light attenuation at those wavelengths and uncertainties in atmospheric corrections particularly at shorter wavelengths (Lee & Carder 2004, Aurin & Dierssen 2012) Cloud cover and solar glint are additional factors that may affect the accuracy of the satellite-derived R_{rs} estimates and associated QAA retrievals. Additionally, small scale spatial heterogeneity in distributions as well as changing environmental conditions over the time window for matchups (± 24hrs) could have contributed to observed differences between the QAA-derived products and in-situ observations.

Another factor influencing the performance of the QAA algorithm involves the choice of the spectral slope value of *a*dg. Spectral slopes of CDOM and NAP are known to vary widely in continental margins (Vodacek 1992, Kirk 1994, Babin et al. 2003b). The S_{CDOM} values determined during this study ranged from 0.01-0.022 nm^{-1}, while S_{NAP} ranged from 0.005 -0.02 nm^{-1}. The QAA uses a standard spectral slope of 0.015 nm^{-1} for S_{dg}. Lee and Carder (2004) noted that ideally in-situ S_{dg} values should be used as it is difficult to accurately determine just from R_{rs} values. Since $a_{\varphi}(\lambda)$ is calculated by subtraction of $a_{dg}(\lambda)$ from a(λ), uncertainty in the spectral slope used in the QAA can be an additional source of error in $a_{\varphi}(\lambda)$.

Considering all these issues the results obtained in this study provides some promise to the usage of QAA in the NGOM. Repeated validation of QAA with in-situ data and R_{rs} data from multi-platform should be undertaken in future. The use of in-situ R_{rs} to derive QAA products would provide much needed information to further investigate the uncertainty budget in the region and is thus recommended for future

assessment of remote sensing algorithms and derived products in NGOM. The low uncertainty associated with the QAA_a_{dg} values are particularly promising and provides confidence to the quantitative use of satellite derived QAA_a_{dg} maps in NGOM.

Conclusion

Large spatial gradients in light absorption properties existed between estuarine-inner shelf waters with mid-shelf and slope waters. Seasonal differences evident in the bio-optical properties were largely influence by regional hydrodynamics including seasonal fluctuations in river discharge and wind driven transport and mixing which supports the primary hypothesis. The secondary hypothesis that phytoplankton processes control the spectral properties of CDOM and NAP was not confirmed.

The QAA performed reasonably well in retrieval of absorption products and results from this study may be useful in further refining the algorithm. Areas for consideration in refining the algorithm include adjustments in the spectral slope and improvements in Rrs retrievals particularly at shorter wavelengths. The parameters provided in this study can also aid in tuning of other OCAs.

CHAPTER V

VARIABILITY OF PHYTOPLANKTON LIGHT ABSORPTION PROPERTIES OF PHYTOPLANKTON IN THE LARGE RIVER DOMINATED CONTINENTAL MARGIN OF THE NORTHERN GULF OF MEXICO

Introduction

Primary production at the base of marine food webs is an important carbon transport pathway in the ocean. Global net primary production (PP) is about 104.9 Pg C yr^{-1} of which about 30% occurs in the coastal ocean (Bianchi & Allison 2009b). Light absorbing capacity of phytoplankton represented as $a^*_\varphi(\lambda)$, chlorophyll *a* (Chl *a*) specific coefficient of absorption, has been used as a key parameter in estimating PP (Platt & Sathyendranath 1988, Sathyendranath 1991). Several remote sensing studies (e.g., Marra et al. (2007)) have argued $a^*_\varphi(\lambda)$ to be a better predictor of surface PP than Chl *a*. A simple example of a bio-optical PP model (Morel 1991) has the form

$$p(z) = \emptyset(z)[c^z_{Chl}].a^*_\varphi.PAR\ (z) \qquad (10)$$

where p(z), ∅ (z), c_{chl}^z, $a^*_\varphi(z)$, and PAR(z) are, respectively, the primary production, photosynthetic quantum yield, chlorophyll concentration, phytoplankton chlorophyll-specific absorption, and photosynthetically available radiation at depth z. The use of ocean color algorithms to estimate PP has the advantage of extending estimates of PP over much wider spatial and temporal scales than is possible by conventional ship-based methods. Estimates of PP derived from remote sensing are important in understanding other aspects of the carbon cycle, such as has been the focus of several modeling studies examining carbon cycling and hypoxia in the northern Gulf of Mexico (Green et al. 2008a, Green & Gould 2008, Fennel et al. 2011).

Besides the importance of $a^*_\varphi(\lambda)$ for its application in remote sensing models to estimate PP, variations in $a^*_\varphi(\lambda)$ also provides information about the ecological dynamics of phytoplankton populations. Light absorption properties of phytoplankton have been widely studied in the various regions of world oceans (Sosik & Mitchell 1995, Stuart et al. 1998, Lohrenz et al. 2003a, Bricaud 2004). Studies have shown that natural variability in $a^*_\varphi(\lambda)$ can be related to the composition and physiology of phytoplankton communities (groups, size pigment composition and packaging effect) structure (Hoepffner & Sathyendranath 1992, Ciotti et al. 2002, Lohrenz et al. 2003a, Bricaud et al. 2004). The complexity and dynamic nature of phytoplankton communities in continental margin waters of the northern Gulf of Mexico was described in Chapter-II of this dissertation. It can be therefore expected that significant differences in $a^*_\varphi(\lambda)$ also exists in the different water types (as previously described in Chapter II) and varies seasonally in the northern Gulf of Mexico.

Continental margin waters of the northern Gulf of Mexico are optically complex case 2 waters (D'Sa et al. 2007, D'Sa & DiMarco 2009) where optical constituents such as colored dissolved organic matter (CDOM) and non-algal particles (NAP) contribute significantly to the total non-water absorption. In the previous chapter (Chapter IV) it was shown that large contributions from the CDOM and NAP in the region can lead to over- or underestimation of Chl *a* and a^*_φ, using both, a semi analytical (Lee et al. 2002) and an empirical (O'Reilly et al. 2000) algorithm. Large uncertainties in Chl *a* and a^*_φ can propagate to large errors in model estimates of PP.

Studies on specific absorption coefficients of phytoplankton in the continental margin of northern Gulf of Mexico have been rare. Previous work by Green and Gould

(2008) characterized the spatial and temporal distributions in satellite derived $a^*_\varphi(\lambda)$in the region. However, their work along with other (D'Sa 2008, Naik et al. 2011, Schaeffer et al. 2011a) was mainly focused on shallow inner shelf waters of northern Gulf of Mexico. All these previous works studied and described the relationship of $a^*_\varphi(\lambda)$ to environmental variables and other optical constituents. The effects of pigment composition, size structure and pigment packaging on the overall variability of a $a^*_\varphi(\lambda)$ in the regions remains unexplored.

On the basis of the bio-optical data collected during the Gulf Carbon cruise (www.gulfcarbon.org) this chapter focuses on describing the variability in $a^*_\varphi(\lambda)$ in relation to controlling biological factors including pigment composition, size structure, and package effects. Previous studies (D'Sa 2008, Green & Gould 2008) reported that high $a_\varphi(\lambda)$ and high biomass (Chl *a*) were generally associated with larger celled phytoplankton cells that dominate the coastal margins of the region. Based on such observations it can be hypothesized that pigment packaging (a shelf shading phenomenon in large cells) are important and can explain most of the spatial variability in $a^*_\varphi(\lambda)$, chlorophyll a (Chl *a*) specific absorption coefficient of phytoplankton. Besides pigment packaging variability in $a^*_\varphi(\lambda)$ can also be attributed to variations in phytoplankton cell size and pigment composition in the northern Gulf of Mexico. The relative importance of each of the above factors contributing to changes in $a^*_\varphi(\lambda)$ was also tested in this study.

Materials and Method

Pigment Analyses

For pigment analysis, seawater samples were filtered through a 47 mm Whatman GF/F glass-fiber filters and filters were immediately frozen and stored in liquid nitrogen until analysis. Sample volumes ranged from approximately 0.2 liters in shallow estuarine end member stations to 4 liters in the deep offshore slope waters. The details of the HPLC analyses are described in Chapter II of this dissertation. For comparisons between pigment composition and pigment absorption spectra, pigment data were grouped into three major categories of accessory pigments including i) PSC (photosynthetic carotenoids, sum of fucoxanthin, peridinin, 19′-Hex and 19′-But), ii) PPC (photo protective carotenoids, sum of zeaxanthin, diadinoxanthin, alloxanthin and β-carotene) iii) Total Chlorophyll-*b*(TChlb) (sum of Chlb and Divinyl Chlorophyll-*b* (DVChlb) and iv) Total Chlorophyll-*c* (TChlc) (sum of Chlorophyll c_1, c_2 and c_3).

The proportions of phytoplankton biomass as chlorophyll *a* associated with major size fractions were estimated using the method originally developed by Vidussi et al. (2000) and modified by Uitz et al. (2006) and Hirata et al. (2011) . The method is based on the relative abundance of diagnostic pigments (DP) as defined in Table 2.1. The relative contribution to TChl *a* by picoplankton (< 2µm), nanoplankton (2-20 µm) and microplankton (>20µm) can be estimated from the following relationships (Hirata et al. 2011).

$$\text{Micro (\%)} = (1.41[\text{Fuco}] + 1.41\ [\text{Peri}]/\ \text{DP}\ ) \times 100 \quad (11)$$

$$\text{Nano (\%)} = (0.60[\text{Allo}] + 0.3519\ [\text{But}] + 1.271\ [\text{Hex}] + 1.01\ [\text{Chlb}]/\ \text{DP}\ ) \times 100 \quad (12)$$

$$\text{Pico (\%)} = (0.86[\text{Zea}]/\ \text{DP}\ ) \times 100 \quad (13)$$

$$DP = \Sigma (1.41\ [Fuco] + 1.41[Peri] + 0.60\ [Allo] + 0.3519\ [But] + 1.271\ [Hex] + 0.86\ [Zea] + 1.01[TChlb \quad (14)$$

The DP method has provided reliable results in both regional (Vidussi et al. 2001) and global applications (Uitz et al. 2006), and was thus selected for use in this study to examine differences in size structure of phytoplankton populations in the NGOM. The method does have limitations in that some pigments can occur in more than one size class of phytoplankton. For example, Fuco and Peri are marker pigments for both diatoms and dinoflagellates and generally dominate the microplankton size class. However, Fuco is a precursor of 19′-Hex and can also co-occur in the nanoplankton group. Nevertheless, the method has performed well in various environments. As an additional means of verification of the method, results in this study will be compared to determinations of algal class abundance in the NGOM from pigment analyses using the chemotaxonomic software CHEMTAX v1.95. Details of the CHEMTAX analyses are provided in Chapter II.

To summarize the size class results, the size index (SI) developed by Bricaud et al. (2004) was used as a single metric to characterize the size structure of the algal population. SI is defined as

$$SI\ (\mu m) = [1*(Pico\ \%) + 5*(Nano\ \%) + 50*\ (Micro\ \%)]/100 \quad (15)$$

This calculation is based on the assumptions that the central size values of pico, nano and micro-phytoplankton are 1, 5 and 50 µm, respectively. Although this assumption is a broad generalization, the SI is useful as a single parameter to characterize the size structure of the algal population, approaching the value of 50 µm for microplankton-

dominated communities and the value of 1 □dominated phytoplankton populations.

Estimation of Packaging Index

The pigment package effect index (Q^*_a (676)) was estimated as the ratio of the Chl *a* specific absorption coefficient (a^*_φ(676)) and the maximum specific absorption coefficient of Chl *a* in solution (0.033 m^2 mg $Chla^{-1}$) at the wavelengths in the vicinity of 676 nm (Johnsen & Sakshaug 2007). This maximum value is based on the assumption that there were minimal package effects in these small celled phytoplankton species. Also implicit in this calculation is the assumption that Chl *a* is the primary light absorbing pigment at 676 nm. The Q^*_a (676) is a dimensionless ratio and ranges between 1 for completely unpackaged pigments to approaching zero for highly packaged pigments. Values of Q^*_a (676) that exceed 1 were likely an indication of unaccounted absorption contributions (see explanation given in Bricaud et al. (1995) and Bricaud et al. (2004) Bricaud et al.(1995) and Bricaud (2004). Another assumption of this approach for estimating pigment packaging is that the maximum (i.e. unpackaged) weight-specific pigment absorption coefficients are similar for all types of phytoplankton populations included in the analysis. This assumption can be questioned as chlorophyll *a*-specific absorption at 675 nm varies among species due to differences in pigment-protein complexes, macromolecular configurations, and cellular morphology (Johnsen et al. 1994). However, the approach used in this study is consistent with that used in several previous studies in different regions of the world ocean (Roy et al. 2008, Matsuoka et al. 2009, Naik et al. 2011, Brunelle et al. 2012).

Statistics

Statistics used in this study were conventional descriptive statistical measures such as mean, standard deviations, maximum and minimum values. Normality of the dataset was tested using the Kolmogorov-Smirnov and Shapiro-Wilk tests and in many cases, data did not fit a normal distribution. Thus non-parametric ANOVA (Kruskal-Wallis) and Wilcoxocon Rank tests were employed to evaluate statistical significance.

A multiple linear regression was employed to examine relationships of different variables to phytoplankton chlorophyll-specific absorption. The assumption of independence of error of the multiple linear regressions was verified using the Durbin-Watson statistic and the statistical significance of the model was assessed using the F-ratio. The assumption of multicollinearity of variables used in the model and homoscedasticity of errors was also evaluated. Multicollinearity of variables was tested using the variance inflation factor (VIF), results are provided in the appendix section (Table 1). Homoscedasticity of error distributions was assessed by plotting the standardized residuals of the regression against the unstandardized predictor variables. The statistical tests were performed using IBM SPSS statistics 14.

Results

Variability in Specific Phytoplankton Absorption

The characteristic absorption maximum of phytoplankton chlorophyll-specific absorption, $a^*_{\varphi}(440)$, varied from high values in oligotrophic slope (mean ± SD, 0.083 ± 0.04) and mid-shelf (0.068 ± 0.03) to low values in estuarine (0.047 ± 0.03) and inner shelf (0.038 ± 0.02) waters (Figs.27 & 28). Mean values of $a^*_{\varphi}(440)$ in the estuarine and inner shelf waters were significantly lower than mid-shelf and slope waters (Kruskal-

Wallis, at 0.05 level). The differences observed in $a^*_\varphi(440)$ among the different water types corresponded to differences in chlorophyll concentrations as well, with highest chlorophyll (here given as total chlorophyll a or TChl *a* as determined by HPLC) in estuarine (range: 2-42 mg^{-3}) and inner-shelf (0.7 – 22.3 mg^{-3}) waters and low chlorophyll (0.04 – 3.8 mg^{-3}) in slope waters.

Significant temporal variability in $a^*_\varphi(440)$ was observed in inner shelf and slope waters, while such differences in estuarine and mid-shelf waters were not evident (Kruskal-Wallis test, p = 0.05). For inner shelf waters, mean values of $a^*_\varphi(440)$ were high during summer (mean ± SD, 0.061 ± 0.021) in comparison to other seasons when $a^*_\varphi(440)$ ranged: 0.008-0.07. In slope waters mean $a^*_\varphi(440)$ values during spring 2009 and fall 2009 (0.121 ± 0.06) were almost double the means (Fig. 28) of other periods (0.61 ± 0.019).

Despite the significant spatio-temporal variability in $a^*_\varphi(440)$ values of $a^*_\varphi(440)$ generally followed a non-linear relationship to TChl *a* concentrations that could be described by a power function of the form (Fig. 28 and Table 17)

$$a^*_\varphi(\lambda) = A\,(\lambda)\; TChl\; a^{-B(\lambda)} \qquad (16)$$

The fit applied to the entire dataset yielded the relation

$$a^*_\varphi(440) = 0.053(440)\; TChl\; a^{-0.333(440)}. \qquad (17)$$

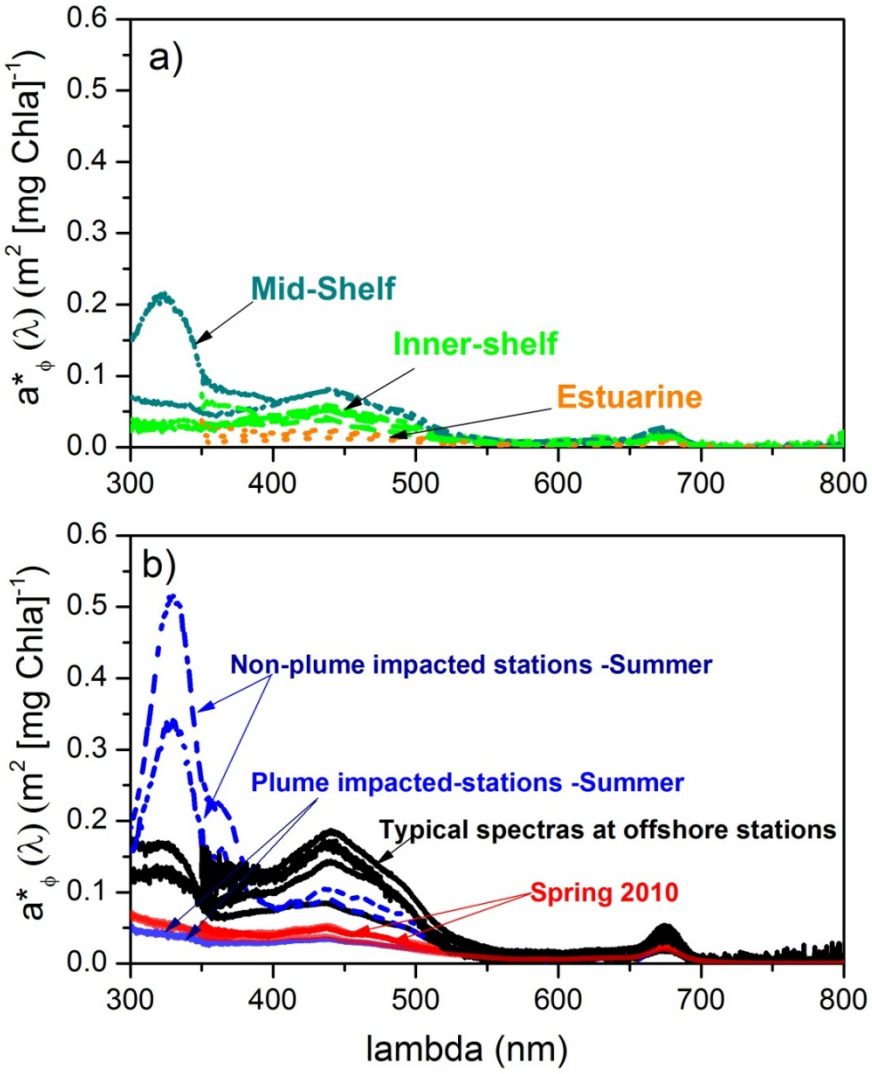

Figure 27. Specific absorption spectra $a^*_\varphi(\lambda)$ at representative stations for each water type showing changes in spectral shape and magnitude in estuarine, inner shelf and mid-shelf waters (a) and in slope waters (b).

The regression coefficients for the combined dataset as well as for the individual water types (Table 17) were in many cases comparable to the ranges reported by Bricaud et al. (1995) and Bricaud et al. (1983) for world oceans (A= 0.03-0.049, B= 0.3-0.38). However, there was considerable scatter in the data (Fig. 28) and such variability

underscores the importance of understanding the major sources of variation in a^*_{φ}. This is considered in the following sections:

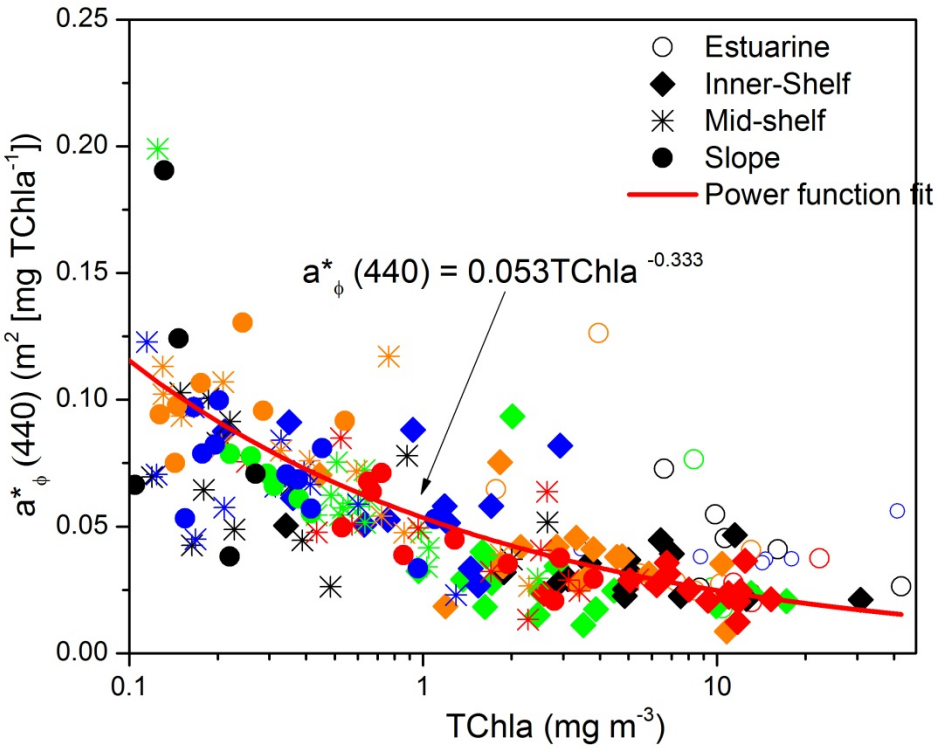

Figure 28. Variations in chlorophyll-specific absorption coefficients of phytoplankton at 440 nm as a function of TChl *a* (Chla+DVChla+Chla-allomers+Chla-epimers). Colors corresponds to different seasons, Winter (green), Spring 2009 (black), summer (July), Fall (orange) and Spring 2010 (red).

Table 17

Showing the Regression Parameters at each Water Types in NGOM

Region	N	A	Std.Dev	B	Std.Dev	r^2
Estuarine	30	0.131	0.04	0.488	0.0176	0.49
Inner-shelf	72	0.0496	0.002	0.303	0.04	0.46
Mid-shelf	70	0.051	0.004	0.327	0.058	0.48
Slope	43	0.046	0.0006	0.442	0.073	0.5
Entire area	215	0.053	0.002	0.333	0.024	0.58

Variability in the Packaging Effect, Pigment composition and Size

To assess variability in pigment packaging, two different proxies were used in this study. The first proxy was the blue-to red (B/R) ratio of $a_{\varphi}(440)$: $a_{\varphi}(675)$ and the other approach (described in methods) was the ratio of observed phytoplankton chlorophyll-specific absorption at 676 nm, $a^*_{\varphi}(676)$, to the maximum of 0.033 m^2 mg $Chla^{-1}$ determined for 33 species (Johnson and Sakshaug, 2007). Accurate determination of the efficiency of pigment packaging (Q^*_a, Morel and Bricaud (1981)), in field samples are not straight forward because of uncertainties related to accurate determination of intercellular pigment composition and cell size (Bricaud et al. 2004, Roy et al. 2008).

Despite such uncertainty, the results from this study (Fig. 29c) compared well with other previous studies (Stuart et al. 1998, Lohrenz et al. 2003a, Lutz et al. 2003)

The B/R ratio in NGOM varied over both spatial and temporal scales from 1.42 - 4.57, a range comparable to that observed in other regions including the Atlantic ocean (range: 2-3.2; by Babin et al. (2003b)), California current system (range: 2-4.5) by Sosik and Mitchell (1995), and Black Sea (range: 2.4- 3.3 by Chami et al. (2005)

Generally, $a_{\varphi}(440)$: $a_{\varphi}(675)$ ratio decreases with increasing cell size; large highly pigmented cells have characteristically higher pigment packaging (Barocio-León et al. 2008). Smaller values in this study were observed in estuarine and inner shelf waters (range 1.42 – 3.77) were consistent with the dominance of larger sized phytoplankton (Fig. 29a & 29b). In contrast, the ratio was higher for the mid-shelf and slope waters (range 1.72 – 4.57), dominated by picophytoplankton (Fig. 30d). Blue to red ratios have been shown to be higher in pico phytoplankton (mainly prochlorophytes and cyanobacteria), typically greater than 2.5 (Stramski & Morel 1990, Moore et al. 1995). Mean $a_{\varphi}(440)$: $a_{\varphi}(675)$ ratios in estuarine (3.07 ± 0.51) and inner-shelf (2.7 ± 0.58) waters were significantly lower (Kruskal-Wallis, $p<0.05$) than ratios for mid-shelf (3.98 ± 1.03) and slope (4.03 ± 1.001) waters. B/R ratios was high in inner shelf (mean ± SD 3.38 ± 0.49) during summer (Fig 29b) and during spring, summer and fall of 2009 (range 2-4.57, median 3.25) in mid-shelf (Fig. 29b). Lowest values in B/R ratios were observed during spring 2010 in the slope waters (Fig. 29b) corresponding to the dominance of microphytoplankton during that period (Fig. 30c & 30d).

Low B/R ratios associated with large celled phytoplankton (microphytoplankton, e.g., diatoms, dinoflagellates) in estuarine and inner shelf waters (Fig. 30a & 30b)

coincided with high levels of pigment packaging and low values of the absorption efficiency factor, Q^*_a (676) (Fig. 29c). High pigment packaging (or low Q^*_a since packaging is proportional to (1- Q^*_a)) was consistently observed in inner shelf (regional mean 0.53 ± 0.21) and estuarine (regional mean 0.45 ± 0.18) waters. Q^*_a (676) and B/R ratios increased significantly (Kruskal Wallis, $p< 0.05$) from estuarine to slope waters (Fig. 29b & c), and could be at least partially attributed to regional differences in phytoplankton size structure from larger microphytoplankton to picophytoplankton.

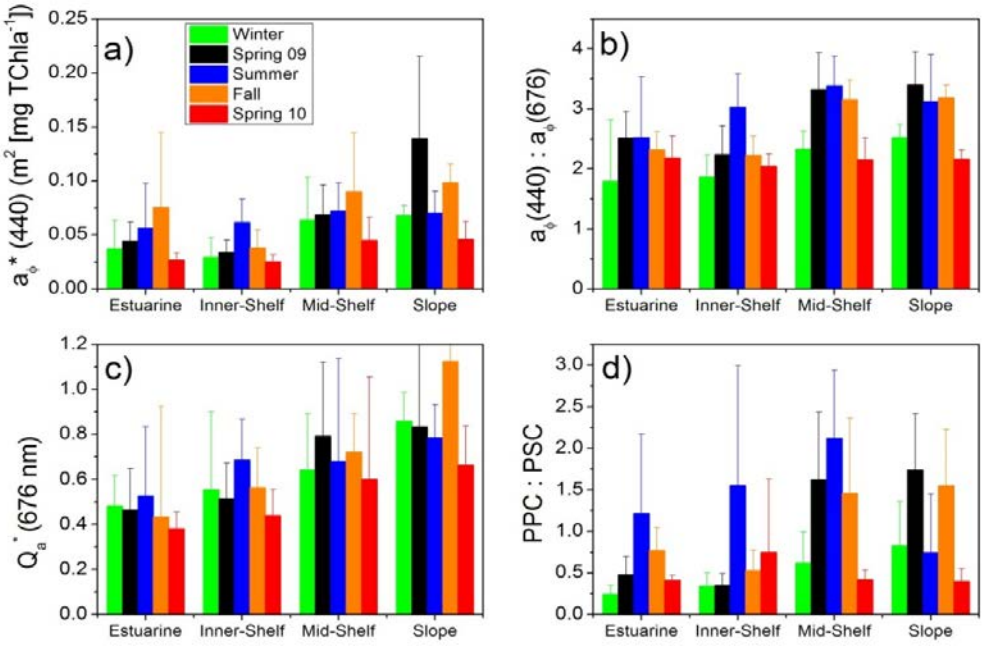

Figure 29. Regional and seasonal variations in (a) chlorophyll-specific absorption properties of phytoplankton ($a^*_\varphi(440)$), (b) the blue-to-red ratio of $a_\varphi(440)$: $a_\varphi(675)$), (c) packaging efficiency (Q^*_a (675)), and (d) ratio of photo protective carotenoids (PPC) and photosynthetic carotenoids (PSC) for surface waters.

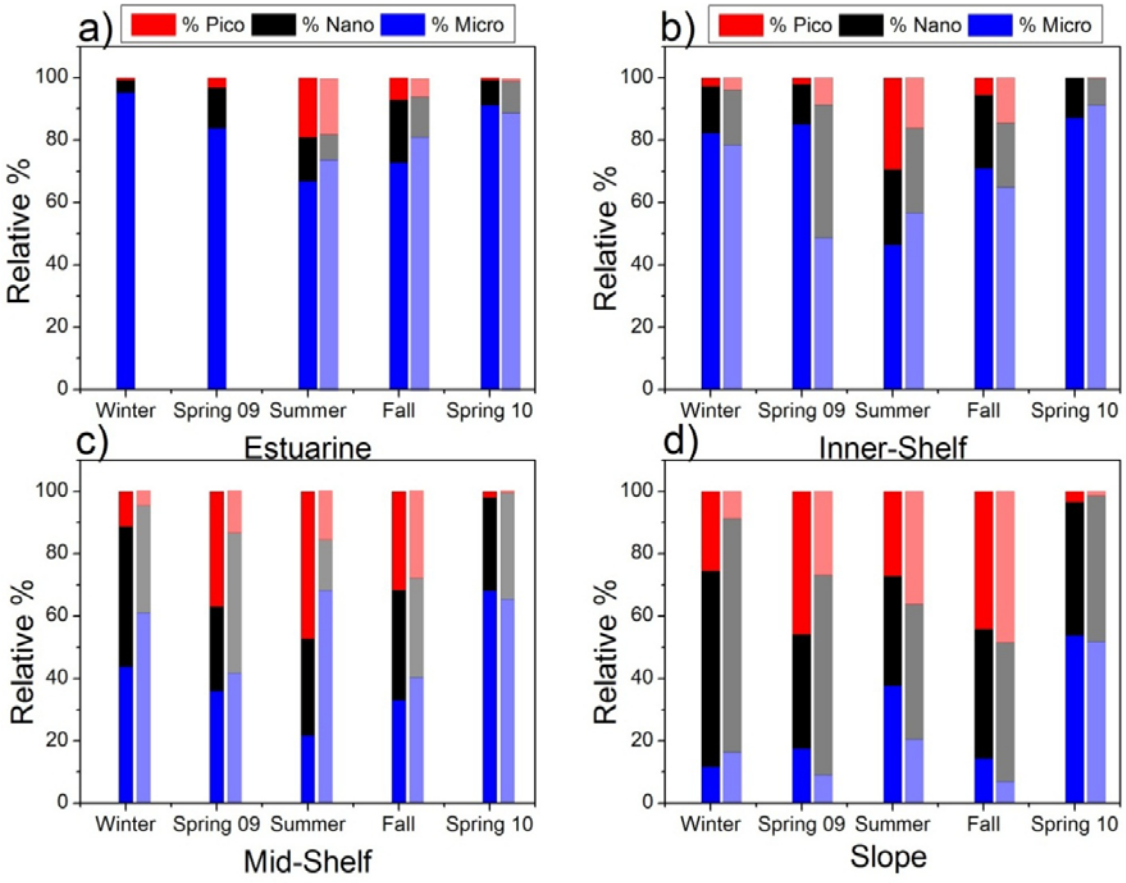

Figure 30. Seasonal variations in the contribution of phytoplankton size fractions at the surface (non-shaded stacked plots) for each water type. The shaded stacked plot represents the contributions of each size fraction at bottom depths for the estuarine, inner-shelf, and mid-shelf water types (a, b, c) and at the subsurface chlorophyll fluorescence maximum for slope waters (d).

However, in to B/R ratios, seasonal differences in $Q^*_a(676)$ within water types were significant only in slope waters. The value of $Q^*_a(676)$ was significantly smaller (Kruskal-Wallis, $p < 0.05$) during spring 2010 in comparison to other periods (Fig 29c), an indication of higher pigment packaging during that time. Photo protective carotenoids (PPC) to photosynthetic carotenoids (PSC) ratios were significantly higher in mid-shelf and slope waters than that of estuarine and inner shelf waters (Fig. 29d). Seasonal variations in the PPC: PSC ratios were also significant within each water type. PPC: PSC

ratios were significantly higher in estuarine (1.32 ± 1.01) and inner shelf (1.59 ± 1.49) waters and were significantly higher (Kruskal-Wallis, $p<0.05$) during summer in comparison to spring (both 2009 and 2010) and winter 2009 (Fig. 29d). In mid-shelf waters, PPC: PSC during winter (0.6 ± 0.38) and spring 2010 (0.41 ± 0.11) were significantly lower (Kruskal-Wallis, $p< 0.05$) than the values observed during other periods (range: 0.37-3.53). Similar trends in PPC: PSC were also observed in the slope waters (Fig. 29d), where ratios were higher for spring and fall of 2009 (range 0.79-3.17) in comparison to spring 2010 (0.39 ± 0.15) and winter 2009 (0.83 ± 0.53).

Distinct regional assemblages in phytoplankton size classes was evident, microphytoplankton mainly dominated estuarine and inner-shelf waters (Fig. 30), while pico and nanophytoplabkton were more prevalent in mid-shelf and slope waters. Proportions of microphytoplankton were significantly lower in summer and fall in estuarine (range: 37-84 %) and inner-shelf (14-77%) waters in comparison to winter (range: 77-99%) and spring (range: 62-98% for 2009 and 2010). Proportions of nano and picophytoplankton were significantly higher during summer and fall than other periods in estuarine and inner shelf waters (Fig. 30a & b). Higher water temperatures and lower discharge conditions may have favored the increased proportions of picophytoplankton (mainly cyanobacteria, See Chapter II). Cyanobacteria have been known to dominate during periods of high temperature and low nutrients conditions (Li 1998).

Significant variability in micro and picophytoplankton size classes were also observed in mid-shelf and slope waters (Fig. 30c & 30d), but such differences existed the nanophytoplankton size group. Microphytoplankton, dominated the mid-shelf (mean ±SD, 68.1 ± 19.5 %) and slope (53.7 ± 27.7 %) communities during spring 2010, for

other periods their contribution to the total community were ~34.2% and 22.3% in mid-shelf and slope waters respectively. Proportions of picophytoplankton during winter and spring 2010 were significantly lower (Kruskal Wallis $p < 0.05$) than that of other periods in mid-shelf waters (Fig. 30c). Picophytoplankton dominated slope waters in spring 2009 and fall (accounted for 45 ± 15.4 % of the community), while they occupied a minor portion of the community during spring 2010 (ranged: 1.9 – 8.7 %). Intermediate proportion of picophytoplankton was observed during winter and summer (26.5 ± 14 %). The low percentage of picophytoplankton during spring 2010 was attributed to the unusually large river discharge (See Fig. 14, Chapter IV) just prior to the cruise (March 2010). This resulted in high nutrient conditions in slope waters, which would have favored microphytoplankton.

Vertical Variability in Chlorophyll-Specific Absorption of Phytoplankton

Vertical variability in phytoplankton chlorophyll-specific absorption was less prominent than the horizontal variations. Some indication of photoacclimations were observed, the ratio of PPC: PSC decreased significantly (Kruskal-Wallis, at p 0.05 levels) indicating increase in PSC with depths (corresponding with decrease in zea; Chl *a*, Fig. 8, Chapter II). At similar depths diminished values of $a_{\varphi}(440)$: $a_{\varphi}(675)$ and $a^*_{\varphi}(440)$ were also observed suggesting flatter spectra in the deep waters consistent with the increase in the levels of pigment packaging. The absorption efficiency index, $Q_a^*(676)$, at CFM, was not significantly different from the surface waters (Kruskal-Wallis, p = 0.05 levels), but, differences were much greater in the stratified months than during the mixed periods (winter and spring 2010) at the slope waters (Fig. 31c).

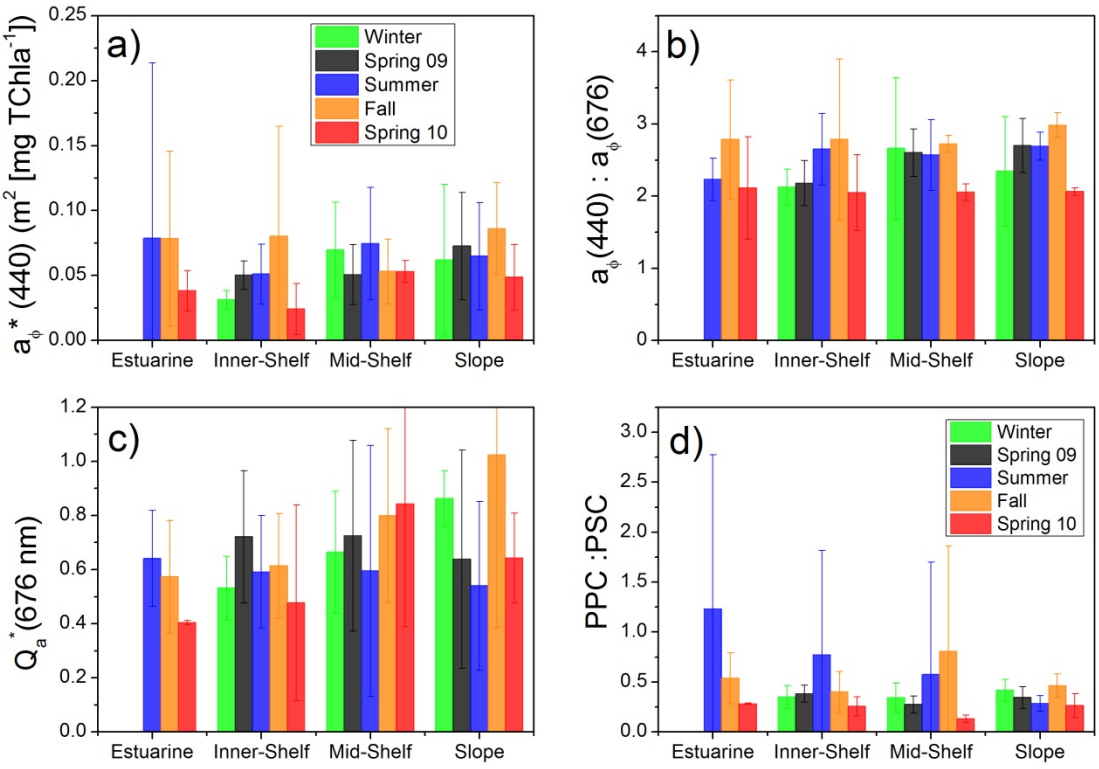

Figure 31. Regional and seasonal variations in phytoplankton bio-optical indices and pigment ratios for samples from near bottom depths in estuarine, inner shelf and mid-shelf water types and the depth of the chlorophyll fluorescence maximum in slope waters. (a) chlorophyll-specific absorption of phytoplankton ($a^*_\varphi(440)$), (b) the ratio of $a_\varphi(440)$: $a_\varphi(675)$, (c) absorption efficiency, (d) ratio of photo protective carotenoids (PPC) to photosynthetic carotenoids (PSC).

Low values $Q_a^*(676)$ at the CFM indicate increased packaging. Ratios of zea : Chl *a* decreased (range 27-74 %) While the ratios of fucoxanthin (fuco) and 19-hexanoloxyfucoxanthin (19′-Hex) to Chl *a* increased from surface to CFM (See Chapter II for details, Fig. 8). The underlying reason of such differences was that phytoplankton were probably photoacclimated at low lights, which led to increases in cellular pigmentation and associated increases in packaging effects.

Discussion

Influence of Cell size and Pigment Packaging.

Phytoplankton size distributions as inferred from the size index (SI) showed a clear trend going from larger to smaller phytoplankton from high TChl *a* to low TChl *a* (Fig. 32a). Large variability particularly in slope waters was attributed to change in community during the summer and spring 2010, size index at the slope stations ranged from 4-40 µm with a mode of 9µm. SI for several slope stations were high which corresponded to periods of high discharge (Spring 2010) and stations affected by Mississippi plume during the offshore transport of the river plume, micro and nanophytoplankton were dominant at those stations.

Values of $a^*_{\varphi}(440)$ generally increased with decreasing SI (Fig. 32b). A clear indication of pigment packaging was a decrease in $a^*_{\varphi}(440)$ and $a^*_{\varphi}(676)$ with the increase in SI (µm)(Fig. 32b). The coefficient of determination (r^2) was 0.43 and 0.21 for relationships of $a^*_{\varphi}(440)$ and $a^*_{\varphi}(676)$ to SI, accounting for about 43% and 21%, respectively, of the variability in the chlorophyll-specific absorption coefficients of phytoplankton. Low values of $Q^*_a(676)$ (Fig. 32d and $a^*_{\varphi}(440)$ (Fig. 32b)) in inner shelf and estuarine waters coincided with , dominance of microphytoplankton. Values of $Q^*_a(676)$ and SI exhibited contrasting relationships to TChl *a* (Fig. 32a & 32c), which was a reflection of the increase in package effect as a function of cell size. Similar observations were also found by Lohrenz et al. (2003a) and Stuart et al. (1998), who reported reductions of 62% and 58%, respectively, in absorption at 440 nm due to package effects in populations dominated by large phytoplankton.

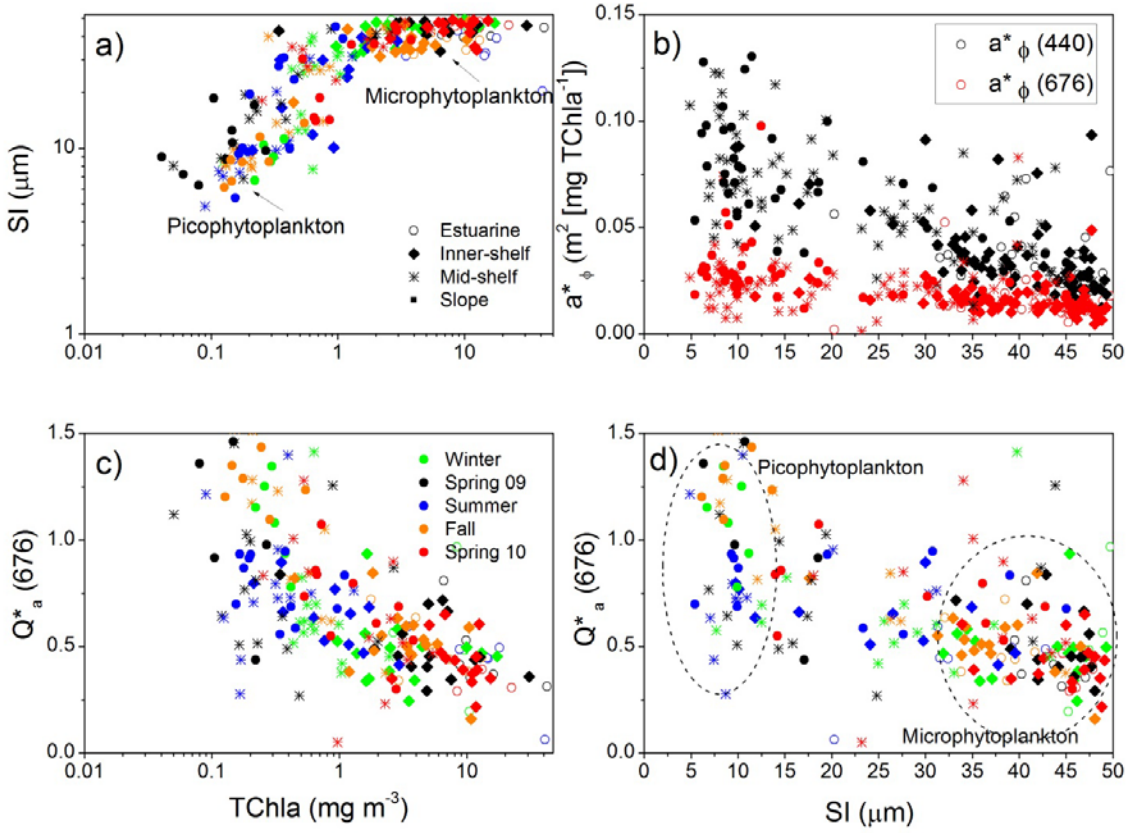

Figure 32. Relationships between size index, SI and TChl *a* (a), between absorption efficiency Q_a*(676) and TChl *a* (b), phytoplankton chlorophyll specific absorption, a^*_{φ}, at 440 nm and 676 nm versus SI (c), and Qa*(676) versus SI (d).

Influence of Pigments on Specific Phytoplankton Absorption.

To further examine the importance of the accessory pigment composition as a factor influencing the chlorophyll-specific absorption of phytoplankton, the relative proportions of four categories of accessory pigments were compared to chlorophyll-specific absorption (Fig. 33). The proportions of each category of accessory pigments relative TChl *a* varied seasonally. The ratio TChlb/TChl *a* varied from 0-0.2 for most of the samples The TChlc/TChl *a* ratio and $a^*_{\varphi}(440)$ was complex and no distinct trend were observed in the dataset (Fig. 33a). Trends in TChlb/TChl *a* (Fig 33b) were slightly

different for estuarine and inner shelf waters, TChlb/TChl *a* ratios were highest during fall (0.074 ± 0.029, median 0.067) while highest values at midhelf and slope waters were during winter (0.128 ± 0.04, median 0.128) when the phytoplankton community was dominated by nanophytoplankton (Fig. 30c & 30d) commonly represents green algae (Chlb and prasinoxanthin). The ratios of TChlb/TChl *a* during spring 2010 were high, high values during that period resulted due to the presence of micro and nanophytoplankton contributing about 96% of the total community.

Higher ratios of PPC:PSC corresponded with higher values of $a^*_{\varphi}(440)$ during spring, fall, and summer of 2009 (Fig. 33c). In general, PPC:PSC ratios were low in estuarine and inner shelf waters and high in mid-shelf and slope waters. These observations were consistent with the view that higher values of $a^*_{\varphi}(440)$ were at least partially due to differences in pigment composition, specifically a higher relative abundance of photo protective pigments. The PPC group of pigments functions to dissipate absorbed energy as heat under high light conditions, and so plays a photo protective role in the cell (Falkowski & Raven 1997). Consistent with the findings in this study, prior investigations have demonstrated that phytoplankton absorption in the blue-green region can be significantly affected by the relative contribution of photo protective pigments (Bricaud et al. 1995). High values of PPC are generally found in high irradiance acclimated cells (Morel & Bricaud 1981) and this was generally consistent with the observations in this study of higher values of $a^*_{\varphi}(\lambda)$ during summer and fall. Cleveland (1995) attributed higher concentrations of PPC to a photoacclimation response to high light conditions at oceanic waters. Higher light penetration in offshore waters is a consequence of lower concentrations of light absorbing constituents including pigments,

colored dissolved organic matter (CDOM) and non-algal particles (NAP)(discussed in Chapter IV). In contrast, relatively high light attenuation in in inshore waters could reduce light exposure of phytoplankton. Observations of low PPC: PSC during summer at some slope stations was attributed to offshore transport of MS river waters (as previously described Chapters II, III, and IV). The presence of MS river waters at several slope stations coincided with shifts in the phytoplankton community from picophytoplankton to microphytopankton. Subsequent changes in pigment composition were also observed, with phytoplankton in the MS water impacted stations characterized by higher relative abundance of PSC.

To explore the effect of photo protective pigments on the shape of the phytoplankton absorption in the blue-green spectral region, a normalized slope of the a_φ spectrum between 488-532 nm was determined following the approach of Eisner et al. (2003): Normalized slope between 488-532 nm in the

$$a_\varphi \text{ spectra} = (a_\varphi(488) - a_\varphi(532)).(a_\varphi(676)(488\text{-}532)^{-1}) \quad (18)$$

The normalized slope was inversely related to PPC:PSC (Fig. 33d), and higher values of the slope generally corresponded to estuarine and inner shelf waters (-0.0173 ± 0.005, median -0.0165). More negative (steeper) normalized slope values were characteristic of mid-shelf and slope populations which was consistent with lower degrees of pigment packaging and phytoplankton acclimation to relatively high irradiance levels. Phytoplankton in slope and mid-shelf waters exhibited characteristics consistent with high light photoacclimation during spring and fall 2009. Evidence in support of this includes deeper euphotic depths (Chapter III), UV absorption peaks indicative of mycosporin-like amino acids (Chapter IV), and high PPC:PSC ratios (this chapter)

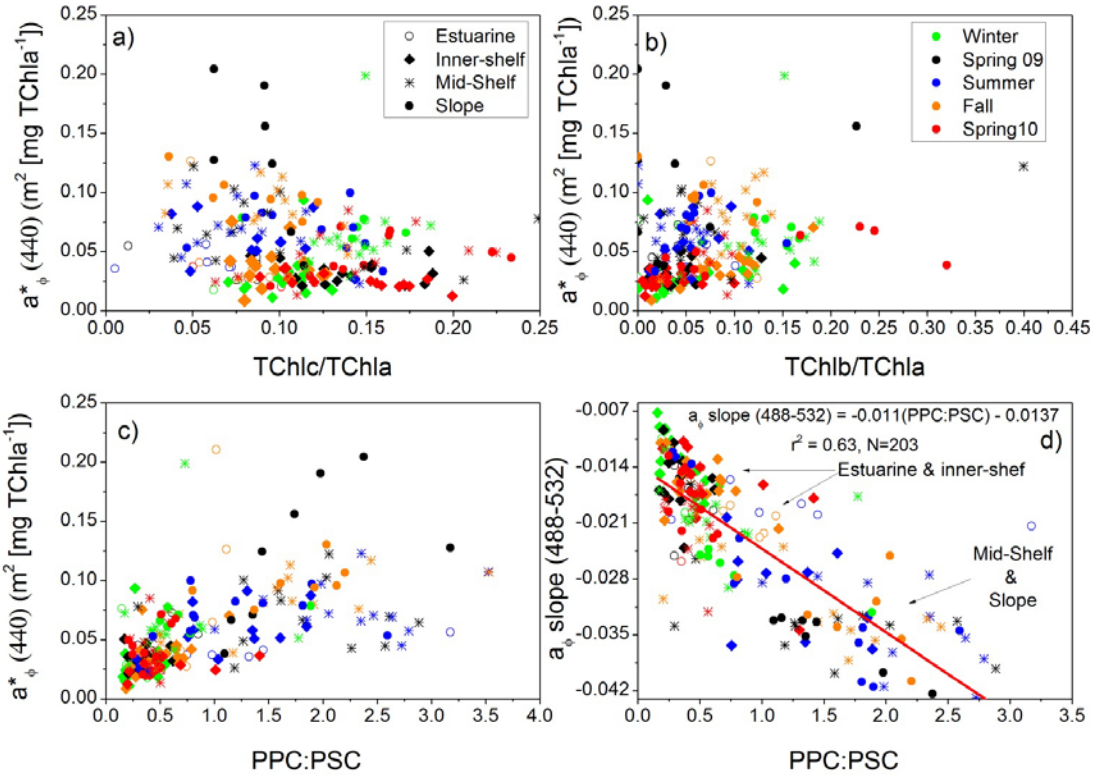

Figure 33. Variation of chlorophyll-specific phytoplankton absorption at 440 nm in relation to accessory pigment ratios including TChla/TChl *a* (a), TChlb/TChlb (b), PPC:PSC (c). The normalized slope of a_φ spectra between 488 and 532 nm (($a_\varphi(488)$ – $a_\varphi(532)$) /($a_\varphi(676)(488–532)$) as a function of the ratio photo protective to photosynthetic carotenoids (PPC:PSC) (d). The line represents a model I regression of normalized slope versus PPC:PSC.

Relative Importance of Pigment Composition and Packaging.

To examine the relative importance of the pigment composition and pigment packaging effects on the chlorophyll-specific phytoplankton absorption coefficient, a stepwise multiple linear regression (IBM SPSS Statistics 14) was used to identify key variables that could account for variability in $a^*_\varphi(440)$. The analysis was performed by setting $a^*_\varphi(440)$ as the dependent variable and the concentrations of the major pigment

groups normalized to Chl *a* along with the absorption efficiency, $Q^*_a(676)$, (as an index of pigment packaging) as the independent variables. In general, the combined effects of pigment packaging and pigment composition accounted for 78.8 - 91.4% of the variation in the chlorophyll-specific absorption coefficient for the entire study period. The variables selected for the model using a forward stepwise criteria was presented in Tables 18, 19 and 20. In the forward stepwise model most significant statistical (lowest p value, $p<0.05$) terms were added to the model at each step, until was no statistically significant term to include. $Q^*_a(676)$ accounted for most of the variability in $a^*_\varphi(440)$ was associated with, and therefore for this study package effects were more important than pigment composition in influencing $a^*_\varphi(440)$. The amounts of variability explained by $Q^*_a(676)$ alone for estuarine-inner shelf, mid-shelf and slope waters were 62.7%, 58.3 % and 84.9 % respectively (Tables 18, 19 and 20).

Table 18

*Multiple Linear Regression Model Summaries for Estuarine and Inner She*lf

Model	R	R Square	Adjusted R Square	Std. Error of the Estimate	Durbin-Watson
1	0.794(a)	0.631	0.627	0.0124125	
2	0.840(b)	0.705	0.699	0.0111563	
3	0.886(c)	0.785	0.779	0.0095680	
4	0.893(d)	0.797	0.788	0.0093523	1.462

a Predictors: (Constant), $Q^*_a(676)$

b Predictors: (Constant), $Q^*_a(676)$, PPC

c Predictors: (Constant), $Q^*_a(676)$, PPC, TChlc

d Predictors: (Constant), $Q^*_a(676)$, PPC, TChlc, TChlb

e Dependent Variable: $a^*_\varphi(440)$

Table 19

Multiple Linear Regression Model Summary for Mid-Shelf

Model	R	R Square	Adjusted R Square	Std. Error of the Estimate	Durbin-Watson
1	0.767(a)	0.589	0.583	0.0227012	
2	0.883(b)	0.780	0.773	0.0167403	
3	0.940(c)	0.884	0.878	0.0122562	1.659

a Predictors: (Constant), $Q^*_{a(}676)$

b Predictors: (Constant), $Q^*_{a(}676)$, PPC

c Predictors: (Constant), $Q^*_{a(}676)$, PPC, TChlc

d Dependent Variable: $a^*_{\varphi}(440)$

Table 20

Multiple Linear Regression Model Summaries for Slope

Model	R	R Square	Adjusted R Square	Std. Error of the Estimate	Durbin-Watson
1	0.923(a)	0.852	0.849	0.0192006	
2	0.948(b)	0.898	0.893	0.0161674	
3	0.959(c)	0.921	0.914	0.0144386	1.726

a Predictors: (Constant), $Q^*_{a(}676)$

b Predictors: (Constant $Q^*_{a(}676)$, PPC

c Predictors: (Constant), $Q^*_{a(}676)$, PPC, TChlb

d Dependent Variable: $a^*_{\varphi}(440)$

Conclusions

The chlorophyll-specific phytoplankton absorption coefficient varied by a factor of approximately 2.5 from estuarine and inner-shelf waters to the slope. The results show that variability in specific phytoplankton absorption was mainly influenced by pigment packaging and community size followed by photo protective pigments. The study clearly indicated the important contribution of PPC pigments (greater than PSC pigments) to the absorption spectrum of phytoplankton in northern Gulf of Mexico.

Differences in the chlorophyll-specific phytoplankton absorption coefficient between spring 2009 and 2010 was attributed to offshore transport of freshwater in spring 2010 following high river discharge. Higher values of PPC: PSC ratios during summer and spring 2009 in surface waters could be explained by phytoplankton acclimation to high light levels. Vertical variations in chlorophyll-specific absorption coefficients were also observed in some cases and attributed to photoacclimation processes and changes in population structure. Variability observed in the optical properties was higher and significant during the stratified month while little differences existed for the mixed periods. The results agrees with the general concept of uniform photoacclimation throughout the water column during non-stratified conditions (when mixed layer depth > euphotic depth), provided that the time required for mixing (that is, the travel time for an algal cell to pass through the light gradient within the mixed layer) is shorter than the time required for photoacclimation. Under stratified conditions (mixed layer depth < euphotic depth), phytoplankton cells in the upper mixed layer would be exposed to higher light levels, exhibiting different photophysiological characteristics from the cells below the mixed layer depths (Falkowski & Wirick 1981). In summary, results from this study

strongly support the view that pigments play a major role in influencing the magnitude and spectral shape of $a^*_{\varphi}(440)$.

The findings from this study emphasize the importance of accounting the variability in magnitude and spectral shape of the chlorophyll-specific absorption coefficient in bio-optical models to estimate primary production. The study also provided important information that will improve the understanding of the ecological and photophysiological characteristics of phytoplankton in northern Gulf of Mexico.

CHAPTER VI

CONCLUSION

Chapter II. Phytoplankton Community Composition among Water Mass Types

The observations from this study supported the primary hypothesis that phytoplankton community in the northern Gulf of Mexico differs among the different water types across the continental shelf. Diatoms, cryptophytes and chlorophytes dominated the estuarine and inner shelf waters in NGOM. In summary, this study has demonstrated that diatoms and cryptophytes dominated the phytoplankton communities in the estuarine and inner shelf waters, except summer, when cyanobacteria were abundant in most of the shelf. Opposite trend was observed in the slope waters where cyanobacteria and prochlorophytes were dominant for majority of the study period, except in summer (July 2009) and spring 2010 (March 2010). Phytoplankton community at several stations (in July 2009) in the slope and most stations (in March 2010) were dominated by diatoms. Under both circumstances seasonal change in winds along with river discharge (during March 2010) lead to offshore transport of freshwater plume to the slope waters.

Chapter III. Relationship between Phytoplankton Community Composition and Environmental Conditions

Results from principal component analysis were in support of the primary hypothesis that differences in phytoplankton community composition will coincide with transitions between stratified and non-stratified periods for all water types in the continental margin of the northern Gulf of Mexico. Principal component analysis (PCA) was successful in determining the important environmental variables during the study..

The results from this study provide strong evidence of preferred mixing regimes between different phytoplankton groups in the northern Gulf of Mexico. Phytoplankton community was found mainly to be dominated by seasonal (thermal) cycles but also showed evidence of variations on shorter time and space scales. The dominant principal component modes of environmental variability (the first two principal components) were mainly associated with water temperature, mixed layer depths, winds, salinity.

Chapter IV. Light Absorption Properties in the NGOM

The primary hypothesis was satisfied and results showed that seasonal difference in bio-optical properties was mainly controlled by regional hydrodynamics; fluctuations in river discharge, wind events, offshore transport of river plume and seasonal mixing. Light absorption properties in NGOM varied and were not spatially homogenous, CDOM and NAP were the main light absorbing components at estuarine and inner shelf margins.

Role of organic matter derived from phytoplankton probably had a minor role in controlling the spectral properties of CDOM and NAP and therefore the secondary hypothesis was not completely satisfied. Terrestrial sources of CDOM can be important source at the offshore slope waters and most likely photo bleaching is the primary process that accounts for the loss of CDOM in offshore waters.

Considering NGOM continental slope to be close to case 1 waters could significantly limit application of global ocean color algorithms particularly those which relies on constant slopes for CDOM, NAP and backscattering ratios. Assessment of remote sensing algorithms (QAA) demonstrated the importance of regional tuning of the algorithms for NGOM. In general, statistical analysis provided evidence of consistent overestimation in the inner-shelf region. QAA_a_{φ} performed considerably well at 443 and

can be used as index to characterize phytoplankton dynamics in the region instead of Chl *a*. Relative uncertainties were much lower for QAA_a_{dg} and results were reasonably promising and will provide confidence if and when satellite derived QAA_a_{dg} maps are used quantitatively in NGOM.

Chapter V. Phytoplankton Light Absorption

Results showed that specific absorption properties of phytoplankton were found to be a function of phytoplankton size, community composition, pigment composition and pigment packaging which supported the primary hypothesis. Absorption coefficients varied closely with variations in chl *a* and were lower for diatoms compared to flagellates and cyanophytes. Chlorophyll-specific coefficients also provided useful information on the level of pigment packaging and were related to the proportion of photosynthetic and photo protective pigments. The results suggests that phytoplankton in the continental margins of the northern Gulf of Mexico were acclimated to different environmental conditions related to seasonal variability in temperature and river discharge. Vertical variations in chlorophyll-specific absorption coefficients were also observed in some cases and attributed to photoacclimation processes and changes in population structure. Variability observed in the optical properties was higher and significant during the stratified month while little differences existed for the mixed periods.

Remarks on application of phytoplankton community information in ecosystem models

The importance of partitioning phytoplankton size structure (micro or picophytoplankton) and functional types is gradually increasing in the ocean modeling community. However there are many ecosystem models that do not include such differentiations (e.g., Earth System Model employed at Max-Planck Institut für

Meteorologie (MIPM) and the Community Climate System Model (CCM 1.4) from National Center for Atmospheric Research). A comparative study (Steinacher et al. 2010) of multiple ecosystem models has highlighted differences in modeled output of PP among models which included both sizes of phytoplankton with those that only included diatoms. Models that included both size classes performed much better than the one that only included diatoms. Again, there are models that include both micro (diatoms) and picophytoplankton, but they tend to pool all picophytoplankton into a single group (Quéré et al. 2005). The results from this study supports previous findings of the ubiquitous nature of the picophytoplankton (Chisholm 1992). The oceanic carbon pump can be significantly impacted based on the dominance of pico-prokaryotes (cyanobacteria and prochlorophytes) or pico-eukaryotes (haptophytes and prasinophytes) (Liu et al. 2009). The pico-eukaryotes (belonging to haptophytes and prasinophytes) along with pico-prokaryotes (prochlorophytes) were found to be important in the present study. Again seasonal differences between the two groups were also noticed. Future models should try to incorporate such partitioning in the pico size fraction in order to better understand the responses of phytoplankton community under the global climate change and ocean acidification scenario.

Remarks on Remote Sensing Applications of Absorption and Chlorophyll-a Specific Absorption

One of the key area of interest in the ocean color community is to derive net primary production from ocean color data (McClain 2009). Phytoplankton absorption and chlorophyll-specific absorption coefficients can influence primary production, since they affect the underwater light transmission and determine the magnitude of

photosynthetically active photons. Besides primary production estimates, chlorophyll-*a* specific absorption can be used to generate size parameters which can reflect composition of microplankton, nano and picoplankton (Ciotti & Bricaud 2006) and can be estimated using remotely sensed reflectance. The results from this study show that phytoplankton community structure, pigment packaging and photo protective pigments play a strong role in determining the chl *a* specific absorption. Significant seasonal variations in each of the factors have been found in the study. Development of season specific bio-optical models may be a better way to estimate primary production and community composition in the region.

APPENDIX A

REGRESSION ANALYSIS OF THE PIGMENT DATA SET FOR EACH GULF CARBON CRUISE.

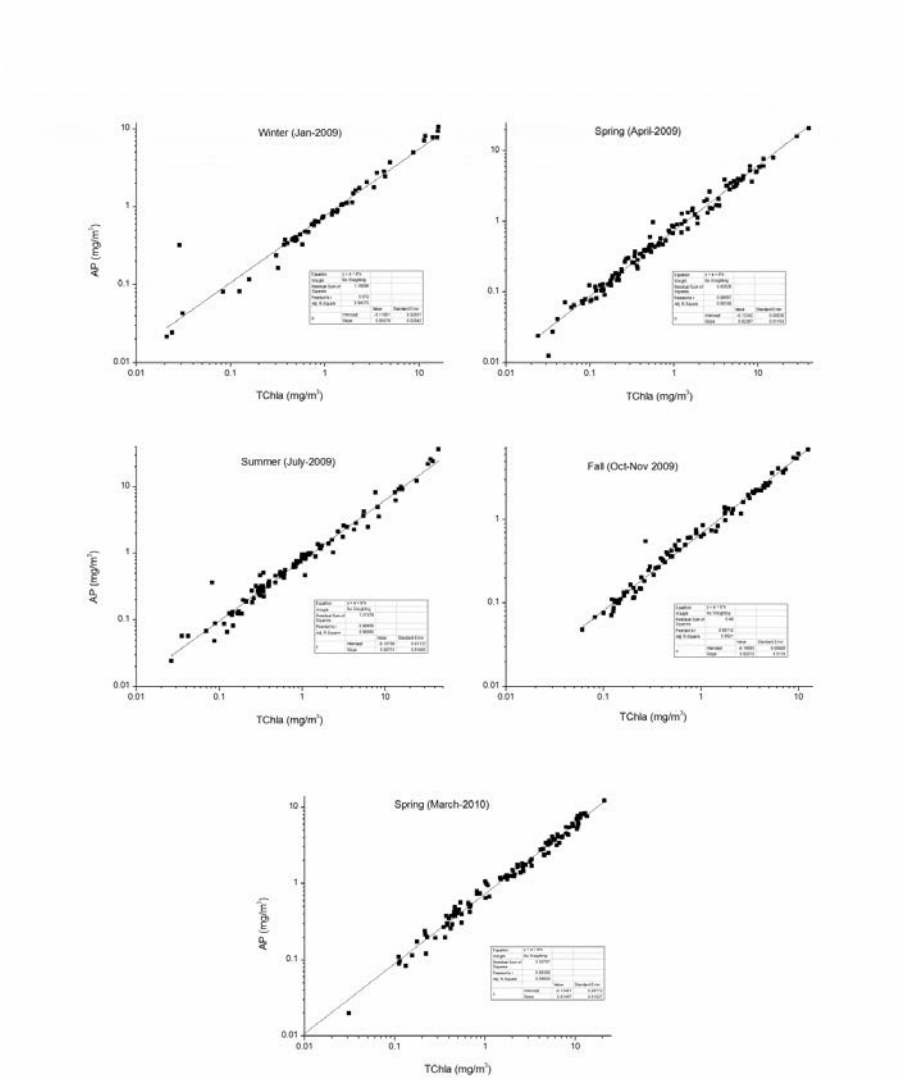

APPENDIX B

CLUSTER ANALYSIS: DENDOGRAM SHOWING DIFFERENT WATER TYPES

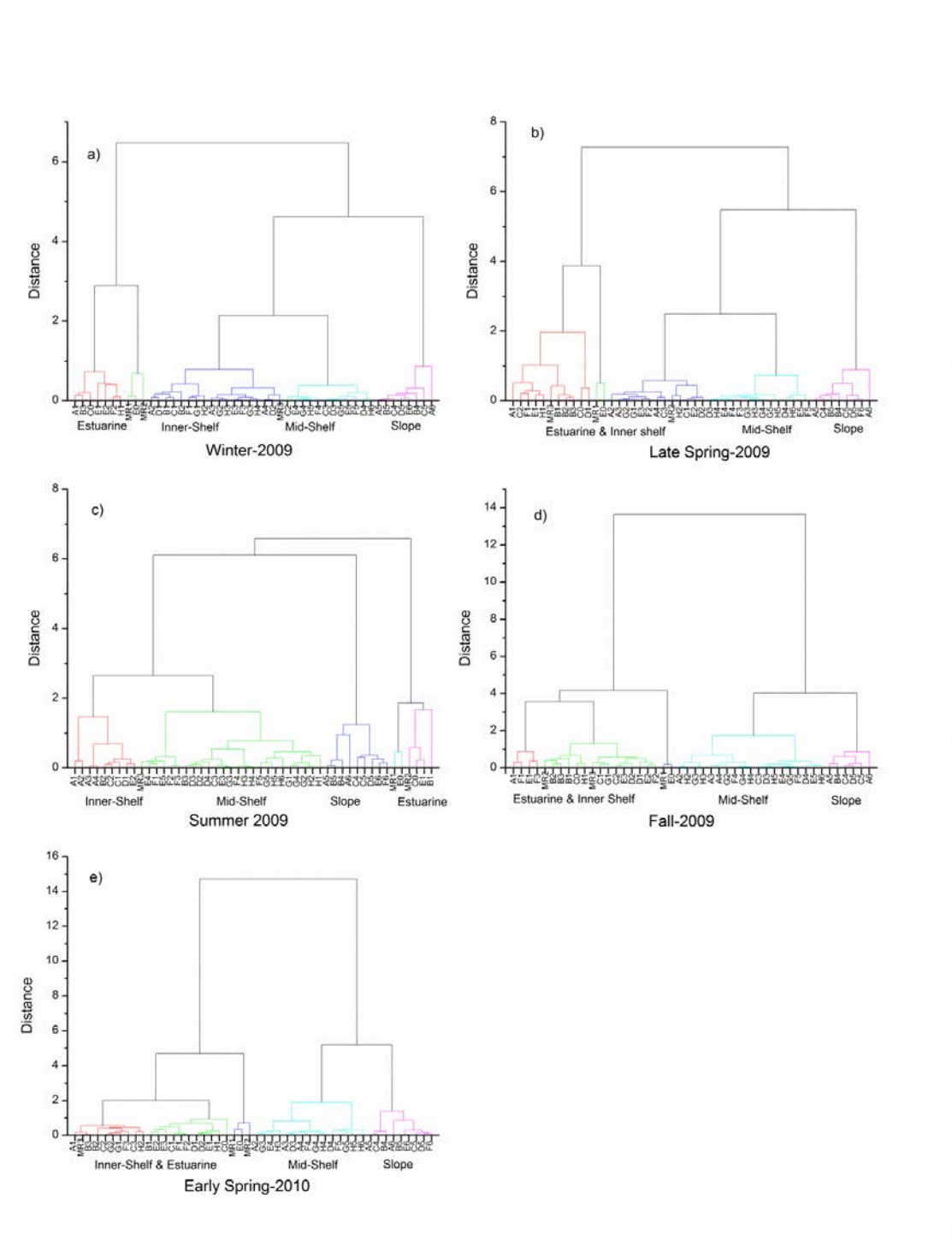

APPENDIX C

CLUSTER ANALYSIS: DENDOGRAM OF SURFACE ACCESSORY PIGMENTS : TCHLA

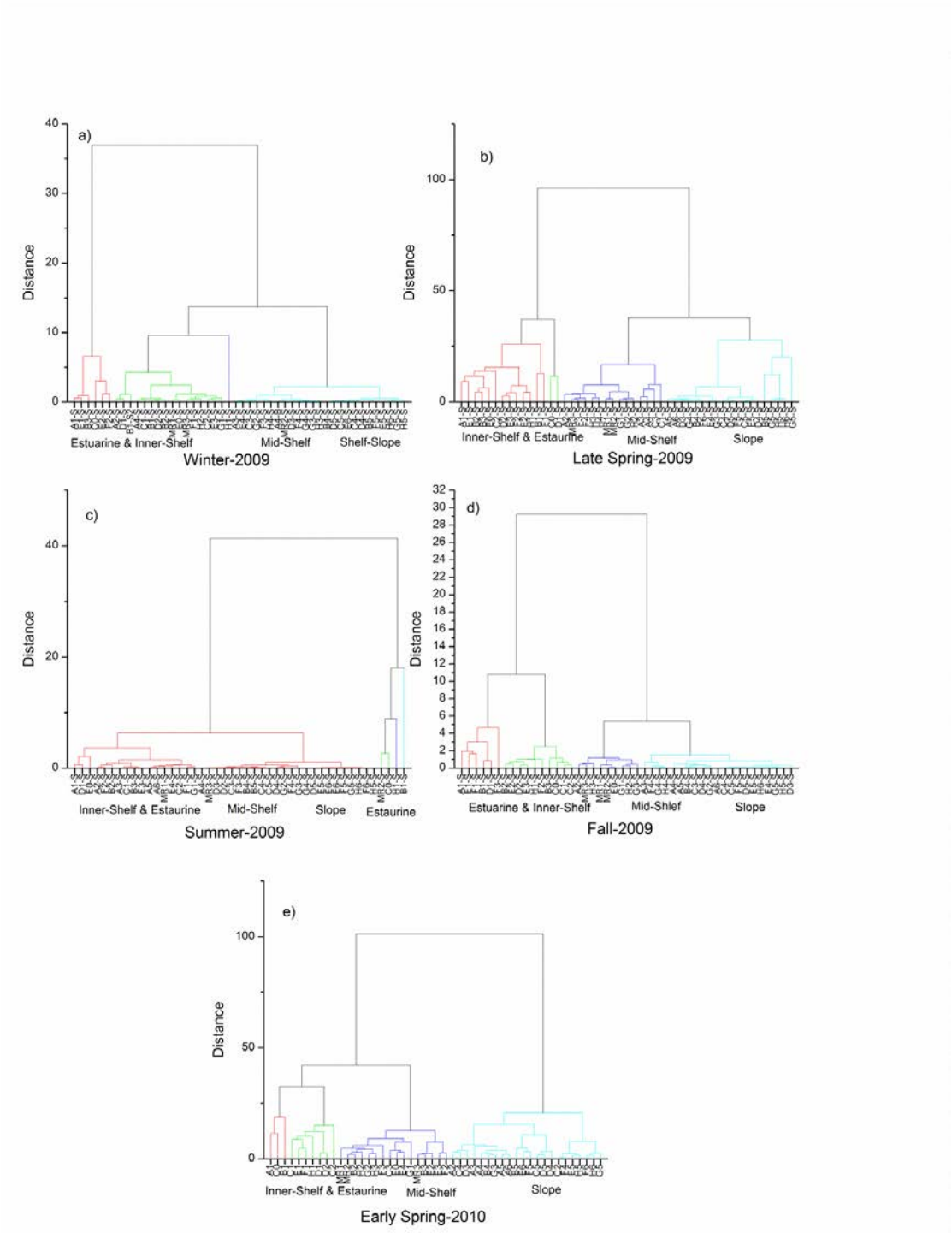

APPENDIX D

CLUSTER ANALYSIS: DENDOGRAM OF SUB SURFACE AND DEEP ACCESSORY PIGMENTS : TCHLA

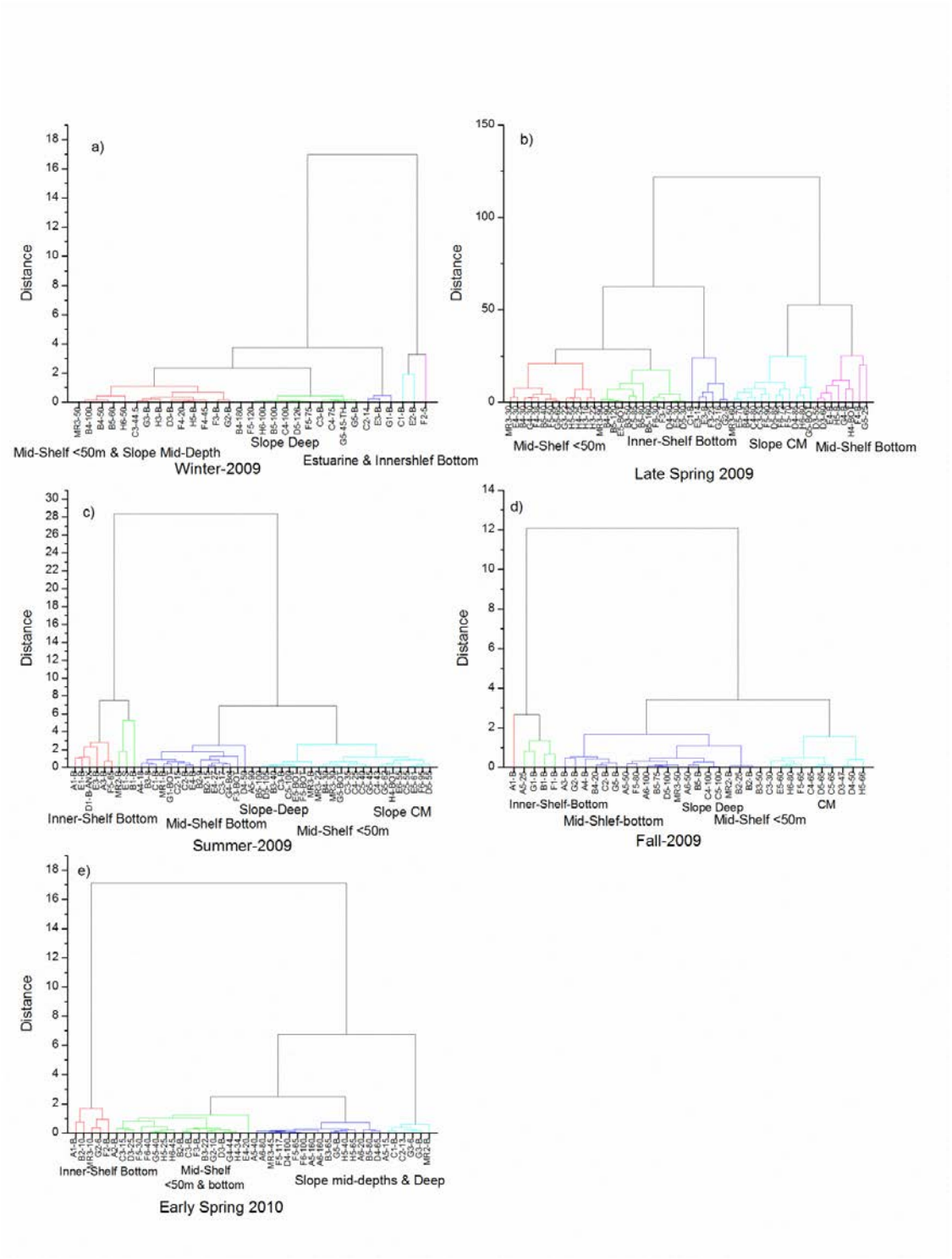

APPENDIX E

HOVMÖLLER DIAGRAM SHOWING THE DISTRIBUTION OF EURUTHERMAL UV DOSE RATE AT LOCAL NOON ON THE SLOPE WATERS (LAT 28N -27N, LON 94 W-87.5W) DERIVED FROM GIOVANNI Level-3 OMI SURFACE UV IRRADIANCE AND EURYTHERMAL DOSE-OMUVBd (JANUARY 2009-APRIL 2010).

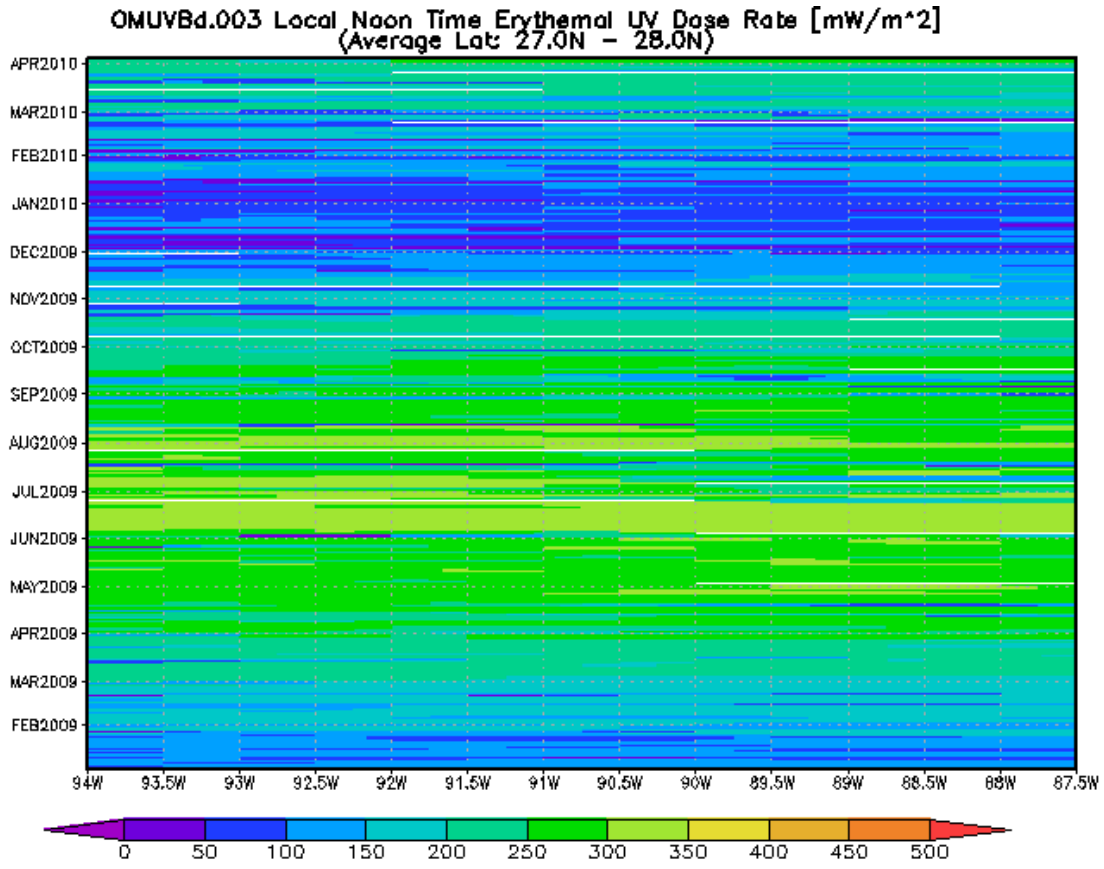

APPENDIX F

RELATIONSHIP BETWEEN S_{CDOM} (275-295) AND TChl *a*.

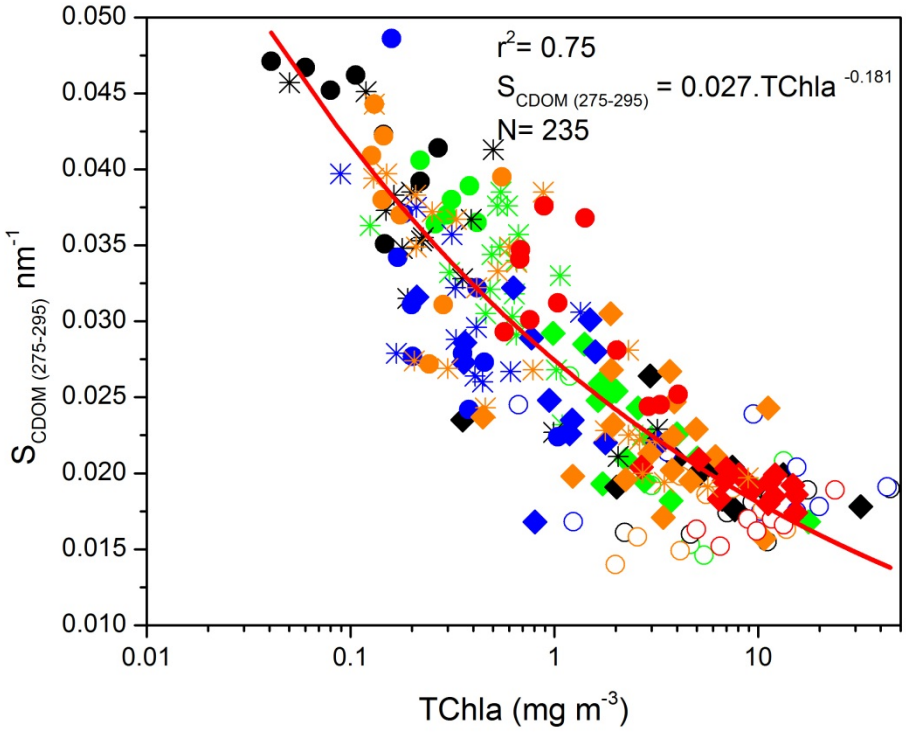

APPENDIX G

DIFFERENCES IN S_{CDOM} (350-500) BETWEEN SURFACE AND BOTTOM (a-c) AND DEEP (d).

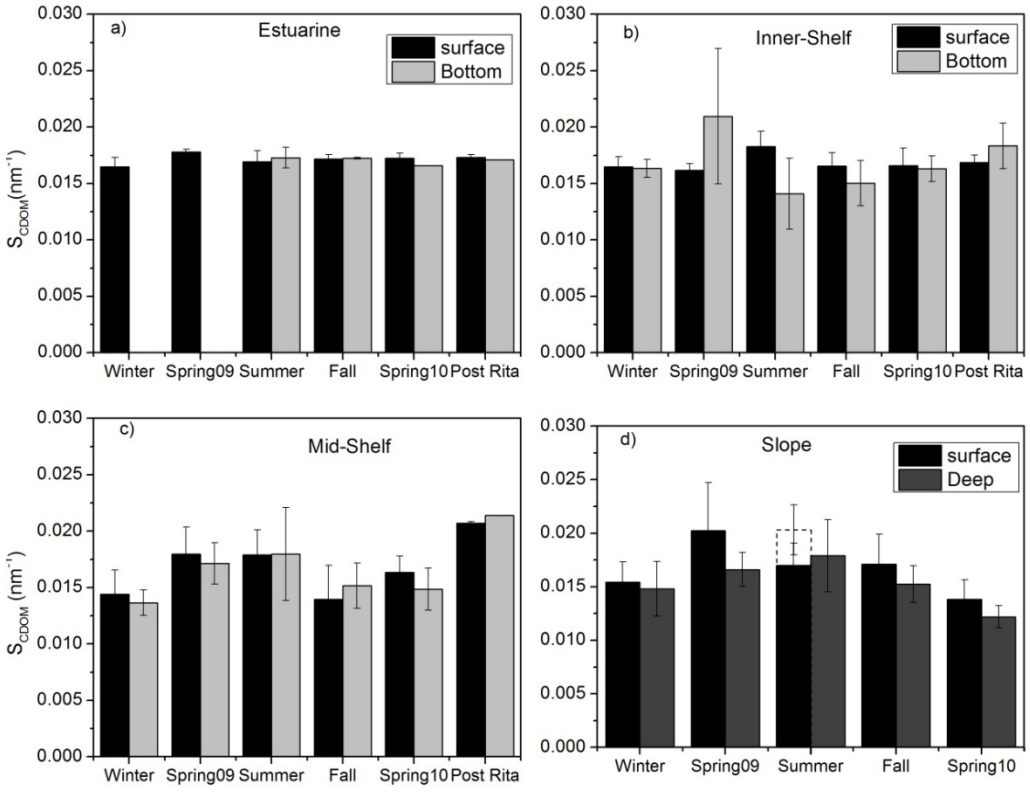

APPENDIX H

SURFACE AND BOTTOM DIFFERNCES IN S_{NAP}

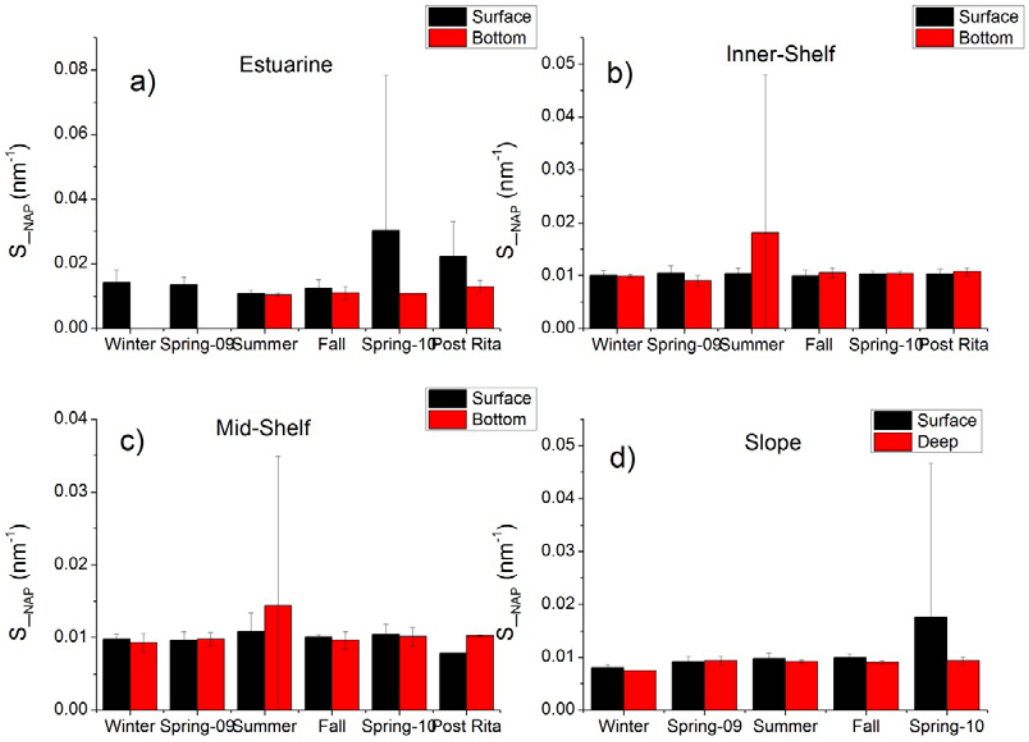

APPENDIX I

SHOWING RELATIONSHIP OF $a^*_{\varphi}(440)$ WITH PHYSICAL AND CHEMICAL VARIABLES, (A) TEMPERATURE, (B) SALINITY AND (C) DIN. WITH THE INCREASE IN SALINITY DIN VALUES DECREASES (D).

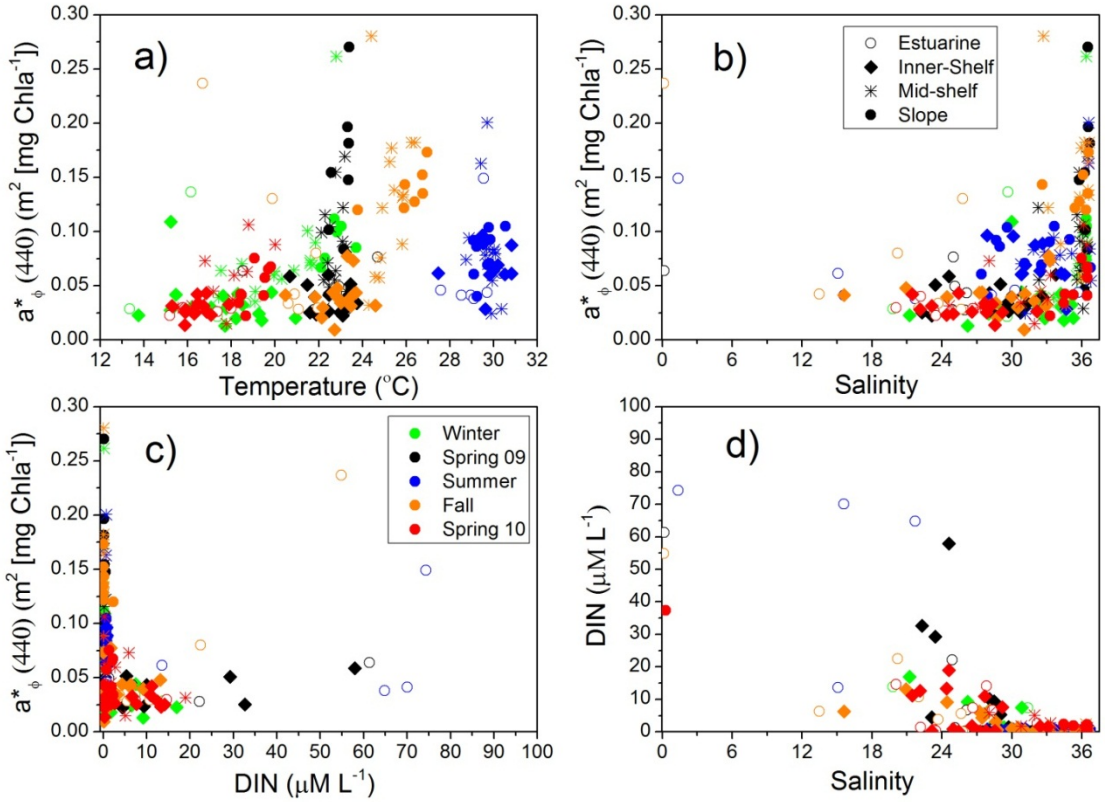

APPENDIX J

SHOWING THE COEFFICIENTS AND VIF GENERATED BY MULTIPLE LINEAR REGRESSION FOR EACH REGION

	Model	Unstandardized coefficients	Std.Err	Standardized Coefficients	p-value	VIF
	(Constant)	0.004	0.003		0.209	
Estuarine	$Q^*_{a(676)}$	0.082	0.005	0.709	0.000	1.055
&	PPC	0.053	0.007	0.707	0.000	4.313
Inner-shelf	TChlc	-0.112	0.019	-0.551	0.000	3.916
	TChlb	0.059	0.025	0.120	0.021	1.223
	(Constant)	-0.025	0.005		0.000	
	$Q^*_{a(676)}$	0.081	0.008	0.555	0.000	1.643
Mid-shelf	PPC	0.128	0.010	0.569	0.000	1.172
	TChlc	0.099	0.013	0.440	0.000	1.859
	(constant)	-0.02	0.007		0.005	
	$Q^*_{a(676)}$	0.087	0.006	0.790	0.000	1.268
Slope	PPC	0.108	0.019	0.355	0.000	1.856
	TChlb	0.076	0.023	0.193	0.002	1.643

All the model fits were significant ($p<0.05$). The assumption that the errors in the regressions were independent and that there was no autocorrelation was verified using the Durbin-Watson test (test results were close to 2), shows that there was no meaningful autocorrelation (Bhargava et al. 1982). The potential for multicollinearity among the independent variables was examined using the variance inflation factor (VIF). VIF values were always less than 5 (Table 5.6), which was evidence of absence of multicollinearity (Farrar & Glauber 1967) and within acceptable limits for these statistical models (Hair 2010).

LITRATURE CITED

Adolf JE, Yeager CL, Miller WD, Mallonee ME, Harding LW (2006) Environmental forcing of phytoplankton floral composition, biomass, and primary productivity in chesapeake bay, USA. Estuarine, Coastal and Shelf Science 67:108-122

Agustí S, Llabrés M (2007) Solar radiation-induced mortality of marine pico-phytoplankton in the oligotrophic ocean†. Photochemistry and Photobiology 83:793-801

Aiken J, Pradhan Y, Barlow R, Lavender S, Poulton A, Holligan P, Hardman-Mountford N (2009) Phytoplankton pigments and functional types in the atlantic ocean: A decadal assessment, 1995–2005. Deep Sea Research Part II: Topical Studies in Oceanography 56:899-917

Allison DB, Stramski D, Mitchell BG (2010) Seasonal and interannual variability of particulate organic carbon within the southern ocean from satellite ocean color observations. Journal of Geophysical Research C: Oceans 115

Allison MA, Kineke GC, Gordon ES, Goñi MA (2000) Development and reworking of a seasonal flood deposit on the inner continental shelf off the atchafalaya river. Continental Shelf Research 20:2267-2294

Álvarez-Góngora C, Herrera-Silveira JA (2006) Variations of phytoplankton community structure related to water quality trends in a tropical karstic coastal zone. Marine pollution bulletin 52:48-60

Anderson GF (1986) Silica, diatoms and a freshwater productivity maximum in atlantic coastal plain estuaries, chesapeake bay. Estuarine, Coastal and Shelf Science 22:183-197

Aufdenkampe AK, Hedges JI, Richey JE, Krusche AV, Llerena CA (2001) Sorptive fractionation of dissolved organic nitrogen and amino acids onto fine sediments within the amazon basin. Limnology and Oceanography 46:1921-1935

Aurin DA, Dierssen HM (2012) Advantages and limitations of ocean color remote sensing in cdom-dominated, mineral-rich coastal and estuarine waters. Remote Sensing of Environment 125:181-197

Babin M, Morel A, Fournier-Sicre V, Fell F, Stramski D (2003a) Light scattering properties of marine particles in coastal and open ocean waters as related to the particle mass concentration. Limnology and Oceanography 48:843-859

Babin M, Stramski D (2004) Variations in the mass-specific absorption coefficient of mineral particles suspended in water. Limnology and Oceanography 49:756-767

Babin M, Stramski D, Ferrari GM, Claustre H, Bricaud A, Obolensky G, Hoepffner N (2003b) Variations in the light absorption coefficients of phytoplankton, nonalgal particles, and dissolved organic matter in coastal waters around europe. Journal of Geophysical Research C: Oceans 108:4-1

Banse K (1994) Grazing and zooplankton production as a key control of phytoplankton production in open ocean. Oceanography 7:13-17

Barocio-León ÓA, Millán-Núñez R, Santamaría-del-Ángel E, Gonzalez-Silvera A, Trees CC, Orellana-Cepeda E (2008) Bio-optical characteristics of a phytoplankton bloom event off baja california peninsula (30–31°n). Continental Shelf Research 28:672-681

Benner R, Weliky K, Hedges JI (1990) Early diagenesis of mangrove leaves in a tropical estuary: Molecular-level analyses of neutral sugars and lignin-derived phenols. Geochimica et Cosmochimica Acta 54:1991-2001

Bhargava A, Franzini L, Narendranathan W (1982) Serial correlation and the fixed effects model. The Review of Economic Studies 49:533-549

Bianchi TS (2011) The role of terrestrially derived organic carbon in the coastal ocean: A changing paradigm and the priming effect. Proceedings of the National Academy of Sciences of the United States of America 108:19473-19481

Bianchi TS, Allison MA (2009a) Large-river delta-front estuaries as natural "recorders" of global environmental change. Proceedings of the National Academy of Sciences of the United States of America 106:8085-8092

Bianchi TS, Allison MA (2009b) Large-river delta-front estuaries as natural “recorders” of global environmental change. Proceedings of the National Academy of Sciences

Bianchi TS, DiMarco SF, Cowan JH, Jr., Hetland RD, Chapman P, Day JW, Allison MA (2010) The science of hypoxia in the northern gulf of mexico: A review. The Science of the total environment 408:1471-1484

Bianchi TS, Filley T, Dria K, Hatcher PG (2004) Temporal variability in sources of dissolved organic carbon in the lower mississippi river. Geochimica et Cosmochimica Acta 68:959-967

Bidigare RR, Schofield O, Prezelin BB (1989) Influence of zeaxanthin on quantum yield of photosynthesis of synechococcus clone wh-7803 dc2. Marine Ecology Progress Series 56:177-188

Biggs DC (1992) Nutrients, plankton, and productivity in a warm-core ring in the western gulf of mexico. Journal of Geophysical Research: Oceans 97:2143-2154

Biggs DC, Müller-Karger FE (1994) Ship and satellite observations of chlorophyll stocks in interacting cyclone-anticyclone eddy pairs in the western gulf of mexico. Journal of Geophysical Research: Oceans 99:7371-7384

Binding C, Jerome J, Bukata R, Booty W (2008) Spectral absorption properties of dissolved and particulate matter in lake erie. Remote Sensing of Environment 112:1702-1711

Binding CE, Bowers DG, Mitchelson-Jacob EG (2005) Estimating suspended sediment concentrations from ocean colour measurements in moderately turbid waters; the impact of variable particle scattering properties. Remote Sensing of Environment 94:373-383

Bode A, Dortch Q (1996) Uptake and regeneration of inorganic nitrogen in coastal waters influenced by the mississippi river: Spatial and seasonal variations. Journal of Plankton Research 18:2251-2268

Bontempi PS (1995) Phytoplankton distribution and species composition across the texas-louisiana continental shelf during two flow regimes of the mississippi river. Masters, Texas A&M University

Boss E, Pegau WS, Lee M, Twardowski M, Shybanov E, Korotaev G, Baratange F (2004) Particulate backscattering ratio at leo 15 and its use to study particle composition and distribution. Journal of Geophysical Research C: Oceans 109:C01014 01011-01010

Bouman HA, Ulloa O, Scanlan DJ, Zwirglmaier Kand others (2006) Oceanographic basis of the global surface distribution of prochlorococcus ecotypes. Science 312:918-921

Bowers DG, Binding CE (2006) The optical properties of mineral suspended particles: A review and synthesis. Estuarine, Coastal and Shelf Science 67:219-230

Brewin RJW, Hardman-Mountford NJ, Lavender SJ, Raitsos DEand others (2011) An intercomparison of bio-optical techniques for detecting dominant phytoplankton size class from satellite remote sensing. Remote Sensing of Environment 115:325-339

Bricaud A (2004) Natural variability of phytoplanktonic absorption in oceanic waters: Influence of the size structure of algal populations. Journal of Geophysical Research 109

Bricaud A, Babin M, Claustre H, Ras J, Tièche F (2010) Light absorption properties and absorption budget of southeast pacific waters. Journal of Geophysical Research 115

Bricaud A, Babin M, Morel A, Claustre H (1995) Variability in the chlorophyll-specific absorption coefficients of natural phytoplankton: Analysis and parameterization. J Geophys Res 100:13321-13332

Bricaud A, Claustre H, Ras J, Oubelkheir K (2004) Natural variability of phytoplanktonic absorption in oceanic waters: Influence of the size structure of algal populations. J Geophys Res 109:C11010

Bricaud A, Morel A, Babin M, Allali K, Claustre H (1998) Variations of light absorption by suspended particles with chlorophyll a concentration in oceanic (case 1)

waters: Analysis and implications for bio-optical models. J Geophys Res 103:31033-31044

Bricaud A, Morel A, Prieur L (1983) Optical efficiency factors of some phytoplankters. Limnology and Oceanography 28:816-832

Brunelle CB, Larouche P, Gosselin M (2012) Variability of phytoplankton light absorption in canadian arctic seas. J Geophys Res 117:C00G17

Bruyant F, Babin M, Genty B, Prasil Oand others (2005) Diel variations in the photosynthetic parameters of prochlorococcus strain pcc 9511: Combined effects of light and cell cycle. Limnology and Oceanography 50:850-863

Cai W-J (2003) Riverine inorganic carbon flux and rate of biological uptake in the mississippi river plume. Geophysical Research Letters 30

Cai W-J (2011) Estuarine and coastal ocean carbon paradox: Co2sinks or sites of terrestrial carbon incineration? Annual Review of Marine Science 3:123-145

Cai W-J, Hu X, Huang W-J, Murrell MCand others (2011) Acidification of subsurface coastal waters enhanced by eutrophication. Nature Geosci 4:766-770

Campbell JW (1995) The lognormal distribution as a model for bio-optical variability in the sea. Journal of Geophysical Research 100:13,237-213,254

Carder KL, Steward RG, Harvey GR, Ortner PB (1989) Marine humic and fulvic acids: Their effects on remote sensing of ocean chlorophyll. Limnology and Oceanography 34:68-81

Chami M, Shybanov EB, Churilova TY, Khomenko GAand others (2005) Optical properties of the particles in the crimea coastal waters (black sea). J Geophys Res 110:C11020

Chang G, Barnard A, Zaneveld JRV (2007) Optical closure in a complex coastal environment: Particle effects. Appl Opt 46:7679-7692

Chassignet EP, Hurlburt HE, Smedstad OM, Barron CNand others (2005) Assessment of data assimilative ocean models in the gulf of mexico using ocean color. In: Circulation in the gulf of mexico: Observations and models, Vol 161. AGU, Washington, DC, p 87-100

Chassot E, Bonhommeau S, Dulvy NK, Melin F, Watson R, Gascuel D, Le Pape O (2010) Global marine primary production constrains fisheries catches. Ecology letters 13:495-505

Chavez F (2007) The first state of the carbon cycle report (soccr): The north american carbon budget and implications for the global carbon cycle, National Oceanic and Atmospheric Administration, National Climactic Data Center, Ashville, NC

Chavez FP, Messié M, Pennington JT (2011) Marine primary production in relation to climate variability and change. Annual Review of Marine Science 3:227-260

Chavez FP, Strutton PG, Friederich GE, Feely RA, Feldman GC, Foley DG, McPhaden MJ (1999) Biological and chemical response of the equatorial pacific ocean to the 1997-98 el nino. Science 286:2126-2131

Chen RF, Bissett P, Coble P, Conmy Rand others (2004) Chromophoric dissolved organic matter (cdom) source characterization in the louisiana bight. Marine Chemistry 89:257-272

Chen RF, Gardner GB (2004) High-resolution measurements of chromophoric dissolved organic matter in the mississippi and atchafalaya river plume regions. Marine Chemistry 89:103-125

Chen X, Lohrenz SE, Wiesenburg DA (2000) Distribution and controlling mechanisms of primary production on the louisiana-texas continental shelf. Journal of Marine Systems 25:179-207

Chisholm SW (1992) Phytoplankton size. In: Woodhead PGFAD (ed) Primary productivity and biogeochemical cycles in the sea. Plenum Press, New York, p 213-237

Ciotti AM, Bricaud A (2006) Retrievals of a size parameter for phytoplankton and spectral light absorption by colored detrital matter from water-leaving radiances at seawifs channels in a continental shelf region off brazil. Limnology and Oceanography: Methods 4:237-253

Ciotti ÁM, Lewis MR, Cullen JJ (2002) Assessment of the relationships between dominant cell size in natural phytoplankton communities and the spectral shape of the absorption coefficient. Limnology and Oceanography 47:404-417

Claustre H (1994) The trophic status of various oceanic provinces as revealed by phytoplankton pigment signatures. Limnology and Oceanography 39:1206-1210

Cleveland JS (1995) Regional models for phytoplankton absorption as a function of chlorophyll a concentration. J Geophys Res 100:13333-13344

Coble PG, Lisa L Robins, Kendra L. Daly, Wei-Jun Cai, Katja Fennel, Steven E. Lohrenz (2010) A preliminary carbon budget for gulf of mexico

Collier JL (2000) Flow cytometry and the single cell in phycology. Journal of Phycology 36:628-644

Conmy RN, Coble PG, Chen RF, Gardner GB (2004) Optical properties of colored dissolved organic matter in the northern gulf of mexico. Marine Chemistry 89:127-144

D'Sa EJ (2008) Colored dissolved organic matter in coastal waters influenced by the atchafalaya river, USA: Effects of an algal bloom. Journal of Applied Remote Sensing 2

D'Sa EJ, DiMarco SF (2009) Seasonal variability and controls on chromophoric dissolved organic matter in a large river-dominated coastal margin. Limnology and Oceanography 54:2233-2242

D'Sa EJ, Miller RL (2003) Bio-optical properties in waters influenced by the mississippi river during low flow conditions. Remote Sensing of Environment 84:538-549

D'Sa EJ, Miller RL, Del Castillo C (2006) Bio-optical properties and ocean color algorithms for coastal waters influenced by the mississippi river during a cold front. Applied Optics 45:7410-7428

D'Sa EJ, Miller RL, McKee BA (2007) Suspended particulate matter dynamics in coastal waters from ocean color: Application to the northern gulf of mexico. Geophysical Research Letters 34

Dagg M, Benner R, Lohrenz S, Lawrence D (2004) Transformation of dissolved and particulate materials on continental shelves influenced by large rivers: Plume processes. Continental Shelf Research 24:833-858

Dagg M, Sato R, Liu H, Bianchi TS, Green R, Powell R (2008) Microbial food web contributions to bottom water hypoxia in the northern gulf of mexico. Continental Shelf Research 28:1127-1137

Dagg MJ, Breed GA (2003) Biological effects of mississippi river nitrogen on the northern gulf of mexico—a review and synthesis. Journal of Marine Systems 43:133-152

Del Castillo CE, Miller RL (2008) On the use of ocean color remote sensing to measure the transport of dissolved organic carbon by the mississippi river plume. Remote Sensing of Environment 112:836-844

Del Vecchio R, Blough NV (2004) Spatial and seasonal distribution of chromophoric dissolved organic matter and dissolved organic carbon in the middle atlantic bight. Marine Chemistry 89:169-187

Demers S, Roy S, Gagnon R, Vignault C (1991) Rapid light-induced changes in cell fluorescence and in xanthophyll-cycle pigments of alexandrium excavaum (dynophyceae) and thalassiosira pseudomonas (bacillariophyceae):. Marine Ecology Progress Series 76:185-193

Dortch Q, Whitledge TE (1992) Does nitrogen or silicon limit phytoplankton production in the mississippi river plume and nearby regions? Continental Shelf Research 12:1293-1309

Eisner LB, Twardowski MS, Cowles TJ, Perry MJ (2003) Resolving phytoplankton photoprotective : Photosynthetic carotenoid ratios on fine scales using in situ spectral absorption measurements. Limnology and Oceanography 48:632-646

Estapa ML, Boss E, Mayer LM, Roesler CS (2012) Role of iron and organic carbon in mass-specific light absorption by particulate matter from louisiana coastal waters. Limnology and Oceanography 57:97-112

Falkowski PG, Barber RT, Smetacek V (1998) Biogeochemical controls and feedbacks on ocean primary production. Science 281:200-206

Falkowski PG, Raven JA (1997) Aquatic photosynthesis, Vol 256. Blackwell Science Malden, MA

Falkowski PG, Wirick CD (1981) A simulation model of the effects of vertical mixing on primary productivity. Marine Biology 65:69-75

Farnham IM, Johannesson KH, Singh AK, Hodge VF, Stetzenbach KJ (2003) Factor analytical approaches for evaluating groundwater trace element chemistry data. Analytica Chimica Acta 490:123-138

Farrar DE, Glauber RR (1967) Multicollinearity in regression analysis: The problem revisited. The Review of Economics and Statistics 49:92-107

Fennel K, Hetland R, Feng Y, Dimarco S (2011) A coupled physical-biological model of the northern gulf of mexico shelf: Model description, validation and analysis of phytoplankton variability. Biogeosciences 8:1881-1899

Ferrari GM, Bo FG, Babin M (2003a) Geo-chemical and optical characterizations of suspended matter in european coastal waters. Estuarine, Coastal and Shelf Science 57:17-24

Ferrari GM, Bo FG, Babin M (2003b) Geo-chemical and optical characterizations of suspended matter in european coastal waters. Estuarine, Coastal and Shelf Science 57:17-24

Ferreira A, Garcia VMT, Garcia CAE (2009) Light absorption by phytoplankton, non-algal particles and dissolved organic matter at the patagonia shelf-break in spring

and summer. Deep Sea Research Part I: Oceanographic Research Papers 56:2162-2174

Fichot CG, Benner, Ronald (2012) The spectral slope coefficient of chromophoric dissolved organic matter (s₂₇₅₋₂₉₅) as a tracer of terrigenous dissolved organic carbon in river-influenced ocean margins. Limnology and Oceanography 57:1453-1466

Filardo MJ, Dunstan WM (1985) Hydrodynamic control of phytoplankton in low salinity waters of the james river estuary, virginia, u.S.A. Estuarine, Coastal and Shelf Science 21:653-667

Furuya K, Hayashi M, Yabushita Y, Ishikawa A (2003) Phytoplankton dynamics in the east china sea in spring and summer as revealed by hplc-derived pigment signatures. Deep Sea Research Part II: Topical Studies in Oceanography 50:367-387

Gattuso J-P, Frankignoulle M, Wollast R (1998) Carbon and carbonate metabolism in coastal aquatic ecosystems. Annual Review of Ecology and Systematics 29:405-434

Gibb SW, Barlow RG, Cummings DG, Rees NW, Trees CC, Holligan P, Suggett D (2000) Surface phytoplankton pigment distributions in the atlantic ocean: An assessment of basin scale variability between 50°n and 50°s. Progress In Oceanography 45:339-368

Gibb SW, Cummings DG, Irigoien X, Barlow RG, Fauzi R, Mantoura C (2001) Phytoplankton pigment chemotaxonomy of the northeastern atlantic. Deep-Sea Research Part II: Topical Studies in Oceanography 48:795-823

Gieskes WW, Kraay GW (1986) Floristic and physiological differences between the shallow and the deep nanophytoplankton community in the euphotic zone of the open tropical atlantic revealed by hplc analysis of pigments. Marine Biology 91:567-576

Goericke R, Montoya JP (1998) Estimating the contribution of microalgal taxa to chlorophyll a in the field--variations of pigment ratios under nutrient- and light-limited growth. Marine Ecology Progress Series 169:97-112

Goericke R, Repeta DJ (1993) Chlorophyll-a and chlorophyll-b and divinyl chlorophyll-a and chlorophyll-b in the open subtropical north atlantic ocean. Marine Ecology Progress Series 101:307-313

Goolsby DA, Battaglin WA, Lawrence GB, Artz RSand others (1999) Flux and sources of nutrients in the mississippi–atchafalaya river basin, NOAA Decision Analysis Series. U.S. Department of Commerce, NOAA Coastal Ocean Program, Silver Spring, MD

Green RE, Bianchi TS, Dagg MJ, Walker ND, Breed GA (2006) An organic carbon budget for the mississippi river turbidity plume and plume contributions to air-sea co2 fluxes and bottom water hypoxia. Estuaries and Coasts 29:579-597

Green RE, Breed GA, Dagg MJ, Lohrenz SE (2008a) Modeling the response of primary production and sedimentation to variable nitrate loading in the mississippi river plume. Continental Shelf Research 28:1451-1465

Green RE, Gould RW (2008) A predictive model for satellite-derived phytoplankton absorption over the louisiana shelf hypoxic zone: Effects of nutrients and physical forcing. Journal of Geophysical Research 113

Green RE, Gould RW, Ko DS (2008b) Statistical models for sediment/detritus and dissolved absorption coefficients in coastal waters of the northern gulf of mexico. Continental Shelf Research 28:1273-1285

Greg Mitchell B, Holm-Hansen O (1991) Bio-optical properties of antarctic peninsula waters: Differentiation from temperate ocean models. Deep Sea Research Part A Oceanographic Research Papers 38:1009-1028

Guillou L, Eikrem W, Chrétiennot-Dinet M-J, Le Gall Fand others (2004) Diversity of picoplanktonic prasinophytes assessed by direct nuclear ssu rdna sequencing of environmental samples and novel isolates retrieved from oceanic and coastal marine ecosystems. Protist 155:193-214

Guo X, Cai W-J, Huang W-J, Wang Yand others (2012) Carbon dynamics and community production in the mississippi river plume. Limnology and Oceanography 57:1-17

Hair JF (2010) Multivariate data analysis : A global perspective, Vol. Pearson Education, Upper Saddle River, N.J.; London

Helms JR, Stubbins A, Ritchie JD, Minor EC, Kieber DJ, Mopper K (2008) Absorption spectral slopes and slope ratios as indicators of molecular weight, source, and photobleaching of chromophoric dissolved organic matter. Limnology and Oceanography 53:955-969

Hernandez-Becerril DU, Aquino-Cruz A, Salas-De-Leon DA, Signoret-Poillon M, Monreal-Gomez MA (2012) Studies on picophytoplankton in the southern gulf of mexico: Pigment analysis and potential importance of the picoeukaryote prasinophyte micromonas pusilla. Marine Biology Research 8:331-340

Hernes PJ, Robinson AC, Aufdenkampe AK (2007) Fractionation of lignin during leaching and sorption and implications for organic matter “freshness&#8221. Geophys Res Lett 34:L17401

Higgins HW, Mackey DJ, Clementson L (2006) Phytoplankton distribution in the bismarck sea north of papua new guinea: The effect of the sepik river outflow. Deep Sea Research Part I: Oceanographic Research Papers 53:1845-1863

Hirata T, Hardman-Mountford NJ, Brewin RJW, Aiken Jand others (2011) Synoptic relationships between surface chlorophyll-a and diagnostic pigments specific to phytoplankton functional types. Biogeosciences 8:311-327

Hoepffner N, Sathyendranath S (1992) Bio-optical characteristics of coastal waters: Absorption spectra of phytoplankton and pigment distribution in the western north atlantic. Limnology & Oceanography 37:1660-1679

Hofmann EE, Cahill B, Fennel K, Friedrichs MAMand others (2011) Modeling the dynamics of continental shelf carbon. Annual Review of Marine Science 3:93-122

Hoogstraten A, M. Peters, K. R. Timmermans, Baar aHJWd (2011) Combined effects of inorganic carbon and light on phaeocystis globosa scherffel (prymnesiophyceae). Biogeosciences Discuss:12353–12380

Hooker SB, VanHeukelem L, Thomas CS, Claustre Hand others (2005) The second sea-wifs hplc analysis round-robin experiment (seaharre-2).

Hooker, S.B., L. Clementson, C.S. Thomas, L. Schlüter, M. Allerup, J. Ras, H. Claustre, C. Normandeau, J. Cullen, M. Kienast, W. Kozlowski, M. Vernet, S. Chakraborty, S. Lohrenz, M. Tuel, D. Redalje, P. Cartaxana, C.R. Mendes, V. Brotas, S.G. Prabhu Matondkar, S.G. Parab, A. Neeley, and E. Skarstad Egeland,

2012: The Fifth SeaWiFS HPLC Analysis Round-Robin Experiment (SeaHARRE-5). NASA Tech. Memo 2012-217503, NASA Goddard Space Flight Center, Greenbelt, Maryland, (in press)

Hulburt EM (1963) The diversity of phytoplankton populations in oceanic, coastal, and estuarine regions. Journal of Marine Research:81-93

Iglesias-Rodriguez MD, Halloran PR, Rickaby REM, Hall IRand others (2008) Phytoplankton calcification in a high-co2 world. Science 320:336-340

IOCCG (2006) Remote sensing of inherent optical properties: Fundamental test for algorithms, and applications.

Jackson RH, Williams PJlB, Joint IR (1987) Freshwater phytoplankton in the low salinity region of the river tamar estuary. Estuarine, Coastal and Shelf Science 25:299-311

Jeffrey SW, Mantoura RFC, Wright SW, International Council of Scientific Unions. Scientific Committee on Oceanic R, Unesco (1997) Phytoplankton pigments in oceanography : Guidelines to modern methods, Vol. UNESCO Pub., Paris

Jochem FJ (2003) Photo- and heterotrophic pico- and nanoplankton in the mississippi river plume: Distribution and grazing activity. Journal of Plankton Research 25:1201-1214

Johnsen G, Nelson NB, Jovine RVM, Prezelin BB (1994) Chromoprotein- and pigment-dependent modeling of spectral light absorption in two dinoflagellates, p'orocenkzm mh&mzm and heterocapsa pygmaea. Marine Ecology Progress Series 114:245-258

Johnsen G, Sakshaug E (2007) Biooptical characteristics of psii and psi in 33 species (13 pigment groups) of marine phytoplankton, and the relevance for pulse-amplitude-modulated and fast-repetition-rate fluorometry1. Journal of Phycology 43:1236-1251

Johnson AG, Kelley JT (1984) Temporal, spatial, and textural variation in the mineralogy of mississippi river suspended sediment. Journal of Sedimentary Research 54:67-72

Johnson ZI, Zinser ER, Coe A, McNulty NP, Woodward EMS, Chisholm SW (2006) Niche partitioning among prochlorococcus ecotypes along ocean-scale environmental gradients. Science 311:1737-1740

Jolliff JK, Kindle JC, Penta B, Helber Rand others (2008) On the relationship between satellite-estimated bio-optical and thermal properties in the gulf of mexico. Journal of Geophysical Research 113

Justić D, Rabalais NN, Eugene Turner R, Wiseman Jr WJ (1993) Seasonal coupling between riverborne nutrients, net productivity and hypoxia. Marine pollution bulletin 26:184-189

Kana TM, Glibert PM (1987) Effect of irradiances up to 2000 μe m-2 s-1 on marine synechococcus wh7803-i. Growth, pigmentation, and cell composition. Deep Sea Research Part A, Oceanographic Research Papers 34:479-495

Kara AB, Rochford PA, Hurlburt HE (2000) An optimal definition for ocean mixed layer depth. J Geophys Res 105:16803-16821

Kirk JTO (1994) Light and photosynthesis in aquatic ecosystems, Vol. Cambridge University Press, Cambridge, UK

Ko DS, R.H. Preller, P.J. Martin (2003) An experimental real-time intra americas sea ocean nowcast/forecast system for coastal prediction AMS 5th Conference on Coastal Atmospheric and Oceanic Prediction and Processes, p 97–100

Kostadinov TS, Siegel DA, Maritorena S, Guillocheau N (2012) Optical assessment of particle size and composition in the santa barbara channel, california. Applied Optics 51:3171-3189

Kozlowski WA, Deutschman D, Garibotti I, Trees C, Vernet M (2011) An evaluation of the application of chemtax to antarctic coastal pigment data. Deep Sea Research Part I: Oceanographic Research Papers 58:350-364

Lambert CD, Bianchia TS, Santschi PH (1998) Cross-shelf changes in phytoplankton community composition in the gulf of mexico (texas shelf/slope): The use of plant pigments as biomarkers. Continental Shelf Research 19:1-21

Latasa M (2007) Improving estimations of phytoplankton class abundances using chemtax. Marine Ecology Progress Series 329:13-21

Latasa M, Scharek R, Gall FL, Guillou L (2004) Pigment suites and taxonomic groups in prasinophyceae. Journal of Phycology 40:1149-1155

Latasa M, Scharek R, Vidal M, Vila-Reixach G, Gutiérrez-Rodríguez A, Emelianov M, Gasol JM (2010) Preferences of phytoplankton groups for waters of different trophic status in the northwestern mediterranean sea. Marine Ecology Progress Series 407:27-42

Laurion I, Blouin F, Roy S (2004) Packaging of mycosporine-like amino acids in dinoflagellates. Marine Ecology Progress Series 279:297-303

Laurion I, Frédérick Blouin, Roy S (2003) The quantitative filter technique for measuring phytoplankton absorption: Interference by maas in the uv waveband. Limnol Oceanogr Methods 1:1-9

Laza-Martinez A, Seoane S, Zapata M, Orive E (2007) Phytoplankton pigment patterns in a temperate estuary: From unialgal cultures to natural assemblages. Journal of Plankton Research 29:913-929

Lee Z, Carder KL (2004) Absorption spectrum of phytoplankton pigments derived from hyperspectral remote-sensing reflectance. Remote Sensing of Environment 89:361-368

Lee Z, Carder KL, Arnone RA (2002) Deriving inherent optical properties from water color: A multiband quasi-analytical algorithm for optically deep waters. Applied Optics 41:5755-5772

Lehrter JC, Murrell MC, Kurtz JC (2009) Interactions between freshwater input, light, and phytoplankton dynamics on the louisiana continental shelf. Continental Shelf Research 29:1861-1872

Lewitus AJ, White DL, Tymowski RG, Geesey ME, Hymel SN, Noble PA (2005) Adapting the chemtax method for assessing phytoplankton taxonomic composition in southeastern u.S. Estuaries. Estuaries 28:160-172

Li WKW (1998) Annual average abundance of heterotrophic bacteria and synechococcus in surface ocean waters. Limnology and Oceanography 43:1746-1753

Li X, Bianchi TS, Yang Z, Osterman LE, Allison MA, DiMarco SF, Yang G (2011) Historical trends of hypoxia in changjiang river estuary: Applications of chemical biomarkers and microfossils. Journal of Marine Systems 86:57-68

Lindell D, Post AF (1995) Ultraplankton succession is triggered by deep winter mixing in the gulf of aqaba (eilat) red sea. Limnology and Oceanography 40:1130-1141

Liu H, Dagg M, Campbell L, Urban-Righ J (2004) Picophytoplankton and bacterioplankton in the mississippi river plume and its adjacent waters. Estuaries 27:147-156

Liu H, Probert I, Uitz J, Claustre Hand others (2009) Extreme diversity in noncalcifying haptophytes explains a major pigment paradox in open oceans. Proceedings of the National Academy of Sciences of the United States of America 106:12803-12808

Llabrés M, Agustí S (2006) Picophytoplankton cell death induced by uv radiation: Evidence for oceanic atlantic communities. Limnology and Oceanography 51:21-29

Lohrenz S, Cai W-J, Chen X, Tuel M (2008a) Satellite assessment of bio-optical properties of northern gulf of mexico coastal waters following hurricanes katrina and rita. Sensors 8:4135-4150

Lohrenz SE (2000) A novel theoretical approach to correct for pathlength amplification and variable sampling loading in measurements of particulate spectral absorption by the quantitative filter technique. Journal of Plankton Research 22:639-657

Lohrenz SE, Carroll CL, Weidemann AD, Tuel M (2003a) Variations in phytoplankton pigments, size structure and community composition related to wind forcing and water mass properties on the north carolina inner shelf. Continental Shelf Research 23:1447-1464

Lohrenz SE, Fahnenstiel GL, Redalje DG, Lang GA, Dagg MJ, Whitledge TE, Dortch Q (1999) Nutrients, irradiance, and mixing as factors regulating primary production in coastal waters impacted by the mississippi river plume. Continental Shelf Research 19:1113-1141

Lohrenz SE, Redalje DG, Cai W-J, Acker J, Dagg M (2008b) A retrospective analysis of nutrients and phytoplankton productivity in the mississippi river plume. Continental Shelf Research 28:1466-1475

Lohrenz SE, Weidemann AD, Tuel M (2003b) Phytoplankton spectral absorption as influenced by community size structure and pigment composition. Journal of Plankton Research 25:35-61

Loisel H, Mériaux X, Berthon J-F, Poteau A (2007) Investigation of the optical backscattering to scattering ratio of marine particles in relation to their biogeochemical composition in the eastern english channel and southern north sea. Limnology and Oceanography 52:739-752

Lorbacher K, Dommenget D, Niiler PP, Köhl A (2006) Ocean mixed layer depth: A subsurface proxy of ocean-atmosphere variability. J Geophys Res 111:C07010

Lutz VA, Sathyendranath S, Head EJH, Li WKW (2003) Variability in pigment composition and optical characteristics of phytoplankton in the labrador sea and the central north atlantic. Marine Ecology Progress Series 260:1-18

Mackey DJ, Higgins HW, Mackey MD, Holdsworth D (1998) Algal class abundances in the western equatorial pacific: Estimation from hplc measurements of chloroplast pigments using chemtax. Deep-Sea Research Part I: Oceanographic Research Papers 45:1441-1468

Mackey MD, Mackey DJ, Higgins HW, Wright SW (1996) Chemtax - a program for estimating class abundances from chemical markers: Application to hplc measurements of phytoplankton. Marine Ecology Progress Series 144:265-283

Margalef R (1978) Life-forms of phytoplankton as survival alternatives in an unstable environment. Oceanol Acta: pp. 493–509

Marra J, Trees CC, O'Reilly JE (2007) Phytoplankton pigment absorption: A strong predictor of primary productivity in the surface ocean. Deep Sea Research Part I: Oceanographic Research Papers 54:155-163

Martin PJ (2000) Description of the navy coastal ocean model version 1.0, Washington, D. C.

Martínez-López B, Zavala-Hidalgo J (2009) Seasonal and interannual variability of cross-shelf transports of chlorophyll in the gulf of mexico. Journal of Marine Systems 77:1-20

Marty J-C, Chiavérini J, Pizay M-D, Avril B (2002) Seasonal and interannual dynamics of nutrients and phytoplankton pigments in the western mediterranean sea at the dyfamed time-series station (1991–1999). Deep Sea Research Part II: Topical Studies in Oceanography 49:1965-1985

Marty J-C, Garcia N, Raimbault P (2008) Phytoplankton dynamics and primary production under late summer conditions in the nw mediterranean sea. Deep Sea Research Part I: Oceanographic Research Papers 55:1131-1149

Massolo S, Messa R, Rivaro P, Leardi R (2009) Annual and spatial variations of chemical and physical properties in the ross sea surface waters (antarctica). Continental Shelf Research 29:2333-2344

Matsuoka A, Larouche P, Poulin M, Vincent W, Hattori H (2009) Phytoplankton community adaptation to changing light levels in the southern beaufort sea, canadian arctic. Estuarine, Coastal and Shelf Science 82:537-546

Mayer LM (1994) Surface area control of organic carbon accumulation in continental shelf sediments. Geochimica et Cosmochimica Acta 58:1271-1284

McClain CR (2009) A decade of satellite ocean color observations. Ann Rev Mar Sci 1:19-42

Meade RH (1996) River sediment input to major delta. In: Milliman J, Haq, B.U. (ed) Sea-level rise and coastal subsidence. Kluwer Academic Publishers, Dordrecht, Netherlands, p 63-85

Meglen RR (1992) Examining large databases: A chemometric approach using principal component analysis. Marine Chemistry 39:217-237

Mélin F, Zibordi G, Berthon J-F (2007) Assessment of satellite ocean color products at a coastal site. Remote Sensing of Environment 110:192-215

Mendes CR, Sá C, Vitorino J, Borges C, Tavano Garcia VM, Brotas V (2011) Spatial distribution of phytoplankton assemblages in the nazaré submarine canyon region (portugal): Hplc-chemtax approach. Journal of Marine Systems 87:90-101

Meyer AA, Tackx M, Daro N (2000) Xanthophyll cycling in phaeocystis globosa and thalassiosira sp.: A possible mechanism for species succession. Journal of Sea Research 43:373-384

Moore LR, Anton FP, Rocap G, Chisholm SW (2002) Utilization of different nitrogen sources by the marine cyanobacteria prochlorococcus and synechococcus. Limnology and Oceanography 47:989-996

Moore LR, Chisholm SW (1999a) Photophysiology of the marine cyanobacterium prochlorococcus: Ecotypic differences among cultured isolates. Limnology and Oceanography 44:628-638

Moore LR, Chisholm SW (1999b) Photophysiology of the marine cyanobacterium prochlorococcus: Ecotypic differences among cultured isolates. Limnology and Oceanography 44:628-638

Moore LR, Goericke R, Chisholm SW (1995) Comparative physiology of synechococcus and prochlorococcus: Influence of light and temperature on growth, pigments, fluorescence and absorptive properties. Marine Ecology Progress Series 116:259-276

Morel A (1991) Light and marine photosynthesis: A spectral model with geochemical and climatological implications. Progress In Oceanography 26:263-306

Morel A, Bricaud A (1981) Theoretical results concerning light absorption in a discrete medium, and application to specific absorption of phytoplankton. Deep Sea Research Part A Oceanographic Research Papers 28:1375-1393

Morel A, Maritorena S (2001) Bio-optical properties of oceanic waters: A reappraisal. Journal of Geophysical Research C: Oceans 106:7163-7180

Morrison JR, Nelson NB (2004) Seasonal cycle of phytoplankton uv absorption at the bermuda atlantic time-series study (bats) site. Limnology and Oceanography 49:215-224

Muller-Karger FE, Walsh JJ, Evans RH, Meyers MB (1991) On the seasonal phytoplankton concentration and sea surface temperature cycles of the gulf of

mexico as determined by satellites. Journal of Geophysical Research 96:12,645-612,665

Murray SP, United States. Minerals Management Service. Gulf of Mexico OCSR, Louisiana State University . Coastal Studies I (1998) An observational study of the mississippi-atchafalaya coastal plume final report, Vol. U.S. Dept. of the Interior, Minerals Management Service, Gulf of Mexico OCS Region, New Orleans [La.] (1201 Elmwood Park Blvd., New Orleans 70123-2394)

Murrell MC, Lores EM (2004) Phytoplankton and zooplankton seasonal dynamics in a subtropical estuary: Importance of cyanobacteria. Journal of Plankton Research 26:371-382

Murtugudde R, Beauchamp J, McClain CR, Lewis M, Busalacchi AJ (2002) Effects of penetrative radiation on the upper tropical ocean circulation. Journal of Climate 15:470-486

Muylaert K, Gonzales R, Franck M, Lionard Mand others (2006) Spatial variation in phytoplankton dynamics in the belgian coastal zone of the north sea studied by microscopy, hplc-chemtax and underway fluorescence recordings. Journal of Sea Research 55:253-265

Naik P, D'Sa EJ, Grippo M, Condrey R, Fleeger J (2011) Absorption properties of shoal-dominated waters in the atchafalaya shelf, louisiana, USA. International Journal of Remote Sensing 32:4383-4406

Nelson JR, Guarda S (1995) Particulate and dissolved spectral absorption on the continental shelf of the southeastern united states. J Geophys Res 100:8715-8732

Nelson NB, Siegel DA, Michaels AF (1998) Seasonal dynamics of colored dissolved material in the sargasso sea. Deep Sea Research Part I: Oceanographic Research Papers 45:931-957

Not F, Latasa M, Scharek R, Viprey Mand others (2008) Protistan assemblages across the indian ocean, with a specific emphasis on the picoeukaryotes. Deep Sea Research Part I: Oceanographic Research Papers 55:1456-1473

O'Reilly JE, Maritorena S, O'Brien MC, Siegel DAand others (2000) Volume 11, seawifs postlaunch calibration and validation analyses, part 3. NASA Technical Memorandum - SeaWIFS Postlaunch Technical Report Series:1-49

Odriozola AL, Varela R, Hu C, Astor Y, Lorenzoni L, Müller-Karger FE (2007) On the absorption of light in the orinoco river plume. Continental Shelf Research 27:1447-1464

Opsahl S, Benner R (1995) Early diagenesis of vascular plant tissues: Lignin and cutin decomposition and biogeochemical implications. Geochimica et Cosmochimica Acta 59:4889-4904

Paerl HW (1996) A comparison of cyanobacterial bloom dynamics in freshwater, estuarine and marine environments. Phycologia 35:25-35

Paerl HW, Valdes LM, Pinckney JL, Piehler MF, Dyble J, Moisander PH (2003) Phytoplankton photopigments as indicators of estuarine and coastal eutrophication. BioScience 53:953-964

Partensky F, Hoepffner N, Li WKW, Ulloa O, Vaulot D (1993) Photoacclimation of prochlorococcus sp. (prochlorophyta) strains isolated from the north atlantic and the mediterranean sea. Plant Physiology 101:285-296

Paul JH, Alfreider A, Kang JB, Stokes RA, Griffin D, Campbell L, Ornolfsdottir E (2000a) Form ia rbcl transcripts associated with a low salinity/high chlorophyll plume ('green river') in the eastern gulf of mexico. Marine Ecology Progress Series 198:1-8

Paul JH, Alfreider A, Wawrik B (2000b) Micro- and macrodiversity in rbcl sequences in ambient phytoplankton populations from the southeastern gulf of mexico. Marine Ecology Progress Series 198:9-18

Pinckney JL, Wee JL, Hou A, Walker ND (2009) Phytoplankton community structure responses to urban effluent inputs following hurricanes katrina and rita. Marine Ecology Progress Series 387:137-146

Platt T, Sathyendranath S (1988) Oceanic primary production: Estimation by remote sensing at local and regional scales. Science 241:1613-1620

Prieur L, Sathyendranath S (1981) An optical classification of coastal and oceanic waters based on the specific spectral absorption curves of phytoplankton pigments, dissolved organic matter, and other particulate materials. Limnology and Oceanography 26:671-689

Qian Y, Jochens AE, Kennicutt Ii MC, Biggs DC (2003) Spatial and temporal variability of phytoplankton biomass and community structure over the continental margin of the northeast gulf of mexico based on pigment analysis. Continental Shelf Research 23:1-17

Quéré CL, Harrison SP, Colin Prentice I, Buitenhuis ETand others (2005) Ecosystem dynamics based on plankton functional types for global ocean biogeochemistry models. Global Change Biology 11:2016-2040

Rabalais N, Turner RE, Dortch Q, Justic D, Bierman V, Jr., Wiseman W, Jr. (2002a) Nutrient-enhanced productivity in the northern gulf of mexico: Past, present and future. Hydrobiologia 475-476:39-63

Rabalais NN, Turner RE, Wiseman Jr WJ (2002b) Gulf of mexico hypoxia, a.K.A. "The dead zone". Annual Review of Ecology and Systematics 33:235-263

Redalje DG, Lohrenz SE, Fahnenstiel GL (1994) The relationship between primary production and the vertical export of particulate organic matter in a river-impacted coastal ecosystem. Estuaries 17:829-838

Robbins LL, P.G. Coble, T.D. Clayton, and W.-J. Cai (2009) Ocean carbon and biogeochemistry scopingworkshop on terrestrial and coastalcarbon fluxes in the gulf of mexico, St. Petersburg, FL

Rochelle-Newall EJ, Fisher TR (2002) Production of chromophoric dissolved organic matter fluorescence in marine and estuarine environments: An investigation into the role of phytoplankton. Marine Chemistry 77:7-21

Rodríguez F, Chauton M, Johnsen G, Andresen K, Olsen LM, Zapata M (2005) Photoacclimation in phytoplankton: Implications for biomass estimates, pigment functionality and chemotaxonomy. Marine Biology 148:963-971

Roesler CS, Perry MJ, Carder KL (1989) Modeling in situ phytoplankton absorption from total absorption spectra in productive inland marine waters. Limnology and Oceanography 34:1510-1523

Roy S, Blouin F, Jacques A, Therriault J-C (2008) Absorption properties of phytoplankton in the lower estuary and gulf of st. Lawrence (canada). Canadian Journal of Fisheries and Aquatic Sciences 65:1721-1737

Sabine CL, Feely RA, Gruber N, Key RMand others (2004) The oceanic sink for anthropogenic co2. Science 305:367-371

Salisbury JE, Campbell JW, Linder E, David Meeker L, Müller-Karger FE, Vörösmarty CJ (2004) On the seasonal correlation of surface particle fields with wind stress and mississippi discharge in the northern gulf of mexico. Deep Sea Research Part II: Topical Studies in Oceanography 51:1187-1203

Sathyendranath S (2000) Remote sensing of ocean color in coastal and other optically-complex waters Dartmouth, Nova Scotia, Canada

Sathyendranath S, Platt, Trevor, Horne, Edward P. W., Harrison, William G., Ulloa, Osvaldo,Outerbridge, Richard, Hoepffner, Nicolas (1991) Estimation of new production in the ocean by compound remote sensing. Nature 353:129-133

Schaeffer BA, Conmy RN, Aukamp J, Craven G, Ferer EJ (2011a) Organic and inorganic matter in louisiana coastal waters: Vermilion, atchafalaya, terrebonne, barataria, and mississippi regions. Marine pollution bulletin 62:415-422

Schaeffer BA, Sinclair GA, Lehrter JC, Murrell MC, Kurtz JC, Gould RW, Yates DF (2011b) An analysis of diffuse light attenuation in the northern gulf of mexico hypoxic zone using the seawifs satellite data record. Remote Sensing of Environment 115:3748-3757

Schiller RV, Kourafalou VH, Hogan P, Walker ND (2011) The dynamics of the mississippi river plume: Impact of topography, wind and offshore forcing on the fate of plume waters. J Geophys Res 116:C06029

Schlüter L, Henriksen P, Nielsen TG, Jakobsen HH (2011) Phytoplankton composition and biomass across the southern indian ocean. Deep-Sea Research Part I: Oceanographic Research Papers 58:546-556

Schlüter L, Lauridsen TL, Krogh G, JØRgensen T (2006) Identification and quantification of phytoplankton groups in lakes using new pigment ratios – a comparison between pigment analysis by hplc and microscopy. Freshwater Biology 51:1474-1485

Schlüter L, Møhlenberg F (2003) Detecting presence of phytoplankton groups with non-specific pigment signatures. Journal of Applied Phycology 15:465-476

Schlüter L, Møhlenberg F, Havskum H, Larsen S (2000) The use of phytoplankton pigments for identifying and quantifying phytoplankton groups in coastal areas: Testing the influence of light and nutrients on pigment/chlorophyll a ratios. Marine Ecology Progress Series 192:49-63

Schoemann V, Becquevort S, Stefels J, Rousseau V, Lancelot C (2005) Phaeocystis blooms in the global ocean and their controlling mechanisms: A review. Journal of Sea Research 53:43-66

Schofield O, Arnone RA, Bissett WP, Dickey TDand others (2004) Watercolors in the coastal zone: What can we see? Biological Sciences:144

Seoane S, Garmendia M, Revilla M, Borja A, Franco J, Orive E, Valencia V (2011) Phytoplankton pigments and epifluorescence microscopy as tools for ecological status assessment in coastal and estuarine waters, within the water framework directive. Marine pollution bulletin 62:1484-1497

Seoane S, Zapata M, Orive E (2009) Growth rates and pigment patterns of haptophytes isolated from estuarine waters. Journal of Sea Research 62:286-294

Shank GC, Evans A (2011) Distribution and photoreactivity of chromophoric dissolved organic matter in northern gulf of mexico shelf waters. Continental Shelf Research 31:1128-1139

Shank GC, Zepp RG, Whitehead RF, Moran MA (2005) Variations in the spectral properties of freshwater and estuarine cdom caused by partitioning onto river and estuarine sediments. Estuarine, Coastal and Shelf Science 65:289-301

Shen Y, Fichot CG, Benner R (2012) Floodplain influence on dissolved organic matter composition and export from the mississippi-atchafalaya river system to the gulf of mexico. Limnology and Oceanography 57:1149-1160

Siegel DA, Maritorena S, Nelson NB, Behrenfeld MJ, McClain CR (2005) Colored dissolved organic matter and its influence on the satellite-based characterization of the ocean biosphere. Geophysical Research Letters 32

Siegel DA, Maritorena S, Nelson NB, Hansell DA, Lorenzi-Kayser M (2002) Global distribution and dynamics of colored dissolved and detrital organic materials. J Geophys Res 107:3228

Smayda TJ (1980) Physiological ecology of phytoplankton chapter in phytoplankton species succession, Vol. Blackwell Scientific Publications

Smith SV, Hollibaugh JT (1993) Coastal metabolism and the oceanic organic carbon balance. Rev Geophys 31:75-89

Sokal RR, Rolf FJ (1973) *Introduction to biostatistics*, Vol. Dover, Minecola, N.Y.

Sommaruga R, Hofer JS, Alonso-Saez L, Gasol JM (2005) Differential sunlight sensitivity of picophytoplankton from surface mediterranean coastal waters. Applied and environmental microbiology 71:2154-2157

Son YB, Gardner WD, Mishonov AV, Richardson MJ (2009) Multispectral remote-sensing algorithms for particulate organic carbon (poc): The gulf of mexico. Remote Sensing of Environment 113:50-61

Sosik HM, Mitchell BG (1995) Light absorption by phytoplankton, photosynthetic pigments and detritus in the california current system. Deep-Sea Research Part I: Oceanographic Research Papers 42:1717-1748

Steinacher M, Joos F, FrÃ¶licher TL, Bopp Land others (2010) Projected 21st century decrease in marine productivity: A multi-model analysis. Biogeosciences 7

Steinberg DK, Carlson CA, Bates NR, Johnson RJ, Michaels AF, Knap AH (2001) Overview of the us jgofs bermuda atlantic time-series study (bats): A decade-scale look at ocean biology and biogeochemistry. Deep Sea Research Part II: Topical Studies in Oceanography 48:1405-1447

Stramski D, Morel A (1990) Optical properties of photosynthetic picoplankton in different physiological states as affected by growth irradiance. Deep Sea Research Part A Oceanographic Research Papers 37:245-266

Stramski D, Reynolds RA, Babin M, Kaczmarek Sand others (2008) Relationships between the surface concentration of particulate organic carbon and optical properties in the eastern south pacific and eastern atlantic oceans. Biogeosciences 5:171-201

Stuart V, Sathyendranath S, Platt T, Maass H, Irwin BD (1998) Pigments and species composition of natural phytoplankton populations: Effect on the absorption spectra. Journal of Plankton Research 20:187-217

Suess E (1970) Interaction of organic compounds with calcium carbonate—i. Association phenomena and geochemical implications. Geochimica et Cosmochimica Acta 34:157-168

Tassan S, Ferrari GM (1998) Measurement of light absorption by aquatic particles retained on filters: Determination of the optical pathlength amplification by the 'transmittance-reflectance' method. Journal of Plankton Research 20:1699-1709

Ting CS, Rocap G, King J, Chisholm SW (2002) Cyanobacterial photosynthesis in the oceans: The origins and significance of divergent light-harvesting strategies. Trends in Microbiology 10:134-142

Twardowski MS, Boss E, Sullivan JM, Donaghay PL (2004) Modeling the spectral shape of absorption by chromophoric dissolved organic matter. Marine Chemistry 89:69-88

Twardowski MS, Donaghay PL (2002) Photobleaching of aquatic dissolved materials: Absorption removal, spectral alteration, and their interrelationship. J Geophys Res 107:3091

Uher G, Hughes C, Henry G, Upstill, Goddard RC (2001) Non‐conservative mixing behavior of colored dissolved organic matter in a humic‐rich, turbid estuary. Geophys Res Lett 28:3309-3312

Uitz J, Claustre H, Morel A, Hooker SB (2006) Vertical distribution of phytoplankton communities in open ocean: An assessment based on surface chlorophyll. Journal of Geophysical Research C: Oceans 111

Van Heukelem L, Thomas CS (2001) Computer-assisted high-performance liquid chromatography method development with applications to the isolation and analysis of phytoplankton pigments. Journal of Chromatography A 910:31-49

Vanderbloemen L, Müller-Karger F (2001) Chlorophyll concentrations along the west florida shelf. Earth System Monitor 11:1-4

Vargo GA, Heil CA, Fanning KA, Dixon LKand others (2008) Nutrient availability in support of karenia brevis blooms on the central west florida shelf: What keeps karenia blooming? Continental Shelf Research 28:73-98

Veldhuis MJW, Kraay GW (2004) Phytoplankton in the subtropical atlantic ocean: Towards a better assessment of biomass and composition. Deep-Sea Research Part I: Oceanographic Research Papers 51:507-530

Vidussi F, Claustre H, Manca BB, Luchetta A, Marty J-C (2001) Phytoplankton pigment distribution in relation to upper thermocline circulation in the eastern mediterranean sea during winter. Journal of Geophysical Research: Oceans 106:19939-19956

Vidussi F, Marty J-C, Chiavérini J (2000) Phytoplankton pigment variations during the transition from spring bloom to oligotrophy in the northwestern mediterranean sea. Deep Sea Research Part I: Oceanographic Research Papers 47:423-445

Viprey M, Guillou L, Ferréol M, Vaulot D (2008) Wide genetic diversity of picoplanktonic green algae (chloroplastida) in the mediterranean sea uncovered by a phylum-biased pcr approach. Environmental Microbiology 10:1804-1822

Vodacek A (1992) An explanation of the spectral variation in freshwater cdom fluorescence. Limnology and Oceanography 37:1808-1813

Vodacek A, Blough NV, DeGrandpre MD, Peltzer ET, Nelson RK (1997) Seasonal variation of cdom and doc in the middle atlantic bight: Terrestrial inputs and photooxidation. Limnology and Oceanography 42:674-686

Walker ND, Wiseman WJ, Rouse LJ, Babin A (2005) Effects of river discharge, wind stress, and slope eddies on circulation and the satellite-observed structure of the mississippi river plume. Journal of Coastal Research 216:1228-1244

Walsh JJ, Jolliff JK, Darrow BP, Lenes JMand others (2006) Red tides in the gulf of mexico: Where, when, and why? J Geophys Res 111:C11003

Ward JH, Jr. (1963) Hierarchical grouping to optimize an objective function. Journal of the American Statistical Association 58:236-244

Wawrik B, Paul JH (2004) Phytoplankton community structure and productivity along the axis of the mississippi river plume in oligotrophic gulf of mexico waters. Aquatic Microbial Ecology 35:185-196

Wawrik B, Paul JH, Campbell L, Griffin D, Houchin L, Fuentes-Ortega A, Muller-Karger F (2003) Vertical structure of the phytoplankton community associated with a coastal plume in the gulf of mexico. Marine Ecology Progress Series 251:87-101

Worden AZ, Nolan JK, Palenik B (2004) Assessing the dynamics and ecology of marine picophytoplankton: The importance of the eukaryotic component. Limnology and Oceanography 49:168-179

Woźniak SB, Stramski D, Stramska M, Reynolds RAand others (2010) Optical variability of seawater in relation to particle concentration, composition, and size distribution in the nearshore marine environment at imperial beach, california. Journal of Geophysical Research C: Oceans 115

Wright S, Ishikawa A, Marchant H, Davidson A, van den Enden R, Nash G (2009a) Composition and significance of picophytoplankton in antarctic waters. Polar Biology 32:797-808

Wright SW, Ishikawa A, Marchant HJ, Davidson AT, Enden RL, Nash GV (2009b) Composition and significance of picophytoplankton in antarctic waters. Polar Biology 32:797-808

Wright SW, van den Enden RL (2000) Phytoplankton community structure and stocks in the east antarctic marginal ice zone (broke survey, january–march 1996) determined by chemtax analysis of hplc pigment signatures. Deep Sea Research Part II: Topical Studies in Oceanography 47:2363-2400

Wright SW, van den Enden RL, Pearce I, Davidson AT, Scott FJ, Westwood KJ (2010) Phytoplankton community structure and stocks in the southern ocean (30–80°e) determined by chemtax analysis of hplc pigment signatures. Deep Sea Research Part II: Topical Studies in Oceanography 57:758-778

Wysocki LA, Bianchi TS, Powell RT, Reuss N (2006) Spatial variability in the coupling of organic carbon, nutrients, and phytoplankton pigments in surface waters and

sediments of the mississippi river plume. Estuarine, Coastal and Shelf Science 69:47-63

Zapata M, Jeffrey SW, Wright SW, Rodríguez F, Garrido JL, Clementson L (2004) Photosynthetic pigments in 37 species (65 strains) of haptophyta: Implications for oceanography and chemotaxonomy. Marine Ecology Progress Series 270:83-102

Zepp RG, Schlotzhauer PF (1981) Comparison of photochemical behavior of various humic substances in water: Iii. Spectroscopic properties of humic substances. Chemosphere 10:479-486

Zhou JL, Rowland S, Fauzi R, Mantoura C, Braven J (1994) The formation of humic coatings on mineral particles under simulated estuarine conditions - a mechanistic study. Water Research 28:571-579